

Development and application of chemical tools for the design and synthesis of bioactive molecules

Janice Lawandi

A thesis submitted to McGill University in partial fulfillment of the requirements of the degree of Doctor of Philosophy

Department of Chemistry
McGill University
Montreal, QC, Canada
December 2009

© Janice Lawandi 2009

*On fait la science avec des faits comme une maison avec des pierres;
mais une accumulation de faits n'est pas plus une science
qu'un tas de pierres n'est une maison.*

*Science is built up of facts, as a house is built of stones;
but an accumulation of facts is no more a science
than a heap of stones is a house.*

Henri Poincaré, La Science et l'Hypothèse, 1905

Copyright statement

Some of the material included in the following thesis is adapted from published papers and is under copyright:

Chapter 1 reproduces material published in Lawandi, J.; Gerber-Lemaire, S.; Juillerat-Jeanneret, L.; Moitessier, N. Inhibitors of prolyl-oligopeptidases for the therapy of human diseases: Defining diseases and inhibitors. *J. Med. Chem.* **2009**, *in press* © American Chemical Society (ACS). The ACS grants blanket permission for authors to use their work in their dissertation, as described at the following URL: <http://pubs.acs.org/copyright/forms/dissertation.pdf>.

Chapter 2 reproduces material published in Lawandi, J.; Toumieux, S.; Seyer, V.; Campbell, P.; Thielges, S.; Juillerat-Jeanneret, L.; Moitessier, N. Constrained peptidomimetics reveal detailed geometric requirements of covalent prolyl oligopeptidase inhibitors. *J. Med. Chem.* **2009**, *52*, 6672-6684. © American Chemical Society (ACS). The ACS grants blanket permission for authors to use their work in their dissertation, as described at the following URL: <http://pubs.acs.org/copyright/forms/dissertation.pdf>.

Chapters 3, 4 and 5 are drafts of manuscripts to be submitted for publication.

Abstract

In the field of drug design and development, medicinal chemists use a variety of tools to quickly generate a series of hit compounds controlling a specific biological target and culminating in a lead compound. Process chemists seek efficient methods to synthesize the lead compounds provided by the medicinal chemists and using readily available and inexpensive starting materials, shortcuts and simpler routes. With this in mind, we aimed to design, develop and apply chemical tools to generate hit compounds, but also developing new simpler methods to make pharmaceutically relevant compounds. In this context, this thesis has two goals. In the first part, we focused on the enzyme prolyl oligopeptidase, reviewing its involvement in neurological disorders, such as Alzheimer's disease, and the efforts of several researchers to synthesize potent, selective inhibitors resembling the natural substrates of this enzyme. We proposed another method, using small pseudopeptidic and peptidomimetic inhibitors as chemical tools to better understand the shape, size and electronics of inhibitors and generate a more potent, selective prolyl oligopeptidase inhibitor. From our series of compounds, we discovered a few potent and highly selective, covalent inhibitors, one of them pseudo-peptidic ($IC_{50} = 3-7$ nM) and the other peptidomimetic ($IC_{50} = 20-700$ nM). In the second part of this thesis, with the goal of being able to exploit sugars in medicinal chemistry, we first reviewed the methods that exist to regioselectively functionalize the various hydroxyls of hexopyranosides. We compiled these methods into a table which chemists could consult when they are seeking to perform a specific reaction on a specific sugar. We then proposed to use a hydrogen bond accepting protecting group which can direct subsequent reactions to specific sites on sugars in an effort to reduce the number of protection and deprotection steps. We applied this protecting-directing group and developed methods to regio- and stereoselectively glycosylate sugars (> 80% yield of one regioisomer), one of the most challenging and complex reactions in the field of carbohydrate chemistry.

Résumé

Lors de la conception d'un nouveau principe actif, les chimistes médicaux disposent d'un grand nombre d'outils leur permettant de générer rapidement une série de composés ayant une action spécifique. L'optimisation du procédé chimique requiert l'utilisation et le développement de méthodes toujours plus simples, rapides et peu coûteuses. Ainsi, nous avons souhaité concevoir et utiliser quelques outils chimiques permettant de résoudre certains de ces problèmes. Cette thèse présente des outils spécifiques à la chimie médicinale et la chimie des procédés. Dans un premier temps, nous nous sommes intéressés à une enzyme : la prolyl oligopeptidase. Nous avons tout d'abord répertorié un grand nombre de données, quant à son implication dans certains troubles neurologiques (ex. : maladie d'Alzheimer), ainsi que de nombreux programmes de recherche visant le développement de nouveaux inhibiteurs conçus à partir de la structure du substrat naturel. Dans l'optique de mieux comprendre l'environnement chimique du site de liaison de l'enzyme et concevoir notre propre inhibiteur sélectif, nous avons synthétisé et testé une série de composés pseudo-peptidiques et peptidomimétiques. Lors de cette étude, nous avons identifié deux inhibiteurs covalents, actifs et sélectifs : l'un pseudo-peptidique ($IC_{50} = 3-7$ nM), l'autre peptidomimétique ($IC_{50} = 20-700$ nM). Dans la deuxième partie de cette thèse, nous avons rapporté les méthodes déjà existantes permettant une fonctionnalisation régiosélective des différents groupements alcools des hexopyranosidases afin de rendre plus accessible l'utilisation des sucres en chimie médicinale. La compilation de cette recherche bibliographique dans une table permettra aux chimistes de facilement sélectionner la méthode la plus adéquate. Afin de réduire le nombre d'étapes (protections et déprotections) associées à la chimie des sucres, nous avons appliqué le groupement protecteur-directeur développé précédemment dans notre laboratoire à une des plus complexes réactions de la chimie des sucres, obtenant ainsi une méthode de glycosylation directe, régio- et stéréosélective (> 80% rendement pour un seul isomère).

Acknowledgements

This thesis would not have been possible without the guidance, enthusiasm and motivation of my supervisor, Nicolas Moitessier, who made a point of being available literally at any hour of the day, working on my projects with me, answering my questions, and genuinely taking an interest every step of the way.

This thesis would also not have been possible without our collaboration with Lucienne Juillerat-Jeanneret who performed all the biological assays and provided us with her wisdom gained from working with our target enzyme for so many years.

I would like to thank Fred Morin for all his advice, but also for working so hard to maintain the NMR machines for hours of spectroscopy without which this thesis would not have been complete. And to Nadim Saadeh, I really appreciate all the time he takes to keep the MS machines up and running, on top of the time he devotes to analyzing our samples. I must thank Richard Rossi, Fred Kluck and George Kopf for attempting to fix all the equipment that was broken along the way. Fay Nurse, Sandra Aerssen, and the secretaries: I don't know if the department would run so smoothly without them. To Chantal Marotte, such a patient listener, she provides us all with comfort and a hug, in good times and bad times. I most heartily thank Linda Cooper for providing two wonderful courses on writing in science. I enjoyed her courses immensely; attending them was never a chore. I am forever thankful that she shared her passion for clear writing with me, and of course for all her advice and guidance.

I am very grateful for the numerous awards I received over the years which allowed me to focus on my research, namely from NSERC (1 year), FQRNT (2.5 years) and the CIHR/Chemical biology training program (1 year).

To my lab mates who provided me with lots of laughs, I thank them all, especially Chris Corbeil, Joris De Schutter, Pablo Englebienne, Mitch Huot, Devin Lee, Eric Therrien and especially Sabine Thielges who taught me so much and is a good friend to this day. Having supervised eight undergraduate students, I

cannot name them all, but I am especially indebted to Bilal Mammah for the hard work and entertainment and Christine Najjar, who is so dedicated and a real friend. I am especially grateful to those who accepted and consumed all my baking. To Carla, Erica, Eva, Patricia, Rae and Vishya: my inspiration.

I must thank Steven and Sandra at Nautilus and my gym buddies who motivated me to actually leave the lab for at least one hour, twice a week. To the instructors at Moksha yoga who gave me a quiet place to unwind and relax, especially to Lana, Sara, and Christina. They helped me clear my mind, even if just for an hour.

I am forever indebted to Concordia University where I learned so many practical skills and gained the confidence to continue my education. Concordia also introduced me to friends who have loved and supported me through it all.

Finally, I owe my deepest gratitude to my family and my friends for all the love and support they provided me over all these years. To my parents, I know this thesis is for me, but it is also for them. They made this possible. I am grateful.

Contribution(s) of authors

This thesis contains 6 original thesis chapters. Chapters 1 and 2 are published articles, while Chapters 3, 4 and 5 are drafts which we plan on submitting for publication.

Professor Nicolas Moitessier, as my supervisor, is a co-author of all the articles presented here.

Chapter 1: I reviewed all reported prolyl oligopeptidase inhibitors and wrote the related sections, while Lucienne Juillerat-Jeannet and Sandrine Gerber reviewed the biological applications for targeting prolyl oligopeptidase.

Chapter 2: I prepared the protein and scaffold structures for docking, and ran the docking using FITTED. I also synthesized most of the bicyclic scaffolds, with assistance from Sabine Thielges, Sylvestre Toumieux and Philip Campbell. I functionalized the scaffolds into potential covalent inhibitors of prolyl oligopeptidase. Under my supervision, Valentine Seyer, an undergraduate student, synthesized the dipeptides. Lucienne Juillerat-Jeannet performed the biological assays.

Chapter 3: I reviewed the methods to selectively functionalize hexopyranoside carbohydrates.

Chapter 4: Nicolas Moitessier initiated this research and I performed most of the chemistry in this chapter.

Chapter 5: I performed all the chemistry in this chapter.

Table of contents

Copyright statement.....	i
Abstract	ii
Résumé	iii
Acknowledgements.....	iv
Contribution(s) of authors.....	vi
Table of contents.....	vii
List of figures.....	xii
List of schemes	xv
List of tables.....	xix
List of abbreviations	xx
Thesis outline.....	1
Chapter 1 Inhibitors of prolyl oligopeptidases for the therapy of human diseases: Defining diseases and inhibitors	3
1.1 Abstract.....	4
1.2 Introduction.....	4
1.3 Proline-specific exo- and endopeptidases	6
1.3.1 Proline-specific peptidases.....	6
1.3.2 Proline-specific exopeptidases: the family of Pro-aminodipeptidases, CD26/DPPIV and FAP- α /seprase.....	6
1.4 POP and other proline-specific peptidases as potential therapeutic targets	9
1.4.1 POP as a therapeutic target	9
1.4.2 POP and protein aggregation	9
1.4.3 Role of POP in the central nervous system (CNS)	12
1.4.4 POP inhibition in animal models	13
1.4.5 Passage through the blood brain barrier (BBB).....	14
1.4.6 Clinical trials.....	17
1.5 POP structural information	18
1.6 POP inhibition.....	20
1.6.1 Proline-specific proteases	20
1.6.2 Potent and selective inhibition	20
1.6.3 Inhibition of POP in human diseases	21
1.7 Peptididic, pseudo-peptididic and peptidomimetic POP inhibitors	22

Table of contents

1.7.1	Modification of P3 for optimal binding	23
1.7.2	Modification of P2 for optimal binding	25
1.7.3	Modification of P1 for optimal binding	28
1.7.4	P1' substitution, covalent versus non-covalent inhibitor	30
1.7.5	Non-peptidic POP inhibitors	31
1.7.6	Selectivity of POP inhibitors	33
1.7.7	Structure-based design of POP inhibitors	34
1.8	Conclusions and prospects	35
1.8.1	POP and POP-like inhibition	35
1.8.2	Selective and potent POP inhibitors	37
1.9	References	39
Chapter 2 Constrained peptidomimetics reveal detailed geometric requirements of covalent prolyl oligopeptidase inhibitors		57
2.1	Abstract	58
2.2	Introduction	58
2.3	Results	60
2.3.1	Computer-Aided Design of constrained inhibitors	60
2.3.2	Chemistry	63
	Synthesis of the pseudopeptidic inhibitors	63
	Synthesis of the bicyclic scaffolds	64
	Functionalization of the scaffolds to covalent inhibitors	67
	Confirming the stereochemistry of the various diastereomers	68
2.3.3	Biological Evaluation	70
	Enzyme inhibition in cell extracts	70
	Enzyme inhibition in intact living cells	73
2.4	Discussion	77
2.4.1	POP and other prolyl peptidases	77
2.4.2	Constrained POP inhibitors	78
2.4.3	POP activity and selectivity in intact cells	81
2.5	Conclusion	83
2.6	Experimental section	84
2.6.1	Synthesis	84
	General remarks	84
	Synthesis of the dipeptides	84

Synthesis of the bicyclic scaffolds	93
General procedure for formation of the amides	102
General procedure for formation of the nitriles	105
2.6.2 HPLC analysis of purity.....	110
2.6.3 Docking study	111
2.6.4 Biological evaluations.....	112
2.7 References.....	113
Chapter 3 The reactivity of the hydroxyls of different sugars is condition dependent..	119
3.1 Abstract.....	120
3.2 Introduction.....	120
3.3 Selective methods to functionalize sugars based on the intrinsic reactivity of the hydroxyls.....	123
3.3.1 4-Dimethylaminopyridine (DMAP) catalyzed acylations of alcohols	124
3.3.2 DMAP-catalyzed acylation of sugars	125
3.3.3 Silyl.....	128
3.3.4 Glycosylations on minimally protected acceptors	130
3.3.5 The influence of the hydrogen bond network	131
3.4 Extrinsic methods which internally deliver the reagent.....	134
3.4.1 DMAP-based catalysts.....	135
3.4.2 Peptidic catalysts.....	137
3.5 Extrinsic methods which pre-functionalize the sugar	139
3.5.1 Organotin derivatives.....	139
Acylation via stannyl ether derivatives	139
Acylation via stannylene acetals	140
3.5.2 Organoboron derivatives.....	145
3.5.3 Salt additives	146
3.6 The role of the acylating agent.....	151
3.7 Tethering.....	155
3.7.1 Orthoesters	155
3.7.2 Peptidic tethers.....	156
3.8 Methods for selective deprotection of sugars	157
3.8.1 Selective removal of an acyl group.....	157
3.8.2 Selective cleavage of 4,6- <i>O</i> -benzylidenes	158
3.8.3 Selective removal of benzyls	160

Table of contents

3.8.4	Selective deprotection of silyl groups	161
3.9	Summary	162
3.10	Conclusion and outlook	162
3.11	References.....	172
Chapter 4	Regioselective glycosylation of position 2 of sugars using directing-protecting groups	183
4.1	Abstract.....	184
4.2	Introduction.....	184
4.2.1	Background.....	184
4.2.2	Challenges of regioselective glycosylations	188
4.2.3	Objectives and methods	188
4.3	Results and discussion	190
4.3.1	Preparation of the 6- <i>O</i> -protected glucopyranosides.....	190
4.3.2	Preparation of the glycosyl donor and reference compounds for glycosylation	195
4.3.3	Regioselectivity of the glycosylation reaction with a benzylated glycosyl donor	197
4.3.4	Optimization of the glycosylation methodology with a benzylated glycosyl donor	201
4.4	Postulated mechanism.....	204
4.5	Conclusion	206
4.6	Experimental section.....	207
4.6.1	General remarks	207
4.6.2	Synthesis	208
	Synthesis of the first series of 6- <i>O</i> -monoprotected carbohydrates ⁵	208
	Synthesis of the second series of 6- <i>O</i> -monoprotected carbohydrates ⁵	210
	Synthesis of the glycosyl donor	216
	Synthesis of reference compounds.....	217
	Glycosylations	226
4.7	References.....	237
Chapter 5	Regio- and stereoselective glycosylation of position 3 of sugars using directing-protecting groups.....	239
5.1	Abstract.....	240
5.2	Introduction.....	240
5.2.1	Background.....	240

5.2.2	Revisiting the challenges of regioselective glycosylation	242
5.2.3	Objectives and methods	242
5.3	Results and discussion	244
5.3.1	Preparation of the hydrogen bond donating protecting group and optimization of its coupling to a sugar	245
5.3.2	Regioselectivity of the glycosylation reaction with a benzoylated glycosyl donor	251
5.3.3	Effect of pre-incubating the acceptor with TMSOTf prior to reacting with a benzoylated glycosyl donor	259
5.4	Revised mechanism	261
5.5	Conclusion	263
5.6	Experimental section.....	264
5.6.1	General remarks	264
5.6.2	Synthesis	265
	Synthesis of hydrogen-bond donating protecting group and its coupling to a sugar and other 6-O-protected sugars not mentioned in Chapter 4	265
	Synthesis of the glycosyl donor	271
	Glycosylations	273
5.7	References.....	278
Chapter 6	Conclusions and contributions to knowledge	279
Appendix	281
	Supplementary information for Chapter 2	281
	Supplementary information for Chapter 5	282

List of figures

Figure 1.1 Alignment of the primary POP sequences from various species (bovine, pig, mouse, rat, human, chicken). The residues in direct contact with the bound inhibitor 1 (see below) are highlighted in red.	8
Figure 1.2 Selected POP inhibitors.	11
Figure 1.3 Selected POP inhibitors.	18
Figure 1.4 Crystal structure of inhibitor 1-1 bound to porcine POP (left). Phe173, Cys255, Tyr473, Phe476, catalytic Ser554, Ile591, Trp595 and Arg643 are shown. Structure and affinities for POP from various species for inhibitor 1 (right).	19
Figure 1.5 Interaction sites (Sx) of POP active site with portions (Px) of substrate or inhibitor.	21
Figure 1.6 P3 substitutions.	25
Figure 1.7 P2 substitutions.	28
Figure 1.8 P1 substitutions.	29
Figure 1.9 Reactive functional groups.	31
Figure 1.10 Examples of non-peptidic POP inhibitors.	32
Figure 1.11 Selective POP inhibitors.	34
Figure 1.12 General considerations to design inhibitors of either DPPIV, DPP8, DPP9, POP or FAP- α /seprase.	37
Figure 1.13 Achieving selectivity for POP over DPPIV, DPP8, DPP9 and FAP- α /seprase.	37
Figure 1.14 Optimal pharmacophore for achieving potency for POP (top), key interactions between inhibitors and POP (bottom).	38
Figure 2.1 Selected POP inhibitors.	59
Figure 2.2 Pseudo peptidic inhibitors inspired from 2-1 and 2-7.	61
Figure 2.3 Docked designed covalent inhibitor (2-8b, green) overlaid with crystal structure of Cbz-Pro-prolinal (2-2, yellow).	63
Figure 2.4 Selected NOE identifying the stereochemistry of the isolated compounds.	68
Figure 2.5 Comparison of ^1H NMR spectra, confirming stereochemistry of isolated diastereomers. The peaks refer to the two hydrogen atoms on carbon # 5 (see 2-8b in Figure 2.4).	69

Figure 2.6 Dose-response of POP activity by 2-11a, 2-11b, 2-12a, 2-12b and 8b in intact cells (PBS) and in cell extracts (PBS-Triton).	76
Figure 2.7 Effect of cyclization on inhibitory potency.	80
Figure 2.8 (a) Structure of Cbz-Pro-prolinal co-crystalized with POP. (b) Docked structures of 2-12a, 2-12b, 2-8a and 2-8b (yellow) superposed to the crystal structure of Cbz-Pro-prolinal (green).	82
Figure 2.9 Effect of cyclization on inhibitory potency.	83
Figure 3.1 Position numbering of methyl α -D-glucopyranoside (3-1), mannopyranoside (3-2) and galactopyranoside (3-3) as well as methyl β -D-glucopyranoside (3-4).	121
Figure 3.2 A few examples of silyl protection of 1,2-, 1,3- and 1,4-diols (3-20, 3-21 and 3-22) which Corey developed.	129
Figure 3.3 Davies proposed intramolecular hydrogen bond networks of methyl α -D-glucopyranoside (3-1) and the α -anomer of glucose (3-33).	132
Figure 3.4 Kurahashi Muzutani and Yoshida proposed the hydrogen bond network of octyl- α -D-glucopyranoside supports DMAP-catalyzed acylation of the 4-OH (3-34a) over the 3-OH (3-34b), the 2-OH (3-34c) and the 6-OH (3-34d).	133
Figure 3.5 Stannylene acetal of methyl α -D-glucopyranoside (3-52) compared to methyl β -D-glucopyranoside (3-53).	141
Figure 3.6 Acetate counterion can direct acylation to secondary hydroxyls.	152
Figure 3.7 Mechanism for acetate-facilitated acetyl migration.	154
Figure 3.8 Some examples of linkers which researchers use to tether the glycosyl donor to the acceptor.	155
Figure 3.9 Peptide tethering glycosyl acceptor and donor for glycosylation.	156
Figure 3.10 Two possible paths for cleavage of 4,6- <i>O</i> -benzylidene, either by Path a, leading to a 6- <i>O</i> benzyl ether or, by Path b, leading to a 4- <i>O</i> benzyl ether.	158
Figure 4.1 First series of 6- <i>O</i> and 4,6- <i>O</i> -protected methyl α -D-glucopyranosides. Protecting groups selected are those which carbohydrate chemists typically use.	191
Figure 4.2 Second series of 6- <i>O</i> -protected methyl α -D-glucopyranosides. Protecting groups chosen feature one or two pyridyl ring which has been shown to hydrogen-bond with the sugar.	191
Figure 4.3 More 6- <i>O</i> -protected hexopyranosides to verify the scope of our method	202
Figure 4.4 The influence of the di-pyridyl-based protecting group on the regioselectivity of reactions.	204

List of figures

Figure 5.1 Illustration of the neighbouring group participation of an acyl group at position 2 and its effects on the stereoselectivity of a subsequent reaction with a nucleophile. ..	243
Figure 5.2 Series of 6- <i>O</i> -protected glucopyranoside acceptors and 2,3,4,6-tetra-benzoylated glucopyranose donor 5-4 which were used to optimize the regio- and stereoselectivity of the glycosylation reaction.	245
Figure 5.3 Stacked NMR spectra of products of glycosylation of methyl 6- <i>O</i> -TBDPS α -D-glucopyranoside (5-7), showing the crude mixture (top spectrum, in dark blue) containing only the two disaccharides (middle and bottom spectra, shown in light blue and purple) and the starting material (spectrum not shown).	253
Figure 5.4 COSY of 5-31.	254
Figure 5.5 COSY of 5-32.	254
Figure 5.6 HSQC of 5-31.	255
Figure 5.7 HSQC of 5-32.	255
Figure 5.8 HMBC of 5-31. In red, the interaction of C2 with H1' is circled and in blue, the interaction of C1' with H2 is circled.	256
Figure 5.9 HMBC of 5-32. In red, the interaction of C1' with H3 is circled and in blue, the interaction of C3 with H1' is circled.	256
Figure 5.10 NMR titration of the 5-1 with increasing amounts of TMSOTf: 0 equivalents of TMSOTf (indigo), 0.5 equivalents of TMSOTf (teal), 1 equivalent of TMSOTf (purple), 1.5 equivalents of TMSOTf (plum).	259
Figure 5.11 Revised postulated mechanism.	262
Figure A.1 COSY of 5-36.	282
Figure A.2 HSQC of 5-36.	282
Figure A.3 HMBC of 5-36.	283
Figure A.4 COSY of 5-37.	283
Figure A.5 HSQC of 5-37.	284
Figure A.6 HMBC of 5-37.	284
Figure A.7 COSY of 5-38.	285
Figure A.8 HSQC of 5-38.	285
Figure A.9 HMBC of 5-38.	286

List of schemes

Scheme 2.1 Synthesis of the pseudopeptidic inhibitors.	64
Scheme 2.2 Synthesis of the bicyclic scaffolds.	65
Scheme 2.3 Synthesis of the bicyclic scaffolds (part 2).	66
Scheme 2.4 Functionalization of the scaffolds to covalent inhibitors.	67
Scheme 3.1 Benzoylation of methyl α -D-glucopyranoside.	121
Scheme 3.2 Benzoylation of methyl 6-deoxy- α -D-mannopyranoside.	122
Scheme 3.3 Mechanism of DMAP catalysis using acylating agents such as acetic anhydride or acetyl chloride.	124
Scheme 3.4 DMAP-catalyzed acetylation of octyl- β -D-glucopyranoside.	125
Scheme 3.5 DMAP-catalyzed acetylation of octyl- α -D-glucopyranoside.	125
Scheme 3.6 Regioselective acylation of position 2 over position 3 of 4,6-O-benzylidene methyl α -D-glucopyranoside.	126
Scheme 3.7 Morère <i>et al.</i> apply a combination of bases to selectively functionalize methyl α -D-glucopyranoside.	127
Scheme 3.8 Regioselective acylation using benzoic acid, DMAP and BOP-Cl.	128
Scheme 3.9 A one-step protection of two positions of a fructopyranoside.	129
Scheme 3.10 Controlled TBDPS migration.	130
Scheme 3.11 Glycosylation of allyl 2-acetamido-6-O-TBDPS-2-deoxy- β -D-glucopyranoside with a galactose trichloroacetimidate.	130
Scheme 3.12 Mannosylation of allyl 6-O-TBDPS- α -D-mannopyranoside.	131
Scheme 3.13 Some possible hydrogen bonds that could explain why the 2-OH of allyl 6-O-TBDPS β -D-mannopyranoside (shown in 3-35a-a'') reacts more than in the α -form (shown in 3-3-a-a').	134
Scheme 3.14 Acetylation catalyzed by DMAP analogues.	135
Scheme 3.15 Acylation catalyzed by tri-peptide containing DMAP.	136
Scheme 3.16 Acylation catalyzed by tetra-peptide containing DMAP.	137
Scheme 3.17 Selective acetylation of position 3 over position 4 of a glucosamine substrate 3-42, catalyzed by peptide 3-43.	138
Scheme 3.18 Optimized acylation catalyzed by a short peptide.	138

List of schemes

Scheme 3.19 Chiral diamine (3-47) catalyzed acylation of methyl-6- <i>O</i> -TBDPS- β -D-glucopyranoside (3-46).	139
Scheme 3.20 Stannyl ethers promote regioselective acylations.	140
Scheme 3.21 Selective benzylation via a stannylene acetal intermediate.	141
Scheme 3.22 Stannylene acetal 3-55 for regioselective acylation of a partially protected galactopyranoside 3-54.	142
Scheme 3.23 Stannylene acetal for regioselective acylation of a partially protected mannopyranoside.	142
Scheme 3.24 Selective oxidation at position 3 of a 3,4-stannylene acetal of a galactopyranoside.	143
Scheme 3.25 Selective benzylation of position 3 of a galactopyranoside and a glucopyranoside.	143
Scheme 3.26 Glycosylation of a galactopyranoside acceptor via a stannylene acetal intermediate.	144
Scheme 3.27 TBAF mediated glycosylation of a 3,4- <i>O</i> -stannylene acetal yields a 3- <i>O</i> -glycoside.	144
Scheme 3.28 A peracetylated bromide glycosyl donor reacts with an activated 3,4-boronate of a fucopyranoside.	146
Scheme 3.29 Avela compare sodium hydride the reactivity of 4,6- <i>O</i> -benzylidene-methyl- α -D-glucopyranoside to copper(II) chloride used following treatment with sodium hydride.	147
Scheme 3.30 Selective alkylation in the presence of copper(II) chloride.	148
Scheme 3.31 Acetylation using zinc(II) chloride.	148
Scheme 3.32 Selective benzylation in the presence of nickel(II) chloride.	149
Scheme 3.33 Selective benzylation in the presence of copper(II) chloride.	149
Scheme 3.34 Optimized conditions to acylate a sugar using copper(II) acetylacetonate.	149
Scheme 3.35 Selective functionalization of methyl α -L-rhamnopyranoside with molybdenum(V) chloride.	150
Scheme 3.36 Stepwise protection of methyl α -D-glucopyranoside (3-1) with catalytic dimethyl tin(IV) chloride.	150
Scheme 3.37 Detailed mechanism of DMAP-catalyzed acylations illustrating the role of the counterion (X^-) or base.	152

Scheme 3.38 Multi-benzoylation of methyl α -D-glucopyranoside.	153
Scheme 3.39 Selective glycosylations through ortho esters.	156
Scheme 3.40 Wang's method for selective removal of the anomeric acyl group of various peracylated glycopyranosides.	157
Scheme 3.41 Selective deacetylation with lithium hydroperoxide.	158
Scheme 3.42 Two methods to cleave 4,6- <i>O</i> -benzylidenes using borane, yielding either the 4- <i>O</i> or the 6- <i>O</i> benzyl ether.	159
Scheme 3.43 First experimental evidence on mechanism of benzylidene ring opening reaction using either a borane or a silane reducing agent.	160
Scheme 3.44 Selective de-benzylation.....	161
Scheme 3.45 Selective removal of TBDMS groups from a persilylated D-gluconolactone using BCl ₃	161
Scheme 4.1 Regioselective mannosylation at position 3 of 6- <i>O</i> -TBDPS-allyl- α -mannopyranoside (4-1).	185
Scheme 4.2 Manipulation of the hydrogen bond network renders position 3 more nucleophilic, but also hindered and position 2, less hindered, but also less nucleophilic.	186
Scheme 4.3 General glycosylation reaction between 13 different glycosyl acceptors and one glycosyl donor which would lead to the formation of 84 possible disaccharides. ...	189
Scheme 4.4 Revised method to screen different 6- <i>O</i> -protected glucopyranosides, first glycosylating to form potentially 84 products, then deprotecting position 6 of these to obtain only 6 possible products identical for all the reactions and which can easily be analyzed using HPLC.	190
Scheme 4.5 Synthesis of 4-15.	192
Scheme 4.6 Synthesis of 4-16.	192
Scheme 4.7 Synthesis of 4-4.	193
Scheme 4.8 Preparation of 4-17 via saponification of 4-26, followed by Mitsunobu coupling to 4-19.	194
Scheme 4.9 Alternate route to 4-17, coupling saponified 4-26 prior to reduction.....	194
Scheme 4.10 Formation of 2,3,4,6-tetra-benzylated glucopyranose trichloroacetimidate 4-31.	195
Scheme 4.11 Preparation of reference compounds 4-36a, 4-36b, 4-37a and 4-37b.	196
Scheme 4.12 Preparation of reference compounds 4-41a and 4-41b.....	197

List of schemes

Scheme 4.13 Postulated mechanisms.....	205
Scheme 5.1 Optimized reaction conditions from Chapter 4, for glycosylating a 6- <i>O</i> -monoprotected glucopyranoside with a tetra-benzylated glucopyranose donor.	241
Scheme 5.2 Synthesis of the protecting group 5-15 and its coupling to 5-16.....	246
Scheme 5.3 Preparation of 5-21 and its coupling to 5-16.....	248
Scheme 5.4 Coupling the indyl diphenyl methanol to a 2,3,4-tribenzylated methyl α -D-glucopyranoside.	250
Scheme 5.5 Formation of the 2,3,4,6-tetra-benzoylated glucopyranose trichloroacetimidate 5-4.	252

List of tables

Table 1.1 Selected potential neuropeptide substrates of POP. ^{32,50}	12
Table 2.1. Inhibition of POP activity and DPP-IV endoprotease activity in cell extracts.	71
Table 2.2 Inhibition of POP endoprotease activity in intact living cells	74
Table 2.3 IC ₅₀ values [nM] for the inhibition of POP endoproteolytic activity activity in intact living cells and in cell extracts.	77
Table 2.4 HPLC analysis of purity of final compounds	111
Table 3.1 Summary of the available methods to selectively functionalize position 2, 3 or 4 of hexopyranosides.	164
Table 4.1 Regioselectivity of the glycosylation of the secondary hydroxyl groups of 4-4, 4-8-4-18.	199
Table 4.2 Regioselectivity of glycosylation of the secondary hydroxyl groups of 4-4, 4-16, 4-42, 4-43 and 4-44. *	203
Table 5.1 Methods tested to chlorinate (or mesylate) the indol-2-yl diphenylmethanol prior to coupling to methyl α -D-glucopyranoside.	247
Table 5.2 Attempts to directly couple the indyl-diphenyl methanol to a sugar.	249
Table 5.3 Coupling of 5-21 to octyl β -D-glucopyranoside (5-26).	251
Table 5.4 Results of glycosylation experiments performed with 2,3,4,6-tetrabenzoylated glucopyranose trichloroacetimidate (5-4). * [§]	258
Table 5.5 Glycosylation experiment in which the acceptor was pre-incubated with TMSOTf (1 equiv.) prior to adding in the donor (1 equiv.) and more TMSOTf (2-4 equiv.). * [§]	260

List of abbreviations

THF: tetrahydrofuran	Ts: tosyl
EA: ethyl acetate	All: allyl
H: hexane	Bn: benzyl
Et ₂ O: diethyl ether	Bz: benzoyl
ACN: acetonitrile	Boc: tert-butoxycarbonyl
DMF: dimethylformamide	Ar: aryl
DMSO: dimethyl-sulfoxide	t-Bu: tert-butyl
Pyr: pyridine	TBDMS: tert-butyldimethylsilyl
Tol: toluene	TBDPS: tert-butyldiphenylsilyl
DME: ethylene glycol dimethyl ether	Cbz: benzyloxycarbonyl
	Tr: trityl
DBU: 1,8-diazabicyclo(5.4.0)undec-7-ene	Me: methyl
CSA: camphor-10-sulfonic acid	Oct: octyl
pTSA: p-toluenesulfonic acid	Et: ethyl
TBAF : tetrabutylammonium fluoride	Ms: methane sulfonyl
DMS: dimethylsulfide	Bz: benzoyl
DIPEA: diisopropylethylamine	Ac: acetyl
DMAP: 4-dimethylaminopyridine	Ph: phenyl
TFA: trifluoroacetic acid	Tf: trifluoromethanesulfonyl
TFAA: trifluoroacetic anhydride	TMS: trimethylsilyl
DCC: N,N'-dicyclohexylcarbodiimide	Piv: pivaloyl
EDC: N-(3-dimethylaminopropyl)-N'-ethyl carbodiimide	<i>i</i> -Pr: iso-propyl
HOBt: 1-hydroxybenzotriazole	FMOC: fluorenylmethoxycarbonyl
DIAD: diisopropyl azodicarboxylate	
AMC: 7-amino-4-methylcoumarin	

POP: prolyl oligopeptidase	Mol. Wt.: molecular weight
DPP: dipeptidyl peptidase	quant.: quantitative
FAP: fibroblast activating protein	mol: moles
PPCE: post-proline cleaving enzyme	DFT: density functional theory
BBB: blood-brain barrier	pdb: protein data bank
CNS: central nervous system	rt: room temperature
	°C: degrees Celsius
	equiv.: equivalents
NMR: Nuclear Magnetic Resonance	TLC: thin-layer chromatography
s: singlet	Rf: the retention factor, is defined as
bs: broad singlet	the distance traveled by the
t: triplet	compound divided by the distance
q: quartet	traveled by the solvent
m: multiplet	
COSY: correlation spectroscopy	
HSQC: Heteronuclear Single Quantum	
Coherence	
HMBC: Heteronuclear Multiple-bond	
Coherence	
NOESY: Nuclear Overhauser Effect	
Spectroscopy	
HR: high resolution	
ESI: electrospray ionization	
EI: electron impact	
MS: mass spectrometry	
m/z: mass-to-charge ratio	

[This page was intentionally left blank]

Thesis outline

As medicinal chemists, we often take clues from Nature when designing drugs. For example, in structure-based drug design, medicinal chemists design scaffold-based drugs to control (either activating or blocking) a specific, biologically-relevant target, knowing the three-dimensional structure of their target. In ligand-based drug design, new scaffolds are contrived from known inhibitors or substrates of the target. Applying this strategy, medicinal chemists targeting the enzyme prolyl oligopeptidase (POP) have been designing novel inhibitors. In Chapter 1, we will review the potential role of the enzyme POP in a variety of neurological disorders, as well as the inhibitors that medicinal chemists have designed and assayed thus far to validate POP as a therapeutic target. From our review, we proposed a pharmacophore which medicinal chemists could use to design novel, more selective and potent POP inhibitors. We also noted that there are several enzymes which have very similar substrate specificity and act similarly to POP, an issue that is largely ignored when researchers design POP inhibitors. In Chapter 2, we designed and synthesized a series of pseudopeptidic and constrained, bicyclic potential inhibitors, having specific three-dimensional shapes and sizes. These compounds were conceived in order to better understand the geometric constraints of a selective and potent drug to target POP in organisms expressing multiple enzymes with very similar functions.

In addition to amino acids, Nature also possesses a library of carbohydrates to build up complex structures with very specific and diverse shapes and sizes. Inspired by Nature, a few medicinal chemists aim to utilize and incorporate simple carbohydrate building blocks as scaffolds. In fact, these seemingly simple scaffolds allow researchers to access a wide variety of shapes and sizes, offering more diversity than any other commonly used starting material, such as amino acids. Yet, considering the potential of carbohydrate-based drugs, few embark on incorporating them into their scaffold design as these seemingly simple building blocks are, synthetically, quite complex to use because they offer a number of similar functional groups. More research needs to be done before medicinal

chemists can truly exploit the possibilities that carbohydrate-based drug design could offer. Chemists need easy, efficient, non-toxic methods to incorporate carbohydrates into their synthetic routes. Thus, in the second part of this thesis, starting with Chapter 3, we will review the available methods to selectively functionalize and glycosylate sugars, finding that researchers have developed a few methods, either taking advantage of the innate reactivity of the hydroxyls of carbohydrates to functionalize carbohydrates, incorporating diverse additives and catalysts into their methods, or pre-functionalizing the substrate prior to performing the reactions of interest. From this study, we found that most methods were inefficient, only applicable to a specific substrate or using reagents that could never be used in a medicinal chemistry setting (based on toxicity and cost). Following this review, in Chapter 4 and Chapter 5, we will offer details on our method to selectively functionalize carbohydrates, in which we selectively protect the most easily accessed position of a carbohydrate (the primary hydroxyl) with a group that can actually modify and manipulate the accessibility and reactivity of the other hydroxyls of the substrate. In these chapters, we will demonstrate that this protecting group can actually be applied to the most complex of reactions in carbohydrate chemistry: the glycosylation reaction. We applied our simpler, protecting group strategy to regio- and stereo-selectively glycosylate a carbohydrate to produce a single disaccharide in yields greater than 80%, which is higher than any reported methods for this reaction.

In the final chapter, Chapter 6, we briefly summarize the results and contributions to knowledge of this thesis.

Chapter 1 Inhibitors of prolyl oligopeptidases for the therapy of human diseases: Defining diseases and inhibitors

This chapter, aside from a few corrections, is reproduced with permission from Lawandi, J.; Gerber-Lemaire, S.; Juillerat-Jeanneret, L.; Moitessier, N. “Inhibitors of prolyl-oligopeptidases for the therapy of human diseases: Defining diseases and inhibitors.” *Journal of Medicinal Chemistry* **2010**, *in press*. Copyright 2010 American Chemical Society.

1.1 Abstract

Within the last 10 years, brain-cell-expressed prolyl oligopeptidases (POPs) have been linked to a number of neurological disorders while microorganism-derived POPs have been associated with the infectious potential of pathogens. The selective inhibition of POPs over other peptide-cleaving enzymes became a promising strategy for the treatment of a variety of human disorders, including Chagas disease. POPs cleave proline-containing peptides and neuropeptides on the carboxy-side of internal proline residues. However, their wide distribution in most organs and cells, as well as the number of other prolyl peptidases, represent a formidable challenge for achieving selective inhibition. Herein, we will review the biological roles of POPs and discuss the various strategies for designing and synthesizing inhibitors and the results of these strategies, while also considering how selectivity is achieved. The research highlighted herein will facilitate, if not guide future designs of therapeutics towards POPs.

1.2 Introduction

The activity and lifetime of proteins or peptides in living organisms are highly dependent on their processing by proteolytic enzymes also known as proteases. Proteases perform different tasks including post-translational modifications of proteins (e.g., cleavage of inactive zymogens to the corresponding active enzymes), regulation of peptide functions and digestion of proteins into smaller peptides. Some proteases, the exopeptidases, can only cleave a few amino acids off the *C*-terminal or *N*-terminal ends of proteins, while others, the endopeptidases, can hydrolyze internal peptide bonds. Most proteases are highly specific and can only process a limited number of substrates with defined amino acid sequences. Similarly, some substrates are only processed by a very small number of proteases. For instance, many biologically active peptides are protected from general proteolytic degradation by evolutionarily conserved prolines.^{1,2} Proline residues impose conformational constraints and kinks in the secondary structure and folding of peptides or proteins,³ which in turn require very specific

enzymes to process them. In fact, only a few proteolytic enzymes, referred to as proline-specific proteases, can accommodate the particular shape of proline-containing peptides in their active site and cleave off the amino acid chain adjacent to proline residues. Among these enzymes, prolyl oligopeptidase (POP, EC 3.4.21.26) is a post-proline-endopeptidase, cleaving peptides on the carboxy-side of proline residues located in the core of peptide chains.

Over the last two decades, researchers have linked abnormal mammalian POP activity to neurological disorders. To better understand and treat these different diseases and to minimize toxicity and side effects, inhibitors of POP must be potent and also selective for the target enzyme. Given the many seemingly similar enzymes grouped under proline-specific proteases, we aim to first highlight the similarities and differences between a few of the enzymes of this family. In a subsequent part of this perspective article, we will focus on one proline-specific peptidase, POP, and discuss the structure-activity relationship of inhibitors developed as potential therapeutic drugs treating neurological disorders. Furthermore, we will discuss two possible pharmacophores, one encompassing features to achieve selectivity for POP over other proline-specific proteases, and another one ranking features to improve inhibitor potency. We believe that the data collected within this review will guide the future development of novel, selective POP inhibitors as more effective candidate drugs (CDs).

This perspective article focuses on a selection of reports that illustrate our discussion on POP inhibitors and their inhibitory potency and selectivity. In no way do we claim to detail an exhaustive review of all the literature in this domain. However, most of the key articles and inhibitors are covered and are representative of the literature and patents as of today. Männistö and co-workers recently reviewed several POP inhibitors evaluated in preclinical animal models, which will only be mentioned when appropriate.⁴

1.3 Proline-specific exo- and endopeptidases

1.3.1 Proline-specific peptidases

Researchers have found proline-specific proteases and peptidases in bacteria, protozoa, plants and animals, including mammals. Despite close similarities between proline-specific peptidases in these different organisms (most of them belong to the serine-protease class of enzymes), these enzymes do not seem to share similar functions. For example, mammalian proline-specific peptidases can easily process small peptides (such as small peptide hormones), but can only cleave larger proteins once proteases have processed them into smaller fragments, whereas proline-specific proteases from microorganisms can digest larger substrates.⁵⁻⁷ The expression of proline-specific proteases and peptidases in almost all living organisms suggests that they play major roles in regulating biological functions via the processing of critical biologically active peptides.

1.3.2 Proline-specific exopeptidases: the family of Pro-aminodipeptidases, CD26/DPPIV and FAP- α /seprase

Dipeptidyl peptidase IV (DPPIV/CD26, EC 3.4.14.5) is a dimeric type II integral membrane glycoprotein (Mol. Wt. 220 kDa), mainly expressed by epithelia. DPPIV is a strict exopeptidase which releases X-Pro (or X-Ala) dipeptide from the free *N*-terminus of peptides. DPPIV is itself a target of great therapeutic interest and inhibitors of DPPIV are clinically used for the treatment of type 2 diabetes.⁸ Clearly, selectivity for POP over DPPIV is critical for the development of POP inhibitors as drugs.

Fibroblast activation protein- α (FAP- α /seprase)⁹ is a dimeric type II integral membrane prolyl dipeptidase with a molecular weight and an enzymatic activity comparable to DPPIV, but also displaying endoproteolytic gelatinase and collagenase activities^{8,10-16} comparable to POP. However, FAP- α /seprase may respond differently to some inhibitors developed against POP.¹⁷ FAP- α /seprase is a cell surface antigen of reactive fibroblasts in cancer, such as melanoma or

sarcoma,¹ found at remodeling stroma, in tumors and healing wounds,¹⁸ and in serum.¹⁷ In fact, Santos and co-workers recently found that they could reduce tumor sizes in mice by inhibiting FAP- α /seprase, demonstrating that FAP is a potential therapeutic target.¹⁹ The DPPIV family of proline-specific exopeptidases will not be reviewed in detail here since many recent reviews have been published.^{20,21}

Prolyl oligopeptidases have received different names such as post-proline cleaving enzyme (PPCE)^{22,23} and proline endopeptidase (PEP)^{24,25} before they were named prolyl oligopeptidases. The POP enzyme family evolved before the archae, prokaryota and eukaryota and was highly conserved during evolution (Figure 1.1). In mammals, prolyl oligopeptidase (POP) (EC 3.4.21.26) is a post-proline-endopeptidase of 80 kDa, which belongs to the S9a subfamily.^{1,2,12,26-28} Mammalian POP is widely expressed, and most highly in the brain.²⁶ Proline-specific endoproteases are also widely distributed in plants, bacteria and fungi. POP may be secreted and is involved in the invasive properties of parasites.²⁹

Proline-specific serine proteases, including POP, exhibit similarities in their catalytic behaviour: preference for proline in the substrate's P1-position, similar rate constants, and a mechanism of substrate-assisted catalysis, which means that the interaction between enzyme and substrate promotes conformational changes in the substrate, a productive binding resulting in hydrolysis of the prolyl-bond.³⁰ Given these similarities, selective POP inhibition over other proline-specific exo- and endopeptidases remains a challenge.

Chapter 1

A5D7C6	MSLSFYQPDVYRDETAQVQDYHGHHKICDPYAWLEDPDSEQTKAFVEAQNKITVPFLEQCPIR	60	A5D7C6_BOVIN
P23687	MSLSFYQPDVYRDETAQVQDYHGHHKICDPYAWLEDPDSEQTKAFVEAQNKITVPFLEQCPIR	60	PPCE_PIG
Q9QUR6	MSLSFYQPDVYRDETSVQDYHGHHKICDPYAWLEDPDSEQTKAFVEAQNKITVPFLEQCPIR	60	PPCE_MOUSE
O70196	MSLSFYQPDVYRDETSVQDYHGHHKICDPYAWLEDPDSEQTKAFVEAQNKITVPFLEQCPIR	60	PPCE_RAT
P48147	MSLSFYQPDVYRDETAQVQDYHGHHKICDPYAWLEDPDSEQTKAFVEAQNKITVPFLEQCPIR	60	PPCE_HUMAN
Q5ZMI7	MQAFQYQPEVYRDEAAVLDYHGHHKISDPYAWLEDPDSEQTKAFVEAQNKITVPFLEQCPIR	60	Q5ZMI7_CHICK

A5D7C6	GLYKERMTLEYDYPKYSCHFKKGRYFYFYNTGLQNRVLYVQDSLEGEARVFLDPNTLS	120	A5D7C6_BOVIN
P23687	GLYKERMTLEYDYPKYSCHFKKGRYFYFYNTGLQNRVLYVQDSLEGEARVFLDPNTLS	120	PPCE_PIG
Q9QUR6	GLYKERMTLEYDYPKYSCHFKKGRYFYFYNTGLQNRVLYVQDSLEGEARVFLDPNTLS	120	PPCE_MOUSE
O70196	GLYKERMTLEYDYPKYSCHFKKGRYFYFYNTGLQNRVLYVQDSLEGEARVFLDPNTLS	120	PPCE_RAT
P48147	GLYKERMTLEYDYPKYSCHFKKGRYFYFYNTGLQNRVLYVQDSLEGEARVFLDPNTLS	120	PPCE_HUMAN
Q5ZMI7	GLFKERMTLEYDYPKYSCHFKKGRYFYFYNTGLQNRVLYVQDSLADAKVFLDPNKL	120	Q5ZMI7_CHICK

A5D7C6	DDGTVALRGYAFSEDEGEYFAYGLSASGSDWVTIKFMKVDGAKELPDVLERVK	180	A5D7C6_BOVIN
P23687	DDGTVALRGYAFSEDEGEYFAYGLSASGSDWVTIKFMKVDGAKELPDVLERVK	180	PPCE_PIG
Q9QUR6	DDGTVALRGYAFSEDEGEYFAYGLSASGSDWVTIKFMKVDGAKELPDVLERVK	180	PPCE_MOUSE
O70196	DDGTVALRGYAFSEDEGEYFAYGLSASGSDWVTIKFMKVDGAKELPDVLERVK	180	PPCE_RAT
P48147	DDGTVALRGYAFSEDEGEYFAYGLSASGSDWVTIKFMKVDGAKELPDVLERVK	180	PPCE_HUMAN
Q5ZMI7	DDGTVALRGYAFSEDEGEYFAYGLSSGSDWVTIKFMKVGAEELPDVLERVK	180	Q5ZMI7_CHICK

A5D7C6	DGKGMFYNAYPQODGKSDGTETSTNLHQKLCYHVLGTDQSEDIACAEFPDEPKWGGAEI	240	A5D7C6_BOVIN
P23687	DGKGMFYNAYPQODGKSDGTETSTNLHQKLCYHVLGTDQSEDIACAEFPDEPKWGGAEI	240	PPCE_PIG
Q9QUR6	DGKGMFYNSYPQODGKSDGTETSTNLHQKLCYHVLGTDQSEDIACAEFPDEPKWGGAEI	240	PPCE_MOUSE
O70196	DGKGMFYNSYPQODGKSDGTETSTNLHQKLCYHVLGTDQSEDIACAEFPDEPKWGGAEI	240	PPCE_RAT
P48147	DGKGMFYNSYPQODGKSDGTETSTNLHQKLCYHVLGTDQSEDIACAEFPDEPKWGGAEI	240	PPCE_HUMAN
Q5ZMI7	DGKGMFYNCYPKODGKSDGTETSTNLHQKLCYHVLGTDQSEDIACAEFPDEPKWGGAEI	240	Q5ZMI7_CHICK

A5D7C6	SDDGRYVLLSIREGDDPVNRLWYCDLQESNGITGILKWKVLIDNFEGEYDYVTNEGTVF	300	A5D7C6_BOVIN
P23687	SDDGRYVLLSIREGDDPVNRLWYCDLQESNGITGILKWKVLIDNFEGEYDYVTNEGTVF	300	PPCE_PIG
Q9QUR6	SDDGRYVLLSIREGDDPVNRLWYCDLQESNGITGILKWKVLIDNFEGEYDYVTNEGTVF	300	PPCE_MOUSE
O70196	SDDGRYVLLSIREGDDPVNRLWYCDLQESNGITGILKWKVLIDNFEGEYDYVTNEGTVF	300	PPCE_RAT
P48147	SDDGRYVLLSIREGDDPVNRLWYCDLQESNGITGILKWKVLIDNFEGEYDYVTNEGTVF	300	PPCE_HUMAN
Q5ZMI7	SDDGRYVLLSIREGDDPVNRLWYCDLQESNGITGILKWKVLIDNFEAEYDYVTNEGTVF	300	Q5ZMI7_CHICK

A5D7C6	TFKTNRHSPNYRLINIDFTDPEESKWKVLVPEHEKDVLWVACVRSNLFVLCYLHDVKNT	360	A5D7C6_BOVIN
P23687	TFKTNRHSPNYRLINIDFTDPEESKWKVLVPEHEKDVLWVACVRSNLFVLCYLHDVKNT	360	PPCE_PIG
Q9QUR6	TFKTNRHSPNYRLINIDFTDPEESKWKVLVPEHEKDVLWVACVRSNLFVLCYLHDVKNT	360	PPCE_MOUSE
O70196	TFKTNRHSPNYRLINIDFTDPEESKWKVLVPEHEKDVLWVACVRSNLFVLCYLHDVKNT	360	PPCE_RAT
P48147	TFKTNRHSPNYRLINIDFTDPEESKWKVLVPEHEKDVLWVACVRSNLFVLCYLHDVKNT	360	PPCE_HUMAN
Q5ZMI7	TFKTNRHSPNYRLINIDFTDPEESKWKVLVPEHEKDVLWVACVRSNLFVLCYLHDVKNT	360	Q5ZMI7_CHICK

A5D7C6	LQLHDLATGALLKTFPLEVGSVVGYSQKKDTEIFYQFTSFLSPGIIYHCDLTKEELEPR	420	A5D7C6_BOVIN
P23687	LQLHDLATGALLKTFPLEVGSVVGYSQKKDTEIFYQFTSFLSPGIIYHCDLTKEELEPR	420	PPCE_PIG
Q9QUR6	LQLHDLTTGALLKTFPLDVGSIIVGYSQKKDSEIFYQFTSFLSPGIIYHCDLTKEELEPR	420	PPCE_MOUSE
O70196	LQLHDLTTGALLKTFPLDVGSIIVGYSQKKDSEIFYQFTSFLSPGIIYHCDLTKEELEPR	420	PPCE_RAT
P48147	LQLHDLTTGALLKTFPLDVGSIIVGYSQKKDTEIFYQFTSFLSPGIIYHCDLTKEELEPR	420	PPCE_HUMAN
Q5ZMI7	LQLHDLATGAHLKTFPLDVGSIIVGYSQKKDTEIFYQFTSFLSPGIIYHCDLTKEELEPR	420	Q5ZMI7_CHICK

A5D7C6	VFREVTVKGIDASDYQTVQIFYPSKDGTKIPMFIVHKKGIKLDGSHPAFLYG	480	A5D7C6_BOVIN
P23687	VFREVTVKGIDASDYQTVQIFYPSKDGTKIPMFIVHKKGIKLDGSHPAFLYG	480	PPCE_PIG
Q9QUR6	VFREVTVKGIDASDYQTVQIFYPSKDGTKIPMFIVHKKGIKLDGSHPAFLYG	480	PPCE_MOUSE
O70196	VFREVTVKGIDASDYQTVQIFYPSKDGTKIPMFIVHKKGIKLDGSHPAFLYG	480	PPCE_RAT
P48147	VFREVTVKGIDASDYQTVQIFYPSKDGTKIPMFIVHKKGIKLDGSHPAFLYG	480	PPCE_HUMAN
Q5ZMI7	VFREVTVKGIDPSYQTVQIFYPSKDGTKIPMFIVHKKGIKLDGSHPAFLYG	480	Q5ZMI7_CHICK

A5D7C6	TPNYSVSRLIFVRHMGGLAVANIRGGGEYGETWHKGGILANKQNCFFDDFQCAAEYLIKE	540	A5D7C6_BOVIN
P23687	TPNYSVSRLIFVRHMGGLAVANIRGGGEYGETWHKGGILANKQNCFFDDFQCAAEYLIKE	540	PPCE_PIG
Q9QUR6	TPNYSVSRLIFVRHMGGLAVANIRGGGEYGETWHKGGILANKQNCFFDDFQCAAEYLIKE	540	PPCE_MOUSE
O70196	TPNYSVSRLIFVRHMGGLAVANIRGGGEYGETWHKGGILANKQNCFFDDFQCAAEYLIKE	540	PPCE_RAT
P48147	TPNYSVSRLIFVRHMGGLAVANIRGGGEYGETWHKGGILANKQNCFFDDFQCAAEYLIKE	540	PPCE_HUMAN
Q5ZMI7	TPSYVSRLIFVRHMGGLAVANIRGGGEYGETWHKGGILANKQNCFFDDFQYAAKYLIKE	540	Q5ZMI7_CHICK

A5D7C6	GYTSPKRLTINGGNGGLLVATCANQRPDLFGCVIAQVGVMDMLKFKHYT	600	A5D7C6_BOVIN
P23687	GYTSPKRLTINGGNGGLLVATCANQRPDLFGCVIAQVGVMDMLKFKHYT	600	PPCE_PIG
Q9QUR6	GYTSPKRLTINGGNGGLLVAAACANQRPDLFGCVIAQVGVMDMLKFKHYT	600	PPCE_MOUSE
O70196	GYTSPKRLTINGGNGGLLVAAACANQRPDLFGCVIAQVGVMDMLKFKHYT	600	PPCE_RAT
P48147	GYTSPKRLTINGGNGGLLVAAACANQRPDLFGCVIAQVGVMDMLKFKHYT	600	PPCE_HUMAN
Q5ZMI7	GYTAPKRLTINGGNGGLLVAAACANQRPDLFGCVIAQVGVMDMLKFKHYT	600	Q5ZMI7_CHICK

A5D7C6	CSDNKQHFEWLKYSPHLNVKLPEADDIQYPSMLLLTADHDDRVPVPLSLKFIATLQYIV	660	A5D7C6_BOVIN
P23687	CSDNKQHFEWLKYSPHLNVKLPEADDIQYPSMLLLTADHDDRVPVPLSLKFIATLQYIV	660	PPCE_PIG
Q9QUR6	CSDTKQHFEWLKYSPHLNVKLPEADDIQYPSMLLLTADHDDRVPVPLSLKFIATLQYIV	660	PPCE_MOUSE
O70196	CSDNKQHFEWLKYSPHLNVKLPEADDIQYPSMLLLTADHDDRVPVPLSLKFIATLQYIV	660	PPCE_RAT
P48147	CSDNKQHFEWLKYSPHLNVKLPEADDIQYPSMLLLTADHDDRVPVPLSLKFIATLQYIV	660	PPCE_HUMAN
Q5ZMI7	CSDHKEQFEWLKYSPHLNVKLPEADDIQYPSMLLLTADHDDRVPVPLSLKFIATLQYIV	660	Q5ZMI7_CHICK

A5D7C6	GRSRKQNNPLLHVDTKAGHGAGKPTAKVIEEVSMDMAFIARCLNIDWIP	710	A5D7C6_BOVIN
P23687	GRSRKQNNPLLHVDTKAGHGAGKPTAKVIEEVSMDMAFIARCLNIDWIP	710	PPCE_PIG
Q9QUR6	GRSRKQSNPLLHVDTKAGHGAGKPTAKVIEEVSMDMAFIARCLNIEWIP	710	PPCE_MOUSE
O70196	GRSRKQSNPLLHVDTKAGHGAGKPTAKVIEEVSMDMAFIARCLNIEWIP	710	PPCE_RAT
P48147	GRSRKQSNPLLHVDTKAGHGAGKPTAKVIEEVSMDMAFIARCLNVDWIP	710	PPCE_HUMAN
Q5ZMI7	GRSRKQTNPLLHVDTKAGHGAGKPTAKVIEEVSMDMAFIARCLNLDWIE	710	Q5ZMI7_CHICK

Figure 1.1 Alignment of the primary POP sequences from various species (bovine, pig, mouse, rat, human, chicken). The residues in direct contact with the bound inhibitor 1 (see below) are highlighted in red.

1.4 POP and other proline-specific peptidases as potential therapeutic targets

1.4.1 POP as a therapeutic target

Researchers have shown that POP participates in several aspects and functions of the central nervous system (CNS), including learning, memory, mood, hypertension, eating, and in some neurodegenerative diseases such as Alzheimer's and Parkinson's diseases. Subsequently, POP has been identified as a potential target in cognitive function, memory and neurodegenerative disorders such as amnesia, Alzheimer's disease and depression (detailed reviews in references 31-33). As a result, researchers have designed inhibitors targeting POP for its role in neurological diseases. Although correlations and straightforward conclusions were not always obvious, preclinical studies suggested an interest mainly for memory and learning disorders compared to other disorders. We have found little information on the potential of such molecules in infectious, oncological or inflammatory disorders, and their possible therapeutic role in these diseases will not be discussed here.

1.4.2 POP and protein aggregation

In vitro, POP inhibitors suppressed the production of β -amyloid in cells.³⁴ However, POP activity may be responsible for generating β -amyloid, but this activity is inhibitor- or cell-dependent,³⁵ suggesting either that several proteases with comparable specificity are acting or that the enzymes are located in different cell compartments. *In vivo*, POP inhibitors have been mainly evaluated in animal models of Alzheimer's disease (models such as the brain of aged mouse or aged rat and transgenic mice expressing human amyloid precursor protein, APP), generally improving the deteriorated cognitive and memory functions, as well as decreasing the amyloid deposition.³⁶⁻⁴¹ Although seemingly linked with Alzheimer's disease, POP was not found to be associated with activated glial cells in amyloid plaques in the brains of people with the disease.³⁷ In addition,

conflicting results have been reported in the literature. For example, Kohsaka and Nakajima showed that the POP inhibitors **1-2** (JTP-4819³⁴) or **1-3** (Y-29794³⁸) (Figure 1.3) abolished the formation of β -amyloid.^{34,38} Others demonstrated that POP inhibitors had no effect on β -amyloid levels in certain cell types, indicating that other proteases are involved or that the enzymes producing the β -amyloid peptides, as well as the β -amyloid precursor, were located in different cell compartments than the β -amyloid peptides.³⁵ Researchers noted, through immunostaining, that POP and amyloid β -peptide were co-localized in the brain of age-accelerated mice,⁴² although POP activity seems to be associated with neuronal damage rather than with β -amyloid accumulation.⁴³ In this latter report, only POP-like activity was determined, without precise characterization of the exact enzyme.

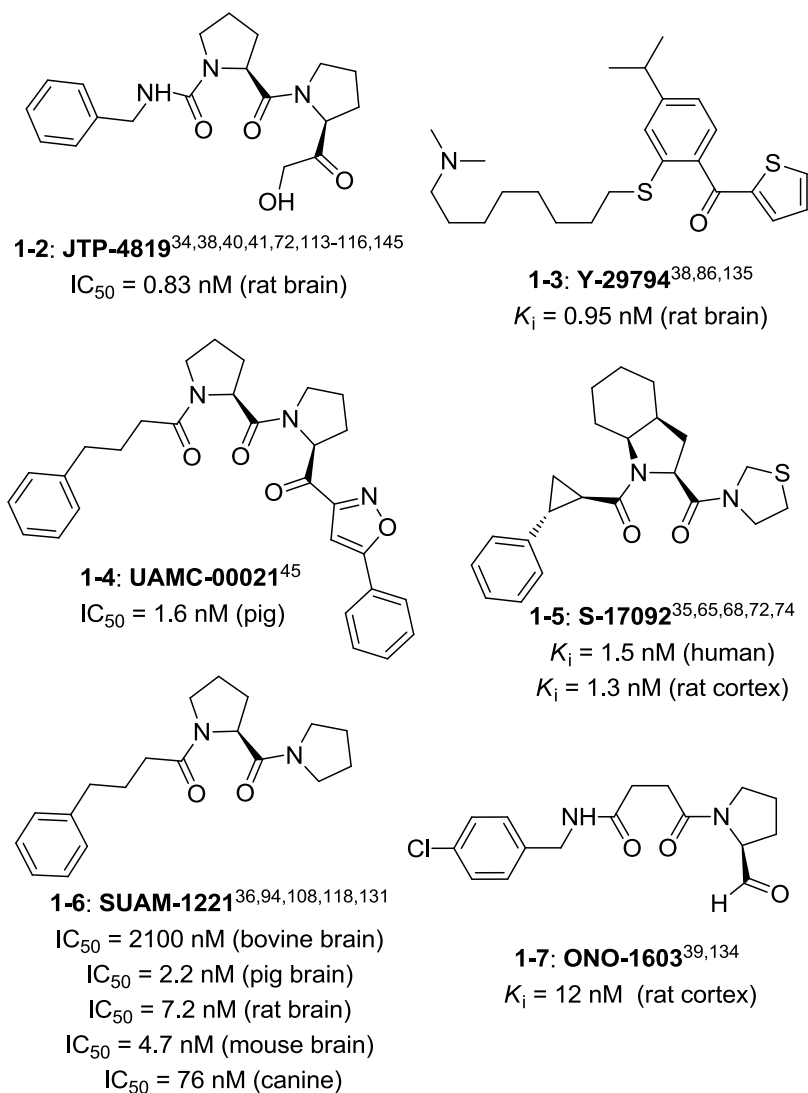


Figure 1.2 Selected POP inhibitors.

Fragments of several other intracellular proteins of the CNS, that are also known to aggregate, are potential substrates for POP,⁴⁴ suggesting that POP inhibitors may have an effect on neurodegenerative disorders, slowing the aggregation of a number of proteins. *In vitro* recombinant POP accelerated the aggregation of α -synuclein,⁴⁵ a protein found in the Lewy body in the brains of people suffering from Parkinson's disease. The presence of POP caused α -synuclein to aggregate, without truncating α -synuclein. Interestingly, when POP inhibitors were added (for example, **1-1** and **1-4** (UAMC 00021⁴⁵)), α -synuclein aggregation was reversed. Whereas α -synuclein is not a substrate for POP, POP

can hydrolyze fragments of α -synuclein at the Pro138-Asp139 bonds,⁴⁴ suggesting cooperation between several proteases.

1.4.3 Role of POP in the central nervous system (CNS)

Männistö demonstrated that POP and/or POP-like activity is distributed throughout the CNS of humans and rats,^{46,47} possibly indicating a role for POP in motor functions, and also at the cellular level in protein processing and secretion.^{37,48} Männistö co-localized POP with components of the inositol-phosphate pathways^{46,47} and with several neuropeptides.^{47,49}

Table 1.1 Selected potential neuropeptide substrates of POP.^{32,50}

Bioactive substrates of POP	Peptide sequence	References
Angiotensin I	DRVYIHPFHL	52,54,55
Bradykinin	pGLUGGWPRPGPEIPP	56
potentiating peptide		
Bradykinin	RPPGFSPFR	52,57
Luliberin (LHRH)	pEHWSYGLRPGNH ₂	54,58
Melantropin	SYSMEHFRWGKPVNH ₂	59
Neurotensin	pELYENKPRRPYIL	52,60
Oxytocin	CYIQNCPLGNH ₂	52,61
Substance P	RPKPQQFFGLM	52,55
Thyroliberin	pEHPNH ₂	54,62,63
Tuftsins	TKPR	59
Vasopressin	CYFQNCPRG	55

LHRH: leuteinizing hormone releasing hormone.

From these studies, the interaction of POP with the components of the inositol-phosphate pathways has been postulated in neurological diseases. However, researchers have yet to confirm the exact mode-of-action and the peptide mediator(s) involved, postulating only that several neuropeptides may be involved.^{32,50} In fact, the actual neuropeptide substrates of POP remain uncertain, although the enzyme has the ability to hydrolyze several peptide hormones and neuropeptides *in vitro* (Table 1.1).^{1,8,12,27,51-53}

Neurons in the brain express POP, but the level of expression is different in various areas of the brain, and is age-dependent.³⁷ POP is a synaptosomal membrane peptidase²⁷ localized intracellularly,⁴⁸ mainly in the perinuclear space, associated with the cytoskeletal tubulin in human neuroblastoma and glioma cells. POP inhibition does not change the intracellular localization of POP, nor its association with tubulin. Thus, association of POP with tubulin is independent of its peptidase activity. In glioma cells, antisense techniques or POP inhibition resulted in increased inositol 1,4,5-triphosphate concentrations with decreased POP activity, further supporting that POP is involved in this pathway. Substance P (one of the substrates of POP *in vitro*) may mediate this process, binding to its neurokinin-1 receptor and may modulate cellular pathways important in learning and memory function.⁶⁴ Thus, the cellular localization of POP suggests functions, such as intracellular trafficking, sorting and secretion.

1.4.4 POP inhibition in animal models

POP inhibitors showed beneficial effects, reducing cognitive deficits in monkeys having Parkinson's disease symptoms induced by the drug 1-methyl-4-phenyl-1,2,3,6-tetrahydropyridine (MTPT), killing neurons in specific regions of the brain.⁶⁵ Morain hypothesized that the inhibitors reduced neuropeptide degradation.^{40,41,66-68}

In animal models from preclinical studies, POP inhibitors could reverse age-related or neurodegeneration-related memory loss. Alterations in the inositol pathway explain, at least in part, the effects of POP inhibitors for bipolar

disorders in experimental models. Synthetic POP inhibitors increase concentrations of some neuropeptides, which are potential substrates of POP, supporting the role of POP in some neurological disorders. POP-like activity decreased in brain extracts of animals treated with these inhibitors. We note that the preclinical and clinical evaluations of POP inhibitors suffer from several problems. The role of POP in the brain may go beyond neuropeptide processing, including regulating intracellular pathways, neuroprotection, perhaps even acting as an anti-apoptosis agent. In addition, most published information evaluated “POP-like” activity, without detailed characterization of the actual protease displaying the activity in order to confirm enzyme identity. Neuropeptides may have multiple hydrolysis sites and associated peptidases, in addition to a site for POP.

1.4.5 Passage through the blood brain barrier (BBB)

Researchers have reported many synthetic POP inhibitors, of which most are substrate-like short amino acid pseudopeptides which have little potential of crossing the BBB, a very unfavourable pharmacokinetics characteristic. In most preclinical studies, researchers evaluated the inhibition of POP-like activity in animal brain extracts after the animals were treated with POP inhibitors. However, in their published papers, researchers did not definitely prove the mechanism of a transport of POP inhibitors across the BBB. None measured the levels of the inhibitors in brain extracts, and more importantly, the distribution of the inhibitors between the brain compartments, in particular the brain vasculature forming the BBB, and the brain parenchyma. Some authors have used artificial membranes to evaluate permeability to membrane models, but this is still not representative of the BBB.^{69,70}

The lone fact that these molecules have an effect on CNS pathologies does not prove that they were physically transported into the brain parenchyma: inhibitors may indirectly act in the blood, they may be trapped in the CNS vasculature where they exert their action, or they may in fact reach the brain parenchyma.

Techniques to study these possibilities are established but not easy to perform: using (mostly radioactive, but not always) inhibitors, animals are bled before their organs are removed, and the organs and the blood can be separately evaluated to determine whether the inhibitors are present (or absent) in each; to differentiate whether inhibitors are trapped either in the brain vasculature or the brain parenchyma, brain vessels are separated from brain parenchyma, and again, researchers can properly determine whether the inhibitors and enzyme are present (or absent) in the two compartments. To the best of our knowledge and according to the published papers, researchers have not systematically separated the organs from the blood, nor brain vessels from brain parenchyma, nor have they thoroughly characterized and analyzed the contents of each, therefore none have definitely proved inhibitor transport across the BBB. The vascular density of the brain is too high for researchers to perform autoradiography to localize radioactive molecules. Although fluorescent reporters could be attached to inhibitors, these fluorescent tags may alter their bio-disposition.

In order for researchers to successfully develop efficient treatments for the diseases of the CNS, therapeutic agents must be transported across the specialized vascular system of the brain, the blood-brain barrier (BBB), a huge obstacle in the development of therapies of the CNS, preventing the brain from taking up most (>98%) small molecules and all large molecules using transvascular routes after the inhibitors are administered intravenously.⁷¹ The BBB is a system of vascular cellular structures mainly represented by tight junctions between endothelial cells, and an ensemble of enzymes, receptors, efflux pumps and transporter systems which all control and limit the access of molecules to the brain, either by paracellular or trans-cellular pathways. The presence of tight junctions between cells, precluding molecules of any size from diffusing para-cellularly, the lack of fenestrae and the low occurrence of pinocytic vesicles differentiate endothelial cells of the BBB from endothelial cells of the rest of the body. Numerous detoxifying enzymes as well as drug efflux systems such as the ATP-driven efflux pumps of the multidrug resistance (MDR) pathways can expel many hydrophilic as well as hydrophobic agents. Furthermore, a basement membrane of

perivascular cells and the astrocytes' extended processes, the astrocyte end-feet which cover the vast majority of the abluminal surface of the BBB capillaries and which contact the endothelial cells, also help to seal the interstitial space of the brain from the circulating plasma. Therefore, all the structures forming the BBB constitute a diffusion barrier not only for large molecules, but also for small molecules. Also, under normal conditions, the lack of pinocytosis of endothelial cells of the BBB limits trans-cellular transport, which alone can move therapeutic agents across the BBB.

The BBB is naturally breached in a few sites along the mid-line of the brain, known as the circumventricular organs. Here the capillaries are fenestrated, allowing relatively free exchange between the blood and the brain. Besides these few sites, the BBB is the bottleneck of the development of drugs for CNS diseases. Transport across the BBB requires transport across the luminal and abluminal membranes of the capillaries and the associated cells forming the BBB and across the basement membrane surrounding these cells. Whereas passive diffusion allows a few lipid-soluble molecules to pass freely from the blood to the interstitium of the brain, ionic solutes are unable to cross. And, even if the brain cerebral endothelium takes them up, these solutes will be trapped in the endothelium or efflux pumps will extrude them toward the blood. These ionic solutes will not reach the brain parenchyma. Therefore, most therapeutic drugs do not cross the BBB, unless invasive processes or chemical modifications of drugs with recognition and transcytosis ligands open the BBB (for a more detailed review see 71). Families of influx transporters expressed at the BBB include the carrier-mediated transporters of small molecules, the receptor-mediated transporters, or adsorptive-mediated endocytosis. However, the drugs must structurally resemble the normal transporter substrates in order to be recognized. A small molecule that is an inhibitor of POP, but also resembling a natural BBB transporter substrate would have to be designed in order for the POP inhibitor to cross the BBB in this way.

1.4.6 Clinical trials

The role of proline-specific peptidase activity has been almost exclusively studied in preclinical models of neurological diseases and clinical data of POP inhibitors are scarce. Among the very few inhibitors investigated in humans, **1-5** (S-17092⁷²) and **1-2** are the most widely studied (and reported) POP inhibitors. **1-2** was orally administered to young healthy male volunteers as a single daily dose, or three times per day, for one week.⁷³ In this study, the plasma and urine concentration of **1-2** were determined; standard plasma assays were performed and the plasma level of several neuropeptides was quantified. Overall, researchers observed acceptable pharmacodynamics and pharmacokinetics profiles with the only abnormal finding being a transient elevation in plasma cholinesterase in the multiple-dose study. They observed no strong evidence of changes in plasma neuropeptide levels, whereas in a pre-clinical study in rats, the researchers noted brain neuropeptide levels increased in animals treated with **1-2**.⁴⁰

In another pre-clinical study, the Morain group found that, 60 min after oral administration of **1-5**, POP-like activity was reduced in all brain regions whereas levels of substance P and α -melanocyte-stimulating hormone increased.^{68,72} This study in rodents was followed by studies in humans. A short (1 week) human phase I exploratory trial with **1-5** (Figure 1.3) single and repeated doses, in healthy elderly volunteers showed that circulating POP-like activity was inhibited, but circulating levels of neuropeptides were not measured.^{72,74} The inhibitor was rapidly absorbed after oral administration (within one hour) and the inhibition of POP-like activity in the blood lasted from 0.5 h - 1 h (peak) to 12 h. However, the researchers did not characterize and identify the enzyme responsible for this POP-like activity in the blood, therefore we cannot be sure that this decreased enzyme activity was due to POP inhibition and not inhibition of an enzyme with a similar function. The percentage of enzyme inhibition was not obviously different between doses, but the duration of inhibition was dose-dependent. The inhibitor was well tolerated and no abnormalities in standard laboratory parameters were detected. The Morain group used electroencephalography (EEG) to measure drug

penetration into the human brain, drug efficacy and the duration of the drug's effects. Increased alpha band in quantitative EEG, as well as improved cognitive memory tests, were observed in the volunteers, but these effects were not-dose-dependent.

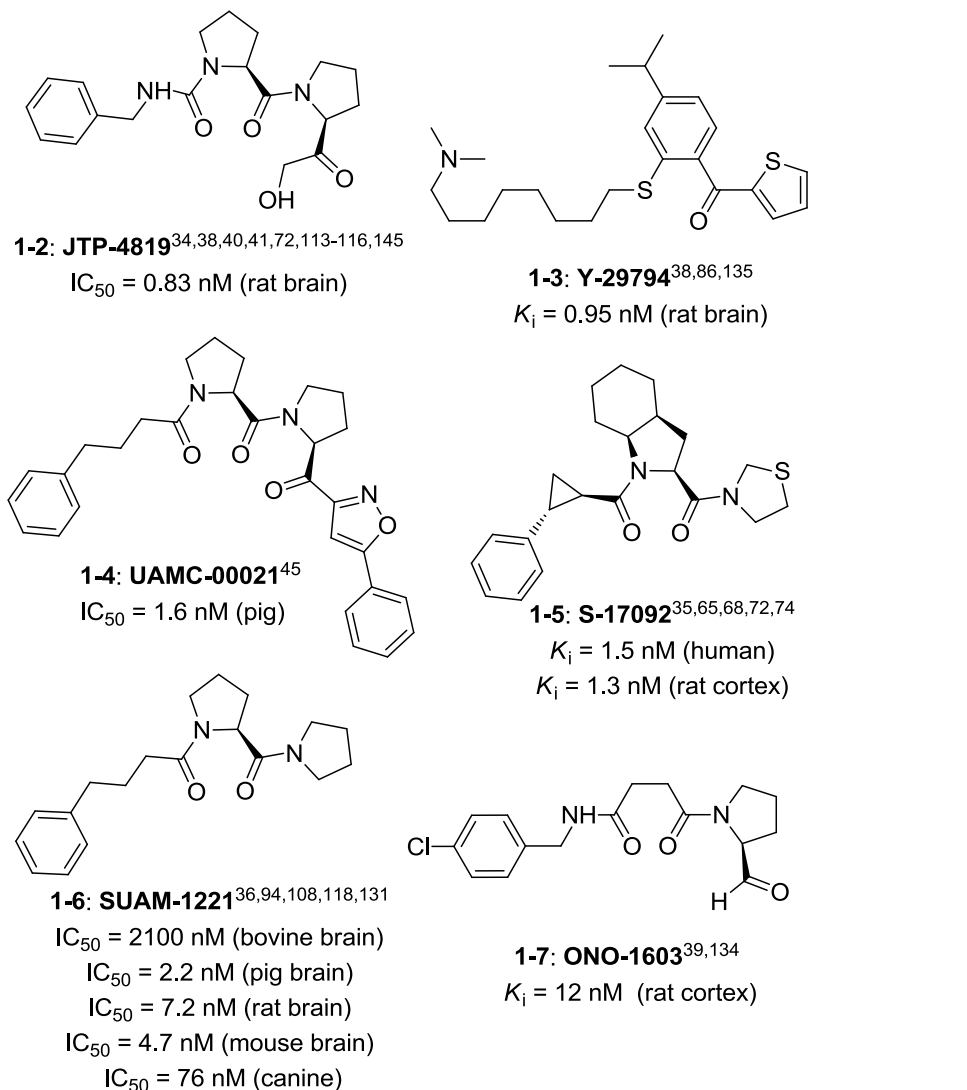
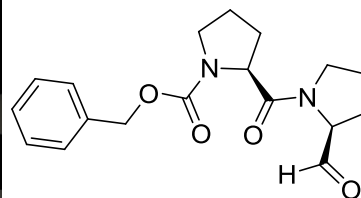
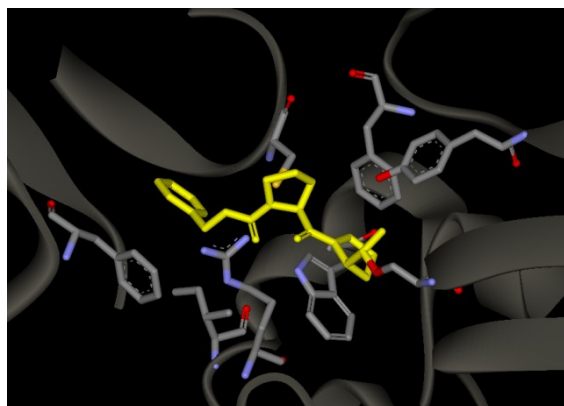


Figure 1.3 Selected POP inhibitors.

1.5 POP structural information

A number of crystal structures of POP either unbound (PDB codes: 1vz2,³⁰ 1h2w⁷⁵) or bound to various ligands (1h2y,⁷⁵ 1o6g⁷⁶) have been reported, but the catalytic serine was mutated to alanine for many of these structures (1uoq,⁷⁷ 1uoo,⁷⁷ 1h2z⁷⁵). Two structures include **1-1** covalently bound to porcine POP

(1qfs²⁸, Figure 1.4, porcine muscle POP, resolution 2.00 Å and 1h2y,⁷⁵ porcine brain POP Y473F, resolution 1.78 Å) and another includes Cbz-Ala-prolinal covalently bound to microbial POP (2bkl,⁷⁸ *Myxococcus xanthus* POP, resolution 1.50 Å) resulting in information on the binding mode of covalent inhibitors. Structures of POP cocrystallized with non covalently bound inhibitors (3eq9) have been reported as well.⁷⁹



1-1^{5,83}: K_i = 14 nM (rabbit brain)
 K_i = 0.35 nM (mouse brain)
 K_i = 0.21-5 nM (bovine brain)
 K_i = 0.50 nM (*Flavobacterium meningosepticum*)

Figure 1.4 Crystal structure of inhibitor 1-1 bound to porcine POP (left). Phe173, Cys255, Tyr473, Phe476, catalytic Ser554, Ile591, Trp595 and Arg643 are shown. Structure and affinities for POP from various species for inhibitor 1 (right).

The crystal structure of purified porcine brain POP shows a cylindrical structure (60x50Å) consisting of an α/β -peptidase domain, where the central tunnel of an unusual β -propeller covers the catalytic triad (Ser554, His680 and Asp641).²⁸ The crystal structure of POP in complex with the inhibitor Cbz-Pro-prolinal²⁸ suggests conformational changes, consistent with the observation that the rate-limiting step of catalysis involves a conformational change.⁸⁰ In this early report, reagents (such as *N*-ethylmaleimide) react with an unpaired cysteine (Cys255) on the propeller domain of the enzyme, impairing important conformational changes and inhibiting the enzyme. Interestingly, when crystallized, the rigid seven-bladed propeller acts as a gate which appears to be too narrow to allow passage of the substrate, thus controlling the selectivity of the enzyme. In addition, the active site entry is narrower than the average diameter of most peptides and small proteins, thus preventing longer sequences from uncontrolled degradation. The lack of an apparent entrance for the substrate

further supports substantial conformational changes of POP prior to substrate binding, involving flexible regions of the protein. A small tunnel between the flexible *N*-terminal segment of the peptidase domain and the facing hydrophilic loop of the propeller domain was identified as a possible entry passage for the substrate.

1.6 POP inhibition

1.6.1 Proline-specific proteases

Researchers have linked proline-specific protease activity with several human diseases, such as cancer, neurodegenerative or immunological/inflammatory disorders. Thus, modulating the activity of proline-specific proteases may be a relevant therapeutic approach. Substrates for proline-specific proteases include autocrine peptides (produced by the cells expressing the proteases) or paracrine peptides (produced by cells other than the cells expressing the proteases). Therefore, inhibitors may be developed for the inhibition of extracellular proteases, either secreted or whose catalytic site is inserted in the outer cell membrane, or for the inhibition of intracellular proteases. While drugs developed for inhibiting extracellular protease activity have been very successful, targeting intracellular proteases and evaluating inhibitors in intact cells has been much more difficult.⁸¹

Since comparable proline-specific peptidase activities are found in many locations in and outside cells, the exact site, mode of action, and biological target(s) of these inhibitors cannot necessarily be attributed to inhibition of one enzyme. To avoid side-effects and toxicity of inhibitors, researchers must develop compounds that selectively inhibit proline-specific protease activity of one enzyme.

1.6.2 Potent and selective inhibition

With data suggesting that POP inhibitors can modulate memory and other neurological disorders, interest in mammalian POP and POP inhibitors increased.

To this end, hundreds of natural or synthetic compounds have been tested.⁸² Many of them are substrate analogs, of which **1-1**, **1-2**, **1-7** (ONO1603³⁹), **1-6** (SUAM-1221³⁶) and **1-5**, are the most studied. However, the reported inhibitors were evaluated on POP enzymes from several species, including microorganisms and mammals. For instance, testing **1-1** on *Flavobacterium meningosepticum*,⁵ as well as rabbit,⁸³ mouse,⁸⁴ and bovine origin⁵ revealed species-dependent K_i values (Figure 1.4). Therefore, comparing inhibitory potency of molecules between species is not recommended as a screening strategy, and published information must carefully address this. In this article, we will therefore focus our discussion on mammalian POP inhibitors. All the available biological data, and the species that this data applies to, is given.

1.6.3 Inhibition of POP in human diseases

The S1 site of POP typically accommodates a proline residue. However, POP sometimes can also accommodate an alanine residue, although the rate of hydrolysis at this residue is much lower than with proline. The S1' site is typically occupied by a hydrophobic residue, located on the right side of the scissile bond (Figure 1.5), although arginine may also be at that location, as in neurotensin, a substrate of POP.

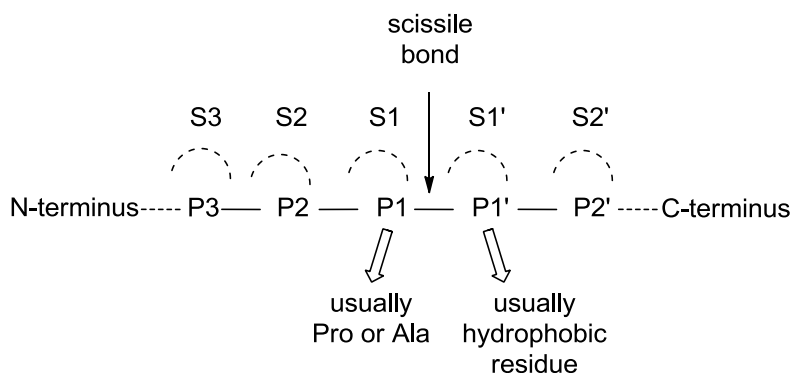


Figure 1.5 Interaction sites (S_x) of POP active site with portions (P_x) of substrate or inhibitor.

As reviewed above, brain cell-expressed prolyl oligopeptidases (POPs) have been linked to a number of neurological disorders. The selective inhibition of POPs over other peptide-cleaving enzymes as a therapeutic approach has been

explored, mainly with the development of peptidic and pseudo-peptidic inhibitors, as well as a few non-peptidic molecules. To develop more potent and selective POP inhibitors, medicinal chemists need to better understand the key inhibitor sites for selectivity and potency. By highlighting and comparing the beneficial and detrimental changes to the sites of POP inhibitors, we will define an optimal pharmacophore of POP inhibitors. In this perspective article, we will develop this pharmacophore by grouping known-inhibitors according to their key sites (P3, P2, P1), in relation to mammalian POP. For the following sections of this article, we will review all structural changes to each of these key inhibitor sites (P3, P2, P1). When necessary, we will mention recent (from 2000 to present), relevant patents, since De Nanteuil, Portevin, and Lepagnol provided an extensive review of inhibitors patented prior to 1998.⁸² Furthermore, we have noted that many of the patented compounds closely resemble compounds previously published in journals. Among several examples, a series of compounds (structures not disclosed) very similar to **1-3** were patented as POP inhibitors in 2009.⁸⁵

1.7 Peptididic, pseudo-peptididic and peptidomimetic POP inhibitors

From as early as 1983, with the discovery by the Wilk group that **1-1** selectively inhibited POP from rabbit brain ($K_i = 14$ nM) over a number of other peptidases such as papain, trypsin and chymotrypsin,⁸³ researchers have thoroughly investigated the effects of structural changes at P1, P2 and P3 of peptidic, pseudopeptidic and peptidomimetic inhibitors. Early efforts came from academia with groups in the US,^{22,56,86} Japan,^{5,22,23,87-99} Belgium,^{100,101} France,¹⁰²⁻¹⁰⁶ Hungary,^{79,107} as well as from industrial research groups (e.g., Zeria Pharmaceuticals,^{108,109} Ajinomoto,¹¹⁰ Meiji Seika Kaisha,^{111,112} Japan Tobacco,^{40,41,76,113-116} Pfizer,¹¹⁷ and Servier^{36,72}). Most of the research efforts, from academia and the pharmaceutical industry, focused on developing pseudo-peptidic and peptidomimetic POP inhibitors. Recently, a group from Finland has further developed a number of pseudo-peptidic inhibitors,¹¹⁸⁻¹²⁸ as did industrial

efforts from Genentech¹²⁹ and GlaxoSmithKline.¹³⁰ Interestingly, to our knowledge, all the reported inhibitors bind to the S3, S2, S1 sites of the catalytic site while only one (**1-4**)⁴⁵ of these reported small molecule inhibitors may fill the S1', S2' and S3' pockets of POP.

1.7.1 Modification of P3 for optimal binding

We selected inhibitors with representative variations at P3 and depicted them in Figure 1.6. Tight binding of inhibitors to POP often requires a hydrophobic group at P3 (e.g., Cbz group of **1-1**) to interact with the hydrophobic S3 pocket lined with several nonpolar residues such as Phe173, Met235, Cys255, Ile591 and Ala594.²⁸ In fact, most of the known substrates feature a polar or hydrophobic residue, but no charged residues at this position. When the Cbz group was replaced with a phenyl-acyl group of varying chain length (**1-6**)^{36,108,131} Figure 1.3), a chain length of 3 carbon atoms (phenylbutanoyl) was found to be optimal for low nanomolar inhibition of POP originating from various species. The obtained potency of **1-6** on bovine brain POP was comparable to the IC₅₀ of **1-8** having a shorter Cbz group at P3.⁹⁴ Clearly, the substitution of an oxygen by two methylene groups is reasonable.^{94,131} When the floppy chain of **1-6** was constrained (**1-9a-d**),¹⁰⁹ the observed IC₅₀ on canine brain POP was improved (by one to two orders of magnitude). Further investigation of the P3 site with acyl and alkenyl groups of varying chain length led to the conclusion that octanoyl (**1-10**) was the longest acyl group that could be tolerated at P3 to favorably fill and interact with the S3 pocket of POP.¹⁰⁷ Not only do longer alkyl chains lead to poor solubility, but probably also to steric clashes in the S3 pocket and large entropy penalties upon binding, resulting in less potent inhibitors.¹⁰⁷ Although most of the reported investigations on P3 inhibitor-enzyme interaction recommend flexible linkers to properly fill the S3 site of POP and to avoid any detrimental clashes with the protein, long and rigid moieties have also been successfully introduced (**1-11**). However, additional changes to these molecules were also required to achieve potent inhibition, rendering their direct comparison

with other inhibitors difficult.¹²⁴ Similarly, the large and bulky fluorescein tag was best tolerated at P3 if a five-carbon linker was employed although high nanomolar activities were still recorded with a single carbon.¹²⁵

The Toide group successfully replaced the oxygen of the Cbz group with a nitrogen (as in **1-2**).^{113,114} This demonstrates that a hydrogen bond donor (**1-2**), a hydrogen bond acceptor (**1-1**) and a methylene group (**1-6**) are tolerated at position P3.

Researchers also modified the phenyl of the Cbz group of **1-1**. SAR data show that the phenyl ring could successfully be replaced with isosteric heterocycles (**1-12**),¹⁰⁸ large, more rigid groups such as 3-phenoxybenzoyl (**1-13**)⁹⁷ or Fmoc (**1-14**),⁸⁶ non aromatic groups such as 3-cyclohexylpropionyl (**1-15**)⁹⁷ and *tert*-butyl (**1-16**)¹²¹ and also with constrained (i.e., cyclized) moieties such as tetrahydronaphthylacetyl (**1-9a-d**) and indanoylacetyl (**1-17a-b**).¹⁰⁹ Similarly, Portevin *et al.* successfully introduced (2-phenylcyclopropyl)carbonyl (**1-18**) as a rigidified version of 4-phenylbutanoyl, yielding an even more potent inhibitor (IC₅₀ of 1.2 nM on POP from rat brain).³⁶ More recently, Kanai *et al.* explored different highly rigid aromatic groups at P3, preparing phthalimido (**1-19**), quinoxalinone (**1-20**) and the bulkier hydantoinyl (**1-21**) derivatives,⁷⁹ while Jarho *et al.* focused on pyridine (**1-22**), all with varying acyl chain lengths.¹²⁷ The introduction of an ionizable group such as pyridine is expected to increase the water solubility of the otherwise hydrophobic phenyl rings. In fact, Jarho and co-workers noted that the logP of the inhibitor dropped significantly while the inhibitor potency was maintaining (IC₅₀ of 2.1 nM on POP from pig brain), when they substituted the phenyl ring by a pyridine ring.¹²⁷ The introduction at P3 of diaminophosphinyl substituents has also been investigated as surrogates for the Cbz group of **1** and analogues.¹³²

Although size (length, bulk, etc.) has been thoroughly investigated, only a few reports detail stereochemical requirements of the P3 subsite (**1-17a,b**).^{95,109} These studies demonstrate that configuration does not have a major impact on potency (one order of magnitude for **1-17a** vs. **1-17b**).

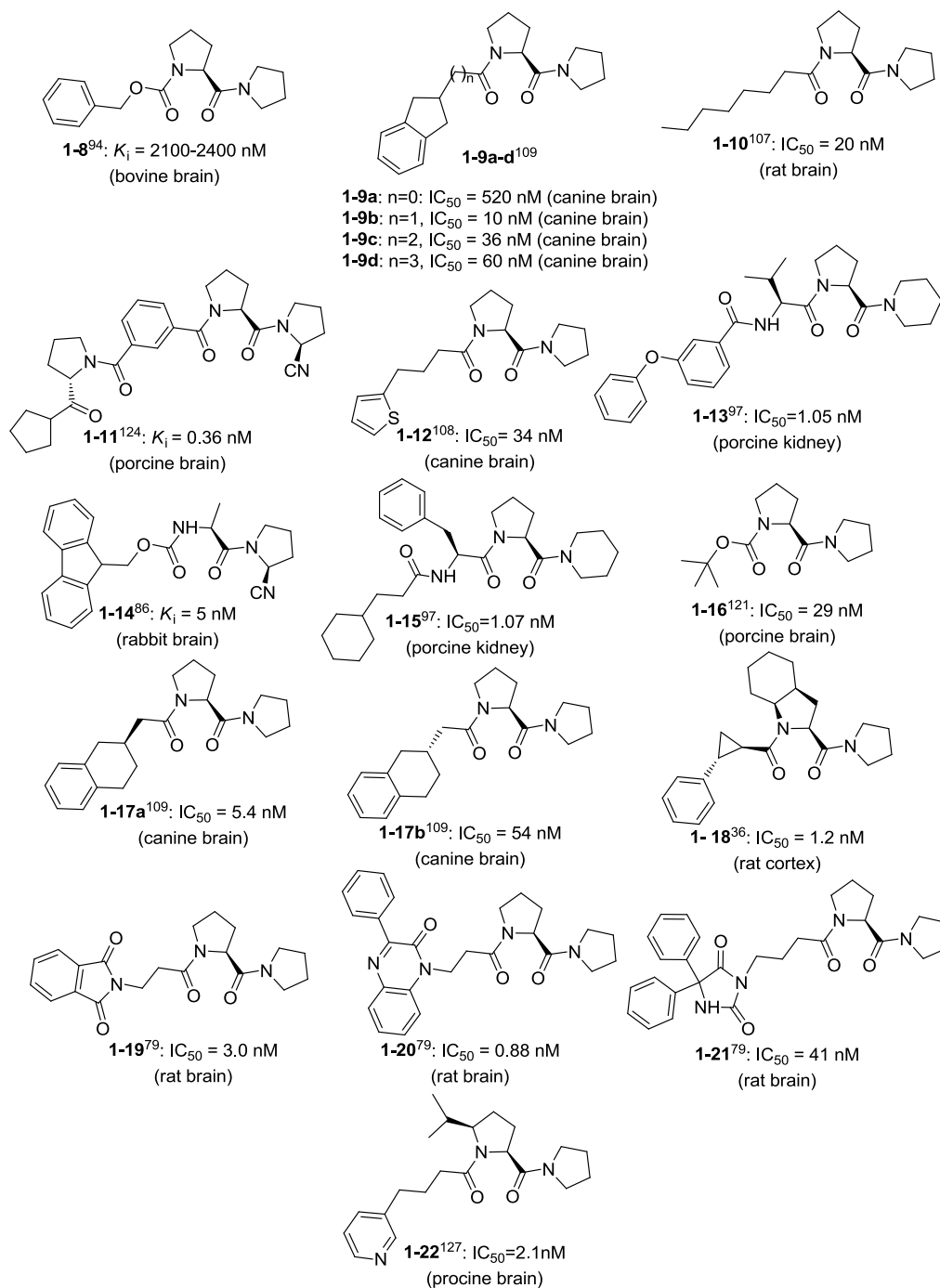


Figure 1.6 P3 substitutions.

1.7.2 Modification of P2 for optimal binding

The S2 pocket of POP has no distinguishing feature that would entail substrate or inhibitor selectivity at this site, although a few residues (Asn534, Tyr453 and

Arg618) may be key as they are conserved in members of the POP family.⁷⁸ A selection of inhibitors highlighting some interesting P2 modifications is given in Figure 1.7. In most cases, P2 was kept as a proline, a proline derivative or a proline mimic. In only a few examples, researchers investigated replacing the proline residue at P2 with other amino acid residues (such as valine in **1-23**).^{6,133} The Yoshimoto group substituted the proline at P2 by thiazolidine-S-oxide, increasing inhibitor potency.⁹⁴ The potency further increased when thiazolidine was used (**1-24**).^{93,94,108} The combined data indicate that subtle changes either steric or electronic in nature affect the inhibitor binding.^{93,94,100,107-109} A few groups searched for a suitable replacement of the P2 amino acid. A few groups have successfully replaced proline with some non-natural amino acids containing perhydroindole (**1-18** and **1-5**), azabicyclo[2.2.2]octane (**1-25**) and azabicyclo[2.2.1]heptane.³⁶ Similarly, tetrahydroisoquinoline (**1-26**),¹⁰²⁻¹⁰⁴ cyclohexyl (**1-27**)¹¹⁷ and indoline (**1-28**)¹¹⁷-based POP inhibitors were reported. Wallén *et al.* functionalized the proline at P2 with either methyl or *tert*-butyl at position 5 of the ring, testing both (*R*) and (*S*) configurations (**1-29**). Although the substitution did not lead to drastic increase or loss of potency, they found that the (*R*) stereochemistry was optimal.¹²¹ These results along with the results for compound **1-30**⁵ clearly indicate that there is some unexplored space in the S2 pocket of the POP binding site that could be filled to improve inhibitor binding. Wallén *et al.* later substituted a cyclopent-2-enecarbonyl (**1-31**) for the proline at P2, yielding inhibitors equipotent to **1-6**, but also more lipophilic which could improve cell permeability.¹²³ However, the cyclopent-2-enecarbonyl-unit of **1-31** could act as a Michael acceptor to any nucleophilic species (with, for example, the thiol of a cysteine side-chain), forming a covalent bond upon binding and leading to undesired side effects. Very recently, researchers showed that substituting the γ -CH₂ of proline with a γ -CF₂-group (**1-32**) could enhance the inhibitory activity by adding an extra hydrogen-bond with the enzyme, but also by inducing a slight shift in the bound pose.⁷⁹ The opening of the ring and the use of a succinic acid core led to the development of **7**.¹³⁴

The carbonyl group between the two pyrrolidine rings of **1-1** has been shown to interact with the protein binding site (PDB code: 1h2y). In fact, removal of this oxygen led to a complete loss of potency (**1-33**).⁹⁴

The stereochemistry at P2 has also been investigated through a variety of inhibitor structures. The Arai group showed that the natural proline stereochemistry is crucial for optimal activity (**1-34** vs. **1-24**).¹⁰⁸ Replacing the asymmetric carbon by a flat sp² carbon or amide nitrogen also led to a significant loss of potency (**1-31** vs. **1-35**, **1-36**).^{123,128}

To date, most of the modifications at P2 are designed to mimic the proline residue of **1-1** and significant changes should be made if we aim to develop more “drug-like” molecules. In this context, phenyl rings have been used successfully.^{85,135} In fact, a closer look at the natural substrates (Table 1.1) reveals that a number of other residues can be tolerated at this position and should guide the design of novel inhibitors. In addition, the activity of a series of Fmoc-aminoacylpyrrolidine-2-nitriles such as **1-14** and **1-37** revealed that an alanine or a charged arginine residue can suitably replace the P2 proline of **1-1** with only a small loss of binding affinity.⁸⁶

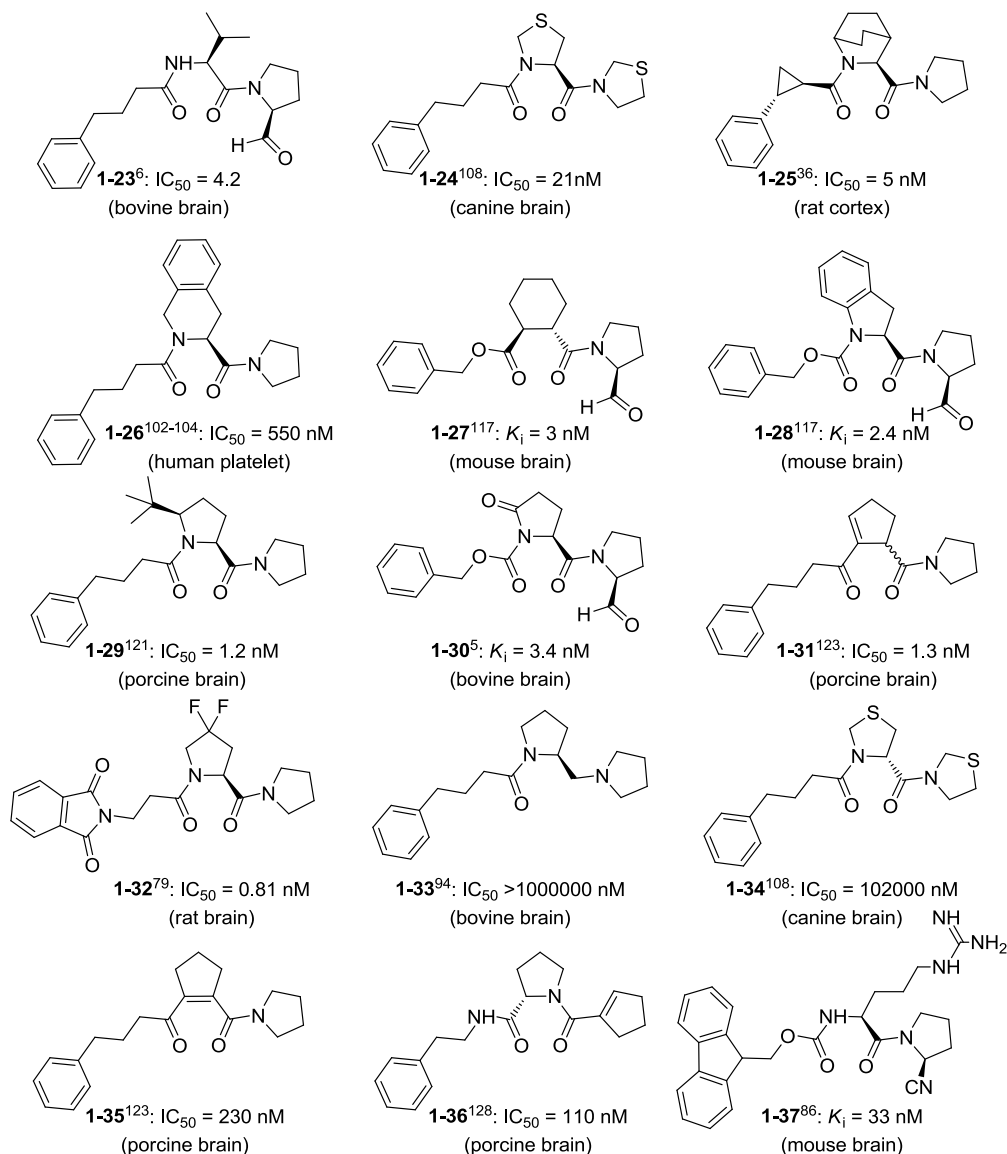


Figure 1.7 P2 substitutions.

1.7.3 Modification of P1 for optimal binding

The S1 pocket is lined with several hydrophobic residues (Trp595, Phe476, Val644, Val580 and Tyr599) allowing the proline ring of its substrate to fit tightly and stack with the indole ring of Trp595, and rendering POP very specific for substrates having residues that can tightly fit within this pocket.²⁸ A selection of P1 modifications are given in Figure 1.8. The chemical nature of the P1 substituent governs whether the designed inhibitor will act covalently or non-covalently. If P1 is a pyrrolidine, the inhibitor acts in a non-covalent fashion (for

example, **1-6**). The pyrrolidine mimics the right-hand-side ring in **1-1**. When comparing non-covalent inhibitors, compounds with a thiazolidine (**1-38**) at P1 were found to be more potent than pyrrolidine- (**1-8**) thiazolidine S-oxide- (**1-39**) and oxazolidine- (**1-40**) containing compounds.^{93,94,104} Portevin *et al.* further explored non-reactive heterocycles at P1 finding comparable potency with 2- and 3-pyrrolines (**1-41**, **1-42**), pyrroles (**1-43**) and isoxazolidine (**1-44**).³⁶ The amide bond was also converted into the thioxo amide bond (**1-45**) but with significant loss of potency.¹⁰⁵ Addition of an oxygen to **1-6** led to **1-46** which demonstrated significantly lower potency.

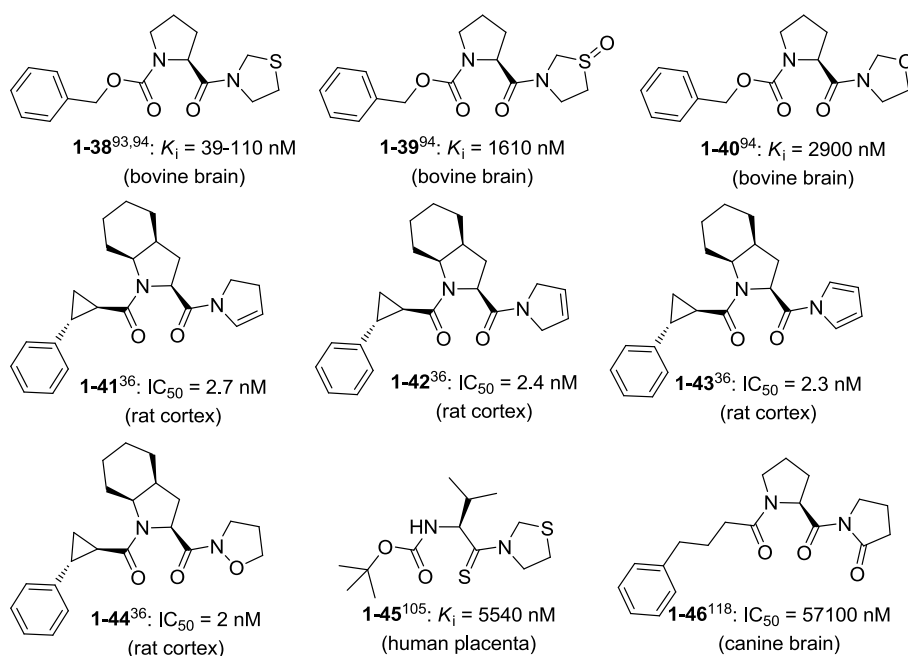


Figure 1.8 P1 substitutions.

Once more, the structural modifications at P1 reported to date focused on proline mimics. However, as we can see from the structures of the substrates, POP is very selective for proline residues (alanine residues are tolerated but with a significant decrease in protease activity) and drastic changes at P1 are expected to correlate with a loss of inhibitory potency.¹⁰⁸ In fact, the oxygen of the P1 ring in **1-40** is most likely facing the catalytic serine oxygen (which reacts with the carbonyl in **1-1**) leading to severe electrostatic repulsions.

1.7.4 P1' substitution, covalent versus non-covalent inhibitor

If the C-terminus at P1 ends with a reactive functional group, such as an aldehyde, hydroxyacetyl or nitrile, then the inhibitor will most likely covalently bind with the catalytic serine of the active site of the enzyme (Figure 1.9).¹³⁶ Researchers introduced phosphonate esters at P1 (structure not shown), which they claimed to induce a covalent bond with the active site serine, resulting in irreversible inhibition of the enzyme.¹³⁷ The formation of a covalent bond has been hypothesized based on kinetic studies and further confirmed by X-ray crystallography of POP co-crystallized with **1-1** (Figure 1.4). Investigation of active-site specific, covalent inhibitors of POP can be traced back as early as 1977 with chloromethyl ketone derivatives of a few dipeptides (Figure 1.9, **1-47**)²² and then the discovery of **1-1** in 1983.^{5,83} Later, SAR studies confirmed that covalent inhibitors were more potent than non-covalent inhibitors (**1-48** vs. **1-1**)^{5,100}.^{121,124} Extensive SAR has shown that aldehydes (**1-49**) could be replaced with α -keto heterocycles like in **1-50**, with a concomitant increase in inhibitory potency.^{106,111,112} Other reactive groups, such as terminal boronates (**1-51**)¹²⁹ and hydroxymethyl ketones (**1-2**),¹¹⁶ were also shown to inhibit POP with improved potency over the corresponding non covalently acting structures. Acetal derivatives of **1-1** and thiazolidine analogues were also prepared as exemplified by ZTTA (**1-52**)¹³⁸ but were less potent, exhibiting high nanomolar inhibitory activity.¹⁰⁰ Further studies showed that α -ketoesters¹¹¹ exhibited nanomolar inhibitory activity.

Vendeville and co-workers closely examined the impact of a reactive group attached to **1-26** showing that aldehydes and nitriles can be advantageously replaced by α -chloromethylketones and α -hydroxymethylketones.¹⁰⁴ However, kinetic studies of analogues of **1-11** revealed that the association and dissociation were faster for the nitrile derivative (KYP-2047, **1-53**)¹²⁶ than for the hydroxymethyl ketone and aldehyde.¹²² As a result, the half life of these covalent inhibitors was controlled by slow dissociation.^{122 126} Similar observations were made with **1-9**, **1-54**, **1-55**.¹⁰⁹

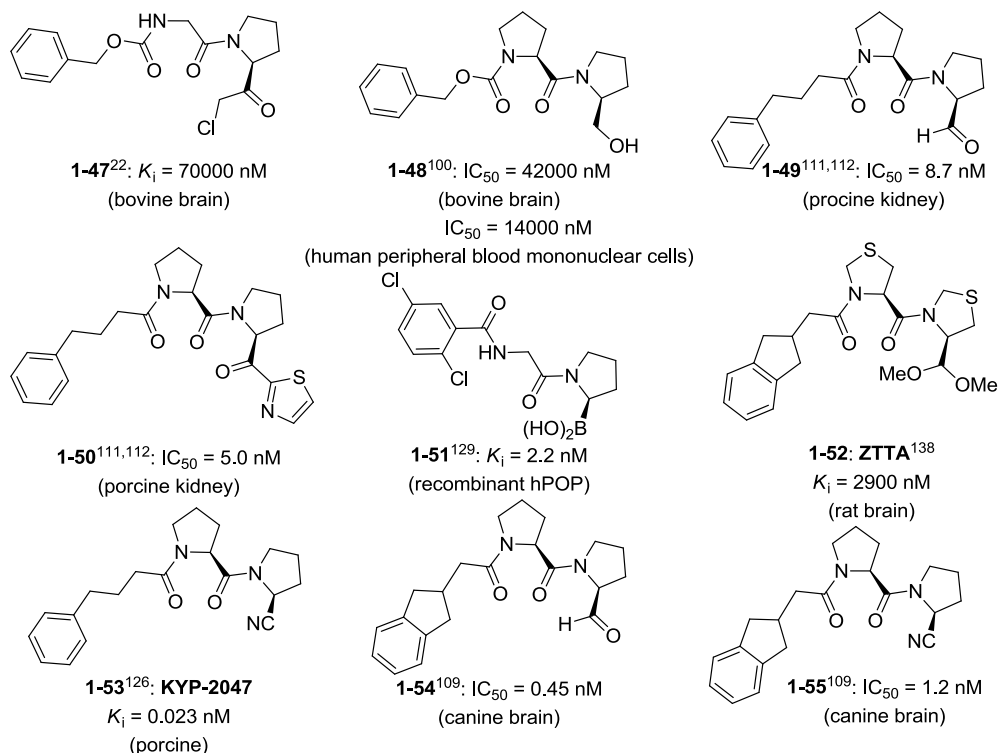


Figure 1.9 Reactive functional groups.

1.7.5 Non-peptidic POP inhibitors

Thus far, very few non-peptidic POP inhibitors have been reported. From a library of traditional Chinese medicine, the natural product berberine (Figure 1.10, **1-56**) was identified as a weak POP inhibitor (IC_{50} found to be 145000 nM).¹³⁹ In particular, berberine was efficient for the treatment of patients with bipolar affective disorders as they present increased levels of POP activity in serum.¹⁴⁰ Later on, further screening of plant extracts led to the discovery of Baicalin (**1-57**) from *Scutellaria baicalensis*. Baicalin was found to act as a prodrug with the sugar moiety being hydrolyzed in the gut. Rat gut β -glucuronidase cleaves baicalin, releasing the active polyphenol portion (baicalein) which can potentially cross the blood brain barrier, and other biological barriers, according to parallel artificial membrane permeability assay data, and inhibit POP in the brain. Baicalin showed POP selectivity, exhibiting significantly less inhibition of DPPIV⁷⁰ The major advantage of compounds like berberine and baicalin is that they have been used in humans for years without noticeable side

effects. This is a clear advantage over novel synthetic inhibitors with *a priori* unknown pharmacokinetic and toxicokinetic profiles.

Inspired by the structure of berberine, isoquinolium derivatives, like **1-58**, were prepared as potential POP inhibitors and other analogues (structures not disclosed) were patented as POP inhibitors in 2008.¹⁴⁰ In addition to being POP inhibitors, these compounds also crossed parallel lipid artificial membranes.⁶⁹ Very recently, Haffner chose to step away from peptidic POP inhibitors by constraining them into pyrrolidinyl pyridone and pyrazinone analogues. All the reported analogues exhibited nanomolar inhibitory potency for POP, and **1-59** could be co-crystallized with the enzyme, showing the key interactions formed in the bound complex.¹³⁰ To our knowledge **1-3** (Figure 1.3) is the only drug-like POP inhibitor that has been discovered by screening of a collection of molecules and not through rational design starting from **1-1**.¹³⁵

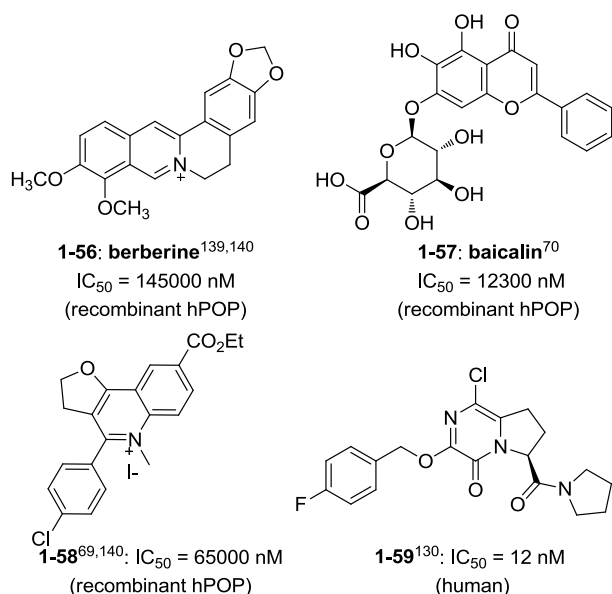


Figure 1.10 Examples of non-peptidic POP inhibitors.

Compounds **1-4**, **1-56** and **1-57** are structurally different from the other inhibitors described above. In fact, the authors do not give details on whether these bind to the active site of POP or an allosteric site.

1.7.6 Selectivity of POP inhibitors

There are three levels of selectivity important in the design of POP inhibitors. The first is that the inhibitors are selective for POP over all other proteases and peptidases. Yoshimoto *et al.* verified that their covalent inhibitor (**1-47**) was selective for POP over other serine proteases like trypsin, chymotrypsin, elastase and papain, Figure 1.11).²² Secondly, the inhibitors must bind selectively to POP and must not bind to other enzymes cleaving peptides at sites adjacent to proline residues, such as dipeptidyl aminopeptidase 2 and IV (DPP2 and DPPIV), aminopeptidase P (APP), and others. For example, selectivity of **1-3** for POP over DPPIV, proline iminopeptidase, APP, prolidase and prolyl-carboxypeptidase was noted, although no explanation for this observation was given.¹¹³ Similarly, synthesized Fmoc-aminoacylpyrrolidine-2-nitriles (**1-14**) selectively inhibited POP over DPPIV (no DPPIV inhibition detected at 5 μ M inhibitor), but no rationalization was given.⁸⁶ Poor selectivity for FAP- α and POP against DPPIV was achieved with synthesized boronate inhibitors (**1-60**, **1-61**), but better selectivity for POP versus DPPIV with decreased FAP- α /seprase inhibitory activity as demonstrated by Wolf and co-workers.^{129,141} Lawandi *et al.* successfully developed a series of bicyclic scaffold-based inhibitors (like **1-62**) to selectively inhibit POP activity over other proline-specific peptidase activity.¹⁴² Finally, as for the third level of selectivity, inhibitors should be able to discriminate between POP from different species (not discussed here).

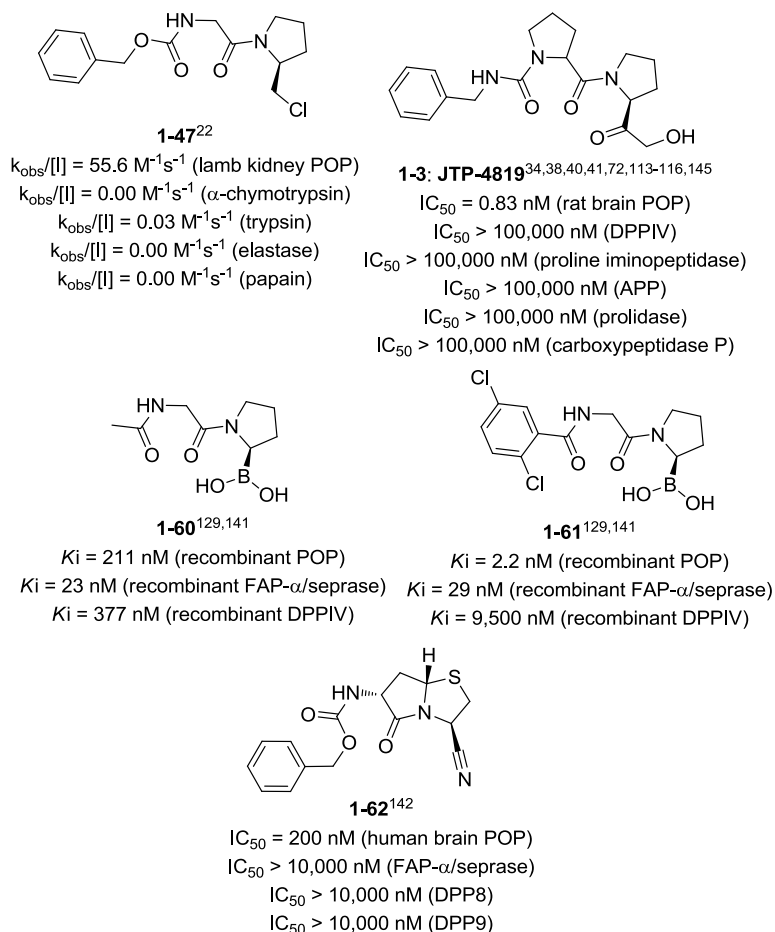


Figure 1.11 Selective POP inhibitors.

1.7.7 Structure-based design of POP inhibitors

The available structural information was further exploited to understand the ligand binding process. For instance, docking inhibitors to the crystal structure 1qfs using GOLD in combination to CoMSIA analysis of the ligands shed light on the key interactions between the ligands and the protein binding site¹²⁴ while docking inhibitors to the crystal structure 1h2w (porcine POP) with AutoDock provided hints on the binding of benzimidazolium derivatives.⁶⁹ Using the linear interaction energy method (LIE),^{143,144} Kánai et al. have attempted to derive binding free energies from computations.⁷⁹ Applied to six different ligands, this molecular dynamics-based method not only identified the weakest binder (no inhibition at 0.1 μM) and the strongest binder within the set, but also predicted the IC_{50} within two orders of magnitude (binding free energies within 2.5 kcal). More

recently, Lawandi *et al.* have reported the successful development of novel, potent and selective inhibitors (**1-62**), guided by docking with the program FITTED which considers covalently bound inhibitors.¹⁴²

1.8 Conclusions and prospects

1.8.1 POP and POP-like inhibition

Researchers focused on developing POP inhibitors because they hypothesized that compounds able to positively modulate the brain levels of neuropeptides which are important in cognitive process, neurodegeneration or in age-related cognitive decline, may be of clinical and therapeutic interest. Researchers have demonstrated some of these positive effects, *in vivo*, in preclinical animal models of these diseases of the CNS and in the few reported phase 1 clinical trials, none of the inhibitors showed any toxicological or safety problems. Toward this goal of treating diseases of the CNS, researchers have studied behavioral pharmacology in animals, evaluated enzyme inhibition, either in human or animal blood, and in animal brain extracts, and for some studies, researchers even quantified how POP inhibitors affected brain levels of neurotransmitters. Most studies extracted the whole brain from animals and then measured POP activity, without thoroughly characterizing the enzyme affected. Furthermore, in many cases of potentially effective POP inhibitors, no *in vivo* testing has been reported for their potential application in other diseases where *in vitro* cell models suggested a role for POP in infectious, oncological or inflammatory disorders. In this Perspective, we restricted our evaluation of their possible clinical interest to CNS disorders.

Despite promising preclinical and clinical results, researchers have yet to evaluate POP inhibitors in large human clinical trials for memory disorders. Furthermore, several aspects of the physiology of POP and its inhibitors are missing and must be addressed before their therapeutic interests can be clearly evaluated:

- Where is (are) the exact target enzyme(s) of POP inhibitors located?
- Are these enzymes intracellular or extracellular?

- Which are the exact biological substrates of POP and POP-like enzymes?
- Do these POP inhibitors pass the BBB? And, if yes, how?
- Are these inhibitors trapped in the cerebral vasculature, where they may exert their effects?
- What is the role and the impact of other POP-like activities in the evaluation of inhibitors in biological models?

A number of biological processes and diseases are linked to POP and will most likely motivate more research on this enzyme towards the development of POP inhibitors. POP activity may lead to both quantitative and qualitative changes in the signaling potential of bioactive peptides and inhibitors of POP activity may be developed as valuable chemotherapeutic agents for neurological disorders. For instance, the use of **1-2** has shown promising applications for the treatment of sensorimotor dysfunctions caused by brain trauma.¹⁴⁵ A combination of physical therapy with drug treatment with **1-2** induced enhanced functional recovery in rats with focal forebrain ischemia.¹⁴⁵ However, the observed effects may originate from families of proline-specific enzymes having comparable activity, but having either related or unrelated sequence and structure homology. Researchers have yet to pinpoint the exact origin of the observed effects of these inhibitors. The published information on neurological diseases reviewed here suggests multiple targets for the inhibitors of the proline-specific proteases and peptidases. The effects of the reported inhibitors may result from an indirect effect regulating other pathways than the pathways initially targeted.

Given the expression of these proline-specific enzymatic activities in most tissues, if not in most cells, an approach to consider for future development includes the preparation of pro-drugs, combining, for example, a POP inhibitor with a cell-targeting agent (for examples, see references 71, 146) in order to improve the delivery of these potential therapeutic agents to the cells to be treated.

Both natural and synthetic compounds have been evaluated for their effects on proline-specific endoproteases. However, in most cases enzymes from different species, either from microorganisms or mammals, have been used to evaluate

many of the reported inhibitors. Translating inhibitor potentials measured on POP from one species to a different species must be done very carefully, knowing that differences exist between proline-specific endoproteases of different origin. Furthermore, the therapeutic potential of the known proline-specific endoprotease inhibitors and of future generations of inhibitors can only be exploited if we can develop an inhibitor exhibiting a high level of selectivity for an enzyme of one species.

1.8.2 Selective and potent POP inhibitors

In order to guide the design of novel selective inhibitors, we summarized the necessary SAR data in Figure 1.12, Figure 1.13 and Figure 1.14. We can combine the information from Figure 1.12 into a first pharmacophore (Figure 1.13) to develop inhibitors selective for POP over other proline-specific proteases including FAP- α /seprase, DPPIV, DPP8 and DPP9.^{129,147,148}

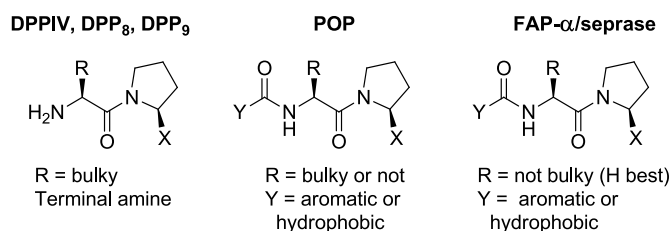


Figure 1.12 General considerations to design inhibitors of either DPPIV, DPP8, DPP9, POP or FAP- α /seprase.

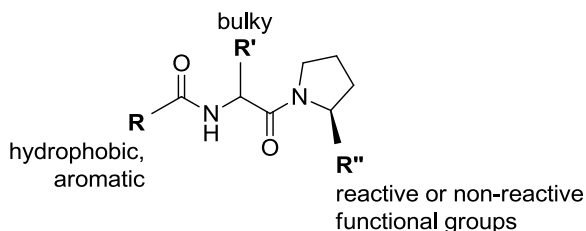


Figure 1.13 Achieving selectivity for POP over DPPIV, DPP8, DPP9 and FAP- α /seprase.

We have also combined all the information from the structure-activity relationship data into a schematic representation of the functional/structural requirements of a peptidomimetic POP inhibitor that can be visualized and used for the design of future generations of potent, selective inhibitors.

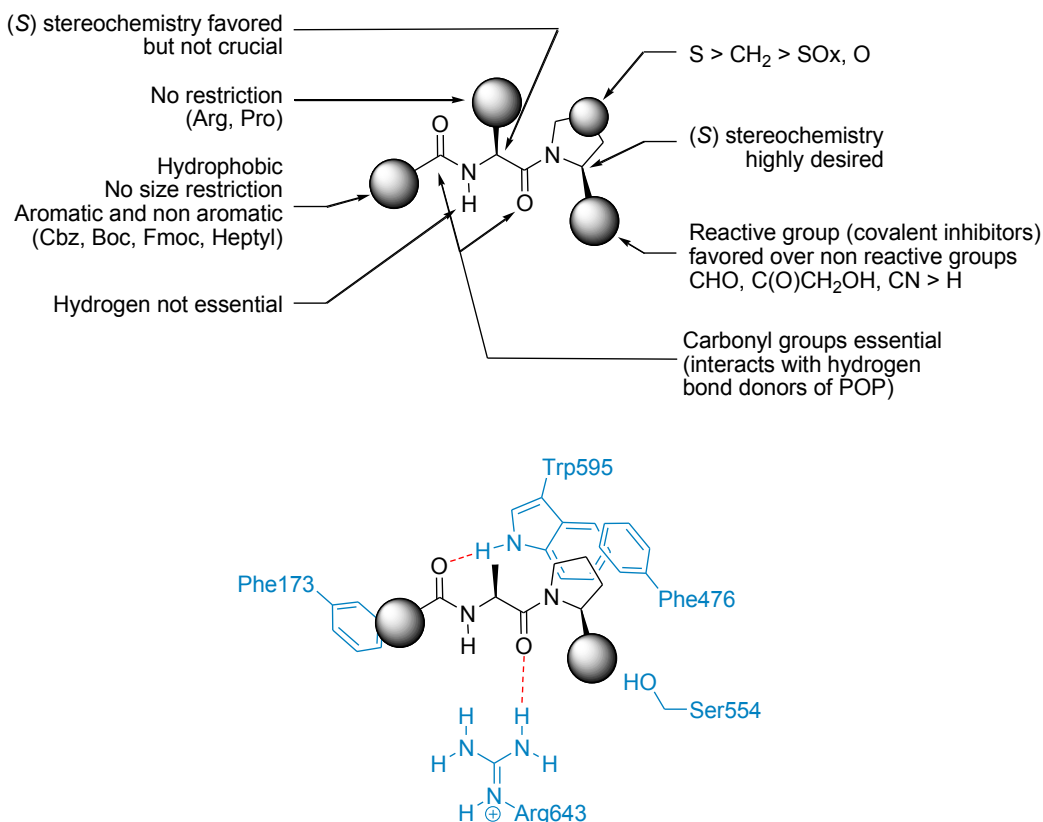


Figure 1.14 Optimal pharmacophore for achieving potency for POP (top), key interactions between inhibitors and POP (bottom).

Covalent inhibitors are more potent than the non-covalent inhibitors developed thus far, although subnanomolar non covalent inhibitors have been discovered (**1-20**). This is not surprising given the trends in drug design towards incorporating covalent modifiers highlighted in a few recent reviews.^{149,150}

Generally, there is a need to direct future drug design towards more drug-like, non-peptidic compounds. Very few studies on drug-like molecules have been reported. In fact, only **1-37**, analogues of **1-37** and **1-3**¹³⁵ have been derived from a hit discovered by screening while most of the other inhibitors mimic **1-1**. Given the availability of crystal structures,^{28,76} we were surprised to find that only a few potent POP inhibitors were developed using computational methods based on these structures. Drug-like candidates could be obtained by virtual screening for example, a strategy we are currently exploring in our laboratories.

1.9 References

1. Rosenblum, J. S.; Kozarich, J. W. Prolyl peptidases: A serine protease subfamily with high potential for drug discovery. *Curr. Opin. Chem. Biol.* **2003**, 7, 496-504.
2. Polgár, L. The prolyl oligopeptidase family. *Cell. Mol. Life Sci.* **2002**, 59, 349-362.
3. Yaron, A.; Naider, F. Proline-dependent structural and biological properties of peptides and proteins. *Crit. Rev. Biochem. Mol. Biol.* **1993**, 28, 31-81.
4. Männistö, P. T.; Venäläinen, J.; Jalkanen, A.; García-Horsman, J. A. Prolyl Oligopeptidase: A Potential Target for the Treatment of Cognitive Disorders. *Drug News Perspect.* **2007**, 20, 293-306.
5. Yoshimoto, T.; Kawahara, K.; Matsubara, F.; Kado, K.; Tsuru, D. Comparison of inhibitory effects of prolinal-containing peptide derivatives on prolyl endopeptidases from bovine brain and *Flavobacterium*. *J. Biochem.* **1985**, 98, 975-979.
6. Saito, M.; Hashimoto, M.; Kawaguchi, N.; Fukami, H.; Tanaka, T.; Higuchi, N. Synthesis and inhibitory activity of acyl-peptidyl-prolinal derivatives toward post-proline cleaving enzyme as nootropic agents. *J. Enzym. Inhib.* **1990**, 3, 163-178.
7. Santana, J. M.; Grellier, P.; Schrével, J.; Teixeira, A. R. L. A *Trypanosoma cruzi*-secreted 80 kDa proteinase with specificity for human collagen types I and IV. *Biochem. J.* **1997**, 325, 129-137.
8. Mentlein, R. Therapeutic assessment of glucagon-like peptide-1 agonists compared with dipeptidyl peptidase IV inhibitors as potential antidiabetic drugs. *Expert Opin. Invest. Drugs* **2005**, 14, 57-64.
9. Park, J. E.; Lenter, M. C.; Zimmermann, R. N.; Garin-Chesa, P.; Old, L. J.; Rettig, W. J. Fibroblast activation protein, a dual specificity serine protease expressed in reactive human tumor stromal fibroblasts. *J. Biol. Chem.* **1999**, 274, 36505-36512.

10. Busek, P.; Malik, R.; Sedo, A. Dipeptidyl peptidase IV activity and/or structure homologues (DASH) and their substrates in cancer. *Int. J. Biochem. Cell Biol.* **2004**, 36, 408-421.
11. Mentlein, R. Dipeptidyl-peptidase IV (CD26)-role in the inactivation of regulatory peptides. *Regul. Pept.* **1999**, 85, 9-24.
12. Cunningham, D. F.; O'Connor, B. Proline specific peptidases. *Biochimica et Biophysica Acta - Protein Structure and Molecular Enzymology* **1997**, 1343, 160-186.
13. Šedo, A.; Malík, R. Dipeptidyl peptidase IV-like molecules: Homologous proteins or homologous activities? *Biochimica et Biophysica Acta - Protein Structure and Molecular Enzymology* **2001**, 1550, 107-116.
14. Kelly, T. Evaluation of seprase activity. *Clin. Exp. Metastas.* **1999**, 17, 57-62.
15. Gorrell, M. D. Dipeptidyl peptidase IV and related enzymes in cell biology and liver disorders. *Clin. Sci.* **2005**, 108, 277-292.
16. Chen, W. T.; Kelly, T.; Ghersi, G. DPPIV, seprase, and related serine peptidases in multiple cellular functions. In *Curr. Top. Dev. Biol.*, 2003; Vol. 54, pp 207-232.
17. Collins, P. J.; McMahon, G.; O'Brien, P.; O'Connor, B. Purification, identification and characterisation of seprase from bovine serum. *Int. J. Biochem. Cell. B.* **2004**, 36, 2320-2333.
18. Aimes, R. T.; Zijlstra, A.; Hooper, J. D.; Ogbourne, S. M.; Sit, M. L.; Fuchs, S.; Gotley, D. C.; Quigley, J. P.; Antalis, T. M. Endothelial cell serine proteases expressed during vascular morphogenesis and angiogenesis. *Thromb. Haemostasis* **2003**, 89, 561-572.
19. Santos, A. M.; Jung, J.; Aziz, N.; Kissil, J. L.; Puré, E. Targeting fibroblast activation protein inhibits tumor stromagenesis and growth in mice. *J. Clin. Invest.* **2009**, doi: 10.1172/JCI38988.

20. Juillerat-Jeanneret, L.; Gerber-Lemaire, S. The prolyl-aminodipeptidases and their inhibitors as therapeutic targets for fibrogenic disorders. *Mini reviews in medicinal chemistry* **2009**, 9, 215-226.
21. Juillerat-Jeanneret, L. Prolyl-specific peptidases and their inhibitors in biological processes. *Curr. Chem. Biol.* **2008**, 2, 97-109.
22. Yoshimoto, T.; Orlowski, R. C.; Walter, R. Postproline cleaving enzyme: Identification as serine protease using active site specific inhibitors. *Biochemistry* **1977**, 16, 2942-2948.
23. Yokosawa, H.; Nishikata, M.; Ishii, S. N-Benzylloxycarbonyl-valyl-prolinal, a potent inhibitor of post-proline cleaving enzyme. *J. Biochem.* **1984**, 95, 1819-1821.
24. Friedman, T. C.; Orlowski, M.; Wilk, S. Prolyl endopeptidase: Inhibition in vivo by N-benzylloxycarbonyl-prolyl-prolinal. *J. Neurochem.* **1984**, 42, 237-241.
25. Wilk, S. Prolyl endopeptidase. *Life Sci.* **1983**, 33, 2149-2157.
26. Irazusta, J.; Larrinaga, G.; González-Maeso, J.; Gil, J.; Meana, J. J.; Casis, L. Distribution of prolyl endopeptidase activities in rat and human brain. *Neurochem. Int.* **2002**, 40, 337-345.
27. O'Leary, R. M.; Gallagher, S. P.; O'Connor, B. Purification and characterization of a novel membrane-bound form of prolyl endopeptidase from bovine brain. *Int. J. Biochem. Cell Biol.* **1996**, 28, 441-449.
28. Fülöp, V.; Böcskei, Z.; Polgár, L. Prolyl oligopeptidase: an unusual beta-propeller domain regulates proteolysis. *Cell* **1998**, 94, 161-170.
29. Bastos, I. M. D.; Grellier, P.; Martins, N. F.; Cadavid-Restrepo, G.; De Souza-Ault, M. R.; Augustyns, K.; Teixeira, A. R. L.; Schrével, J.; Maigret, B.; Da Silveira, J. F.; Santana, J. M. Molecular, functional and structural properties of the prolyl oligopeptidase of *Trypanosoma cruzi* (POP Tc80), which is required for parasite entry into mammalian cells. *Biochem. J.* **2005**, 388, 29-38.
30. Szeltner, Z.; Rea, D.; Juhasz, T.; Renner, V.; Fülöp, V.; Polgár, L. Concerted structural changes in the peptidase and the propeller domains of prolyl

oligopeptidase are required for substrate binding. *J. Mol. Biol.* **2004**, 340, 627-637.

31. Mantle, D.; Falkous, G.; Ishiura, S.; Blanchard, P. J.; Perry, E. K. Comparison of proline endopeptidase activity in brain tissue from normal cases and cases with Alzheimer's disease, Lewy body dementia, Parkinson's disease and Huntington's disease. *Clin. Chim. Acta* **1996**, 249, 129-139.

32. García-Horsman, J. A.; Männistö, P. T.; Venäläinen, J. I. On the role of prolyl oligopeptidase in health and disease. *Neuropeptides* **2007**, 41, 1-24.

33. Williams, R. S. B. Prolyl oligopeptidase and bipolar disorder. *Clin. Neurosci. Res.* **2004**, 4, 233-242.

34. Shinoda, M.; Toide, K.; Ohsawa, I.; Kohsaka, S. Specific inhibitor for prolyl endopeptidase suppresses the generation of amyloid β protein in NG108-15 cells. *Biochem. Biophys. Res. Commun.* **1997**, 235, 641-645.

35. Petit, A.; Barelli, H.; Morain, P.; Checler, F. Novel proline endopeptidase inhibitors do not modify A β 40/42 formation and degradation by human cells expressing wild-type and Swedish mutated β -amyloid precursor protein. *Br. J. Pharmacol.* **2000**, 130, 1613-1617.

36. Portevin, B.; Benoist, A.; Rémond, G.; Herve, Y.; Vincent, M.; Lepagnol, J.; De Nanteuil, G. New prolyl endopeptidase inhibitors: In vitro and in vivo activities of azabicyclo[2.2.2]octane, azabicyclo[2.2.1]heptane, and perhydroindole derivatives. *J. Med. Chem.* **1996**, 39, 2379-2391.

37. Roßner, S.; Schulz, I.; Zeitschel, U.; Schliebs, R.; Bigl, V.; Demuth, H. U. Brain prolyl endopeptidase expression in aging, APP transgenic mice and Alzheimer's disease. *Neurochem. Res.* **2005**, 30, 695-702.

38. Kato, A.; Fukunari, A.; Sakai, Y.; Nakajima, T. Prevention of amyloid-like deposition by a selective prolyl endopeptidase inhibitor, Y-29794, in senescence-accelerated mouse. *J. Pharmacol. Exp. Ther.* **1997**, 283, 328-335.

39. Katsube, N.; Sunaga, K.; Aishita, H.; Chuang, D. M.; Ishitani, R. ONO-1603, a potential antidementia drug, delays age-induced apoptosis and suppresses

overexpression of glyceraldehyde-3-phosphate dehydrogenase in cultured central nervous system neurons. *J. Pharmacol. Exp. Ther.* **1999**, 288, 6-13.

40. Toide, K.; Shinoda, M.; Fujiwara, T.; Iwamoto, Y. Effect of a novel prolyl endopeptidase inhibitor, JTP-4819, on spatial memory and central cholinergic neurons in aged rats. *Pharmacol., Biochem. Behav.* **1997**, 56, 427-434.

41. Toide, K.; Shinoda, M.; Iwamoto, Y.; Fujiwara, T.; Okamiya, K.; Uemura, A. A novel propyl endopeptidase inhibitor, JTP-4819, with potential for treating Alzheimer's disease. *Behav. Brain Res.* **1997**, 83, 147-151.

42. Fukunari, A.; Kato, A.; Sakai, Y.; Yoshimoto, T.; Ishiura, S.; Suzuki, K.; Nakajima, T. CoLocalization of prolyl endopeptidase and amyloid P-peptide in brains of senescence-accelerated mouse. *Neurosci. Lett.* **1994**, 176, 201-204.

43. Laitinen, K. S. M.; Van Groen, T.; Tanila, H.; Venäläinen, J.; Männistö, P. T.; Alafuzoff, I. Brain prolyl oligopeptidase activity, is associated with neuronal damage rather than β -amyloid accumulation. *NeuroReport* **2001**, 12, 3309-3312.

44. Brandt, I.; Vriendt, K. D.; Devreese, B.; Beeumen, J. V.; Dongen, W. V.; Augustyns, K.; Meester, I. D.; Scharpé, S.; Lambeir, A. M. Search for substrates for prolyl oligopeptidase in porcine brain. *Peptides* **2005**, 26, 2536-2546.

45. Brandt, I.; Gérard, M.; Sergeant, K.; Devreese, B.; Baekelandt, V.; Augustyns, K.; Scharpé, S.; Engelborghs, Y.; Lambeir, A. M. Prolyl oligopeptidase stimulates the aggregation of α -synuclein. *Peptides* **2008**, 29, 1472-1478.

46. Myöhänen, T. T.; Venäläinen, J. I.; Tupala, E.; Garcia-Horsman, J. A.; Miettinen, R.; Männistö, P. T. Distribution of immunoreactive prolyl oligopeptidase in human and rat brain. *Neurochem. Res.* **2007**, 32, 1365-1374.

47. Myöhänen, T. T.; Venäläinen, J. I.; Garcia-Horsman, J. A.; Männistö, P. T. Spatial association of prolyl oligopeptidase, inositol 1,4,5-triphosphate type 1 receptor, substance P and its neurokinin-1 receptor in the rat brain: An immunohistochemical colocalization study. *Neuroscience* **2008**, 153, 1177-1189.

48. Schulz, I.; Zeitschel, U.; Rudolph, T.; Ruiz-Carrillo, D.; Rahfeld, J. U.; Gerhartz, B.; Bigl, V.; Demuth, H. U.; Roßner, S. Subcellular localization suggests novel functions for prolyl endopeptidase in protein secretion. *J. Neurochem.* **2005**, 94, 970-979.
49. Myöhänen, T. T.; Venäläinen, J. I.; Garcia-Horsman, J. A.; Piltonen, M.; Männistö, P. T. Cellular and subcellular distribution of rat brain prolyl oligopeptidase and its association with specific neuronal neurotransmitters. *J. Comp. Neurol.* **2008**, 507, 1694-1708.
50. Brandt, I.; Scharpé, S.; Lambeir, A. M. Suggested functions for prolyl oligopeptidase: A puzzling paradox. *Clin. Chim. Acta* **2007**, 377, 50-61.
51. Polgár, L. Oligopeptidase B: A new type of serine peptidase with a unique substrate-dependent temperature sensitivity. *Biochemistry* **1999**, 38, 15548-15555.
52. Orłowski, M.; Wilk, E.; Pearce, S.; Wilk, S. Purification and properties of a prolyl endopeptidase from rabbit brain. *J. Neurochem.* **1979**, 33, 461-469.
53. Weber, A. E. Dipeptidyl peptidase IV inhibitors for the treatment of diabetes. *J. Med. Chem.* **2004**, 47, 4135-4141.
54. Knisatschek, H.; Bauer, K. Characterization of 'thyroliberin-deamidating enzyme' as a post-proline-cleaving enzyme: Partial purification and enzyme-chemical analysis of the enzyme from anterior pituitary tissue. *J. Biol. Chem.* **1979**, 254, 10936-10943.
55. Moriyama, A.; Nakanishi, M.; Sasaki, M. Porcine muscle prolyl endopeptidase and its endogenous substrates. *J. Biochem.* **1988**, 104, 112-117.
56. Koida, M.; Walter, R. Post proline cleaving enzyme. Purification of this endopeptidase by affinity chromatography. *J. Biol. Chem.* **1976**, 251, 7593-7599.
57. Greene, L. J.; Spadaro, A. C. C.; Martins, A. R. Brain endo-oligopeptidase B: A post-proline cleaving enzyme that inactivates angiotensin I and II. *Hypertension* **1982**, 4, 178-184.
58. Mendez, M.; Cruz, C.; Joseph-Bravo, P.; Wilk, S.; Charli, J. L. Evaluation of the role of prolyl endopeptidase and pyroglutamyl peptidase I in the metabolism of LHRH and TRH in brain. *Neuropeptides* **1990**, 17, 55-62.

59. Tate, S. S. Purification and Properties of a Bovine Brain Thyrotropin-Releasing-Factor Deamidase. *Eur. J. Biochem.* **1981**, 118, 17-23.
60. Camargo, A. C. M.; Almeida, M. L. C.; Emson, P. C. Involvement of Endo-Oligopeptidases A and B in the Degradation of Neurotensin by Rabbit Brain. *J. Neurochem.* **1984**, 42, 1758-1761.
61. Walter, R.; Shlank, H.; Glass, J. D.; Schwartz, I. L.; Kerenyi, T. D. Leucylglycinamide released from oxytocin by human uterine enzyme. *Science* **1971**, 173, 827-829.
62. Hersh, L. B.; McKelvy, J. F. Enzymes involved in the degradation of thyrotropin releasing hormone (TRH) and luteinizing hormone releasing hormone (LH-RH) in bovine brain. *Brain Res.* **1979**, 168, 553-564.
63. Bøler, J.; Enzmann, F.; Folkers, K.; Bowers, C. Y.; Schally, A. V. The identity of chemical and hormonal properties of the thyrotropin releasing hormone and pyroglutamyl-histidyl-proline amide. *Biochem. Biophys. Res. Commun.* **1969**, 37, 705-710.
64. Schulz, I.; Gerhartz, B.; Neubauer, A.; Holloschi, A.; Heiser, U.; Hafner, M.; Demuth, H. U. Modulation of inositol 1,4,5-triphosphate concentration by prolyl endopeptidase inhibition. *Eur. J. Biochem.* **2002**, 269, 5813-5820.
65. Schneider, J. S.; Giardiniere, M.; Morain, P. Effects of the prolyl endopeptidase inhibitor S 17092 on cognitive deficits in Chronic low dose MPTP-treated monkeys. *Neuropsychopharmacol.* **2002**, 26, 176-182.
66. Kovács, G. L.; De Wied, D. Peptidergic modulation of learning and memory processes. *Pharmacol. Rev.* **1994**, 46, 269-291.
67. Barelli, H.; Petit, A.; Hirsch, E.; Wilk, S.; De Nanteuil, G.; Morain, P.; Checler, F. S 17092-1, a highly potent, specific and cell permeant inhibitor of human proline endopeptidase. *Biochem. Biophys. Res. Commun.* **1999**, 257, 657-661.
68. Bellemère, G.; Morain, P.; Vaudry, H.; Jégou, S. Effect of S 17092, a novel prolyl endopeptidase inhibitor, on substance P and α -melanocyte-

stimulating hormone breakdown in the rat brain. *J. Neurochem.* **2003**, 84, 919-929.

69. Tarragó, T.; Masdeu, C.; Gómez, E.; Isambert, N.; Lavilla, R.; Giralt, E. Benzimidazolium salts as small, nonpeptidic and BBB-permeable human prolyl oligopeptidase inhibitors. *ChemMedChem* **2008**, 3, 1558-1565.

70. Tarragó, T.; Kichik, N.; Claasen, B.; Prades, R.; Teixidó, M.; Giralt, E. Baicalin, a prodrug able to reach the CNS, is a prolyl oligopeptidase inhibitor. *Bioorg. Med. Chem.* **2008**, 16, 7516-7524.

71. Juillerat-Jeanneret, L. The targeted delivery of cancer drugs across the blood-brain barrier: chemical modifications of drugs or drug-nanoparticles? *Drug Discov. Today* **2008**, 13, 1099-1106.

72. Umemura, K.; Kondo, K.; Ikeda, Y.; Kobayashi, T.; Urata, Y.; Nakashima, M. Pharmacokinetics and safety of JTP-4819, a novel specific orally active prolyl endopeptidase inhibitor, in healthy male volunteers. *Br. J. Clin. Pharmacol.* **1997**, 43, 613-618.

73. Morain, P.; Lestage, P.; De Nanteuil, G.; Jochemsen, R.; Robin, J. L.; Guez, D.; Boyer, P. A. S 17092: A prolyl endopeptidase inhibitor as a potential therapeutic drug for memory impairment. Preclinical and clinical studies. *CNS Drug Rev.* **2002**, 8, 31-52.

74. Morain, P.; Robin, J. L.; De Nanteuil, G.; Jochemsen, R.; Heidet, V.; Guez, D. Pharmacodynamic and pharmacokinetic profile of S 17092, a new orally active prolyl endopeptidase inhibitor, in elderly healthy volunteers. A phase I study. *Br. J. Clin. Pharmacol.* **2000**, 50, 350-359.

75. Szeltner, Z.; Rea, D.; Renner, V.; Fülöp, V.; Polgár, L. Electrostatic effects and binding determinants in the catalysis of prolyl oligopeptidase. Site specific mutagenesis at the oxyanion binding site. *J. Biol. Chem.* **2002**, 277, 42613-42622.

76. Szeltner, Z.; Rea, D.; Juhasz, T.; Renner, V.; Mucsi, Z.; Orosz, G.; Fülöp, V.; Polgár, L. Substrate-dependent competency of the catalytic triad of prolyl oligopeptidase. *J. Biol. Chem.* **2002**, 277, 44597-44605.

77. Szeltner, Z.; Rea, D.; Renner, V.; Juliano, L.; Fülöp, V.; Polgár, L. Electrostatic environment at the active site of prolyl oligopeptidase is highly influential during substrate binding. *J. Biol. Chem.* **2003**, 278, 48786-48793.
78. Shan, L.; Mathews, II; Khosla, C. Structural and mechanistic analysis of two prolyl endopeptidases: role of interdomain dynamics in catalysis and specificity. *Proc. Natl. Acad. Sci. U. S. A.* **2005**, 102, 3599-35604.
79. Kánai, K.; Arányi, P.; Böcskei, Z.; Ferenczy, G.; Harmat, V.; Simon, K.; Bátori, S.; Náray-Szabó, G.; Hermecz, I. Prolyl oligopeptidase inhibition by N-acyl-pro-pyrrolidine-type molecules. *J. Med. Chem.* **2008**, 51, 7514-7522.
80. Polgár, L. Prolyl endopeptidase catalysis. A physical rather than a chemical step is rate-limiting. *Biochemistry* **1992**, 283, 647-648.
81. Berger, Y.; Bernasconi, C. C.; Schmitt, F.; Neier, R.; Juillerat-Jeanneret, L. Determination of intracellular prolyl/glycyl proteases in intact living human cells and protoporphyrin IX production as a reporter system. *Chem. Biol.* **2005**, 12, 867-872.
82. De Nanteuil, G.; Portevin, B.; Lepagnol, J. Prolyl endopeptidase inhibitors: A new class of memory enhancing drugs. *Drug Future* **1998**, 23, 167-179.
83. Wilk, S.; Orłowski, M. Inhibition of Rabbit Brain Prolyl Endopeptidase by N-Benzyloxycarbonyl-Prolyl-Prolinal, a Transition State Aldehyde Inhibitor. *J. Neurochem.* **1983**, 41, 69-75.
84. Bakker, A. V.; Jung, S.; Spencer, R. W.; Vinick, F. J.; Faraci, W. S. Slow tight-binding inhibition of prolyl endopeptidase by benzyloxycarbonyl-prolyl-prolinal. *Biochem. J.* **1990**, 271, 559-562.
85. Niestroj, A. J.; UHeiser, U.; Demuth, H. U.; Aust, S. Inhibitors of prolyl endopeptidase. US 7,592,467 B2, 2009.
86. Li, J.; Wilk, E.; Wilk, S. Inhibition of prolyl oligopeptidase by Fmoc-aminoacylpyrrolidine-2-nitriles. *J. Neurochem.* **1996**, 66, 2105-2112.
87. Yoshimoto, T.; Fischl, M.; Orłowski, R. C.; Walter, R. Post-proline cleaving enzyme and post-proline dipeptidyl aminopeptidase. Comparison of two

peptidases with high specificity for proline residues. *J. Biol. Chem.* **1978**, 253, 3708-3716.

88. Yoshimoto, T.; Ogita, K.; Walter, R.; Koida, M.; Tsuru, D. Post-proline cleaving enzyme. Synthesis of a new fluorogenic substrate and distribution of the endopeptidase in rat tissues and body fluids of man. *Biochim. Biophys. Acta* **1979**, 569, 184-192.

89. Yoshimoto, T.; Simmons, W. H.; Kita, T.; Tsuru, D. Post-proline cleaving enzyme from lamb brain. *J. Biochem.* **1981**, 90, 325-334.

90. Yoshimoto, T.; Tsukumo, K.; Takatsuka, N.; Tsuru, D. An inhibitor for post-proline cleaving enzyme; distribution and partial purification from porcine pancreas. *J. Pharmacobio-Dyn.* **1982**, 5, 734-740.

91. Yoshimoto, T.; Nishimura, T.; Kita, T.; Tsuru, D. Post-proline cleaving enzyme (prolyl endopeptidase) from bovine brain. *J. Biochem.* **1983**, 94, 1179-1190.

92. Yoshimoto, T.; Kado, K.; Matsubara, F.; Koriyama, N.; Kaneto, H.; Tsuru, D. Specific inhibitors for prolyl endopeptidase and their anti-amnesic effect. *J. Pharmacobio-Dyn.* **1987**, 10, 730-735.

93. Tsuru, D.; Yoshimoto, T.; Koriyama, N.; Furukawa, S. Thiazolidine derivatives as potent inhibitors specific for prolyl endopeptidase. *J. Biochem.* **1988**, 104, 580-586.

94. Yoshimoto, T.; Tsuru, D.; Yamamoto, N.; Ikezawa, R.; Furukawa, S. Structure activity relationship of inhibitors specific for prolyl endopeptidase. *Agric. Biol. Chem.* **1991**, 55, 37-43.

95. Nishikata, M.; Yokosawa, H.; Ishii, S. Synthesis and structure of prolinal-containing peptides, and their use as specific inhibitors of prolyl endopeptidases. *Chem. Pharm. Bull.* **1986**, 34, 2931-2936.

96. Tsuda, M.; Muraoka, Y.; Nagai, M.; Aoya, T.; Takeuchi, T. Poststatin, a new inhibitor of prolyl endopeptidase. VIII. Endopeptidase inhibitory activity of non-peptidyl poststatin analogues. *J. Antibiot.* **1996**, 49, 1022-1030.

97. Tsuda, M.; Muraoka, Y.; Nagai, M.; Aoyagi, T.; Takeuchi, T. Poststatin, a new inhibitor of prolyl endopeptidase. VII. N-cycloalkylamide analogues. *J. Antibiot.* **1996**, 49, 909-920.
98. Tsuda, M.; Muraoka, Y.; Nagai, M.; Aoyagi, T.; Takeuchi, T. Poststatin, a new inhibitor of prolyl endopeptidase. V. Endopeptidase inhibitory activity of poststatin analogues. *J. Antibiot.* **1996**, 49, 890-899.
99. Tsuda, M.; Muraoka, Y.; Someno, T.; Nagai, M.; Aoyagi, T.; Takeuchi, T. Poststatin, a new inhibitor of prolyl endopeptidase. VI. Endopeptidase inhibitory activity of poststatin analogues containing pyrrolidine ring. *J. Antibiot.* **1996**, 49, 900-908.
100. Augustyns, K.; Borloo, M.; Belyaev, A.; Rajan, P.; Goossens, F.; Hendriks, D.; Scharpe, S.; Haemers, A. Synthesis of peptidyl acetals as inhibitors of prolyl endopeptidase. *Bioorg. Med. Chem. Lett.* **1995**, 5, 1265-1270.
101. Bal, G.; Van Der Veken, P.; Antonov, D.; Lambeir, A. M.; Grellier, P.; Croft, S. L.; Augustyns, K.; Haemers, A. Prolylisoxazoles: Potent inhibitors of prolyl oligopeptidase with antitrypanosomal activity. *Bioorg. Med. Chem. Lett.* **2003**, 13, 2875-2878.
102. Vendeville, S.; Bourel, L.; Davioud-Charvet, E.; Grellier, P.; Deprez, B.; Sergheraert, C. Automated parallel synthesis of a tetrahydroisoquinolin-based library: Potential prolyl endopeptidase inhibitors. *Bioorg. Med. Chem. Lett.* **1999**, 9, 437-442.
103. Vendeville, S.; Buisine, E.; Williard, X.; Schrevel, J.; Grellier, P.; Santana, J.; Sergheraert, C. Identification of inhibitors of an 80 kDa protease from *Trypanosoma cruzi* through the screening of a combinatorial peptide library. *Chem. Pharm. Bull.* **1999**, 47, 194-198.
104. Vendeville, S.; Goossens, F.; Debreu-Fontaine, M. A.; Landry, V.; Davioud-Charvet, E.; Grellier, P.; Scharpe, S.; Sergheraert, C. Comparison of the inhibition of human and *Trypanosoma cruzi* prolyl endopeptidases. *Bioorg. Med. Chem.* **2002**, 10, 1719-1729.
105. Stöckel-Maschek, A.; Mrestani-Klaus, C.; Stiebitz, B.; Demuth, H. U.; Neubert, K. Thioxo amino acid pyrrolidides and thiazolidides: New inhibitors of

proline specific peptidases. *Biochim. Biophys. Acta, Protein Struct. Mol. Enzymol.* **2000**, 1479, 15-31.

106. Joyeau, R.; Maoulida, C.; Guillet, C.; Frappier, F.; Teixeira, A. R. L.; Schrével, J.; Santana, J.; Grellier, P. Synthesis and activity of pyrrolidinyl- and thiazolidinyl-dipeptide derivatives as inhibitors of the Tc80 prolyl oligopeptidase from *Trypanosoma cruzi*. *Eur. J. Med. Chem.* **2000**, 35, 257-266.

107. Kánai, K.; Erdo, S.; Susán, E.; Feher, M.; Sipos, J.; Podányi, B.; Szappanos, A.; Hermecz, I. Prolyl endopeptidase inhibitors: N-acyl derivatives of L-thioprolinyl- pyrrolidine. *Bioorg. Med. Chem. Lett.* **1997**, 7, 1701-1704.

108. Arai, H.; Nishioka, H.; Niwa, S.; Yamanaka, T.; Tanaka, Y.; Yoshinaga, K.; Kobayashi, N.; Miura, N.; Ikeda, Y. Synthesis of prolyl endopeptidase inhibitors and evaluation of their structure-activity relationships: In vitro inhibition of prolyl endopeptidase from canine brain. *Chem. Pharm. Bull.* **1993**, 41, 1583-1588.

109. Tanaka, Y.; Niwa, S.; Nishioka, H.; Yamanaka, T.; Torizuka, M.; Yoshinaga, K.; Kobayashi, N.; Ikeda, Y.; Arai, H. New potent prolyl endopeptidase inhibitors: Synthesis and structure- activity relationships of indan and tetralin derivatives and their analogues. *J. Med. Chem.* **1994**, 37, 2071-2078.

110. Asano, M.; Nio, N.; Ariyoshi, Y. Inhibition of prolyl endopeptidase by synthetic beta-casein peptides and their derivatives with a C-terminal prolinol or prolinal. *Biosci., Biotechnol., Biochem.* **1992**, 56, 976-977.

111. Tsutsumi, S.; Okonogi, T.; Shibahara, S.; Ohuchi, S.; Hatsushiba, E.; Patchett, A. A.; Christensen, B. G. Synthesis and structure-activity relationships of peptidyl α -keto heterocycles as novel inhibitors of prolyl endopeptidase. *J. Med. Chem.* **1994**, 37, 3492-3502.

112. Tsutsumi, S.; Okonogi, T.; Shibahara, S.; Patchett, A. A.; Christensen, B. G. α -Ketothiazole inhibitors of prolyl endopeptidase. *Bioorg. Med. Chem. Lett.* **1994**, 4, 831-834.

113. Toide, K.; Iwamoto, Y.; Fujiwara, T.; Abe, H. JTP-4819: A novel prolyl endopeptidase inhibitor with potential as a cognitive enhancer. *J. Pharmacol. Exp. Ther.* **1995**, 274, 1370-1378.
114. Toide, K.; Okamiya, K.; Iwamoto, Y.; Kato, T. Effect of a novel prolyl endopeptidase inhibitor, JTP-4819, on prolyl endopeptidase activity and substance P- and arginine-vasopressin-like immunoreactivity in the brains of aged rats. *J. Neurochem.* **1995**, 65, 234-240.
115. Toide, K.; Fujiwara, T.; Iwamoto, Y.; Shinoda, M.; Okamiya, K.; Kato, T. Effect of a novel prolyl endopeptidase inhibitor, JTP-4819, on neuropeptide metabolism in the rat brain. *Naunyn-Schmiedeberg's Arch. Pharmacol.* **1996**, 353, 355-362.
116. Toide, K.; Shinoda, M.; Iwamoto, Y.; Fujiwara, T.; Abe, H.; Uchida, I. A novel prolyl endopeptidase inhibitor, JTP-4819, for the treatment of Alzheimer's disease: Review of preclinical pharmacology. *CNS Drug Rev.* **1996**, 2, 343-362.
117. Bakker, A. V.; Daffeh, J.; Jung, S.; Vincent, L. A.; Nagel, A. A.; Spencer, R. W.; Vinick, F. J.; Faraci, W. S. Novel in vitro and in vivo inhibitors of prolyl endopeptidase. *Bioorg. Med. Chem. Lett.* **1991**, 1, 585-590.
118. Wallén, E. A. A.; Christiaans, J. A. M.; Saario, S. M.; Forsberg, M. M.; Venäläinen, J. I.; Paso, H. M.; Männistö, P. T.; Gynther, J. 4-Phenylbutanoyl-2(S)-acylpyrrolidines and 4-phenylbutanoyl-L-prolyl-2(S)-acylpyrrolidines as prolyl oligopeptidase inhibitors. *Bioorg. Med. Chem.* **2002**, 10, 2199-2206.
119. Wallén, E. A. A.; Christiaans, J. A. M.; Forsberg, M. M.; Venäläinen, J. I.; Männistö, P. T.; Gynther, J. Dicarboxylic acid bis(L-prolyl-pyrrolidine) amides as prolyl oligopeptidase inhibitors. *J. Med. Chem.* **2002**, 45, 4581-4584.
120. Wallén, E. A. A.; Christiaans, J. A. M.; Jarho, E. M.; Forsberg, M. M.; Venäläinen, J. I.; Männistö, P. T.; Gynther, J. New prolyl oligopeptidase inhibitors developed from dicarboxylic acid bis(L-prolyl-pyrrolidine) amides. *J. Med. Chem.* **2003**, 46, 4543-4551.
121. Wallén, E. A. A.; Christiaans, J. A. M.; Saarinen, T. J.; Jarho, E. M.; Forsberg, M. M.; Venäläinen, J. I.; Männistö, P. T.; Gynther, J. Conformationally

rigid N-acyl-5-alkyl-L-prolyl-pyrrolidines as prolyl oligopeptidase inhibitors. *Bioorg. Med. Chem.* **2003**, 11, 3611-3619.

122. Venäläinen, J. I.; Juvonen, R. O.; Garcia-Horsman, J. A.; Wallén, E. A. A.; Christiaans, J. A. M.; Jarho, E. M.; Gynther, J.; Männistö, P. T. Slow-binding inhibitors of prolyl oligopeptidase with different functional groups at the P1 site. *Biochem. J.* **2004**, 382, 1003-1008.

123. Jarho, E. M.; Venäläinen, J. I.; Huuskonen, J.; Christiaans, J. A. M.; Garcia-Horsman, J. A.; Forsberg, M. M.; Järvinen, T.; Gynther, J.; Männistö, P. T.; Wallén, E. A. A. A cyclopent-2-enecarbonyl group mimics proline at the P2 position of prolyl oligopeptidase inhibitors. *J. Med. Chem.* **2004**, 47, 5605-5607.

124. Jarho, E. M.; Wallén, E. A. A.; Christiaans, J. A. M.; Forsberg, M. M.; Venäläinen, J. I.; Männistö, P. T.; Gynther, J.; Poso, A. Dicarboxylic acid azacycle L-prolyl-pyrrolidine amides as prolyl oligopeptidase inhibitors and three-dimensional quantitative structure-activity relationship of the enzyme-inhibitor interactions. *J. Med. Chem.* **2005**, 48, 4772-4782.

125. Venäläinen, J. I.; Wallén, E. A. A.; Poso, A.; Garcia-Horsman, J. A.; Männistö, P. T. Synthesis and characterization of the novel fluorescent prolyl oligopeptidase inhibitor 4-fluoresceinthiocarbamoyl-6-aminocaproyl-L-prolyl-2(S)-(hydroxyacetyl)pyrrolidine. *J. Med. Chem.* **2005**, 48, 7093-7095.

126. Venäläinen, J. I.; Garcia-Horsman, J. A.; Forsberg, M. M.; Jalkanen, A.; Wallén, E. A. A.; Jarho, E. M.; Christiaans, J. A. M.; Gynther, J.; Männistö, P. T. Binding kinetics and duration of in vivo action of novel prolyl oligopeptidase inhibitors. *Biochem. Pharmacol.* **2006**, 71, 683-692.

127. Jarho, E. M.; Venäläinen, J. I.; Juntunen, J.; Yli-Kokko, A. L.; Vepsäläinen, J.; Christiaans, J. A. M.; Forsberg, M. M.; Järvinen, T.; Männistö, P. T.; Wallén, E. A. A. An introduction of a pyridine group into the structure of prolyl oligopeptidase inhibitors. *Bioorg. Med. Chem. Lett.* **2006**, 16, 5590-5593.

128. Jarho, E. M.; Venäläinen, J. I.; Poutiainen, S.; Leskinen, H.; Vepsäläinen, J.; Christiaans, J. A. M.; Forsberg, M. M.; Männistö, P. T.; Wallén, E. A. A. 2(S)-(Cycloalk-1-enecarbonyl)-1-(4-phenyl-butanoyl)pyrrolidines and 2(S)-(aroyl)-1-

(4-phenylbutanoyl)pyrrolidines as prolyl oligopeptidase inhibitors. *Bioorg. Med. Chem.* **2007**, 15, 2024-2031.

129. Tran, T.; Quan, C.; Edosada, C. Y.; Mayeda, M.; Wiesmann, C.; Sutherlin, D.; Wolf, B. B. Synthesis and structure-activity relationship of N-acyl-Gly-, N-acyl-Sar- and N-blocked-boroPro inhibitors of FAP, DPP4, and POP. *Bioorg. Med. Chem. Lett.* **2007**, 17, 1438-1442.

130. Haffner, C. D.; Diaz, C. J.; Miller, A. B.; Reid, R. A.; Madauss, K. P.; Hassell, A.; Hanlon, M. H.; Porter, D. J. T.; Becherer, J. D.; Carter, L. H. Pyrrolidinyl pyridone and pyrazinone analogues as potent inhibitors of prolyl oligopeptidase (POP). *Bioorg. Med. Chem. Lett.* **2008**, 18, 4360-4363.

131. Atack, J. R.; Suman-Chauhan, N.; Dawson, G.; Kulagowski, J. J. In vitro and in vivo inhibition of prolyl endopeptidase. *Eur. J. Pharmacol.* **1991**, 205, 157-163.

132. Abe, M.; Muraoka, Y.; Kojima, F. Prolyl oligopeptidase inhibitor. WO 2005/027934, 2005.

133. Saito, M.; Hashimoto, M.; Kawaguchi, N.; Shibata, H.; Fukami, H.; Tanaka, T.; Higuchi, N. Synthesis and inhibitory activity of acyl-peptidyl-pyrrolidine derivatives toward post-proline cleaving enzyme; a study of subsite specificity. *J. Enzym. Inhib.* **1991**, 5, 51-75.

134. Katsube, N.; Ishitani, R. A Review of the Neurotrophic and Neuroprotective Properties of ONO-1603: Comparison with Those of Tetrahydroaminoacridine, an Antidementia Drug. *CNS Drug Rev.* **2000**, 6, 21-34.

135. Nakajima, T.; Ono, Y.; Kato, A.; Maeda, J.; Ohe, T. Y-29794 - A non-peptide prolyl endopeptidase inhibitor that can penetrate into the brain. *Neurosci. Lett.* **1992**, 141, 156-160.

136. Kahyaoglu, A.; Haghjoo, K.; Kraicsovits, F.; Jordan, F.; Polgár, L. Benzyloxycarbonylprolylprolinal, a transition-state analogue for prolyl oligopeptidase, forms a tetrahedral adduct with catalytic serine, not a reactive cysteine. *Biochem. J.* **1997**, 322, 839-843.

137. Augustyns, K.; Vanhoof, G.; Borloo, M.; de Meester, I.; Goossens, F.; Haemers, A. Tetrahydroisoquinoline 3-carboxamide derivatives. WO 95/34538, 1995.
138. Shishido, Y.; Furushiro, M.; Tanabe, S.; Nishiyama, S.; Hashimoto, S.; Ohno, M.; Yamamoto, T.; Watanabe, S. ZTTA, a postproline cleaving enzyme inhibitor, improves cerebral ischemia-induced deficits in a three-panel runway task in rats. *Pharmacol., Biochem. Behav.* **1996**, 55, 333-338.
139. Tarragó, T.; Kichik, N.; Segú, J.; Giralt, E. The natural product berberine is a human prolyl oligopeptidase inhibitor. *ChemMedChem* **2007**, 2, 354-359.
140. Giraltlleló, E.; Tarragó Clua, M. T. Therapeutic agent for treatment of bipolar affective disorder in mammals. WO 2008/077978, 2008.
141. Edosada, C. Y.; Quan, C.; Wiesmann, C.; Tran, T.; Sutherlin, D.; Reynolds, M.; Elliott, J. M.; Raab, H.; Fairbrother, W.; Wolf, B. B. Selective inhibition of fibroblast activation protein protease based on dipeptide substrate specificity. *J. Biol. Chem.* **2006**, 281, 7437-7444.
142. Lawandi, J.; Toumieux, S.; Seyer, V.; Campbell, P.; Thielges, S.; Juillerat-Jeanneret, L.; Moitessier, N. Constrained peptidomimetics reveal detailed geometric requirements of covalent prolyl oligopeptidase inhibitors. *J. Med. Chem.* **2009**, 52, 6672-6684.
143. Aqvist, J.; Luzhkov, V. B.; Brandsdal, B. O. Ligand binding affinities from MD simulations. *Acc. Chem. Res.* **2002**, 35, 358-365.
144. Aqvist, J.; Medina, C.; Samuelsson, J. E. A new method for predicting binding affinity in computer-aided drug design. *Protein Eng.* **1994**, 7, 385-391.
145. Sirviö, J.; Lehtimäki, T. Prolyl oligopeptidase inhibitors ameliorating recovery from brain trauma. WO 2005/002624, 2005.
146. Juillerat-Jeanneret, L.; Schmitt, F. Chemical modification of therapeutic drugs or drug vector systems to achieve targeted therapy: Looking for the grail. *Med. Res. Rev.* **2007**, 27, 574-590.
147. Edosada, C. Y.; Quan, C.; Tran, T.; Pham, V.; Wiesmann, C.; Fairbrother, W.; Wolf, B. B. Peptide substrate profiling defines fibroblast activation protein as

an endopeptidase of strict Gly(2)-Pro(1)-cleaving specificity. *FEBS Lett.* **2006**, 580, 1581-1586.

148. Van der Veken, P.; De Meester, I.; Dubois, V.; Soroka, A.; Van Goethem, S.; Maes, M. B.; Brandt, I.; Lambeir, A. M.; Chen, X.; Haemers, A.; Scharpé, S.; Augustyns, K. Inhibitors of dipeptidyl peptidase 8 and dipeptidyl peptidase 9. Part 1: Identification of dipeptide derived leads. *Bioorg. Med. Chem. Lett.* **2008**, 18, 4154-4158.

149. Potashman, M. H.; Duggan, M. E. Covalent modifiers: an orthogonal approach to drug design. *J. Med. Chem.* **2009**, 52, 1231-1246.

150. Smith, A. J.; Zhang, X.; Leach, A. G.; Houk, K. N. Beyond picomolar affinities: quantitative aspects of noncovalent and covalent binding of drugs to proteins. *J. Med. Chem.* **2009**, 52, 225-33.

[This page was intentionally left blank]

Chapter 2 Constrained peptidomimetics reveal detailed geometric requirements of covalent prolyl oligopeptidase inhibitors

We used the criteria generated from our review in Chapter 1 to design a series of pseudopeptidic and constrained, bicyclic potential inhibitors having specific three-dimensional shapes and sizes. These compounds were conceived in order to better understand the geometric constraints of a selective and potent drug to target POP in organisms expressing multiple enzymes with very similar functions. Herein we discuss the synthesis of this series and the results of the biological assays performed on this series.

This chapter, aside from a few additions and corrections, is reproduced with permission from Lawandi, J.; Toumieux, S.; Seyer, V.; Campbell, P.; Thielges, S.; Juillerat-Jeanneret, L.; Moitessier, N. “Constrained peptidomimetics reveal detailed geometric requirements of covalent prolyl oligopeptidase inhibitors.” *Journal of Medicinal Chemistry* **2009**, 52, 6672-6684. Copyright 2009 American Chemical Society.

2.1 Abstract

Prolyl oligopeptidases cleave peptides on the carboxy side of internal proline residues and their inhibition has potential in the treatment of human brain disorders. Using our docking program FITTED, we have designed a series of constrained covalent inhibitors, built from a series of bicyclic scaffolds, to study the optimal shape required for these small molecules. These structures bear nitrile functional groups that we predicted to covalently bind to the catalytic serine of the enzyme. Synthesis and biological assays using human brain-derived astrocytic cells and endothelial cells and human fibroblasts revealed that these compounds act as selective inhibitors of prolyl oligopeptidase activity compared to prolyl-dipeptidyl-aminopeptidase activity, are able to penetrate the cells and inhibit intracellular activities in intact living cells. This integrated computational and experimental study shed light on the binding mode of inhibitors in the enzyme active site and will guide the design of future drug-like molecules.

2.2 Introduction

Prolyl oligopeptidase (POP, EC 3.4.21.26) is a large (about 80 kDa), highly conserved and widely distributed prolyl-selective serine endoprotease. Unlike other serine proteases, prolyl oligopeptidase can accommodate proline residues (and less frequently alanine residues) in its active site, cleaving short peptides on the carboxy side of these residues.¹ Over the last 15 years, abnormal POP activity, particularly in many regions of the brain,² has been linked to a number of diseases.³⁻⁵ As a consequence, POP is believed to be a target for the treatment of neurodegenerative (e.g., Alzheimer's disease) and psychiatric (e.g., bipolar disorder⁶) disorders. A number of POP inhibitors, including covalent inhibitors such as Cbz-Gly-prolinal (**2-1**), Cbz-Pro-prolinal (**2-2**)⁷ and JTP-4819 (**2-3**),^{8, 9} and non covalent inhibitors (e.g., SUAM-1221 (**2-4**)¹⁰ and S-17092-1 (**2-5**)¹¹) have been prepared and evaluated in various experimental models. Some of these POP inhibitors were found to improve memory and learning¹² in animal models of brain disorders and to prevent amyloid-like depositions.¹³⁻¹⁵ A few of these

inhibitors also exhibited good pharmacokinetic and safety profiles and were able to penetrate the blood-brain barrier.¹⁶ However, none has yet reached advanced clinical trials, and drug candidates are yet to be developed.

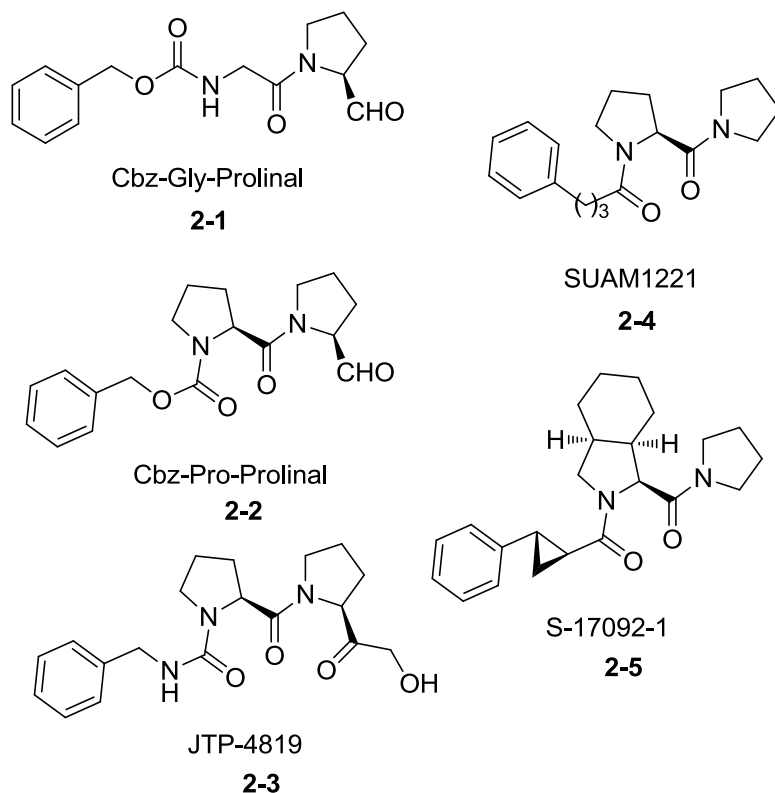


Figure 2.1 Selected POP inhibitors.

Although many POP inhibitors have been reported, a better understanding of the geometric and electronic requirements for a potent and selective POP inhibitor is still necessary in order to design improved POP inhibitors. Our aim in this study was not only to achieve selective inhibition of POP activity over other prolyl-specific proteases but also to reveal the optimal shape, size and electronic requirement of a potent POP inhibitor. To reach these goals, we have exploited an approach integrating structures available from X-ray crystallography data, docking predictions, higher level computations (e.g., density functional theory, DFT) and chemical tools. We have combined and applied all of these techniques, also evaluating the inhibition of enzymatic activity, to reveal insight into binding and inhibition modes that each of them alone cannot predict. Using this strategy, we have designed a series of pseudo peptidic and peptidomimetic inhibitors, many

of which are built around bicyclic scaffolds. These scaffolds closely mimic the known prolyl oligopeptidase inhibitor Cbz-Pro-prolinal (**2-1**, Figure 2.1).

We report herein docking predictions of a series of inhibitors into the active site of POP, followed by the synthesis and biological evaluation of the designed inhibitors in human cells. Of the entire series of compounds, one bicyclic scaffold exhibits high nanomolar inhibition of prolyl oligopeptidase activity and high selectivity over prolyl-dipeptidyl aminopeptidase activity in human brain astrocyte-derived cells, human brain-derived endothelial cells and human fibroblasts. Combining results from the computational modeling and biological evaluation, optimal inhibitor geometry is revealed.

2.3 Results

2.3.1 Computer-Aided Design of constrained inhibitors

We combined structural knowledge from reported inhibitor structures, docking experiments and evaluation of synthetic feasibility to design a series of inhibitors. To date, no crystal structure for the human isoform of prolyl oligopeptidase has been reported. However, a structure of POP from porcine brain (PDB code: 1h2y), which demonstrates 97% identity with the human form is available and can be used for docking experiments.¹⁷

As illustrated in Figure 2.2, this ligand-based design led us to the selected scaffold-based inhibitors, designed to mimic Fmoc-Ala-pyrrolidine-2-carbonitrile (**2-7**), previously shown to be a non-competitive inhibitor selective for POP over DPP-IV,¹⁸ and Cbz-Gly-prolinal (**2-1**). Several pieces of evidence,¹⁸ including a crystal structure of Cbz-Pro-prolinal bound to POP¹⁷ indicate that both inhibitors **2-1** and **2-7** are most likely reacting with the active site serine. For this work, we hypothesized that the designed inhibitors will also bind covalently to POP and covalent docking was carried out.

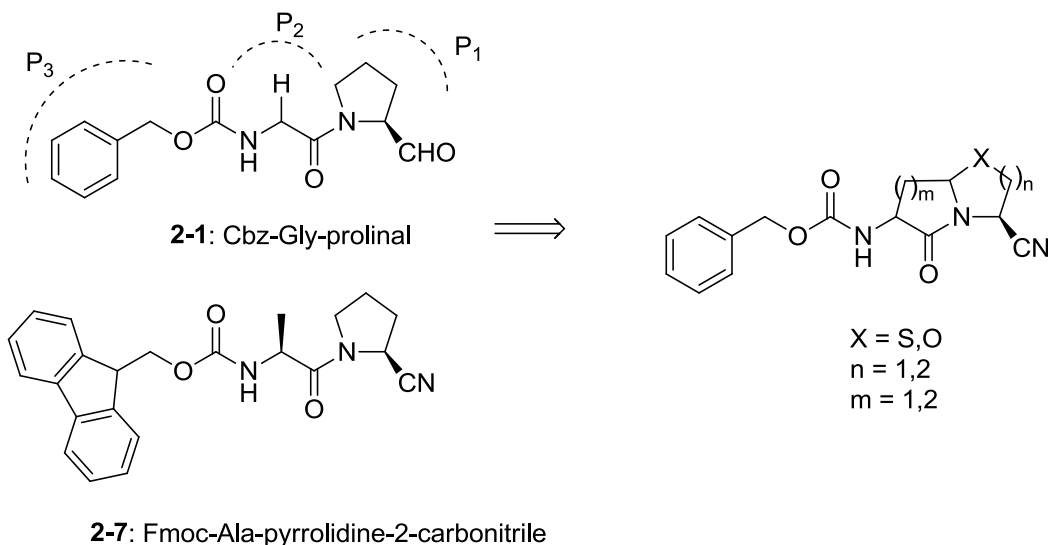


Figure 2.2 Pseudo peptidic inhibitors inspired from 2-1 and 2-7.

We used the latest version of our docking program FITTED (version 2.6)¹⁹⁻²¹ to dock various covalent inhibitors, mainly built around rigid, bicyclic scaffolds. However, we first had to modify the program to perform covalent docking. With the novel implementations in the program, FITTED can now automatically identify reactive functional groups in the ligands (e.g., aldehydes, nitrile), and then dock these ligands, evaluating both the non-covalent and covalent binding modes simultaneously. As mentioned in the design section, we planned to develop constrained structures that would mimic pseudopeptidic inhibitors. The major interaction of these compounds is the covalent bond. However, the scoring of the binding of covalent inhibitors requires to consider the reactivity of the reactive group (i.e., nitrile or aldehyde) which can vary significantly from one compound to another, as shown by Bayly and co-workers on a set of nitrile derivatives.²² As the scoring of covalent bonds would require more advanced and much more time consuming techniques to be accurate, our strategy cannot rely on generated scores. Instead, we applied a strategy that verified that the docked poses maintained the covalent bond and at least 2 of the 3 major interactions observed with these pseudo peptides. We have successfully applied this strategy to the design of metalloenzyme inhibitors as the metal coordination is not well scored either.²³

Typically, a docking program used in conjunction with a scoring function predicting the binding affinity of the docked ligand, gives high scores to good binders. However, none of the currently available scoring functions can handle covalent bonds formed upon docking. Thus, we visually inspected the docked poses, hypothesizing that if the bound pose retained the key interactions observed in the crystal structure, the docked ligand should be active. This assumption has been successfully exploited in other medicinal chemistry programs such as the development of nanomolar metalloprotease inhibitors.²³ Compound **2-2** binds to POP through two hydrogen bonds with the side chains of an arginine (Arg643) and a tryptophan (Trp595), while the 5-membered ring proline ring sits on the aromatic ring of the Trp595 side chain. We predicted, using FITTED, that when bound to POP, the bicyclic structure **2-8b** should retain the key interactions made by **2-2** (Figure 2.3). We therefore prioritized **2-8b** for immediate synthesis. Synthetic routes enabling the synthesis of a small set of analogues of **2-8b**, with different ring sizes and heteroatoms, were developed. By varying only a few atoms of the bicyclic scaffold, small changes in geometry and chemical properties were calculated. For example, DFT calculations were carried out on the analogous scaffolds **2-8b** and **2-9b** and revealed significant differences in the electronic distributions making the nitrile of **2-9b** less reactive (DFT results not shown).

In order to evaluate the impact of the conformational constraint of the bicyclic structures, we also designed and prepared a series of pseudo-peptides, closely resembling the bicyclic scaffolds, in order to compare the bioactivity of the flexible dipeptide to that of the corresponding rigid bicyclic scaffolds. From the docking study, we predicted that the five-membered proline ring of compounds **2-11a** and **2-12a,b** sits on the aromatic side chain of Trp595. Our docking studies also indicated that this interaction should be disrupted when a six-membered ring (**2-14**) is introduced; a loss of potency is expected. We chose to also synthesize **2-14** and test it to validate our docking predictions.

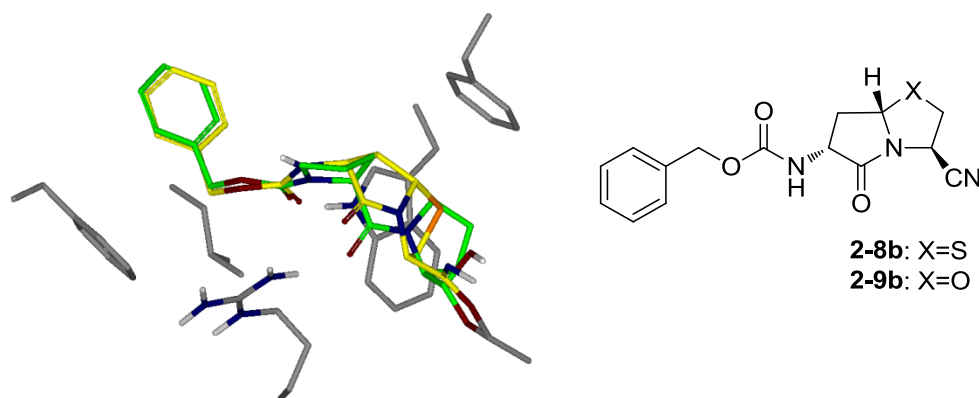
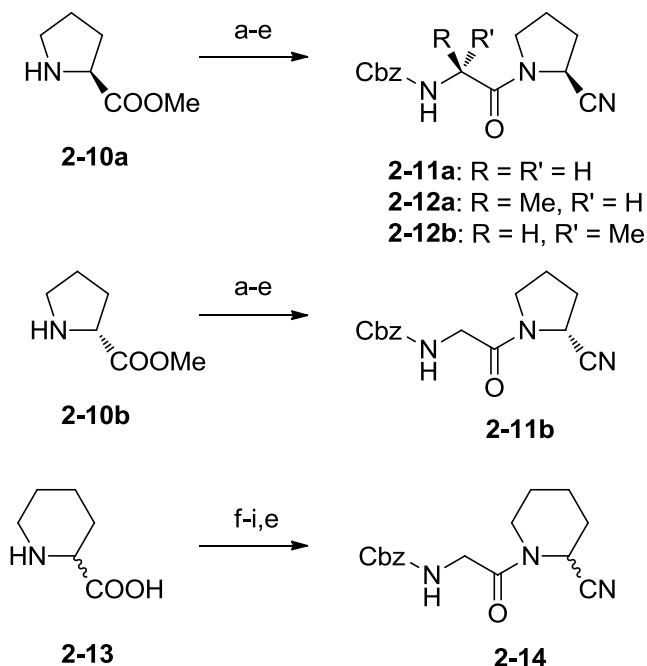


Figure 2.3 Docked designed covalent inhibitor (**2-8b**, green) overlaid with crystal structure of Cbz-Pro-prolinal (**2-2**, yellow).

2.3.2 Chemistry

Synthesis of the pseudopeptidic inhibitors.

The series of pseudo-peptides, incorporating either a piperidine-2-carbonitrile or pyrrolidine-2-carbonitrile moiety, was synthesized as described in Scheme 2.1. To synthesize Cbz-Gly-L/D-pyrrolidine-2-carbonitrile (**2-11a,b**) and Cbz-L/D-Ala-L-pyrrolidine-2-carbonitrile (**2-12a,b**), the pyrrolidine nitrile portions were prepared from L- and D-Pro methyl esters using previously reported procedures (see Experimental Section). Then, the nitrile derivatives were coupled to Cbz protected Ala and Gly residues. In parallel, we also prepared the racemic compound **2-14** from pipecolic acid **2-13**. The procedures used to prepare the pyrrolidine-2-carbonitriles were not as successful on pipecolic acid **2-13**. We therefore used slightly different methods to make **2-14** (listed in steps f-i of Scheme 2.1).



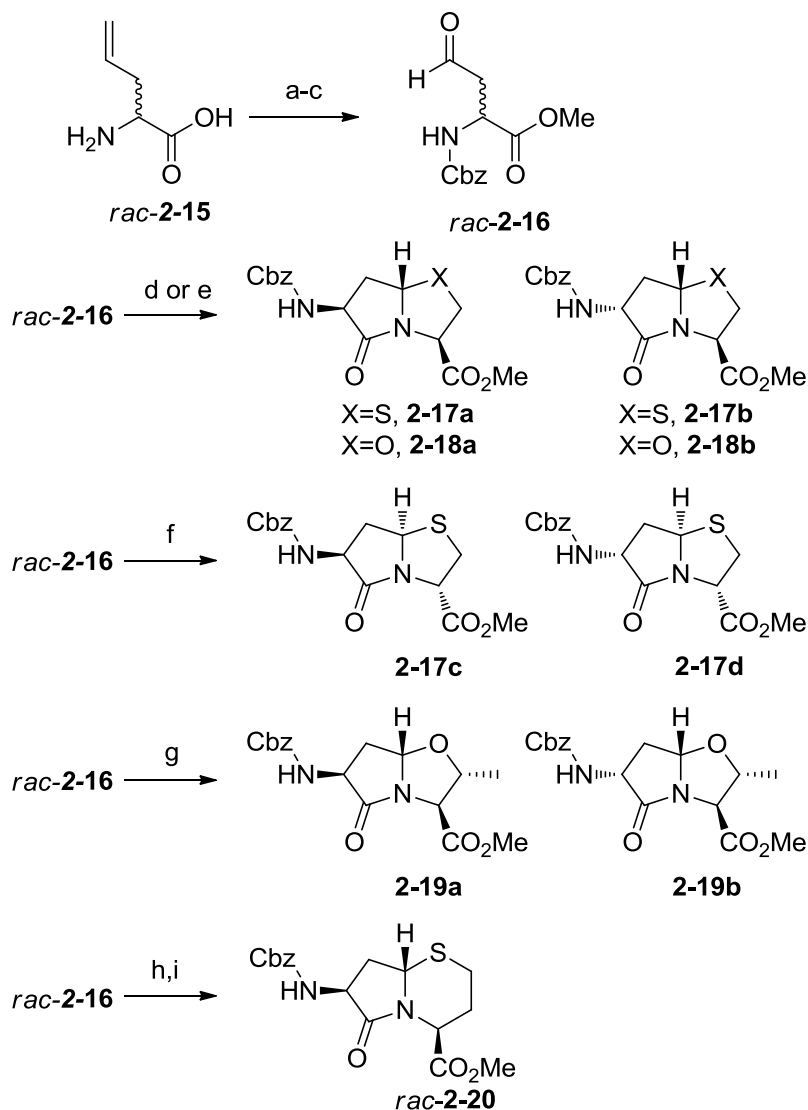
Scheme 2.1 Synthesis of the pseudopeptidic inhibitors.

(a) Boc_2O , Et_3N , DMAP, CH_2Cl_2 , 40%; (b) NH_3 (aq) 28%, THF, 60°C , 89%; (c) $(\text{CF}_3\text{CO})_2\text{O}$, Et_3N , THF, 0°C , 74-83%; (d) $\text{CF}_3\text{CO}_2\text{H}$, CH_2Cl_2 , 0°C , 29-53%; (e) RCOOH (Cbz-Gly-OH or Cbz-Ala-OH or Cbz-D-Ala-OH), Et_3N , HOBT, EDCI, CH_2Cl_2 , 30-65%; (f) Boc_2O , Et_3N , 1,4-dioxane/ H_2O , 82%; (g) ClCO_2Et , Et_3N , THF, -15°C then NH_3 (aq) 28%, rt, 83%; (h) $(\text{CF}_3\text{CO})_2\text{O}$, Et_3N , CH_2Cl_2 , 0°C , 52-68%; (i) HCl, 1,4-dioxane, 90%.

Synthesis of the bicyclic scaffolds.

Following the synthesis of the pseudo dipeptides, we synthesized the (5,5) fused scaffolds as enantiopure compounds or diastereomeric mixtures enriched in the diastereomer that we predicted to be most active from the docking and the initial results from the biological testing (Scheme 2.2).²⁴⁻²⁸ After protection of the amine and acid functions of allyl Gly *rac*-**2-15**,²⁹ we oxidized the alkene to the corresponding aldehyde *rac*-**2-16** in quantitative yields.³⁰ Reaction of this aldehyde (*rac*-**2-16**) with L-Cys-OMe at room temperature, and then at 50°C for several days in pyridine afforded the first two bicyclic structures **2-17a** and **2-17b** after careful chromatographic separation. Alternatively, we repeated this same procedure to prepare the desired bicyclic structures **2-17c** and **2-17d** as a separable 1:1 diastereomeric mixture. The same approach was applied to other

amino acids and we synthesized the scaffolds **2-18a** and **2-18b** from *rac*-**2-16** and L-Ser-OMe and **2-19a** and **2-19b** from *rac*-**2-16** and L-Thr-OMe.



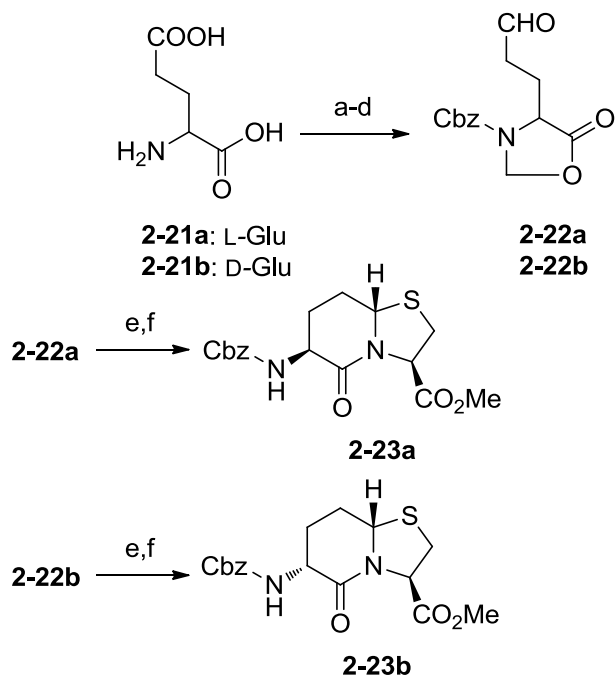
Scheme 2.2 Synthesis of the bicyclic scaffolds.

(a) TMSCl, CH₃OH, 0°C to R.T.; (b) CbzCl, Et₃N, 0°C; (c) O₃, CH₂Cl₂; then DMS (d) L-Cys-OMe, pyridine, molecular sieves; then pyridine, 50°C, 4 days, 48% **2-17a,b** (over 3 steps); (e) L-Ser-OMe, pyridine, molecular sieves; then pyridine, 50°C, 4 days, 49% of **2-18a,b** (over 3 steps); (f) (i) D-Cys-OH, pyridine, molecular sieves; then pyridine, 50°C, 4 days, 33% of **2-17c,d** (over 4 steps); (g) L-Thr-OMe, pyridine, molecular sieves; then pyridine, 50°C, 4 days, 35% of **2-19a,b** (over 3 steps); (h) L-homo-Cys-OH, pyridine, 50°C, 4 days (i) TMSCHN₂, CH₂Cl₂, 32% of *rac*-**2-20** (over 4 steps).

In order to probe the geometric requirement for optimal binding and to probe the computational predictions, the size of the right-hand 5-membered ring was

expanded to **2-20** as a mimic of **2-14**. *rac*-**2-20** was prepared following synthetic routes similar to the one used previously (Scheme 2.2). In contrast to the synthesis of the 5,5-bicyclic structures, none of the other possible diastereomers were isolated in a large enough amount to enable any further transformations. In addition, our docking studies predicted a distorted binding mode and further efforts to make the other isomers were deemed unnecessary.

Two additional diastereomeric scaffolds (**2-23a** and **2-23b**) were prepared from L- and D-Glu (**2-21a,b**) using a modified strategy reported by Subasinghe *et al.*²⁶ This strategy relies on the intermediate **2-22** which upon treatment with Cys afforded the desired structure in a single step (Scheme 2.3). Two additional diastereomeric scaffolds (**2-23a** and **2-23b**) were prepared from L- and D-Glu (**2-21a,b**) using a modified strategy reported by Subasinghe *et al.*²⁶ This strategy relies on the intermediate **2-22** which upon treatment with Cys afforded the desired structure in a single step (Scheme 2.3).

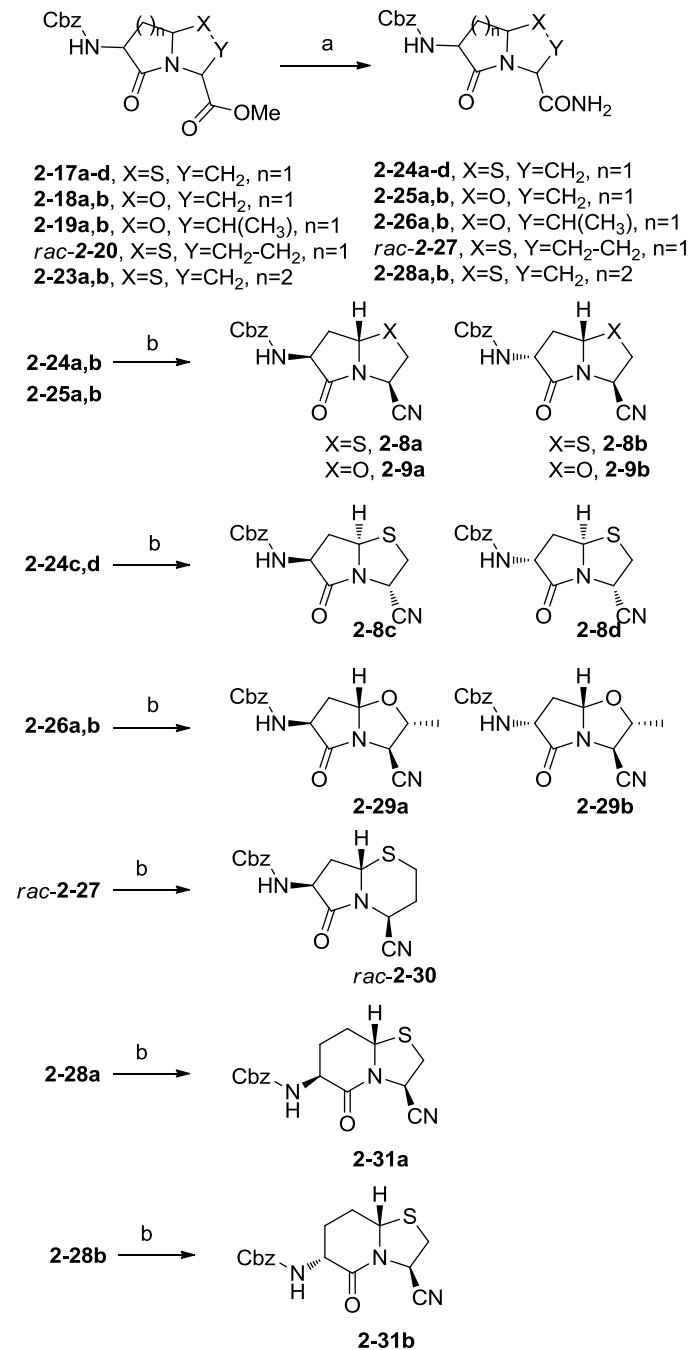


Scheme 2.3 Synthesis of the bicyclic scaffolds (part 2).

(a) CbzCl, 4 N NaOH, 0°C to rt., 21h; (b) (CH₂O)_n, cat. pTsOH, toluene, reflux, 3h; (c) (COCl)₂, cat. DMF, CH₂Cl₂, quant.; (d) LiAl[OtBu]₃H, THF; (e) (i) L-CysOMe•HCl, pyridine, 24 h; (ii) 50°C, 3 days; (f) K₂CO₃, CH₃OH, 6-8% over 6 steps.

Functionalization of the scaffolds to covalent inhibitors.

The covalent functionality was added to each of the scaffolds once formed (Scheme 2.4).



Scheme 2.4 Functionalization of the scaffolds to covalent inhibitors.

(a) NH₃, CH₃OH, rt., quant.; (b) (CF₃CO)₂O, Et₃N, THF, rt., 27-81%.

For this purpose, we converted each of the methyl esters into the corresponding amides, **2-24a** through **2-28b**, using ammonia³¹ which we then transformed into the corresponding nitriles with good to excellent yields by dehydration.³²

Confirming the stereochemistry of the various diastereomers.

Given that **2-17a-d** are reported in the literature,^{25,33} providing stereochemistry identified by NOE experiments, we compared NMR data from our purified compounds to the reported data. For all other bicyclic compounds, both COSY and NOESY experiments were performed to identify the isolated diastereomers (Figure 2.4). In addition, only one stereogenic center is made throughout the synthesis while the other two already appear in the starting amino acids. When racemic allyl glycine was used two stereogenic centers needed to be assigned.

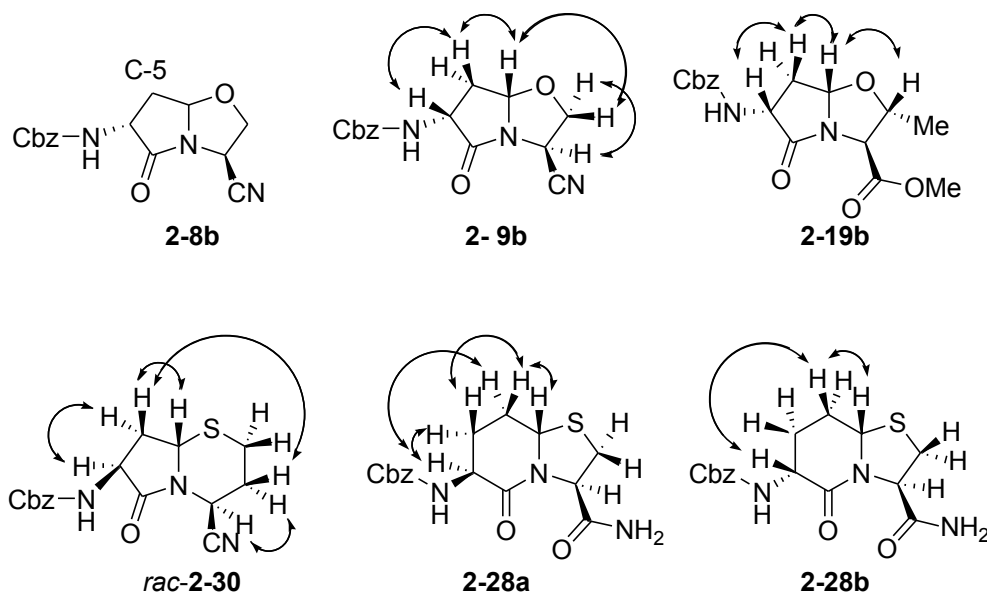


Figure 2.4 Selected NOE identifying the stereochemistry of the isolated compounds.

To further confirm the stereochemistry of the scaffolds, we simply compared the ¹H NMR spectra of the novel scaffolds to those of **2-8a-b** (Figure 2.5).

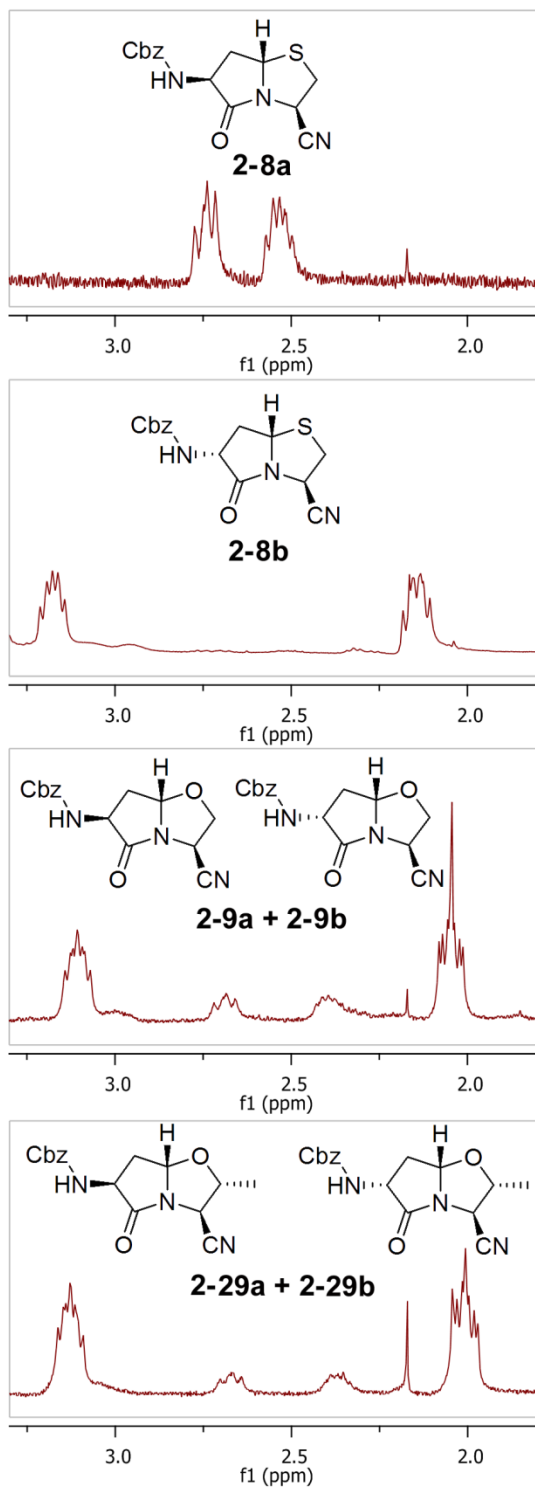


Figure 2.5 Comparison of ^1H NMR spectra, confirming stereochemistry of isolated diastereomers. The peaks refer to the two hydrogen atoms on carbon # 5 (see 2-8b in Figure 2.4).

2.3.3 Biological Evaluation

Enzyme inhibition in cell extracts

POP activity was measured using the fluorogenic substrate Z-Gly-Pro-AMC and prolyl-dipeptidyl-aminopeptidase (DPPIV) activity with the fluorogenic substrate Gly-Pro-AMC using the human brain astrocyte-derived LN18, LN229 and LN2308 glioblastoma cells, the human brain-derived HCEC endothelial cells and the human lung-derived PO03 and skin-derived PG98/5 fibroblasts. The initial inhibition screening experiments were performed using cell extracts, obtained by extracting cell layers in PBS-0.1% Triton X-100 to determine the potential of the developed inhibitors to inhibit total cellular enzyme activities (Table 2.1). All compounds were found to be very selective for POP activity over DPP IV activity in cell extracts.

Table 2.1. Inhibition of POP activity and DPP-IV endoprotease activity in cell extracts.

Compound	Z-Gly-Pro-AMC (POP activity) ^a			Gly-Pro-AMC (DPP IV activity) ^a		
	human astrocyte-derived cells ^b	human brain-derived endothelial cells ^c	human fibroblasts ^d	human astrocyte-derived cells	human brain-derived endothelial cells	human fibroblasts
Z-Pro-NH ₂	+	-	+	-	-	-
Z-Pro-CN	-	+	-	-	-	-
Boc-Pro-CN	-	-	-	-	-	-
Pro-CN	-	-	-	-	-	nd
2-11a	+++	+++	+++	-	-	-
2-11b	+++	+++	+++	-	-	-
2-12a	+++	+++	+++	-	-	-
2-12b	+++	+++	+++	-	-	-
2-14	++	+	+	-	-	-
2-17a	+	-	+	-	-	-
2-17b	-	-	+	-	-	-

2-24a	-	-	-	-	-	-
2-24b	-	-	-	-	-	-
2-8a	+	++	+	-	-	-
2-8b	+++	+++	+++	-	-	-
2-8c	+	+	-	-	-	-
2-8d	+	++	+	-	-	-
2-9a,b	-	-	+	-	-	-
2-29a,b	+	+	-	-	-	-
<i>rac</i>-2-30	-	-	+	-	-	-
2-31a	++	++	++	-	--	--
2-31b	++	++	++	-	-	--

^a -: no inhibition at 100 μ M; +: 10-50% inhibition at 100 μ M; ++: > 50% inhibition at 100 μ M; +++: > 90% inhibition at 20 μ M; nd: not determined; ^b LN18, LN229, LN2308: human glioblastoma cells; ^c HCEC: human brain-derived endothelial cells; ^d PO03: human lung-derived fibroblasts; PG98/5: human skin-derived fibroblasts.

Enzyme inhibition in intact living cells

In order to evaluate the potential of these molecules to inhibit membrane-inserted enzymes as well as to penetrate cells and inhibit intracellular enzymatic activities, the inhibition of POP activity was also evaluated with the same compounds in intact living cells (Table 2.2).

Table 2.2 Inhibition of POP endoprotease activity in intact living cells

Compound	Z-Gly-Pro-AMC (POP activity) ^a		
	human astrocyte-derived cells	human brain-derived endothelial cells	human fibroblasts
Z-Pro-NH ₂	+	-	-
Z-Pro-CN	-	-	+
Boc-Pro-CN	-	-	-
Pro-CN	-	-	-
2-11a	+++	+++	+++
2-11b	+++	+++	+++
2-12a	+++	+++	+++
2-12b	+++	+++	+++
2-14	+	-	-
2-17a	-	-	+
2-17b	-	-	+
2-24a	-	-	-

2-24b	-	-	-
2-8a	-	+	+
2-8b	+++	+++	+++
2-8c	-	-	-
2-8d	-	+	-
2-9a,b	-	-	+
2-29a,b	-	+	-
<i>rac</i>-2-30	-	-	-
2-31a	++	+	++
2-31b	++	++	++

^a -: no inhibition at 100 μ M; +: 10-50% inhibition at 100 μ M; ++: > 50% inhibition at 100 μ M; +++: > 90% inhibition at 20 μ M.

As shown in Table 2.2, the inhibitors not only inhibit POP activity in cell extracts, but also this proteolytic activity in intact living cells. Out of all the compounds tested, compounds **2-11a**, **2-11b**, **2-12a**, **2-12b** and **2-8b** were the best inhibitors of POP activity. In order to obtain more detailed information concerning the potency of **2-11a**, **2-11b**, **2-12a**, **2-12b** and **2-8b** as POP inhibitors, the IC_{50} values were determined in cell extracts and in intact cells (Figure 2.6 and Table 2.3).

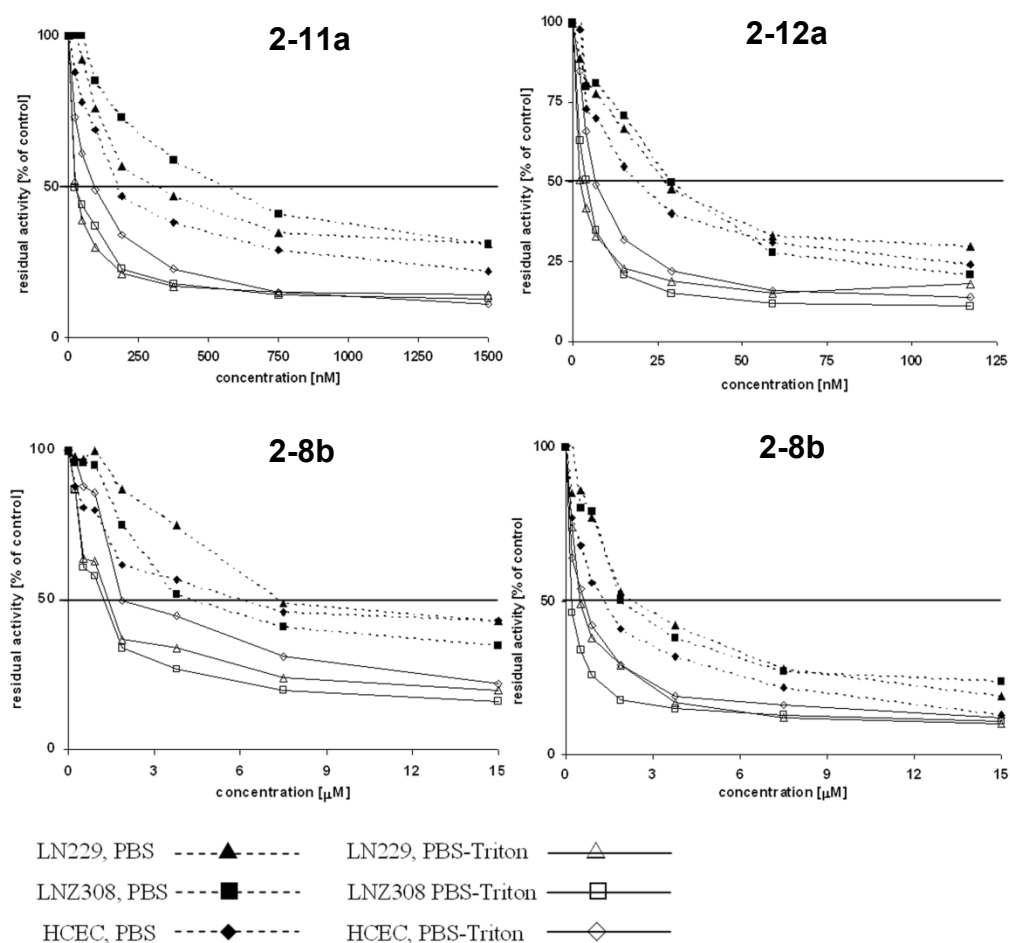


Figure 2.6 Dose-response of POP activity by **2-11a**, **2-11b**, **2-12a**, **2-12b** and **8b** in intact cells (PBS) and in cell extracts (PBS-Triton).

Compounds **2-12a** and **2-11a** are the most potent inhibitors of POP activity of our series, displaying low nanomolar IC_{50} values. They are also very selective over DPPIV activity, both in cell extracts and in intact cells (data not shown). The

inhibition of POP activity, as defined by IC_{50} , is about 10 fold higher in cell extracts than in intact cells, possibly reflecting the partial efficacy of these inhibitors of crossing the cell membrane.

Table 2.3 IC_{50} values [nM] for the inhibition of POP endoproteolytic activity activity in intact living cells and in cell extracts.

Compound	LN229 (nM)		LNZ308 (nM)		HCEC (nM)	
	Intact cells	Cell extract	Intact cells	Cell extract	Intact cells	Cell extract
2-11a	325	20	590	20	180	95
2-11b	3400	430	>4000	430	2800	690
2-12a	28	3	29	5	20	7
2-12b	7,500	1,400	4,700	1,200	6,600	2,000
2-8b	2,000	500	2,500	200	1,300	700

2.4 Discussion

2.4.1 POP and other prolyl peptidases

The family of serine peptidases able to cleave peptide bonds after a prolyl residue comprises exopeptidases such as the cell plasma-membrane anchored DPPIV/CD26 and FAP- α /seprase, and the intracellular DPP8, DPP9, and endopeptidases, mainly represented by the widely distributed intracellular prolyl oligopeptidase (POP). POP and/or POP-like activity have been found in many regions of the brain,^{2,34} and has been associated with the cleavage of oligopeptides involved in memory and the processing of amyloid precursor protein to β -amyloid.¹⁵ Studies on animal models suggested that POP inhibition may lead to improved memory and learning in rodents,^{13,35} to reverse scopolamine-induced amnesia in rats³⁶ and to enhance cognition in Parkinson's disease.³⁷ Human POP levels are reduced in different stages of depression, increased in maniac and

schizophrenic patients, and the enzyme is reactivated to normal levels by antidepressants.³⁸ Conflicting data regarding altered POP activity^{13,39} have been reported in patients with Alzheimer's disease. Thus, POP activity may represent a target for the treatment of neurological disorders. However, FAP- α /seprase, and possibly the DPP8/DPP9 proteases also display post-prolyl hydrolytic endoproteolytic activities.³⁴ Therefore, several proteases may share the endoproteolytic activity attributed to POP. Highly specific POP inhibitors therefore need to be designed in order to further explore this enzyme and its function.

As our long-term aim is to develop POP inhibitors targeting POP expressed in the brain, and as most of the information concerning POP and its inhibitors was obtained in brain models, we evaluated the inhibitory potency of our compounds in human brain-derived cells of astrocytic origin (glioblastoma cells) and endothelial cells as a model of cells forming the blood-brain barrier. As POP and POP activity are widely expressed in many other cells, we also evaluated the inhibitory potential of the inhibitors in human fibroblasts of the lung or the skin, as models for non brain-derived cells. Selectivity for endoproteolytic POP activity over exoproteolytic DPPIV activity can easily be obtained due to the different chemical properties of their catalytic site since DPPIV binds to charged terminal residues while POP does not. Selectivity for other prolyl-specific endoproteolytic activities is challenging and in fact rarely reported.⁴⁰

2.4.2 Constrained POP inhibitors

In contrast to non-covalent competitive inhibitors which can adjust their orientation and translation in the enzyme binding site, the orientation of covalent inhibitors is tightly controlled by the forming covalent bond and any seemingly minor change in shape can have a significant impact on the binding affinity. The docking study and biological testing of the scaffold-based structures revealed **2-8a** and **2-8b** as potent POP inhibitors. The biological evaluation of the analogues provided more in depth information about the required functional groups and

stereochemical features of the inhibitors. First, comparing **2-8a/b** to **2-17a/b** and **2-24a/b** revealed that the nitrile functional group is essential for optimal binding most likely through the postulated covalent bond with the catalytic serine. Then the predicted drop in activity observed from **2-11a** to **2-14** and from **2-8a** to *rac*-**2-30** confirmed that mimicking the Pro ring of Cbz-Gly-prolinal (**2-1**) with a larger ring results in loss of binding affinity. Unlike with the 5-membered ring systems mimicking Pro, this expanded 6-membered ring cannot fit into the binding site without clashing with the enzyme or disrupting the key hydrogen bonds and hydrophobic interactions. The bound pose is distorted when compared to the crystal structure, as revealed by our docking studies.

Furthermore, the replacement of the sulfur atom of **2-8b** by an oxygen atom (in **2-9b**) resulted in a complete loss of activity. Although reduction in inhibitory potency has been observed when moving from thiooxazoline to oxazoline,⁴¹ such a large drop in affinity is unexpected. Again, we hypothesize that these changes are magnified by the fact that these inhibitors bind covalently. This seemingly subtle change actually leads to reduced ring size, C-S bonds being significantly longer than C-O bonds. As for *rac*-**2-30**, the increase to a 6-membered ring resulted in a different shape of the whole molecule, hence a different binding affinity. To further probe the differences between these two structures, DFT calculations were carried out and revealed a significantly different electronic distribution and a much less polarized (i.e., less reactive) nitrile group in **2-9b** when compared to **2-8b**. This reduced reactivity may prevent the covalent binding.

The stereochemistry of the molecular scaffolds was also critical for the inhibition of POP endoproteolytic activity (**2-8a** vs. **2-8b**, **2-8c** or **2-8d**). As expected, the natural amino acid configuration is required at the nitrile position (**2-8a** vs. **2-8c**; **2-8b** vs. **2-8d** or **2-11a** vs. **2-11b**) in order to mimic the natural Pro-containing substrate of the enzyme. More interestingly, the optimal configuration of the left-handed stereogenic center (carbon 6 in Figure 2.7) of the scaffold mimics the D-amino acid configuration (**2-8a** vs. **2-8b**). In order to

investigate this specific observation, we prepared the corresponding pseudo-peptides **2-12a** and **2-12b** (Figure 2.7). When moving from Gly to L-Ala (**2-11a** to **2-12a**), the inhibition increased by an order of magnitude. More interestingly, when the configuration of the Ala residue was inverted (**2-12a** to **2-12b**) (Figure 2.7), inhibition was still observed but dropped by a factor of 500. Similarly, when the Pro stereogenic center is inverted, **2-11a** versus **2-11b**, inhibition is observed, although with a higher IC_{50} for the D-isomer. This data suggests that the stereochemistry at these two centers have an impact on the potency.

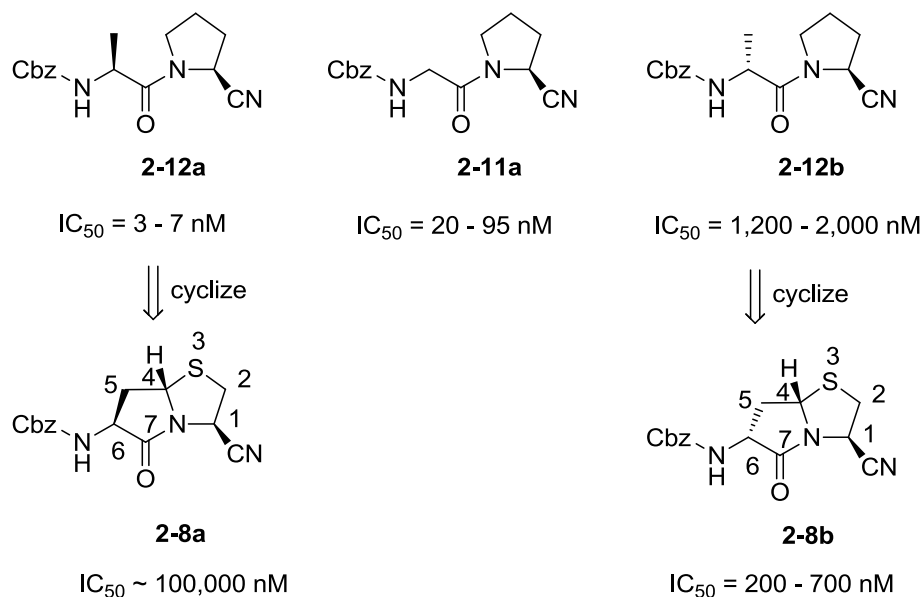


Figure 2.7 Effect of cyclization on inhibitory potency.

As shown in Figure 2.8, the proposed binding mode of **2-12a** is very similar to the experimentally observed binding mode of Cbz-Pro-prolinal. The proline ring stacks on Trp595 and interacts with Phe476, while the terminal phenyl ring interacts with Phe173 and the two hydrogen bonds between carbonyls of the inhibitor and the enzyme are retained. In contrast, **2-12b** does not fit as nicely in the binding site and a hydrogen bond is lost, resulting in a significant drop in potency. When constraining **2-12a** and **2-12b** into **2-8a** and **2-8b**, a loss of activity is observed from **2-12a** to **2-8a**, while a slight increase is observed from **2-12b** to **2-8b**. We rationalize that the stereochemistry of the carbon C1 which is imposed by the synthetic pathway influences the binding (Figure 2.8, Figure 2.9).

Comparing the crystal structure of Cbz-Pro-prolinal, co-crystallized with POP (PDB code: 1h2y), and the docked conformations of **2-12a**, **2-12b**, **2-8a** and **2-8b**, shows that, when compared to **2-8a**, **2-8b** adopts a shape that more closely replicates the interactions of the enzyme with Cbz-Pro-prolinal (Figure 2.8). This observation is consistent with the measured inhibitory potencies of these inhibitors on POP, where we noted that **2-8b** was more potent than all the other bicyclic structures. Interestingly, the binding mode and more specifically of the position of the proline ring of **2-12b** and **2-8b** are fairly similar while the binding mode of **2-12a** and **2-8a** are quite different as are the measured potencies. In practice, the cyclization of **2-12b** corresponds to the substitution of the two hydrogen atoms highlighted by grey spheres of Cbz-D-Pro-prolinal in Figure 2.9 by a covalent bond and to the production of **2-8b**. In contrast, the proline γ -carbon (shown in yellow) is not positioned to be covalently linked to the γ -carbon of the Cbz-L-Pro-prolinal. As a result, when **2-12a** is cyclized into **2-8a**, **2-8a** cannot adopt the bioactive conformation of **2-12a**.

Further docking studies with **2-31c**, an epimer of **2-31a** revealed that the binding mode should be very similar to Cbz-Pro-prolinal and **2-31c** is therefore expected to be a tight binder. Unfortunately, all our synthetic efforts to make **2-31c** proved unsuccessful. This last observation will now guide our future synthetic efforts to make constrained bicyclic POP inhibitors.

2.4.3 POP activity and selectivity in intact cells

The inhibitory potency of these compounds was maintained in intact living cells (Table 2.2). These experiments demonstrate that the developed inhibitors are penetrating the cells, a key feature if POP inhibitors have to be efficient as therapeutic agents for neurodegenerative diseases, since their target enzyme is intracellular. Moreover, when assessed for inhibition toward DPPIV activity, none of the compounds exhibited inhibition at concentrations as high as 100 μ M. This data clearly demonstrates the high selectivity of **2-8a** and **2-8b** for POP activity.

Overall, these molecules achieved excellent selectivity for inhibition of POP endoproteolytic activity over inhibition of DPPIV exoproteolytic activity in soluble enzyme activities extracted from relevant cell models and in human intact living astrocyte-derived cells, human brain-derived endothelial cells and human primary fibroblasts.

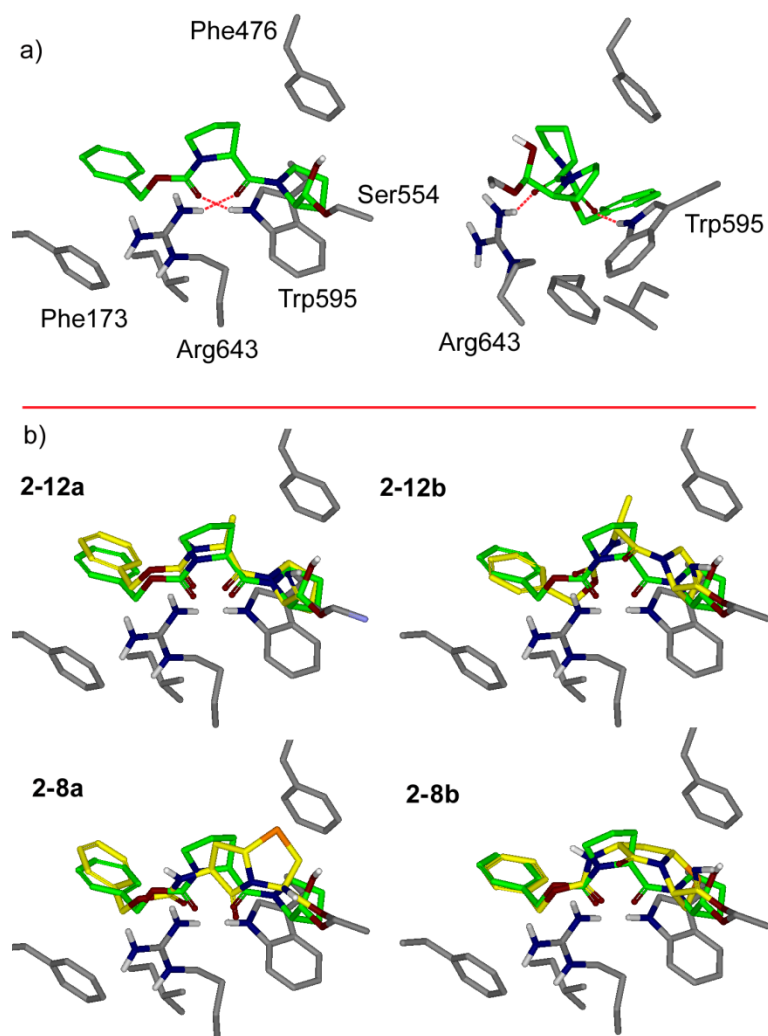


Figure 2.8 (a) Structure of Cbz-Pro-prolinal co-crystalized with POP. (b) Docked structures of 2-12a, 2-12b, 2-8a and 2-8b (yellow) superposed to the crystal structure of Cbz-Pro-prolinal (green).

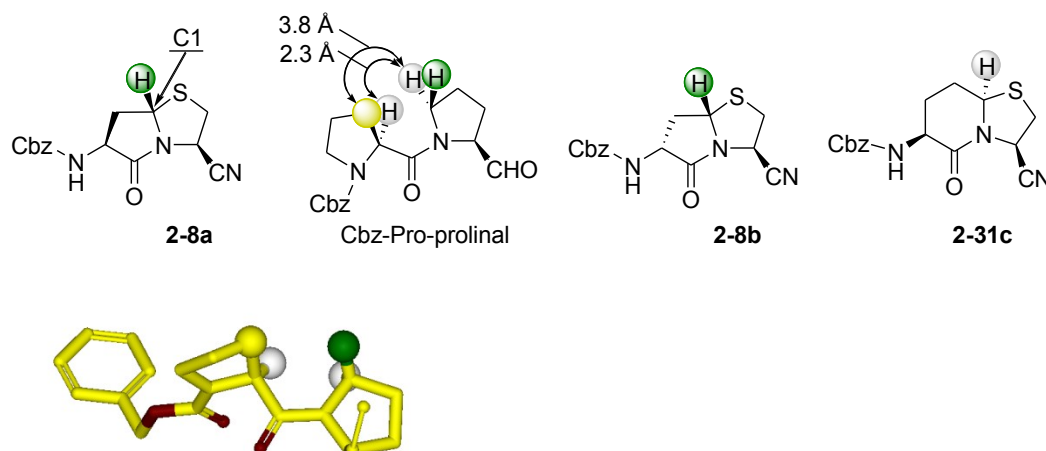


Figure 2.9 Effect of cyclization on inhibitory potency.

2.5 Conclusion

We have used a series of constrained peptidomimetics to better understand some important inhibitor shape requirements leading to more potent inhibitors of prolyl oligopeptidase. We first used a novel feature of our docking program FITTED to dock covalent inhibitors to the binding site of prolyl oligopeptidase and to select a lead scaffold for synthesis. Based on this docking study, two were selected for synthesis (**2-8a** and **2-8b**). In order to validate our predictions, several analogues of different sizes, stereochemistry and shapes were also prepared. Exhaustive biological evaluation confirmed our prediction and identified **2-8b** as a potent, highly selective and cell-permeant POP inhibitor (IC_{50} of 200-700 nM). Through this series of seemingly similar compounds, we demonstrated that scaffolding is very sensitive to seemingly subtle changes such as the substitution of a sulfur atom by an isosteric oxygen atom. The docking studies also identified the configuration of the stereogenic center at the ring junction as a limiting factor for optimal activity and will lead our design of the second generation of more potent inhibitors.

2.6 Experimental section

2.6.1 Synthesis

General remarks

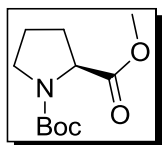
All commercially available reagents were used without further purification, unless otherwise stated. 4 Å molecular sieves were dried at 100°C prior to use. Optical rotations were measured on a JASCO DIP 140 in a 1dm cell at 20°C. FTIR spectra were recorded using a Perkin Elmer Spectrum One FT-IR. ¹H and ¹³C NMR spectra were recorded on Varian mercury 400 MHz, 300 MHz or Unity 500 spectrometers. Chemical shifts are reported in ppm using the residual of chloroform as internal standard (7.26 ppm for ¹H and 77.160 ppm for ¹³C). TLC visualization was performed by UV or by development using KMnO₄, H₂SO₄/MeOH or Mo/Ce solutions. Chromatography was performed on silica gel 60 (230-40 mesh). Low resolution mass spectrometry was performed by ESI using a Thermoquest Finnigan LCQDuo. High resolution mass spectrometry was performed by EI Peak matching (70 eV) on a Kratos MS25 RFA Double focusing mass spectrometer or by ESI on a IonSpec 7.0 tesla FTMS at McGill University. Prior to biological testing, reversed phase HPLC was used to verify the purity of compounds on an Agilent 1100 Series instrument equipped with VWD-detector, C18 reverse column (Agilent, Zorbax Eclipse XDB-C18 150mm*4.6mm, 5µm), UV detection at 254 nm. All measured purities are listed in a table in the experimental section “**HPLC analysis of purity.**” All tested compounds were ≥ 95% pure, except for compounds **2-14**, **2-17a**, **2-24b** (≥ 90% pure) which were not active according to our biological tests.

Synthesis of the dipeptides

(2*S*)-*N*-(*tert*-butoxycarbonyl)proline methyl ester⁴²

To a solution of **L-proline methyl ester hydrochloride** (1.00 g, 6.06 mmol) in 10 mL of dry CH₂Cl₂ was added Boc₂O (2.90 g, 13.3 mmol), Et₃N (0.92 mL, 6.61

mmol) and DMAP (0.81 g, 6.64 mmol) at 0 °C under Ar. After 18 h, the crude mixture was washed with aqueous HCl 0.5 M, saturated aqueous NaHCO₃ solution, H₂O and brine. The organic phase was dried over Na₂SO₄, filtered, concentrated *in vacuo* and purified by flash chromatography (petroleum ether/ethyl acetate; 85/15) to give **(2S)-N-(tert-butoxycarbonyl)proline methyl ester** (0.552 g, 40% yield).



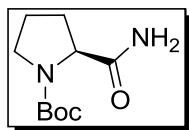
C₁₁H₁₉NO₄ ; Mol. Wt. = 229.27

R_f = 0.35 (Pet Ether/EA, 9:1)

¹H NMR (CDCl₃, 300 MHz) δ 4.21 (dd, 1H), 3.70 (s, 3H), 3.58-3.30 (m, 2H), 2.30-1.75 (m, 4H), 1.40 (s, 9H).

(2S)-N-(tert-butoxycarbonyl)pyrrolidine-2-carboxamide⁴³

(2S)-N-(tert-butoxycarbonyl)proline methyl ester (0.552 g, 2.4 mmol) was heated in a mixture of THF and 28% aqueous NH₃ (2/9, v/v) at 60 °C for 18 h under Ar. The reaction mixture was concentrated to give **Boc-L-Pro-NH₂** (0.460 g, 89%), used in the next step without any further purification.



C₁₀H₁₈N₂O₃ ; Mol. Wt. = 214.26

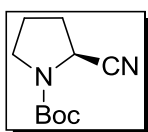
R_f = 0.85 (CH₂Cl₂/Acet, 8:2)

¹H NMR (400 MHz, CDCl₃) δ 7.50-7.01 (m, 2H), 4.87 (m, 1H), 4.35 (m, 1H), 3.44 (m, 1H), 2.00-1.75 (m, 4H), 1.43 (s, 9H).

(2S)-N-(tert-butoxycarbonyl)-pyrrolidine-2-carbonitrile⁴³

TFA anhydride (0.39 mL, 2.80 mmol), was added to a solution of **(2S)-N-(tert-**

butoxycarbonyl)pyrrolidine-2-carboxamide (0.501 g, 2.33 mmol) and Et₃N (0.779 mL, 5.59 mmol) in dry THF (6 mL) under Ar at 0 °C. The reaction was stirred at 0 °C for another 6 h. After addition of CH₂Cl₂, the organic phase was washed with a saturated aqueous NaHCO₃ solution, dried over Na₂SO₄, filtered and concentrated *in vacuo* to afford **(2S)-N-(tert-butoxycarbonyl)-pyrrolidine-2-carbonitrile** (0.393 g, 86%, brown oil) used in the next step without any further purification.



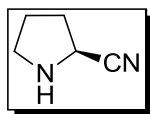
C₁₀H₁₆N₂O₂ ; Mol. Wt. = 196.25

R_f = 0.89 (Pet Ether/EA, 5:4)

¹H NMR (400 MHz, CDCl₃) δ 4.43 (m, 1H), 3.54-3.30 (m, 2H), 2.30-1.98 (m, 4H), 1.49 (s, 9H).

(2S)-pyrrolidine-2-carbonitrile (TFA salt)⁴⁴

(2S)-N-(tert-butoxycarbonyl)-pyrrolidine-2-carbonitrile (0.202 g, 1.03 mmol) was dissolved in dry CH₂Cl₂ (5 mL) under Ar and TFA (2 mL) was added at 0 °C. The reaction was stirred at 0 °C for 2 h. The solvent was evaporated and the product was crystallized in Et₂O, yielding the white TFA salt of **(2S)-pyrrolidine-2-carbonitrile** (0.110 g, 51% yield, white powder).



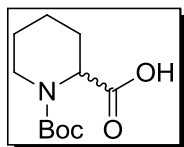
C₅H₈N₂, Mol. Wt. = 96.13

R_f = 0.46 (Pet Ether/EA, 5:2)

¹H NMR (400 MHz, CD₃OD) δ 4.92 (s, 1H), 4.68 (t, 1H), 3.47-3.35 (m, 2H), 2.52-2.43 (m, 1H), 2.32-2.07 (m, 3H).

rac-N-(tert-butoxycarbonyl)-piperidine-2-carboxylic acid⁴⁵

DL-Pipecolinic acid (3.00 g, 23.2 mmol) and Et₃N (3.24 mL, 23.2 mmol) were dissolved in 1,4-dioxane (32 mL) and H₂O (21 mL). Boc₂O (5.58 g, 25.5 mmol) was added, and the solution was stirred for 24 h at rt. The solvent was evaporated, and the residue was extracted in EtOAc. The solution was washed with aqueous 5% HCl and brine. The organic layer was dried over Na₂SO₄, filtered, and evaporated to obtain ***rac-N-(tert-butoxycarbonyl)-piperidine-2-carboxylic acid*** (4.39 g, 82% yield, white powder).



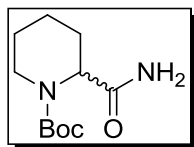
C₁₁H₁₉NO₄, Mol. Wt. = 229.27

R_f = 0.1 (CH₂Cl₂/Acet, 7:3)

¹H NMR (CDCl₃) δ 10.93 (s, 1H), 4.92-4.74 (bd, 1H), 3.98-3.91 (m, 1H), 2.95 (m, 1H), 2.20 (s, 1H), 1.66-1.23 (m, 14H).

rac-N-(tert-butoxycarbonyl)-piperidine-2-carboxamide⁴³

To a solution of ***rac-N-(tert-butoxycarbonyl)-piperidine-2-carboxylic acid*** (4.26 g, 18.6 mmol) and Et₃N (2.60 mL, 18.7 mmol) in dry THF (25 mL) under Ar at -15 °C, was added dropwise a solution of ethyl chloroformate. The resulting reaction mixture was stirred for 1 h. 28% aqueous NH₃ (6 mL) was then added dropwise and the solution was warmed to rt and stirred for another 4 h. The solution was concentrated and the residue extracted with EtOAc, washed with 10% aqueous citric acid, a saturated aqueous NaHCO₃ solution, then brine, dried over Na₂SO₄, filtered and concentrated *in vacuo* to give ***rac-N-(tert-butoxycarbonyl)-piperidine-2-carboxamide*** (3.53 g, 83% yield, oil).



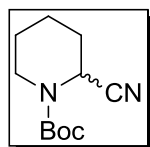
$C_{11}H_{20}N_2O_3$, Mol. Wt. = 228.29

$R_f = 0.70$ (CH_2Cl_2 /Acet, 7:3)

1H NMR (400 MHz, $CDCl_3$) δ 6.12 (m, 2H), 4.70 (m, 1H), 4.11 (m, 1H), 2.70 (m, 1H), 2.25 (m, 1H), 1.46 (s, 9H), 1.70–1.38 (m, 5H).

***rac*-2-piperidine-2-carbonitrile (HCl salt)⁴⁶**

TFA anhydride (0.18 mL, 1.32 mmol), was added to a solution of ***rac*-N-(*tert*-butoxycarbonyl)-piperidine-2-carboxamide** (0.200g, 0.88 mmol) and Et_3N (0.37 mL, 2.64 mmol) in dry CH_2Cl_2 (3 mL) under Ar at 0°C. The reaction was stirred at 0 °C for another 6 h. The solution was washed with water, a HCl solution (0.5N) and a saturated aqueous $NaHCO_3$ solution, dried over Na_2SO_4 , filtered and concentrated *in vacuo* to afford ***rac*-N-(*tert*-butoxycarbonyl)-piperidine-2-carbonitrile** (0.125 g, 68% yield, white crystals)



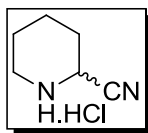
$C_{11}H_{18}N_2O_2$, Mol. Wt. = 210.27

$R_f = 0.90$ (CH_2Cl_2 /Acet, 7:3)

1H NMR (400 MHz, CD_3OD) δ 5.24 (bs, 1H), 4.04 (bs, 1H), 2.92 (bs, 1H), 1.94–1.80 (m, 2H), 1.70–1.68 (m, 3H), 1.45 (s, 9H).

***rac*-2-piperidine-2-carbonitrile**

***rac*-N-(*tert*-butoxycarbonyl)-piperidine-2-carbonitrile** (0.100 g, 0.48 mmol) in 1,4-dioxane (5 mL) was treated with 4 N HCl for 45 min at rt. The reaction mixture was then filtered, washed with Et_2O , concentrated *in vacuo* to afford the HCl salt of ***rac*-2-piperidine-2-carbonitrile** (0.064 g, 92% yield, white powder).



$C_{16}H_{11}ClN_2$, Mol. Wt. = 146.62

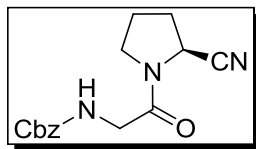
$R_f = 0.1$ (CH_2Cl_2 /Acet, 7:3)

1H NMR (400 MHz, CD_3OD) δ 3.84 (d, 1H), 3.38 (d, 1H), 3.03 (t, 1H), 2.24 (d, 1H), 1.94-1.86 (m, 2H), 1.72-1.69 (m, 3H).

General procedure for dipeptide coupling. Anhydrous Et_3N (2 equiv.) was added dropwise to a stirred solution of amino acid (1 equiv.) (TFA or HCl salt), *N*-benzyloxycarbonyl-glycine or *N*-benzyloxycarbonyl-alanine or *N*-benzyloxycarbonyl-D-alanine (1 equiv.) and HOBT (0.6 equiv.) in CH_2Cl_2 under Ar. The resulting solution was cooled to 0 °C. A solution of 1-ethyl-3-(3-dimethylaminopropyl)carbodiimide hydrochloride (1.05 equiv.) in CH_2Cl_2 was then added dropwise. The reaction mixture was warmed up to rt, stirred until completion (tlc monitoring, 16 to 20h) then washed with 0.2 N aqueous HCl, saturated aqueous $NaHCO_3$, dried over Na_2SO_4 , filtered and concentrated *in vacuo*. Flash chromatography afforded the dipeptides.

N-benzyloxycarbonylamino-glycine-2S-pyrrolidine-2-carbonitrile (2-11a)

Following the general procedure, (2*S*)-pyrrolidine-2-carbonitrile (TFA salt) (0.080 g, 0.38 mmol) reacted with Cbz-Gly-OH afforded after flash chromatography (CH_2Cl_2 /acetone; gradient of 98/2 to 95/5) *N*-benzyloxycarbonylamino-glycine-2*S*-pyrrolidine-2-carbonitrile (**2-11a**) (63 mg, 58%)



$C_{15}H_{17}N_3O_3$, Mol. Wt. = 287.31

$R_f = 0.60$ (CH_2Cl_2 /Acet, 8:2)

IR (cm^{-1}): 2956, 2476, 1716, 1656

$[\alpha]_D = -78.1$ (c 0.96, CH_3OH)

1H NMR ($CDCl_3$, 300 MHz) δ 7.41-7.27 (m, 5H), 5.75 (s, 1H), 5.12 (s, 2H), 4.74 (m, 1H), 4.05 (dd, 1H), 3.94 (dd, 1H), 3.59 (m, 1H), 3.41 (m, 1H), 2.35-2.07 (m, 4H).

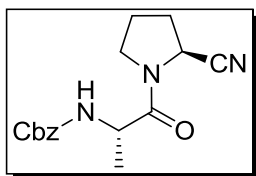
^{13}C NMR ($CDCl_3$, 75 MHz) δ 167.6, 156.5, 136.4, 128.6, 128.3, 128.1, 118.1, 67.1, 46.7, 45.5, 43.6, 30.0, 25.2.

HRMS (ESI+) calc'd for $[C_{15}H_{17}N_3O_3 + Na]^+$: 310.11621. Found: 310.11591.



N-benzyloxycarbonylamino-L-alanine-2S-pyrrolidine-2-carbonitrile (**2-12a**)

Following the general procedure, (2S)-pyrrolidine-2-carbonitrile (TFA salt) (0.075 g, 0.36 mmol) reacted with Cbz-L-Ala-OH afforded, after flash chromatography (petroleum ether/ethyl acetate; gradient of 5/2 to 5/3), N-benzyloxycarbonylamino-L-alanine-2S-pyrrolidine-2-carbonitrile (**2-12a**) (37 mg, 34%).



$C_{19}H_{19}N_3O_3$, Mol. Wt. = 301.34

$R_f = 0.70$ (CH_2Cl_2 /Acet, 7:3)

IR (cm^{-1}): 3314, 2927, 1715, 1653

$[\alpha]_D = -96.4$ (c 0.56, CH_3OH)

1H NMR ($CDCl_3$, 300 MHz) δ 7.39-7.29 (m, 5H), 5.59 (d, 1H), 5.08 (dd, 2H), 4.78 (m, 1H), 4.48 (m, 1H), 3.66 (m, 2H), 2.34-2.11 (m, 3H), 1.65 (m, 1H), 1.38 (d, 3H).

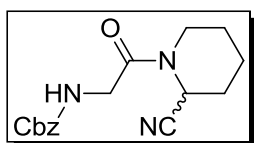
^{13}C NMR (CDCl_3 , 75 MHz) δ 171.8, 155.8, 136.4, 128.7, 128.3, 128.1, 118.2, 67.1, 48.4, 46.6, 46.5, 29.9, 25.4, 18.4.

HRMS (ESI+) calc'd for $[\text{C}_{16}\text{H}_{19}\text{N}_3\text{O}_3 + \text{Na}]^+$: 324.13186. Found: 324.13168.



N-benzyloxycarbonylamino-D-alanine-2S-pyrrolidine-2-carbonitrile (2-12b)

Following the general procedure, (2S)-pyrrolidine-2-carbonitrile (TFA salt) (0.080 g, 0.38 mmol) reacted with Cbz-D-Ala-OH afforded after flash chromatography (hexanes/ethyl acetate; gradient of 5/2 to 6/4) N-benzyloxycarbonylamino-D-alanine-2S-pyrrolidine-2-carbonitrile (**2-12b**) (56 mg, 49%) as a mixture of rotamers.



$\text{C}_{19}\text{H}_{19}\text{N}_3\text{O}_3$, Mol. Wt. = 301.34

R_f = 0.70 ($\text{CH}_2\text{Cl}_2/\text{Acet}$, 7:3)

IR (cm^{-1}): 3308, 2931, 1711, 1652

$[\alpha]_D = -34.6$ (c 0.43, CH_3OH)

^1H NMR (CDCl_3 , 400 MHz) δ 7.41-7.28 (m, 5H), 5.70 (d, 1H), 5.40 (d, 1H), 5.11 (m, 2H), 4.67 (m, 1H), 4.53 (m, 1H), 3.87-3.78 (m, 1H), 3.65-3.42 (m, 1H), 2.42-2.06 (m, 4H), 1.45 (d, 3H), 1.34 (d, 3H).

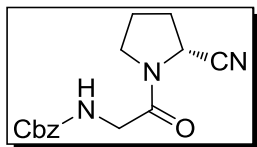
^{13}C NMR (CDCl_3 , 75 MHz) δ 171.5; 155.6, 136.3, 128.7, 128.3, 128.1, 118.1, 67.2, 67.1, 48.5, 48.4, 47.4, 46.9, 46.5, 46.4, 32.4, 30.1, 25.2, 23.2, 18.6, 18.2.

HRMS (ESI+) calc'd for $[\text{C}_{16}\text{H}_{19}\text{N}_3\text{O}_3 + \text{Na}]^+$: 324.13186. Found: 324.13189.



N-benzyloxycarbonylamino-glycine-2R-pyrrolidine-2-carbonitrile (2-11b)

Following the general procedure, (2R)-pyrrolidine-2-carbonitrile (TFA salt) (0.034 g, 0.16 mmol) reacted with Cbz-Gly-OH afforded after flash chromatography (CH_2Cl_2 /acetone gradient of 98/2 to 95/5) N-benzyloxycarbonylamino-glycine-2R-pyrrolidine-2-carbonitrile (**2-11b**) (31 mg, 66%).



$C_{15}H_{17}N_3O_3$, Mol. Wt. = 287.31

$R_f = 0.60$ (CH_2Cl_2 /Acet, 8:2)

IR (cm^{-1}): 3327, 2927, 1722, 1661

$[\alpha]_D = -36.4$ (c 0.88, CH_3OH)

1H NMR ($CDCl_3$, 400 MHz) same as **11a**.

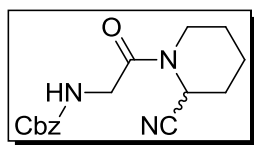
^{13}C NMR ($CDCl_3$, 75 MHz) same as **11a**.

HRMS (ESI+) calc'd for $[C_{15}H_{17}N_3O_3 + Na]^+$: 310.11621. Found: 310.11621.



N-benzyloxycarbonylamino-glycine-*rac*-piperidine-2-carbonitrile (2-14)

Following the general procedure, *rac*-2-piperidine-2-carbonitrile (HCl salt) (0.100 g, 0.691 mmol) reacted with Cbz-Gly-OH afforded after flash chromatography (CH_2Cl_2 /acetone (gradient of 98/2 to 95/5)) **N-benzyloxycarbonylamino-glycine-*rac*-piperidine-2-carbonitrile (2-14)** (31 mg, 30%)



$C_{16}H_{16}N_3O_3$, Mol. Wt. = 301.34

$R_f = 0.87$ (CH_2Cl_2 /Acet, 8:2)

IR (cm^{-1}): 3327, 2950, 1722, 1661

1H NMR ($CDCl_3$, 400 MHz) δ 7.42-7.29 (m, 5H), 5.75 (bs, 1H), 5.68 (bs, 1H), 5.13 (s, 2H), 4.13 (dd, 1H), 3.98 (dd, 1H), 3.70 (m, 1H), 3.31 (m, 1H), 2.08-1.40 (m, 6H).

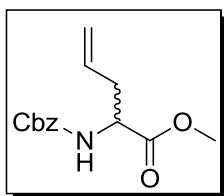
^{13}C NMR ($CDCl_3$, 125 MHz) δ 167.4, 156.4, 136.4, 128.7, 128.2, 117.1, 67.2, 42.9, 42.4, 41.8, 28.4, 25.1, 20.5.

HRMS (ESI+) calc'd for $[C_{16}H_{19}N_3O_3 + Na]^+$: 324.13186. Found: 324.13187.

Synthesis of the bicyclic scaffolds

Methyl (2S)-2-[N-(benzyloxycarbonyl)amino]pent-4-enoate²⁹

To a suspension of allylglycine (*rac*-**2-15**, 550 mg, 4.78 mmol) in 11 mL of dry MeOH at 0 °C was added TMSCl (1.9 mL, 15.0 mmol). The resulting mixture was stirred at 0 °C for 2 h. After stirring for another 12 h at rt, the mixture was cooled to 0 °C and Et₃N (2.70 mL, 19.4 mmol) was slowly added, followed by CBzCl (0.80 mL, 5.68 mmol). The reaction was stirred for 4 h at 0 °C, concentrated *in vacuo*, dissolved in 2M HCl and extracted with EtOAc. The solution was then dried over Na₂SO₄, filtered, concentrated *in vacuo* and used without any further purification in the next reaction.

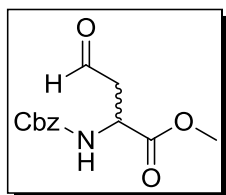


C₁₄H₁₇NO₄, Mol. Wt. = 263.29

R_f = 0.35 (H/EA, 9:1)

Synthesis of *rac*-**2-16**³⁰

Ozone was bubbled through a solution of the oil in CH₂Cl₂ (50 mL) at -78 °C for 30 minutes. Excess of ozone was removed by bubbling Argon through the solution. Dimethyl sulfide (2 mL, excess) was then added. The resulting mixture was stirred at rt for 16 h, concentrated *in vacuo*, re-dissolved in EtOAc, washed with saturated aqueous NaHCO₃, dried over Na₂SO₄, filtered and concentrated to give a colorless oil which was pure enough to be used in the next step without further purification.



$C_{13}H_{15}NO_5$, Mol. Wt. = 265.26

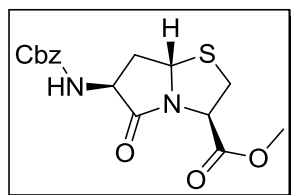
$R_f = 0.1$ (H/EA, 1:1)

General procedure for scaffold synthesis. A solution of L-Cysteine methyl ester (or D-cysteine, L-serine methyl ester, L-threonine methyl ester *rac*-homocysteine) hydrochloride (1.2 to 1.7 equiv.) and aldehyde (*rac*-**2-16**) (1.0 equiv.) in pyridine was stirred at rt for 15 h under Ar and then at 50 °C for 3 days. The excess pyridine was evaporated. When L-Cysteine methyl ester, L-serine methyl ester and L-threonine methyl ester were used, the residue was redissolved in CH_2Cl_2 , washed with 5% aqueous HCl, saturated aqueous $NaHCO_3$, water and brine, dried over Na_2SO_4 , filtered and concentrated *in vacuo*. When D-Cysteine and *rac*-homocysteine were reacted, the residue was acidified to about pH 2 with 1N aqueous HCl and partitioned between CH_2Cl_2 and water. The organic layer was washed with brine, dried over Na_2SO_4 , filtered and concentrated *in vacuo*. The residue was redissolved in THF and treated with a 2.0 M (trimethylsilyl)diazomethane ($TMSCH_2N_2$) solution for 16 h. The solution was then stirred with saturated aqueous $NaHCO_3$, and extracted with CH_2Cl_2 . The organic phase was dried over Na_2SO_4 , filtered and concentrated *in vacuo*. All crude residues were purified by flash chromatography (toluene/diethyl ether, gradient of 9:1 to 8:2) to yield the corresponding bicyclic scaffolds.

(2R,5S,7S)-1-Aza-7-benzyloxycarbonylamino-8-oxo-4-thiabicyclo[3.3.0]octane-2-carboxylic acid methyl ester (2-17a) and (2R,5S,7R)-1-Aza-7-benzyloxycarbonylamino-8-oxo-4-thiabicyclo[3.3.0]octane-2-carboxylic acid methyl ester (2-17b)

Following the general procedure, L-Cys-OMe (1.00 g, 5.84 mmol) and *rac*-**2-16** (1.10 g, 4.15 mmol) afforded the corresponding bicyclic scaffolds **2-17a** (434 mg,

30%) and **2-17b** (265 mg, 18%).



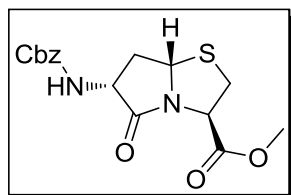
$C_{16}H_{18}N_2O_5$, Mol. Wt. = 350.39

$R_f = 0.35$ (Tol/Ether, 1:1)

2-17a: 1H NMR (300 MHz, $CDCl_3$) δ 7.36 (s, 5H), 5.23 (bd, 1H), 5.19-5.17 (m, 1H), 5.13 (s, 2H), 5.08-5.04 (m, 1H), 4.50-4.42 (q, 1H), 3.78 (s, 3H), 3.53-3.36 (m, 2H), 2.77-2.70 (m, 1H), 2.49-2.39 (m, 1H).

^{13}C NMR (75 MHz, $CDCl_3$) δ 175.0, 170.2, 156.1, 136.1, 128.6, 128.3, 128.3, 67.3, 64.0, 58.6, 53.1, 52.2, 37.1, 30.0.

HRMS (EI+) calc'd for $[C_{16}H_{18}N_2O_5S]^+$: 350.09364. Found: 350.09310.



$C_{16}H_{18}N_2O_5$, Mol. Wt. = 350.39

$R_f = 0.30$ (Tol/Ether, 1:1)

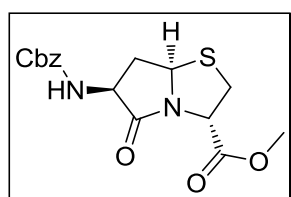
2-17b: 1H NMR (300 MHz, $CDCl_3$) δ 7.35 (s, 5H), 5.35 (bd, 1H), 5.16-5.14 (m, 2H), 5.12 (s, 2H), 4.67 (q, 1H), 3.77 (s, 3H), 3.37-3.35 (m, 2H), 3.26-3.15 (m, 1H), 2.10-2.00 (m, 1H).

^{13}C NMR (75 MHz, $CDCl_3$) δ 171.3, 169.6, 156.05, 136.1, 128.7, 128.4, 128.2, 67.2, 61.7, 57.8, 54.7, 53.1, 38.5, 35.1.

HRMS (EI+) calc'd for $[C_{16}H_{18}N_2O_5S]^+$: 350.09364. Found: 350.09268.

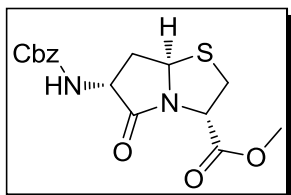
**(2*S*,5*R*,7*S*)-1-Aza-7-benzyloxycarbonylamino-8-oxo-4-thiabicyclo[3.3.0]octane-2-carboxylic acid methyl ester (2-17c) and
(2*S*,5*R*,7*R*)-1-Aza-7-benzyloxycarbonylamino-8-oxo-4-thiabicyclo[3.3.0]octane-2-carboxylic acid methyl ester (2-17d)**

Following the general procedure and treatment with TMSCH₂N₂ (5 mL, excess), D-Cys (1.00 g, 6.35 mmol) and *rac*-**2-16** (1.10 g, 4.15 mmol) afforded the corresponding bicyclic scaffolds **2-17c** (194 mg, 13%) and **2-17d** (291 mg, 20%).



C₁₆H₁₈N₂O₅, Mol. Wt. = 350.39
R_f = 0.30 (Tol/Ether, 1:1)

2-17c: The characterization data are same as for **2-17b**.

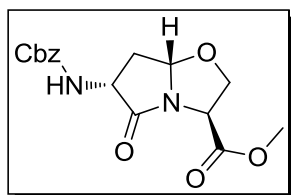


C₁₆H₁₈N₂O₅, Mol. Wt. = 350.39
R_f = 0.35 (Tol/Ether, 1:1)

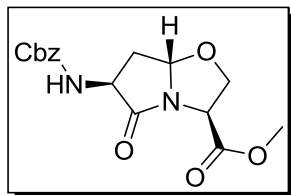
2-17d: The characterization data are the same as for **2-17a**.

**(2*S*,5*S*,7*S*)-1-Aza-7-benzyloxycarbonylamino-8-oxo-4-oxabicyclo[3.3.0]octane-2-carboxylic acid methyl ester and (2-18a) and
(2*R*,5*S*,7*R*)-1-Aza-7-benzyloxycarbonylamino-8-oxo-4-oxabicyclo[3.3.0]octane-2-carboxylic acid methyl ester (2-18b)**

Following the general procedure, L-Ser-OMe (0.250 g, 1.61 mmol) and *rac*-**2-16** (0.250 g, 0.943 mmol) afforded the corresponding bicyclic scaffolds **2-18a** and **2-18b** as an inseparable mixture (154 mg, 49%).



$C_{16}H_{18}N_2O_6$, Mol. Wt. = 334.32



$R_f = 0.45$ (H/EA, 3:7)

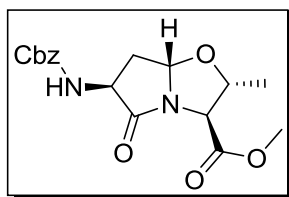
2-18a and 2-18b: 1H NMR (400 MHz, $CDCl_3$) δ 7.35 (s, 5H), 5.30 (bs, 1H), 5.17-5.19 (d, 1H), 5.13 (s, 2H), 5.09-5.07 (d, 1H), 4.49-4.43 (q, 1H) 3.78 (m, 3H), 2.97-2.90 (m, 1H), 2.69-2.64 (m, 1H), 2.52-2.29 (m, 3H), 1.95-1.86 (m, 1H).

^{13}C NMR (125 MHz, $CDCl_3$) δ 177.4, 174.1, 170.4, 170.0, 156.1, 136.2, 128.7, 128.4, 90.8, 89.3, 89.2, 70.0, 67.4, 57.2, 55.2, 54.1, 53.0, 52.9, 52.5, 36.1, 31.1.

HRMS (ESI+) calc'd for $[C_{16}H_{18}N_2O_6 + Na]^+$: 357.10571. Found: 357.10533.

(2S,3R,5S,7S)-1-Aza-7-benzyloxycarbonylamino-8-oxo-4-oxa-6-methylbicyclo[3.3.0]octane-2-carboxylic acid methyl ester and (2-19a)
(2S,3R,5S,7R)-1-Aza-7-benzyloxycarbonylamino-8-oxo-4-oxa-6-methylbicyclo[3.3.0]octane-2-carboxylic acid methyl ester (2-19b)

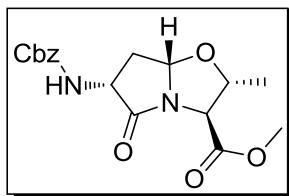
Following the general procedure, L-Thr-OMe (0.680 g, 4.01 mmol) and *rac*-**2-16** (0.825 g, 3.11 mmol) afforded the corresponding bicyclic scaffolds **2-19a** and **2-19b** as an inseparable mixture (380 mg, 35%).



$C_{17}H_{20}N_2O_6$, Mol. Wt. = 348.35

$R_f = 0.47$ (H/EA, 3:7)

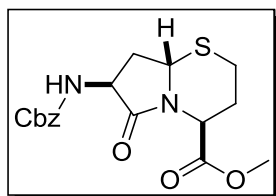
IR (cm^{-1}): 3338, 3018, 1713



2-19a and **2-19b**: 1H NMR (400 MHz, $CDCl_3$) δ 7.33 (s, 8H), 5.60 (bs, 0.5 H), 5.49 (bs, 1H), 5.20-5.19 (bd, 2H), 5.11 (s, 4H), 4.69-4.67 (q, 1H), 4.43-4.42 (q, 0.5 H), 4.26-4.17 (m, 1.5H), 4.11-4.09 (m, 1.5H), 3.76 (d, 6H), 3.08-3.04 (m, 1H), 2.64-2.58 (m, 0.5H), 2.28-2.22 (m, 0.5 H), 1.96-1.89 (m, 2H), 1.49-1.48 (d, 3H), 1.43-1.42 (d, 2H). ^{13}C NMR (100 MHz, $CDCl_3$) δ 177.40, 173.76, 170.19, 169.74, 156.07, 136.14, 128.63, 128.32, 128.25, 128.20, 90.60, 88.79, 79.82, 79.39, 67.28, 67.22, 63.97, 61.59, 54.03, 52.87, 52.45, 35.89, 31.09, 19.85, 19.39. HRMS (ESI+) calc'd for $[C_{17}H_{20}N_2O_6 + Na]^+$: 371.12136. Found: 371.12086.

(2R,6R,8R)-1-Aza-8-benzyloxycarbonylamino-9-oxo-5-thiabicyclo[4.3.0]nonane-2-carboxylic acid methyl ester (*rac*-2-20)

Following the general procedure and treatment with $TMSCH_2N_2$ (5 mL, excess), *rac*-homoCys (0.60 g, 3.50 mmol) and *rac*-2-16 (0.568 g, 2.14 mmol) afforded the corresponding bicyclic scaffolds *rac*-2-20 (250 mg, 32%).



$C_{17}H_{20}N_2O_5$, Mol. Wt. = 364.42

$R_f = 0.65$ (Tol/Ether, 1:1)

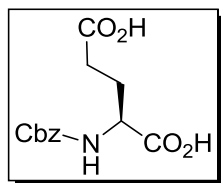
IR (cm^{-1}): 3324, 2953, 1697

^1H NMR (400 MHz, CDCl_3) δ 7.36-7.35 (m, 5H), 5.29 (bd, 1H), 5.19, (d, 1H), 5.12 (s, 2H), 5.07 (dd, 1H), 4.46 (q, 1H), 3.78 (s, 3H), 2.96-2.90 (m, 1H), 2.68 (dt, 1H), 2.49 (m, 1H), 2.39-2.30 (m, 2H), 1.95-1.86 (m, 1H).

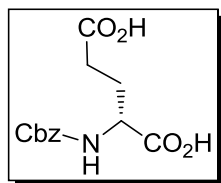
^{13}C NMR (75 MHz, CDCl_3) δ 171.5, 170.3, 156.3, 136.2, 128.7, 128.4, 128.3, 67.3, 54.9, 52.9, 51.9, 51.4, 33.2, 26.8, 25.4. HRMS (ESI+) calc'd for $[\text{C}_{17}\text{H}_{20}\text{N}_2\text{O}_5\text{S} + \text{H}]^+$: 365.11657. Found: 365.11685.

(S)-benzyl 5-oxo-4-(3-oxopropyl)oxazolidine-3-carboxylate (2-22a) and (R)-benzyl 5-oxo-4-(3-oxopropyl)oxazolidine-3-carboxylate (2-22b)

To a solution of L or D-Glutamic acid (5.0 g, 34.0 mmol) in 4 N NaOH (17 mL) at 0°C was added benzyl chloroformate (7.8 mL, 54.7 mmol) dropwise over a period of 10 min, then stirred at rt for 16 hours. The solution was extracted with diethyl ether, acidified to pH 2 with 4N HCl and extracted with ethyl acetate. The organic phase was then dried over Na_2SO_4 , filtered and concentrated *in vacuo* (5.6 g, 59 %, oil).



$\text{C}_{13}\text{H}_{15}\text{NO}_6$, Mol. Wt. = 281.26

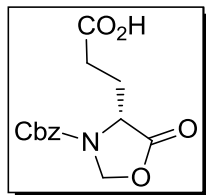
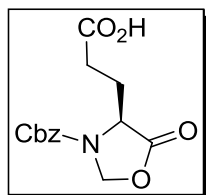


$R_f = 0.1$ (H/EA, 1:1)

^1H NMR (300MHz, acetone- d_6) δ 7.29-7.41 (m, 5H), 6.64-6.66 (d, 1H), 5.09 (s, 2H), 4.29-4.36 (m, 1H), 2.47-2.53 (m, 2H), 2.17-2.28 (m, 1H), 1.98-2.05 (m, 1H).

To a solution of the crude oil (5.6 g, 20.1 mmol) in toluene (125 mL), under Ar, was added paraformaldehyde (4.02 g, excess) and *p*-toluenesulfonic acid (0.40 g, 2.12 mmol equiv.). The mixture was refluxed for 3 h with removal of water using a Dean-Stark, then filtered through a pad of silica and concentrated *in vacuo*. The crude product was purified by flash chromatography (Hex/EtOAc/AcOH, gradient

of 8/2/0.01 to 1/1/0.01) to yield the desired intermediate oxazolidinone (3.02 g, 51%, oil).

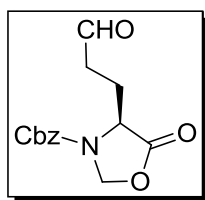


$C_{14}H_{15}NO_6$, Mol. Wt. = 293.27

$R_f = 0.2$ (H/EA, 1:1)

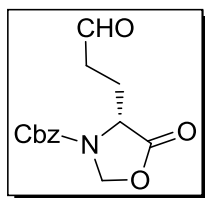
1H NMR (400MHz, $CDCl_3$) δ 7.39-7.35 (m, 5H), 5.55 (br, 1H), 5.24-5.19 (m, 3H), 4.42-4.39 (t, 1H), 2.57-2.15 (m, 4H).

To a stirred solution of the intermediate oxazolidinone (2.08 g, 7.1 mmol) in CH_2Cl_2 (50ml) under Ar were added distilled oxalyl chloride (0.91 mL, 10.6 mmol) and dimethylformamide (0.055 mL, 0.70 mmol). The solution was stirred for 1 h at rt, then the solvents were evaporated to give the crude product (quant. yield) which was immediately dissolved in dry THF (50 mL) and cooled to $-78^\circ C$. To the stirred solution was added lithium tri-*tert*-butoxyaluminum hydride (1.89 g, 7.45 mmol) slowly. The mixture was stirred for 4 h, slowly warming to $0^\circ C$, quenched with water and then filtered through Celite. The filtrate was extracted with CH_2Cl_2 , washed with water and brine, dried over Na_2SO_4 , and concentrated *in vacuo* to afford the aldehyde **2-22a** or **2-22b** which were used without further purification (1.27 g, 65%, orange oil).



$C_{14}H_{15}NO_5$, Mol. Wt. = 277.27

$R_f = 0.6$ (H/EA, 1:1)

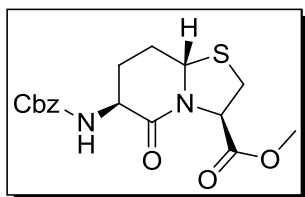


1H NMR (400 MHz, $CDCl_3$) δ 9.70 (br, 1H), 7.41-7.33 (m, 5H), 5.53 (br, 1H), 5.24-5.15 (m, 3H), 4.39-4.36 (t, 1H), 2.70-2.15 (m, 4H).

(2R,5S,8S)-1-Aza-8-benzyloxycarbonylamino-9-oxo-4-

thiabicyclo[3.4.0]nonane-2-carboxylic acid methyl ester (2-23a)

Following the general procedure, L-Cys-OMe (0.45 g, 2.6 mmol) and **2-22a** (0.60 g, 2.16 mmol) provided the cyclized intermediate as an oil. To a solution of this crude mixture in MeOH (25 mL) was added K_2CO_3 (0.40 g, 2.9 mmol). After stirring for another 4h, the reaction was quenched with water and extracted with CH_2Cl_2 . The organic phase was washed with brine, dried over Na_2SO_4 , filtered and concentrated *in vacuo*. The crude product was purified by flash chromatography (Hex/EtOAc, gradient 6/4 to 1/1) to afford the corresponding bicyclic scaffolds **2-23a** (116 mg, 32%).



$C_{17}H_{20}N_2O_5S$, Mol. Wt. = 364.42

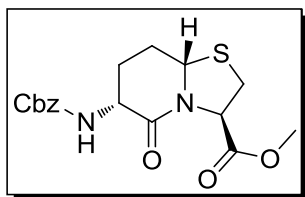
$R_f = 0.35$ (H/EA, 1:1)

1H NMR (300 MHz, $CDCl_3$) δ 7.36-7.31 (m, 5H), 5.51 (br, 1H), 5.13-5.08 (m, 3H), 4.97-4.90 (m, 1H), 4.33-4.16 (m, 1H), 3.76 (s, 3H), 3.41-3.33 (m, 1H), 3.28-3.21 (m, 1H), 2.65-2.53 (m, 1H), 2.43-1.74 (m, 4H).

HRMS (EI+) calc'd for $[C_{17}H_{20}N_2O_5S]^+$: 364.10929. Found: 364.10896.

(2R,5S,8R)-1-Aza-8-benzyloxycarbonylamino-9-oxo-4-thiabicyclo[3.4.0]nonane-2-carboxylic acid methyl ester (2-23b)

As for **2-23a**, L-Cys-OMe (0.95 g, 5.5 mmol), **2-22b** (1.27 g, 4.60 mmol) then K_2CO_3 (0.72 g, 5.2 mmol) afforded after flash chromatography (Hex/EtOAc, gradient 6/4 to 1/1) the corresponding bicyclic scaffolds **2-23b** (372 mg, 25%).



$C_{17}H_{20}N_2O_5S$, Mol. Wt. = 364.42

R_f = 0.35 (H/Ea, 1:1)

IR (cm^{-1}): 3324, 2953, 1697

$[\alpha]_D = -160.0$ (c 0.12, CH_3OH)

1H NMR (300 MHz, $CDCl_3$) δ 7.37 (s, 1H), 5.60-5.46 (m, 1H), 5.39-5.33 (m, 1H), 5.20 (bs, 2H), 4.95 (bs, 1H), 4.39 (bs, 1H), 3.77 (s, 3H), 3.43-3.21 (m, 1H), 3.27-3.17 (m, 1H), 2.31 (bs, 1H), 2.20-2.14 (m, 4H).

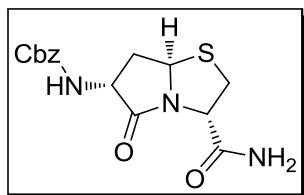
HRMS (EI+) calc'd for $[C_{17}H_{20}N_2O_5S]^+$: 364.10929. Found: 364.10847.

General procedure for formation of the amides

A stirred solution of the ester (either **2-24a-d**, **2-25a,b**, **2-26a,b**, *rac*-**2-27**, **2-28a,b**) in a solution of ammonia in methanol (ca. 7N solution) was reacted for 1h at rt. The corresponding amides were obtained in quantitative yields. Storage leads to partial isomerization. **2-24a,d**, **2-24b,c**, **2-28a** and **2-28b** were fully characterized. However, the other amides (**2-25a,b**, **2-26a,b**, *rac*-**2-27**) were reacted in the next step without further purification.

(2R,5S,7S)-1-Aza-7-benzyloxycarbonylamino-8-oxo-4-thiabicyclo[3.3.0]octane-2-carboxamide (2-24a,d)

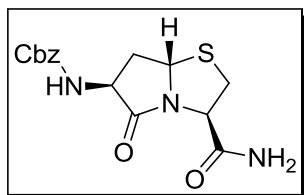
Following the general procedure for formation of the amide, **2-17a** and **2-17d** were reacted to give **2-24a** and **2-24d**.



$C_{15}H_{17}N_3O_4$, Mol. Wt. = 35.38

$R_f = 0.7$ (CH_2Cl_2 /Acet, 1:1)

IR (cm^{-1}): 3333, 2951, 1683



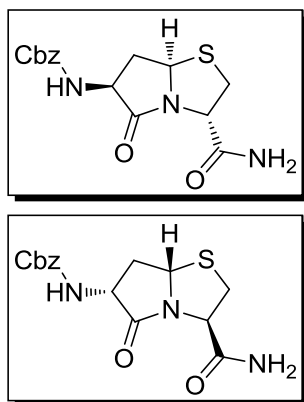
1H NMR (400 MHz, $(CD_3)_2CO$) δ 7.38-7.36 (m, 5H), 7.11 (bd, 2H), 6.76 (bs, 1H), 5.24-5.23 (dd, 1H), 5.10 (s, 2H), 4.81 (t, 1H), 4.37-4.29 (q, 1H), 3.48-3.47 (m, 2H), 2.58-2.52 (m, 2H).

^{13}C NMR (300 MHz, $(CD_3)_2CO$) δ 174.9, 171.9, 156.8, 137.8, 129.2, 128.8, 128.7, 67.0, 64.9, 60.0, 53.4, 37.0, 31.5.

LRMS (ESI+) calc'd for $[C_{15}H_{17}N_3O_4S + Na]^+$: 358.08. Found: 358.17.

(2*R*,5*S*,7*R*)-1-Aza-7-benzyloxycarbonylamino-8-oxo-4-thiabicyclo[3.3.0]octane-2-carboxamide (2-24b,c)

Following the general procedure for formation of the amide, **2-17c** and **2-17d** were reacted to give **2-24b** and **2-24c**.



$C_{15}H_{17}N_3O_4$, Mol. Wt. = 35.38

$R_f = 0.7$ (CH_2Cl_2 /Acet, 1:1)

IR (cm^{-1}): 3334, 1708, 1688

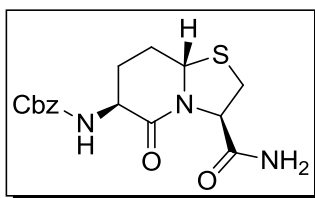
1H NMR (400 MHz, $(CD_3)_2CO$) δ 7.44-7.26 (m, 5H), 7.22 (bs, 1H), 6.75-6.72 (d, 1H), 6.64 (bs, 1H), 5.16 (t, 1H), 5.10 (s, 2H), 4.91-4.89 (m, 1H), 4.84-4.77 (m, 1H), 3.52-3.48 (dd, 1H), 3.91-3.24 (m, 1H), 3.07-3.01 (m, 1H), 2.14-2.05 (m, 1H).

^{13}C NMR (75 MHz, $CDCl_3$) δ 172.4, 171.4, 156.9, 138.0, 129.2, 128.7, 66.8, 62.0, 60.3, 55.2, 38.2, 34.8.

LRMS (ESI+) calc'd for $[C_{15}H_{17}N_3O_4S + Na]^+$: 358.08. Found: 358.15.

(2R,5S,8S)-1-Aza-8-benzyloxycarbonylamino-9-oxo-4-thiabicyclo[3.4.0]nonane-2-carboxamide (2-28a)

Following the general procedure for formation of the amide, **2-23a** was reacted to give **2-28a**.



$C_{16}H_{19}N_3O_4$, Mol. Wt. = 349.40

$R_f = 0.25$ (CH_2Cl_2 /Acet, 6:4)

IR (cm^{-1}): 3309, 2954, 1675, 1644

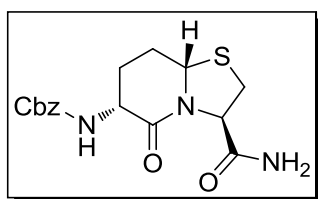
1H NMR (300 MHz, $CDCl_3$) δ 7.41-7.28 (m, 5H), 7.10 (bs, 1H), 5.79 (d, 1H), 5.33-5.28 (m, 2H), 5.08-5.02 (m, 2H), 4.88 (dd, 1H), 3.69 (dd, 1H), 3.53 (dd, 1H), 3.26 (dd, 1H), 2.34 (ddd, 1H), 2.23 (dt, 2H), 1.79 (ddd, 1H).

^{13}C NMR (75 MHz, CDCl_3) δ 171.4, 167.7, 156.7, 135.9, 128.7, 128.5, 128.1, 67.5, 62.1, 61.9, 52.1, 30.8, 28.6, 27.4.

HRMS (EI+) calc'd for $[\text{C}_{16}\text{H}_{19}\text{N}_3\text{O}_4\text{S}]^+$: 349.10963. Found: 349.10893.

(2R,5S,8R)-1-Aza-8-benzoyloxycarbonylamino-9-oxo-4-thiabicyclo[3.4.0]nonane-2-carboxamide (2-28b)

Following the general procedure for formation of the amide, **2-23b** was reacted to give **2-28b**.



$\text{C}_{16}\text{H}_{19}\text{N}_3\text{O}_4$, Mol. Wt. = 349.40

R_f = 0.27 ($\text{CH}_2\text{Cl}_2/\text{Acet}$, 6:4)

IR (cm^{-1}): 3329, 2947, 1671, 1659

^1H NMR (400 MHz, CDCl_3) δ 7.40-7.30 (m, 4H), 6.45 (s, 1H), 5.63 (s, 1H), 5.35 (s, 1H), 5.21-5.15 (m, 1H), 5.13 (s, 2H), 4.86 (t, 1H), 4.34-4.20 (m, 1H), 3.67 (dd, 1H), 3.12 (dd, 1H), 2.48-2.38 (m, 1H), 2.38-2.25 (m, 1H), 2.13-2.02 (m, 1H), 1.87-1.74 (m, 1H).

^{13}C NMR (75 MHz, CDCl_3) δ 171.0, 169.8, 156.3, 136.3, 128.7, 128.4, 128.3, 67.2, 61.8, 61.1, 51.6, 30.2, 29.8, 25.3, 24.9.

HRMS (EI+) calc'd for $[\text{C}_{16}\text{H}_{19}\text{N}_3\text{O}_4\text{S}]^+$: 349.10963. Found: 349.10863.

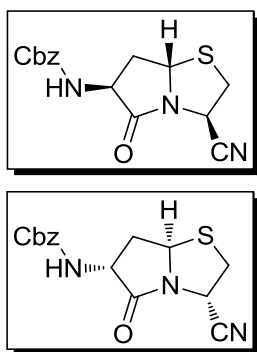
General procedure for formation of the nitriles

To a stirred solution of the amide (either **2-24a,d**, **2-24b,c**, **2-25a,b**, **2-26a,b**, *rac*-**2-27**, **2-28a** or **2-28b**) in dry THF, under Ar, at 0°C, was added TFA anhydride (1.2 equiv.) and Et_3N (2.0 equiv.). The reaction was stirred for 1 to 3 hours at rt. The solution was extracted with CH_2Cl_2 , washed with a saturated NaHCO_3 , dried over Na_2SO_4 and concentrated *in vacuo*. Further purification of the residue by flash column chromatography afforded the nitrile derivative.



(2R,5S,7S)-1-Aza-7-benzyloxycarbonylamino-8-oxo-4-thiabicyclo[3.3.0]octane-2-carbonitrile (2-8a) and (2S,5R,7R)-1-Aza-7-benzyloxycarbonylamino-8-oxo-4-thiabicyclo[3.3.0]octane-2-carbonitrile (2-8d)

Following the general procedure for formation of the nitrile, **2-24a** (238 mg, 0.71 mmol) or **2-24d** (90 mg, 0.12 mmol) afforded **8a** (114 mg, 51%) or **2-8d** (69 mg, 81%).



$C_{15}H_{15}N_3O_3$, Mol. Wt. 317.36

$R_f = 0.8$ (CH_2Cl_2 /Acet, 9:1)

IR (cm^{-1}): 3398, 2935, 1726, 1699

1H NMR (400 MHz, $(CD_3)_2CO$) δ 7.42-7.29 (m, 5H), 7.07 (d, 1H), 5.42-5.41 (m, 1H), 5.40 (d, 1H), 5.10 (s, 2H), 4.39 (q, 1H), 3.74-3.68 (m, 1H), 3.52-3.48 (m, 1H), 2.71-2.55 (m, 2H).

^{13}C NMR (75 MHz, $(CD_3)_2CO$) δ 175.6, 156.8, 137.9, 129.2, 128.8, 118.1, 67.1, 64.5, 52.2, 48.3, 39.0.

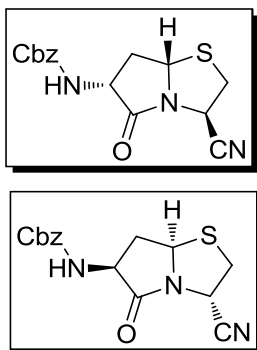
HRMS (ESI+) calc'd for $[C_{15}H_{15}N_3O_3S + Na]^+$: 340.07263. Found: 340.07229.



(2R,5S,7R)-1-Aza-7-benzyloxycarbonylamino-8-oxo-4-thiabicyclo[3.3.0]octane-2-carbonitrile (2-8b) and (2S,5R,7S)-1-Aza-7-benzyloxycarbonylamino-8-oxo-4-thiabicyclo[3.3.0]octane-2-carbonitrile (2-8c)

Following the general procedure for formation of the nitrile, **2-24b** (15 mg,

0.04mmol) or **2-24c** (55 mg, 0.16 mmol) afforded **2-8b** (11 mg, 79%) or **2-8c** (40 mg, 77%).



$C_{15}H_{15}N_3O_3$, Mol. Wt. 317.36

$R_f = 0.8$ (CH_2Cl_2 /Acet, 9:1)

IR (cm^{-1}): 3345, 2941, 1711, 1690

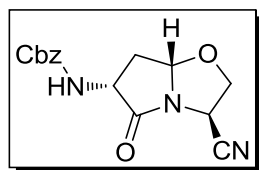
1H NMR (400 MHz, $(CD_3)_2CO$) δ 7.38-7.25 (m, 5H), 6.80 (d, 1H), 5.55-5.51 (m, 1H), 5.75 (t, 1H), 5.08 (s, 2H), 4.79-4.72 (m, 1H), 3.49-3.37 (m, 2H), 3.14-3.07 (m, 1H), 2.26-2.18 (m, 1H).

^{13}C NMR (75 MHz, $(CD_3)_2CO$) δ 172.4, 156.7, 138.0, 129.2, 128.7, 128.7, 117.5, 114.0, 66.9, 61.6, 55.0, 54.8, 48.1, 37.8, 36.6.

HRMS (ESI+) calc'd for $[C_{15}H_{15}N_3O_3S + Na]^+$: 340.07263. Found: 340.07247.

(2S,5S,7S)-1-Aza-7-benzyloxycarbonylamino-8-oxo-4-oxabicyclo[3.3.0]octane-2-carbonitrile and (2-9a) (2R,5S,7R)-1-Aza-7-benzyloxycarbonylamino-8-oxo-4-oxabicyclo[3.3.0]octane-2-carbonitrile (2-9b)

Following the general procedure for formation of the nitrile, **2-25a,b** (17 mg, 0.05 mmol) afforded **2-9a,b** (10 mg, 66%).



$C_{15}H_{15}N_3O_4$, Mol. Wt. = 301.30

$R_f = 0.35$ (CH_2Cl_2 /EA, 9:1)

IR (cm^{-1}): 3332, 2952, 1707

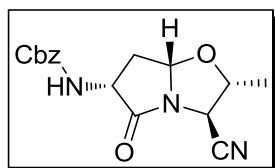
2-9a,b: ^1H NMR (400 MHz, CDCl_3) δ 7.36 (s, 6H), 5.13-5.30 (m, 3H), 5.12 (s, 3H), 4.77-4.84 (m, 1H), 4.59-4.65 (m, 1H), 4.47-4.52 (m, 1H), 4.38-4.43 (m, 0.3H), 4.02-4.24 (m, 1.7H), 3.72-3.78 (m, 0.3H), 3.09-3.16 (m, 1H), 2.67-2.74 (m, 0.3H), 2.36-2.44 (m, 0.3H), 2.01-2.08 (m, 1H).

^{13}C NMR (125 MHz, CDCl_3) δ 174.4, 155.9, 135.9, 128.7, 128.5, 128.4, 128.3, 116.8, 116.4, 90.6, 89.1, 70.7, 70.6, 67.5, 53.7, 45.4, 43.4, 35.1.

HRMS (ESI+) calc'd for $[\text{C}_{15}\text{H}_{15}\text{N}_3\text{O}_4 + \text{Na}]^+$: 324.09548. Found: 324.09527.

(2*S*,3*R*,5*S*,7*S*)-1-Aza-7-benzyloxycarbonylamino-8-oxo-4-oxa-6-methylbicyclo[3.3.0]octane-2-carbonitrile and (2-29a) (2*S*,3*R*,5*S*,7*R*)-1-Aza-7-benzyloxycarbonylamino-8-oxo-4-oxa-6-methylbicyclo[3.3.0]octane-2-carbonitrile (2-29b)

Following the general procedure for formation of the nitrile, **2-26a,b** (100 mg, 0.30 mmol) afforded **2-29a,b** (51 mg, 54%).



$\text{C}_{16}\text{H}_{17}\text{N}_3\text{O}_4$, Mol. Wt. = 315.32

R_f = 0.55 ($\text{CH}_2\text{Cl}_2/\text{EA}$, 9:1)

IR (cm^{-1}): 3332, 2932, 1712

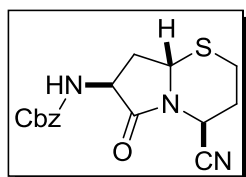
2-29a,b: ^1H NMR (400 MHz, CDCl_3) δ 7.36 (s, 5H), 5.30-5.23 (m, 2H), 5.12 (s, 2H), 4.63 (q, 1H), 4.43 (q, 1H), 4.20 (q, 1H), 3.17-3.09 (m, 1H), 2.71-2.64 (m, 0.1H), 2.41-2.33 (m, 0.1H), 2.05-1.97 (m, 1H), 1.53-1.51 (d, 3H), 1.43 (d, 1H).

^{13}C NMR (75 MHz, CDCl_3) δ 174.4, 155.9, 136.0, 128.7, 128.5, 128.3, 116.5, 116.1, 90.5, 88.9, 80.7, 67.5, 53.5, 51.9, 49.4, 35.3, 18.9, 18.2.

HRMS (ESI+) calc'd for $[\text{C}_{16}\text{H}_{17}\text{N}_3\text{O}_4 + \text{Na}]^+$: 338.11113. Found: 338.11096.

(2R,6R,8R)-1-Aza-8-benzyloxycarbonylamino-9-oxo-5-thiabicyclo[4.3.0]nonane-2-carbonitrile (*rac*-2-30)

Following the general procedure for formation of the nitrile, *rac*-2-27 (59 mg, 0.17 mmol) afforded *rac*-2-30 (24 mg, 42%).



$C_{17}H_{17}N_3O_3S$, Mol. Wt. = 331.39

$R_f = 0.3$ (H/EA, 7:3)

IR (cm^{-1}): 3271, 2952, 1717, 1689

1H NMR (400 MHz, $CDCl_3$) δ 7.36 (s, 5H), 5.42 (bs, 1H), 5.20 (bs, 2H), 5.13 (s, 2H), 4.42 (q, 1H), 3.35 (t, 1H), 2.83-2.79 (m, 1H), 2.53-2.48 (m, 1H), 2.41-2.33 (m, 1H), 2.33-2.17 (m, 1H), 2.00-1.94 (m, 1H).

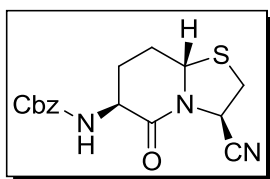
^{13}C NMR (100 MHz, $CDCl_3$) δ 170.5, 156.1, 136.0, 128.7, 128.5, 128.3, 115.9, 67.5, 54.4, 51.4, 41.9, 32.8, 28.2, 24.8.

HRMS (ESI+) calc'd for $[C_{16}H_{17}N_3O_3S + Na]^+$: 354.08828. Found: 354.08831.



(2R,5S,8S)-1-Aza-8-benzyloxycarbonylamino-9-oxo-4-thiabicyclo[3.4.0]nonane-2-carboxylic carbonitrile (2-31a)

Following the general procedure for formation of the nitrile, 2-28a (23 mg, 0.07 mmol) afforded 2-31a (9 mg, 39%).



$C_{16}H_{17}N_3O_3S$, Mol. Wt. = 331.39

$R_f = 0.49$ (H/EA, 6:4)

IR (cm^{-1}): 3366, 2952, 1695, 1656

$[\alpha]_D = -130.8$ (c 0.12, CH_3OH)

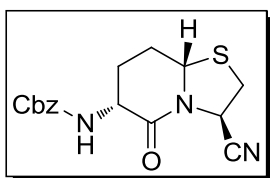
1H NMR (500 MHz, $CDCl_3$) δ 7.42-7.28 (m, 5H), 5.62 (s, 1H), 5.34 (dd, 1H), 5.12 (q, 2H), 4.95 (s, 1H), 4.23 (s, 1H), 3.40 (dd, 1H), 3.31 (dd, 1H), 2.53 (bd, 1H), 2.40 (bd, 1H), 1.97-1.78 (m, 2H).

^{13}C NMR (125 MHz, CDCl_3) δ 167.6, 156.6, 136.3, 128.7, 128.7, 128.6, 128.3, 128.2, 116.7, 67.2, 62.3, 52.3, 48.5, 33.2, 29.8, 27.9, 27.7.

HRMS (EI+) calc'd for $[\text{C}_{16}\text{H}_{17}\text{N}_3\text{O}_3\text{S}]^+$: 331.09906. Found: 331.09817.

(2R,5S,8R)-1-Aza-8-benzyloxycarbonylamino-9-oxo-4-thiabicyclo[3.4.0]nonane-2-carboxylic carbonitrile (2-31b)

Following the general procedure for formation of the nitrile, **2-28b** (40 mg, 0.11 mmol) afforded **2-31b** (10 mg, 27%).



$\text{C}_{16}\text{H}_{17}\text{N}_3\text{O}_3\text{S}$, Mol. Wt. = 331.39

R_f = 0.45 (H/EA, 6:4)

IR (cm^{-1}): 3322, 2926, 1712, 1663

$[\alpha]_D = -208.1$ (c 0.09, CH_3OH)

^1H NMR (500 MHz, CDCl_3) δ 7.36 (s, 5H), 5.74 (s, 1H), 5.68 (s, 1H), 5.12 (s, 3H), 4.30-4.18 (m, 1H), 3.30 (dd, 2H), 2.52-2.31 (m, 2H), 2.19-2.02 (m, 1H), 1.92-1.76 (m, 1H).

^{13}C NMR (125 MHz, CDCl_3) δ 168.7, 156.1, 136.2, 128.7, 128.4, 128.3, 116.8, 67.2, 61.9, 51.8, 48.5, 33.7, 29.8, 24.9.

HRMS (EI+) calc'd for $[\text{C}_{17}\text{H}_{20}\text{N}_2\text{O}_5\text{S}]^+$: 331.09906. Found: 331.09795.

2.6.2 HPLC analysis of purity

To verify the purity of all compounds used for biological tests, analytical reverse phase HPLC was performed on an Agilent 1100 Series instrument equipped with VWD-detector, C18 reverse column (Agilent, Zorbax Eclipse XDB-C18 150mm*4.6mm, 5 μm), UV detection at 254 nm. Depending on the compound, two different conditions were used: condition A (50% acetonitrile, 50% water, 1 mL/min) or condition B (50% methanol, 50% water, 1 mL/min) or condition C (60% water, 40% acetonitrile, 1 mL/min) or condition D (70% water, 30% acetonitrile, 1 mL/min).

Table 2.4 HPLC analysis of purity of final compounds

Compd	Analysis condition	Retention time (min.)	Purity (%)
2-11a	B	4.3	98.7
2-11b	B	4.5	98.8
2-12a	B	5.9	98.0
2-12b	B	5.7	98.2
2-14	B	8.7	92.5
2-17a	A	3.8	91.9 (9:1 of 2-17a : 2-17b)
2-17b	A	3.3	96.7 (1:9 of 2-17a : 2-17b)
2-24a	D	5.2	98.0
2-24b	D	4.7	93.6
2-8a	C	7.3	97.9
2-8b	C	6.7	99.7
2-8c	A	3.5	98.9 (18:1 of 2-8c : 2-8d)
2-8d	A	3.8	96.0 (1:4 of 2-8c : 2-8d)
2-9a,b	A	3.0	95.8 (1:10 of 2-9a : 2-9b)
2-29a,b	B	3.7	98.1 (1:21 of 2-29a : 2-29b)
<i>rac</i> - 2-30	B	7.6	95.7
2-31a	B	5.8	97.6
2-31b	B	6.7	97.3

2.6.3 Docking study

The protein structure (1h2y) was downloaded from the protein databank and prepared as reported previously.¹⁹ It was next prepared for docking using

PROCESS, a module of our docking program FITTED.²¹ The ligands were prepared using Maestro and SMART, a third module of FITTED. They were subsequently docked using the FITTED docking engine and default parameters. For the covalent docking to be used, the Ser554 has been selected as a reactive residue.

2.6.4 Biological evaluations

The human glioblastoma-derived cell lines LN18, LN229 and LN2308 were a kind gift of AC Diserens, Neurosurgery Department, Lausanne, Switzerland, the immortalized human brain-derived HCEC cells have been kindly provided by D. Stanimirovic, Ottawa, Canada, and the human fibroblasts PO03 and PG98/5 cells have been prepared in Lausanne from human lung and skin surgical samples, respectively, according to protocols accepted by the Hospital Ethics Committee.

Cells were routinely grown in DMEM culture medium containing 4.5 g/L glucose, 10% fetal calf serum (FCS) and antibiotics (all from Gibco, Basel, Switzerland). One to two days before evaluation, cells were seeded in 48-well plates (Costar, Corning, NY, USA) in complete medium in order to reach confluence on the day of experiment. On the day of experiment, the culture medium was removed, and either 200 μ L phosphate-buffered saline (PBS, pH 7.2-7.4) were added in half of the wells or 200 μ L PBS containing 0.1 % Triton X-100 (Fluka, Buchs, Switzerland) were added in the other half of the wells, for the evaluation of the inhibition of POP and DPP IV activities in intact cells or cell extracts, respectively. Experiments were performed in duplicate wells.

The synthetic molecules were dissolved at 10 mg/mL in methanol, then diluted 1:10 in H₂O, and 1 or 5 μ L of the water solution were added to duplicate PBS and PBS-Triton wells, followed after 5-10 min at room temperature by Gly-Pro-AMC or Z-Gly-Pro-AMC substrates (1 mg/mL DMSO, both from Bachem, Bubendorf, Switzerland), final concentration 10 μ M. Increase in fluorescence at $\lambda_{ex}/\lambda_{em}$ = 360/460 nm was recorded for 30 min at 37 °C in a thermostated multiwell fluorescence reader (Cytofluor, PerSeptive BioSystems, Switzerland). For the determination of IC₅₀, cells in PBS or in PBS-Triton X-100 were exposed to

decreasing concentrations of the inhibitors, then determination of residual activity was measured, and plotted against inhibitor concentration. IC₅₀ values were determined graphically.

Acknowledgment. We thank CIHR, ViroChem Pharma, NSERC, FQRNT and the Canadian Foundation for Innovation for financial support (NM). JL holds a scholarship from Le Fonds Québécois de la Recherche sur la Nature et les Technologies. We also thank the Swiss Society for Multiple Sclerosis for support to LJJ group.

2.7 References

1. Polgár, L. Prolyl endopeptidase catalysis. A physical rather than a chemical step is rate-limiting. *Biochemistry* **1992**, 283, 647-648.
2. Irazusta, J.; Larrinaga, G.; González-Maeso, J.; Gil, J.; Meana, J. J.; Casis, L. Distribution of prolyl endopeptidase activities in rat and human brain. *Neurochem. Int.* **2002**, 40, 337-345.
3. Szeltner, Z.; Polgár, L. Structure, function and biological relevance of prolyl oligopeptidase. *Curr. Protein Pept. Sci.* **2008**, 9, 96-107.
4. Männistö, P. T.; Venäläinen, J.; Jalkanen, A.; García-Horsman, J. A. Prolyl Oligopeptidase: A Potential Target for the Treatment of Cognitive Disorders. *Drug News Perspect.* **2007**, 20, 293-306.
5. Brandt, I.; Scharpé, S.; Lambeir, A. M. Suggested functions for prolyl oligopeptidase: A puzzling paradox. *Clin. Chim. Acta* **2007**, 377, 50-61.
6. Williams, R. S. B. Prolyl oligopeptidase and bipolar disorder. *Clin. Neurosci. Res.* **2004**, 4, 233-242.
7. Cunningham, D. F.; O'Connor, B. Identification and initial characterisation of a N-benzyloxycarbonyl-prolyl-prolinal (Z-Pro-prolinal)-insensitive 7-(N-benzyloxycarbonyl-glycyl-prolyl-amido)-4-methylcoumarin (Z-Gly-Bro-NH-Mec)-hydrolysing peptidase in bovine serum. *Eur. J. Biochem.* **1997**, 244, 900-903.

8. Toide, K.; Shinoda, M.; Iwamoto, Y.; Fujiwara, T.; Okamiya, K.; Uemura, A. A novel propyl endopeptidase inhibitor, JTP-4819, with potential for treating Alzheimer's disease. *Behav. Brain Res.* **1997**, 83, 147-151.
9. Toide, K.; Shinoda, M.; Miyazaki, A. A novel prolyl endopeptidase inhibitor, JTP-4819. Its behavioral and neurochemical properties for the treatment of Alzheimer's disease. *Rev. Neurosci.* **1998**, 9, 17-29.
10. Saito, M.; Hashimoto, M.; Kawaguchi, N.; Shibata, H.; Fukami, H.; Tanaka, T.; Higuchi, N. Synthesis and inhibitory activity of acyl-peptidyl-pyrrolidine derivatives toward post-proline cleaving enzyme; a study of subsite specificity. *J. Enzym. Inhib.* **1991**, 5, 51-75.
11. Barelli, H.; Petit, A.; Hirsch, E.; Wilk, S.; De Nanteuil, G.; Morain, P.; Checler, F. S 17092-1, a highly potent, specific and cell permeant inhibitor of human proline endopeptidase. *Biochem. Biophys. Res. Commun.* **1999**, 257, 657-661.
12. Toide, K.; Shinoda, M.; Fujiwara, T.; Iwamoto, Y. Effect of a novel prolyl endopeptidase inhibitor, JTP-4819, on spatial memory and central cholinergic neurons in aged rats. *Pharmacol., Biochem. Behav.* **1997**, 56, 427-434.
13. Miyazaki, A.; Toide, K.; Sasaki, Y.; Ichitani, Y.; Iwasaki, T. Effect of a prolyl endopeptidase inhibitor, JTP-4819, on radial maze performance in hippocampal-lesioned rats. *Pharmacol., Biochem. Behav.* **1998**, 59, 361-368.
14. Kato, A.; Fukunari, A.; Sakai, Y.; Nakajima, T. Prevention of amyloid-like deposition by a selective prolyl endopeptidase inhibitor, Y-29794, in senescence-accelerated mouse. *J. Pharmacol. Exp. Ther.* **1997**, 283, 328-335.
15. Shinoda, M.; Toide, K.; Ohsawa, I.; Kohsaka, S. Specific inhibitor for prolyl endopeptidase suppresses the generation of amyloid β protein in NG108-15 cells. *Biochem. Biophys. Res. Commun.* **1997**, 235, 641-645.
16. Morain, P.; Robin, J. L.; De Nanteuil, G.; Jochemsen, R.; Heidet, V.; Guez, D. Pharmacodynamic and pharmacokinetic profile of S 17092, a new orally active prolyl endopeptidase inhibitor, in elderly healthy volunteers. A phase I study. *Br. J. Clin. Pharmacol.* **2000**, 50, 350-359.

17. Szeltner, Z.; Rea, D.; Renner, V.; Fulop, V.; Polgar, L. Electrostatic effects and binding determinants in the catalysis of prolyl oligopeptidase. Site specific mutagenesis at the oxyanion binding site. *J. Biol. Chem.* **2002**, 277, 42613-22.
18. Li, J.; Wilk, E.; Wilk, S. Inhibition of prolyl oligopeptidase by Fmoc-aminoacylpyrrolidine-2-nitriles. *J. Neurochem.* **1996**, 66, 2105-2112.
19. Corbeil, C. R.; Englebienne, P.; Moitessier, N. Docking ligands into flexible and solvated macromolecules. 1. Development and validation of FITTED 1.0. *J. Chem. Inf. Model.* **2007**, 47, 435-449.
20. Corbeil, C. R.; Moitessier, N. Docking ligands into flexible and solvated macromolecules. 3. Impact of input ligand conformation, protein flexibility, and water molecules on the accuracy of docking programs. *J. Chem. Inf. Model.* **2009**, 49, 997-1009.
21. Corbeil, C. R.; Englebienne, P.; Moitessier, N.; Therrien, E. *FITTED Docking Program*. www.fitted.ca **2009**.
22. Oballa, R. M.; Truchon, J. F.; Bayly, C. I.; Chauret, N.; Day, S.; Crane, S.; Berthelette, C. A generally applicable method for assessing the electrophilicity and reactivity of diverse nitrile-containing compounds. *Bioorg. Med. Chem. Lett.* **2007**, 17, 998-1002.
23. Hanessian, S.; Moitessier, N. Sulfonamide-based acyclic and conformationally constrained MMP inhibitors: From computer-assisted design to nanomolar compounds. *Curr. Top. Med. Chem.* **2004**, 4, 1269-1287.
24. Hanessian, S.; McNaughton-Smith, G.; Lombart, H. G.; Lubell, W. D. Design and synthesis of conformationally constrained amino acids as versatile scaffolds and peptide mimetics. *Tetrahedron* **1997**, 53, 12789-12854.
25. Baldwin, J. E.; Freeman, R. T.; Lowe, C.; Schofield, C. J.; Lee, E. A γ -lactam analogue of the penems possessing antibacterial activity. *Tetrahedron* **1989**, 45, 4537-4550.

26. Subasinghe, N. L.; Bontems, R. J.; McIntee, E.; Mishra, R. K.; Johnson, R. L. Bicyclic thiazolidine lactam peptidomimetics of the dopamine receptor modulating peptide Pro-Leu-Gly-NH₂. *J. Med. Chem.* **1993**, 36, 2356-2361.
27. Nagai, U.; Sato, K. Synthesis of a bicyclic dipeptide with the shape of β -turn central part. *Tetrahedron Lett.* **1985**, 26, 647-650.
28. Estiarte, M. A.; Rubiralta, M.; Diez, A.; Thormann, M.; Giralt, E. Oxazolopiperidin-2-ones as type II' β -turn mimetics: Synthesis and conformational analysis. *J. Org. Chem.* **2000**, 65, 6992-6999.
29. Caplan, J. F.; Sutherland, A.; Vederas, J. C. The first stereospecific synthesis of L-tetrahydrodipicolinic acid; a key intermediate of diaminopimelate metabolism. *J. Chem. Soc., Perkin Trans. 1* **2001**, 2217-2220.
30. Kamber, M.; Just, G. γ -Phosphono- γ -lactones. The use of allyl esters as easily removable phosphonate protecting groups. *Can. J. Chem.* **1985**, 63, 823-827.
31. Khalil, E. M.; Pradhan, A.; Ojala, W. H.; Gleason, W. B.; Mishra, R. K.; Johnson, R. L. Synthesis and dopamine receptor modulating activity of substituted bicyclic thiazolidine lactam peptidomimetics of L-prolyl-L-leucyl-glycinamide. *J. Med. Chem.* **1999**, 42, 2977-2987.
32. Wallén, E. A. A.; Christiaans, J. A. M.; Forsberg, M. M.; Venäläinen, J. I.; Männistö, P. T.; Gynther, J. Dicarboxylic acid bis(L-prolyl-pyrrolidine) amides as prolyl oligopeptidase inhibitors. *J. Med. Chem.* **2002**, 45, 4581-4584.
33. Baldwin, J. E.; Lee, E. Synthesis of bicyclic γ -lactams via oxazolidinones. *Tetrahedron* **1986**, 42, 6551-6554.
34. Juillerat-Jeanneret, L. Prolyl-specific peptidases and their inhibitors in biological processes. *Curr. Chem. Biol.* **2008**, 2, 97-109.
35. Morain, P.; Lestage, P.; De Nanteuil, G.; Jochemsen, R.; Robin, J. L.; Guez, D.; Boyer, P. A. S 17092: A prolyl endopeptidase inhibitor as a potential therapeutic drug for memory impairment. Preclinical and clinical studies. *CNS Drug Rev.* **2002**, 8, 31-52.

36. Toide, K.; Iwamoto, Y.; Fujiwara, T.; Abe, H. JTP-4819: A novel prolyl endopeptidase inhibitor with potential as a cognitive enhancer. *J. Pharmacol. Exp. Ther.* **1995**, 274, 1370-1378.
37. Schneider, J. S.; Giardiniere, M.; Morain, P. Effects of the prolyl endopeptidase inhibitor S 17092 on cognitive deficits in Chronic low dose MPTP-treated monkeys. *Neuropsychopharmacol.* **2002**, 26, 176-182.
38. Maes, M. Alterations in plasma prolyl endopeptidase activity in depression, mania, and schizophrenia: Effects of antidepressants, mood stabilizers, and antipsychotic drugs. *Psychiatry Res.* **1995**, 58, 217-225.
39. Mantle, D.; Falkous, G.; Ishiura, S.; Blanchard, P. J.; Perry, E. K. Comparison of proline endopeptidase activity in brain tissue from normal cases and cases with Alzheimer's disease, Lewy body dementia, Parkinson's disease and Huntington's disease. *Clin. Chim. Acta* **1996**, 249, 129-139.
40. Tran, T.; Quan, C.; Edosada, C. Y.; Mayeda, M.; Wiesmann, C.; Sutherlin, D.; Wolf, B. B. Synthesis and structure-activity relationship of N-acyl-Gly-, N-acyl-Sar- and N-blocked-boroPro inhibitors of FAP, DPP4, and POP. *Bioorg. Med. Chem. Lett.* **2007**, 17, 1438-42.
41. Yoshimoto, T.; Tsuru, D.; Yamamoto, N.; Ikezawa, R.; Furukawa, S. Structure activity relationship of inhibitors specific for prolyl endopeptidase. *Agric. Biol. Chem.* **1991**, 55, 37-43.
42. Jones, K.; Woo, K. C. A total synthesis of (-)-ruspolinone. *Tetrahedron* **1991**, 47, 7179-7184.
43. Tang, F. Y.; Qu, L. Q.; Xu, Y.; Ma, R. J.; Chen, S. H.; Li, G. Practical synthesis of structurally important spirodiamine templates. *Synth. Commun.* **2007**, 37, 3793-3799.
44. Caputo, C. A.; Carneiro, F. D. S.; Jennings, M. C.; Jones, N. D. Modular syntheses of oxazolinylamine ligands and characterization of group 10 metal complexes. *Can. J. Chem.* **2007**, 85, 85-95.
45. Heller, B.; Sundermann, B.; Buschmann, H.; Drexler, H. J.; You, J.; Holzgrabe, U.; Heller, E.; Oehme, G. Photocatalyzed [2 + 2 + 2]-cycloaddition of

nitriles with acetylene: An effective method for the synthesis of 2-pyridines under mild conditions. *J. Org. Chem.* **2002**, 67, 4414-4422.

46. Johnson, R. L.; Rajakumar, G.; Yu, K. L.; Mishra, R. K. Synthesis of Pro-Leu-Gly-NH₂ analogues modified at the prolyl residue and evaluation of their effects on the receptor binding activity of the central dopamine receptor agonist, ADTN. *J. Med. Chem.* **1986**, 29, 2104-2107.

Chapter 3 The reactivity of the hydroxyls of different sugars is condition dependent

Previous chapters focused on amino acids and peptides in scaffold design in medicinal chemistry. While amino acids are widely used, medicinal chemists could also investigate carbohydrates as chiral sources. However, given the complexity of carbohydrate chemistry, carbohydrates remain largely under-explored in medicinal chemistry. Herein, we review the existing methods that chemists use to selectively functionalize various carbohydrates, as steps towards exploit carbohydrates as chiral sources.

3.1 Abstract

Glucose can be described as one of Nature's simple building blocks. Yet to an Organic Chemist, this simple building block represents a major challenge because of its multiple hydroxyl groups thereby limiting its applications. How can we target one hydroxyl on a compound that has so many? To address the regioselectivity issue and develop efficient synthetic routes, a few studies were done to better understand the differences in reactivity between the secondary hydroxyls of various sugars, while others focused on how to overcome this order of reactivity, innate in each sugar. We aim to review the studies revealing the differences in reactivity of the hydroxyls of hexopyranosides, also highlighting the various methods available to selectively functionalize or glycosylate a sugar at different positions. From our review, we found that some research groups have utilized the innate differences in reactivity of the hydroxyls to selectively functionalize one position of a sugar over the others. Others used extrinsic factors, such as adding catalysts or introducing other functional groups on the sugar, to overcome the innate order of reactivity. Overall, we realized that many reports contradict each other, and most researchers do not offer any explanations or justifications for the observed trends in reactivity.

3.2 Introduction

Many organisms use sugars as building blocks for more complex structures in nature such as cellulose in plants and chitin in crustaceans. To construct these large polysaccharides, these organisms use powerful enzymes which perform reactions regio- and stereo-selectively on these sugar building blocks. The enzymes build polysaccharides in an efficient process that yields a large amount of the desired product quickly, without wasting energy and without generating undesired side products such as unwanted isomers. As synthetic chemists, we wonder how we could perform such efficient reactions when Nature's seemingly simple building blocks are actually quite complex because of the number of

stereocenters and similar functional groups. More often than not, researchers aiming to perform a reaction at a specific hydroxyl on a sugar will perform a series of protections and deprotections in a process that is wasteful, costly, time consuming, and, in the end, yielding little product. To better understand how one could perform a reaction selectively on a sugar, Williams and Richardson first attempted^{1,2} to rank the secondary hydroxyls of three sugars (methyl α -D-glucopyranoside (**3-1**), methyl α -D-mannopyranoside (**3-2**) and methyl α -D-galactopyranoside (**3-3**), Figure 3.1) according to how reactive each hydroxyl is under benzoylation conditions.

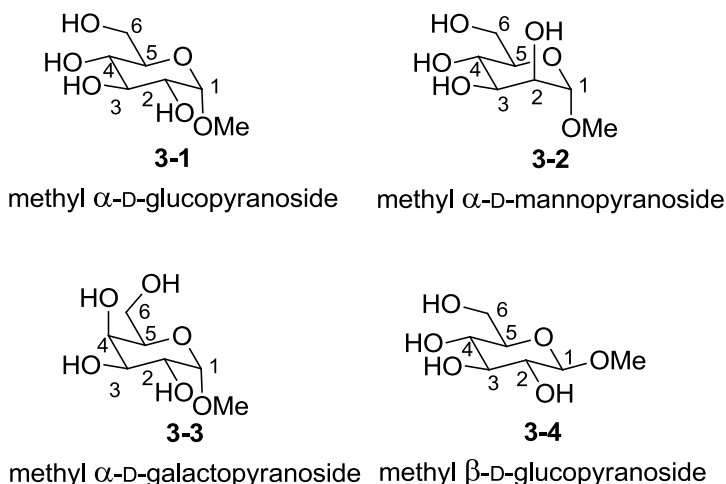
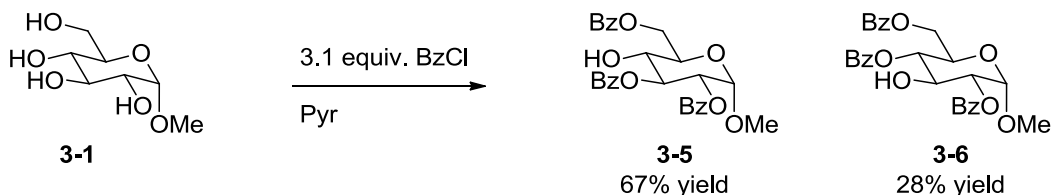


Figure 3.1 Position numbering of methyl α -D-glucopyranoside (**3-1**), mannopyranoside (**3-2**) and galactopyranoside (**3-3**) as well as methyl β -D-glucopyranoside (**3-4**).

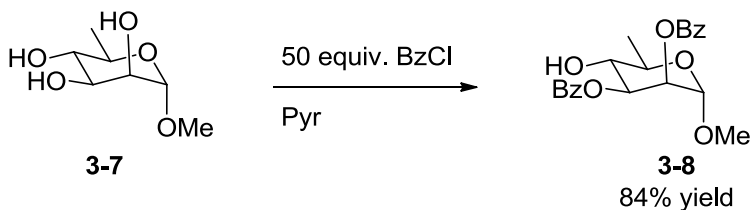


Scheme 3.1 Benzoylation of methyl α -D-glucopyranoside.

By benzoylating each sugar with an excess of benzoyl chloride in pyridine and carefully isolating and analyzing the di- and tri-benzoylated products from the mixture (such as **3-5** and **3-6** in Scheme 3.1), Williams and Richardson established that the primary hydroxyl at position 6 of each of the sugars reacted first (perhaps because this position is the most accessible of them all) and

observed the following reactivity trends for the secondary hydroxyls: 2-OH > 3-OH > 4-OH for the glucopyranoside, 3-OH > 2-OH > 4-OH for the mannopyranoside, and finally 2-OH, 3-OH > 4-OH for the galactopyranoside. Williams and Richardson discussed that intramolecular hydrogen-bonding possibly influences the reactivity of each hydroxyl. While the adjacent anomeric position may contribute an extra hydrogen bond to the 2-OH, thereby increasing the reactivity of the 2-OH of the glucopyranoside, the 2-OH is axial in the mannopyranoside, rendering the 2-OH less reactive than the 3-OH. Intramolecular hydrogen bonding is unlikely in pyridine, the basic solvent used for their benzylation experiments. Interestingly, they observe similar reactivities when they ran their experiments in carbon tetrachloride, a solvent that cannot provide any hydrogen bonding (unlike pyridine), thereby promoting the intramolecular hydrogen bonding of the sugar.

In a second part to the study of hydroxyl reactivity,³ Williams and Richardson examined how reactive the secondary hydroxyls would be under similar benzylation conditions, but when the primary hydroxyl was eliminated from each sugar system; in other words, the 6-OH was replaced with a 6-H (3-7).



Scheme 3.2 Benzylation of methyl 6-deoxy- α -D-mannopyranoside.

Again, the 4-OH does not react under the benzylation conditions used, while the 2-OH and 3-OH of methyl 6-deoxy- α -D-mannopyranoside are benzylated (forming 3-8). They concluded that the hydroxyl (or rather the benzyolated hydroxyl since this position is benzyolated rapidly) at position 6 is not to blame for the “non-reactivity” of the 4-OH. They also confirm the results of Williams and Richardson, namely that the 4-OH is the least reactive. Kondo, Miyahara and Kashimura⁴ also confirmed that the order of reactivity of the secondary hydroxyls of methyl 6-deoxy- α - and β -D-glucopyranosides was the same as the order that

Williams and Richardson previously observed for methyl α - and β -D-glucopyranosides.

This ground-breaking work demonstrates that the hydroxyls of different sugars have different intrinsic reactivity patterns that vary depending on the sugar explored. However, none of these studies reveal whether extrinsic factors, such as the sterics of the reagent, also influence the products formed. Furthermore, neither of these studies provided an easy method to selectively react at one hydroxyl over all the other hydroxyls. Such a method would greatly simplify the number of steps a chemist is required to perform when attempting to react at a specific position of a sugar, thereby reducing the amount of waste generated, the amount of time necessary, and the financial resources required to perform such reactions.

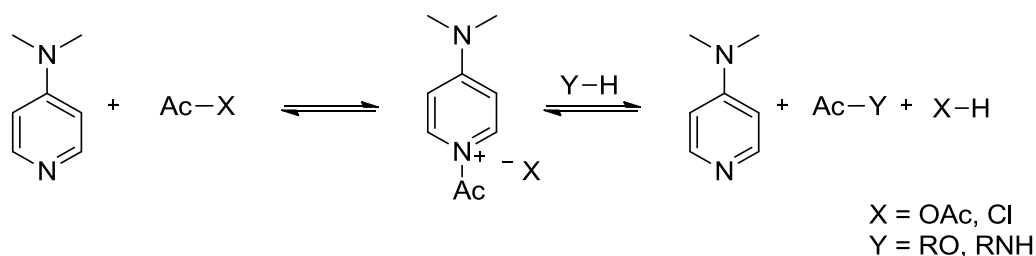
The aim of this chapter is to provide a review of the different methods that chemists have explored over the last 40 years to selectively react at one position of a sugar in a minimal number of reactions, without going through several extra steps of protections and deprotections prior to the desired reaction. For the purpose of this thesis, we will mainly highlight methods applied to selective acylation and glycosylation of hexopyranosides. Many of the methods reviewed here have been successfully applied to furanosides, and also alkylation chemistry of pyranosides. Rather than listing all the reported methods, we have organized these methods according to whether they take advantage of the intrinsic reactivity of the hydroxyls of sugars, or whether extrinsic factors are used to overcome the innate reactivity of the hydroxyls.

3.3 Selective methods to functionalize sugars based on the intrinsic reactivity of the hydroxyls

Several methods take advantage of the innate reactivity of the hydroxyls in order to regioselectively functionalize a sugar.

3.3.1 4-Dimethylaminopyridine (DMAP) catalyzed acylations of alcohols

DMAP and chiral DMAP derivatives are now quite commonly used as catalysts (catalytically or stoichiometrically) in many reactions, including peptide bond formation,⁵ Morita-Baylis Hillman reaction,⁶ and Michael addition.⁷ For carbohydrate chemists especially, DMAP-catalyzed acylation of alcohols represents an essential tool to functionalize sugars. In 1901, Verley and Bolsing⁸ developed the first procedure for acylation of hydroxyls using acetic anhydride and pyridine. This reliable procedure is widely used, even today, for acetylation of carbohydrates. It was not until the late 60's that Höfle and Steglich discovered that DMAP and 4-pyrrolidinopyridine catalyzed the acylation reaction, not only speeding up the reaction but also rendering this new set of conditions applicable to large-scale synthesis.⁹ Fersht and Jencks originally proposed a mechanism for DMAP-catalyzed acylation in 1970 (Scheme 3.3),¹⁰ based on results from a three-part study on the hydrolysis of acetic anhydride (part I),¹¹ catalyzed by pyridine (part II)¹² and other tertiary amines (part III).¹³



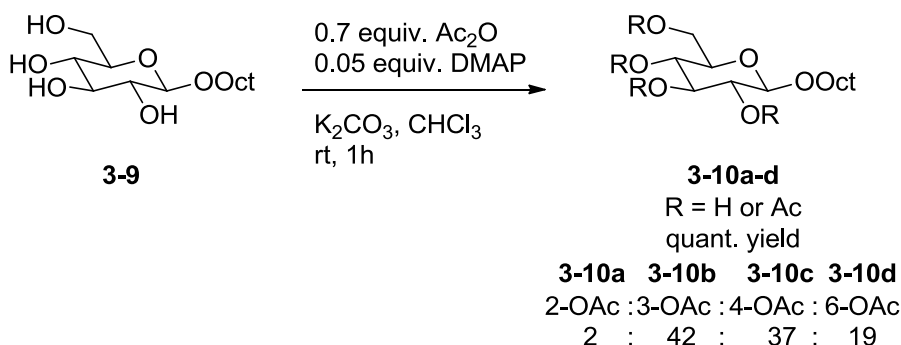
Scheme 3.3 Mechanism of DMAP catalysis using acylating agents such as acetic anhydride or acetyl chloride.

In a review of DMAP-catalyzed acylations, Vorbrüggen briefly discussed the mechanism of this reaction, attempting to rationalize why DMAP is such a powerful catalyst when compared to pyridine and triethylamine. In fact, DMAP and 4-pyrrolidinopyridine catalyze acylation reactions better than other bases due to their nucleophilicity. The nitrogen is acylated, forming N-acylpyridinium salts which exist as ion pairs where the charge renders the N-acylpyridinium more electrophilic.¹⁴ The mechanism of nucleophilic catalysis of 4-

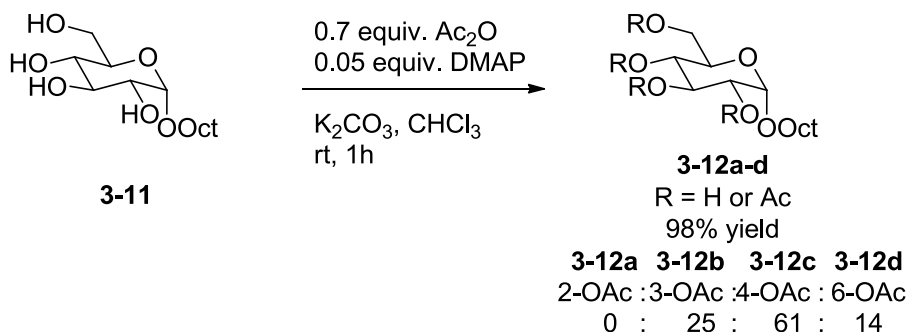
dialkylaminopyridines was further studied in 1979,¹⁵ and again in 2005, when Zipse and co-workers performed a more detailed computational study of DMAP-catalyzed acetylation of alcohols. They not only confirmed the mechanism in Scheme 3.3, but also determined that the hydroxyl that is acetylated is most likely deprotonated by the acetate counterion generated, and not DMAP or other bases used (such as triethylamine).¹⁶

3.3.2 DMAP-catalyzed acylation of sugars

Given the versatility of DMAP, Kurahashi, Mizutani and Yoshida acetylated unprotected carbohydrates using DMAP. They acetylated octyl- β -D-glucopyranoside (**3-9**, Scheme 3.4), as well as the α -anomer (**3-11**, Scheme 3.5), in order to rank the hydroxyls according to their relative reactivity.



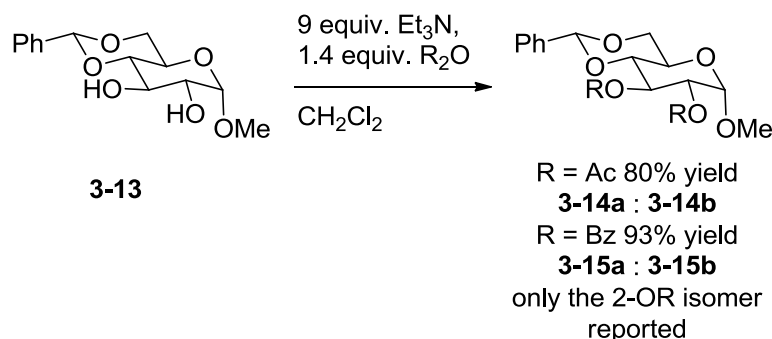
Scheme 3.4 DMAP-catalyzed acetylation of octyl- β -D-glucopyranoside.



Scheme 3.5 DMAP-catalyzed acetylation of octyl- α -D-glucopyranoside.

Unlike the uncatalyzed acylation reactions performed with an excess of acylating agent (mentioned in the introduction), the 6-OH hardly reacts for both

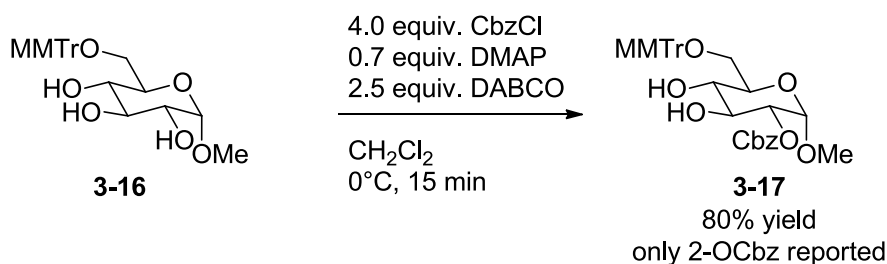
the α - and β -D-glucopyranosides (**3-11** and **3-10**) when a limiting amount of the acylating agent is added to the reaction. Clearly then, the 6-OH is not the most reactive position on the sugar under these conditions, even though it is sterically the least hindered. Furthermore, the 2-OHs of the glucopyranosides hardly react, if at all. The main positions that do react on each of the glucopyranosides are the 3-OH and the 4-OH, which react fairly equally for the β -stereoisomer (Scheme 3.4), while the 4-OH is three times more reactive for the α -stereoisomer (Scheme 3.5). Clearly, the stereochemistry at the anomeric position affects the reactivity of the hydroxyls and the outcome of acetylation. Upon comparing the reactions in Scheme 3.4 and Scheme 3.5 with Scheme 3.1, we find that the acylating agent also differs: in Scheme 3.1, the reagent is an acyl chloride, while in Scheme 3.4 and Scheme 3.5, the reagent is an anhydride, demonstrating that the reactivity may also depend on the acylating agent used (the role of the acylating agent is further discussed in section 3.6). Applying the same conditions to octyl- α - and octyl- β -D-mannopyranosides and octyl- α - and octyl- β -D-galactopyranosides allowed the authors to better understand the effect of the stereochemistry of the hydroxyls at positions 2 and 4 on the relative reactivities of the hydroxyls. In these cases, the stereochemistry of the anomeric position did not affect the order of reactivity of the hydroxyls, which was determined as 4-OH > 6-OH > 3-OH > 2-OH for the mannopyranosides, and as 6-OH > 4-OH \approx 3-OH > 2-OH for the galactopyranosides.¹⁷



Scheme 3.6 Regioselective acylation of position 2 over position 3 of 4,6-O-benzylidene methyl α -D-glucopyranoside.

Using just triethylamine and either acetic or benzoic anhydride, Hung and co-workers¹⁸ showed that various glucopyranosides, such as **3-13**, could be selectively functionalized at position 2 without any catalysts or additives, although an excess (9 equivalents) of triethylamine was used (yields vary between 65 and 93%, Scheme 3.6). Interestingly, they obtain an almost random mono-functionalization of the sugars when pyridine is used instead of triethylamine.

Using benzyl chloroformate, Morère *et al.*¹⁹ mono-functionalized several sugars. Combining two bases in their reaction conditions, namely DMAP and DABCO, Morère *et al.* could selectively install a benzyloxycarbonyl in high yields.

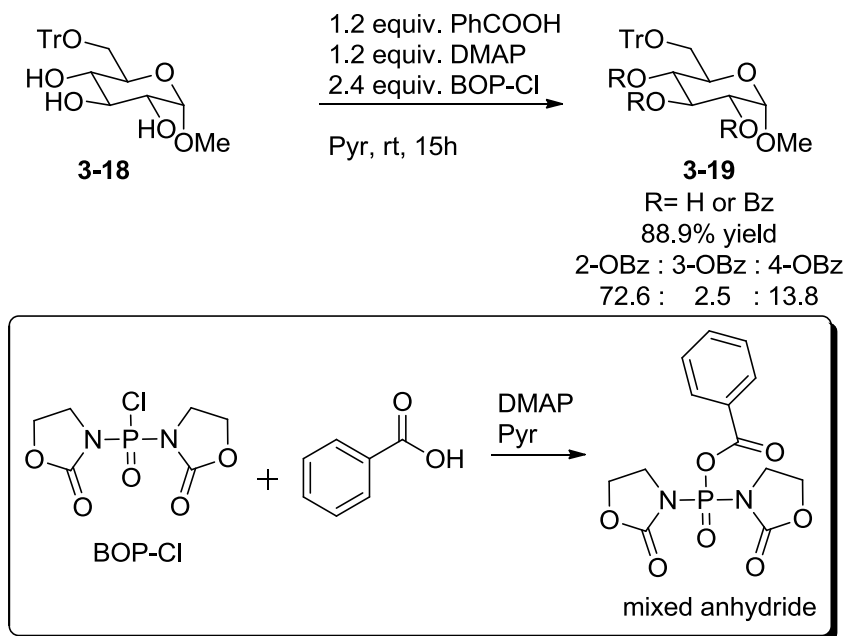


Scheme 3.7 Morère *et al.* apply a combination of bases to selectively functionalize methyl α -D-glucopyranoside.

In fact, they were able to put a benzyloxycarbonyl group at position 2 of 6-*O*-(4-methoxytrityl) methyl α -D-glucopyranoside (**3-16**) (80% yield of **3-17**, Scheme 3.7) and 6-*O*-(4-methoxytrityl) methyl α -D-galactopyranoside (74% yield), and selectively at position 3 (and not position 2) of 6-*O*-(4-methoxytrityl) methyl α -D-mannopyranoside (85% yield). Again for the mannopyranoside, the equatorial position 3 was more reactive compared to the axial 2-OH. Interestingly, when the β -isomer of the glucopyranoside was subjected to the same conditions, a mixture of products, functionalized at either position 2 or 3, was obtained (31% at position 2, 43% at position 3), further demonstrating the influence of the orientation of the anomeric position. The reactivity pattern from Morère mirrors that from Williams and Richardson with benzoyl chloride.

Procopio and colleagues²⁰ selectively acylated position 2 of 6-*O*-trityl methyl α -D-glucopyranoside (**3-18**), yielding **3-19** (72.6 %). They used a combination of

BOP-Cl and DMAP which, along with the desired acid, most likely first form the mixed anhydride of BOP-Cl with that acid (Scheme 3.8). However, the necessary control experiments are not performed to determine, firstly, whether the acyl pyridinium forms from the reaction of DMAP with the mixed anhydride, and secondly, whether a symmetric anhydride forms from the reaction of the mixed anhydride with another equivalent of the acid.



Scheme 3.8 Regioselective acylation using benzoic acid, DMAP and BOP-Cl.

3.3.3 Silyl

A wide variety of silyl ether derivatives of carbohydrates can be formed for the protection of hydroxyls, and, more importantly, 1,2- and 1,3-diols.²¹ For instance, Corey explored di-isopropylsilyl and di-tert-butylsilyl di-triflates to protect 1,2-, 1,3-, and 1,4-diols (a few examples shown in Figure 3.2).²²

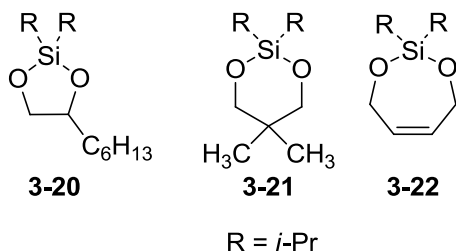
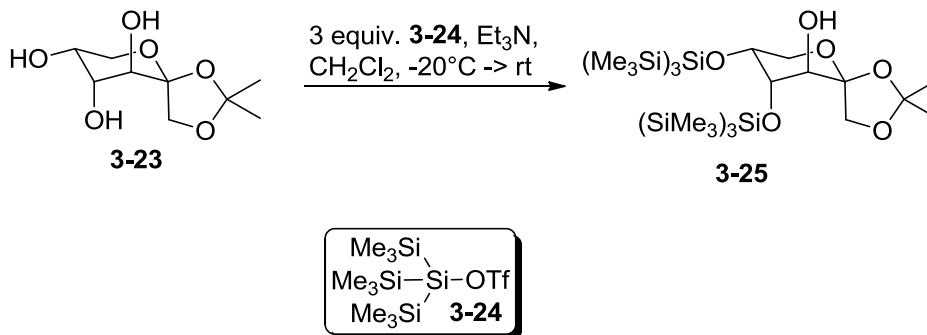


Figure 3.2 A few examples of silyl protection of 1,2-, 1,3- and 1,4-diols (**3-20**, **3-21** and **3-22**) which Corey developed.

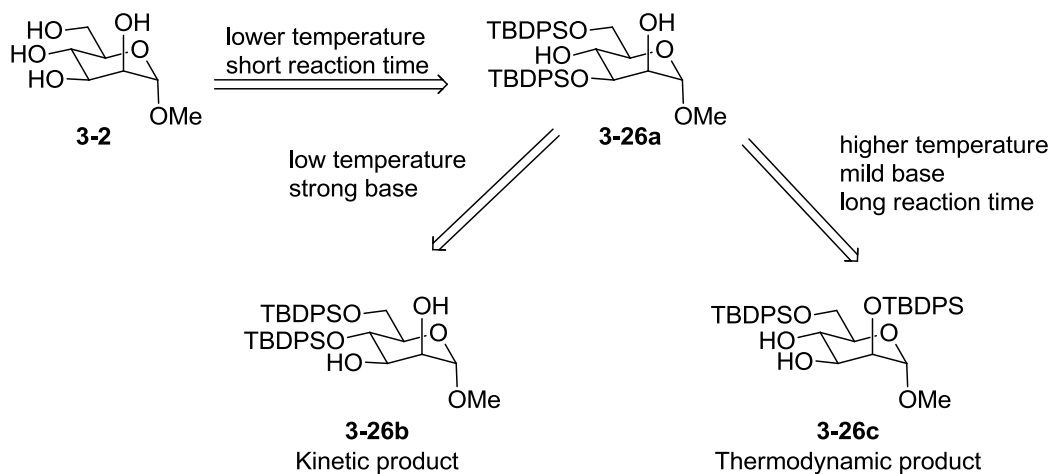
The Miethchen group²³ applied branched oligosilyl triflates with silyl spacers (as in **3-25**) as protecting groups for some fructopyranose sugars (**3-23**), leaving only one secondary hydroxyl available (Scheme 3.9) for further functionalization.



Scheme 3.9 A one-step protection of two positions of a fructopyranoside.

Arias-Peréz and Santos²⁴ disilylated methyl and allyl α -D-mannopyranosides, at various temperatures, to establish the order of reactivity of the secondary hydroxyls from the disilylated products observed. At low temperatures, mainly the 3,6-disilylated product formed, while at higher temperatures, the 2,6-disilylated product was predominant. From this data, Arias-Peréz and Santos not only derived the order of reactivity of the hydroxyls (3-OH > 2-OH > 4-OH), but also that at higher temperatures, the silyl group migrated from position 3 to position 2. In fact, they could manipulate which position the TBDPS group migrated to using different bases: stronger bases like *n*-butyllithium forced migration of the TBDPS from position 3 of **3-26a** to position 4, the less hindered position compared to the 2-OH (kinetic conditions yielding **3-26b**), while softer imidazole base (longer reaction times and higher temperatures) promoted

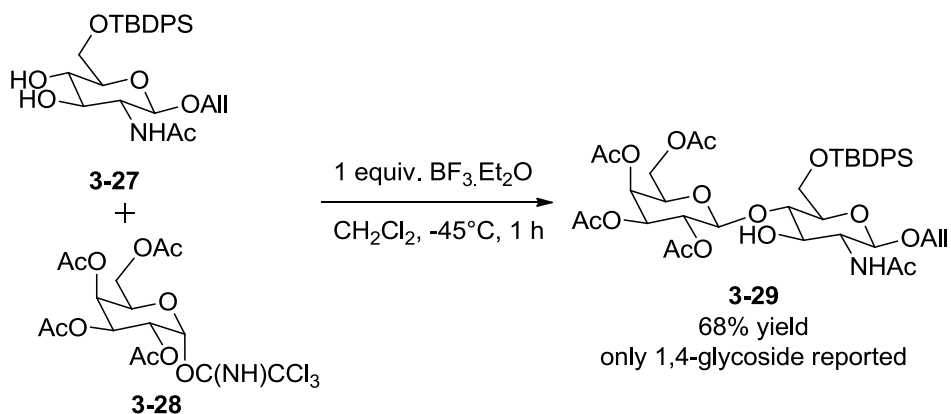
migration from position 3 of **3-26a** to position 2 (the thermodynamic product **3-26c**) (Scheme 3.10).



Scheme 3.10 Controlled TBDPS migration.

3.3.4 Glycosylations on minimally protected acceptors

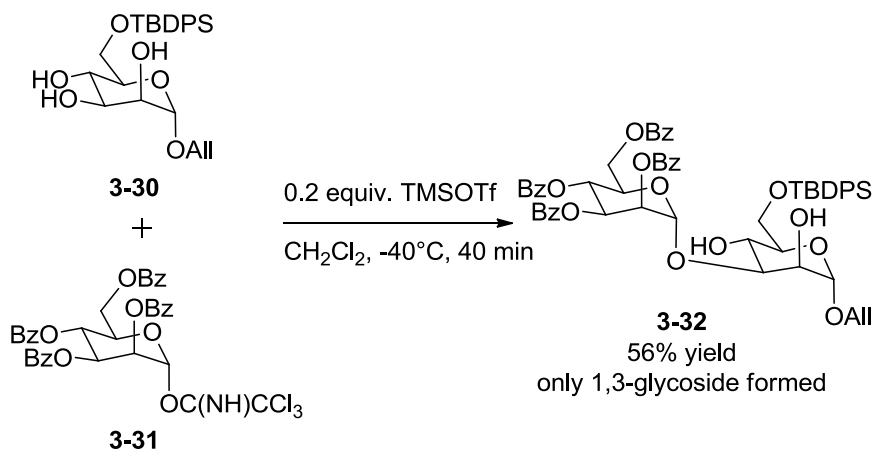
A few groups have glycosylated minimally protected acceptors in order to determine if long synthetic routes of protections and deprotections are actually necessary.



Scheme 3.11 Glycosylation of allyl 2-acetamido-6-O-TBDPS-2-deoxy-β-D-glucopyranoside with a galactose trichloroacetimidate.

The Roy group synthesized N-acetyllactosamine derivatives (such as **3-29**), finding that a 6-O-TBDPS allyl β-D-glucopyranoside acceptor (**3-27**) could be selectively glycosylated with **3-28** at position 4 without protecting any of the other positions of the sugar (Scheme 3.11).²⁵ The Pakulski group investigated the

mannosylation (in other words, glycosylation using a mannose-based donor) of 6-*O*-TBDPS benzyl- α -D-mannopyranoside and allyl α - and β -D-mannopyranoside (**3-30**).²⁶ They observed the α -D-mannopyranosides could be selectively glycosylated with **3-31** at position 3, when the 2-, 3-, and 4-OHs were unprotected.



Scheme 3.12 Mannosylation of allyl 6-*O*-TBDPS- α -D-mannopyranoside.

Their best results were obtained for allyl 6-*O*-TBDPS- α -D-mannopyranoside (**3-30**) when they used either $\text{BF}_3 \cdot \text{OEt}_2$ (70% yield of glycosylation at position 3) or with TMSOTf (56% yield of glycosylation at position 3, Scheme 3.12). Interestingly, for allyl 6-*O*-TBDPS- β -D-mannopyranoside, Pakulski observed lower yields (68% yield or less) and a mixture of disaccharides containing a much higher amount of product mannosylated at position 2. Furthermore, for benzyl 6-*O*-TBDPS- α -D-mannopyranoside, the yields were also significantly lower, although they were able to selectively mannosylate the acceptor at position 3 using TMSOTf (34% yield).

3.3.5 The influence of the hydrogen bond network

In explaining the results of their acylation experiments, Williams and Richardson mentioned the influence of the intramolecular hydrogen bond network.^{1,2} In fact, several groups have investigated this intramolecular hydrogen bond network to better understand the order of reactivity of the hydroxyls on

sugars.^{17,27-32} Surprisingly, Williams and Richardson performed their experiments in pyridine, a solvent that is able to hydrogen bond with the sugar, a fact which renders this inference of the intramolecular hydrogen bond network seemingly less plausible. However, a few groups have discovered that even in hydrogen bonding solvents, although it may be weakened, the intramolecular hydrogen bond network still exists,^{27,31,32} supporting Williams and Richardson's theory that the internal hydrogen bond network influences acetylation reactions of sugars, even when the reactions are performed in pyridine.

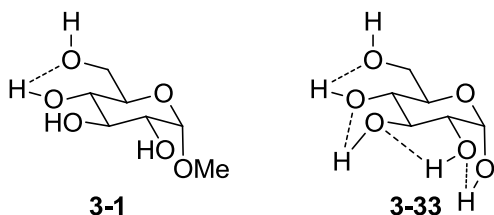


Figure 3.3 Davies proposed intramolecular hydrogen bond networks of methyl α -D-glucopyranoside (3-1) and the α -anomer of glucose (3-33).

From a few ^1H NMR studies, Davies found that for methyl- α -D-glucopyranoside (3-1), only one intramolecular hydrogen bond existed between the hydroxyls at position 4 and 6, while for the α -anomer of glucose (3-33), Davies demonstrated that glucose has an extensive hydrogen bond network, as in Figure 3.3.²⁷ Brewster rationalized the reactivities of the hydroxyls of glucose by determining the acidities of the hydroxyls of α -D-glucopyranose (and β -maltose). To do this, they performed computational calculations using a semiempirical molecular orbital (AM1) framework. From their calculations, Brewster determined that the position 6-OH is the least acidic along with the following order of acidity: 1-OH > 4-OH > 3-OH > 2-OH > 6-OH. This would explain why Kurahashi, Mizutani and Yoshida observe very little acylation of position 6 in their experiments, even though this primary OH is free. On the other hand, position 6-OH sometimes seems the most reactive towards alkylation and acylation because it is the least hindered position and therefore electrophiles can easily access this position.²⁸ Thus if more than an equivalent of acylating agent is used on an unprotected pyranoside, researchers

(such as Williams and Richardson) observe di-acylation, the 6-OH being one of the positions acylated.

Kurahashi, Mizutani and Yoshida propose that the internal hydrogen bond network of octyl- α -D-glucopyranoside (Figure 3.4) can account for the reactivity patterns which they observed experimentally in Scheme 3.5.¹⁷

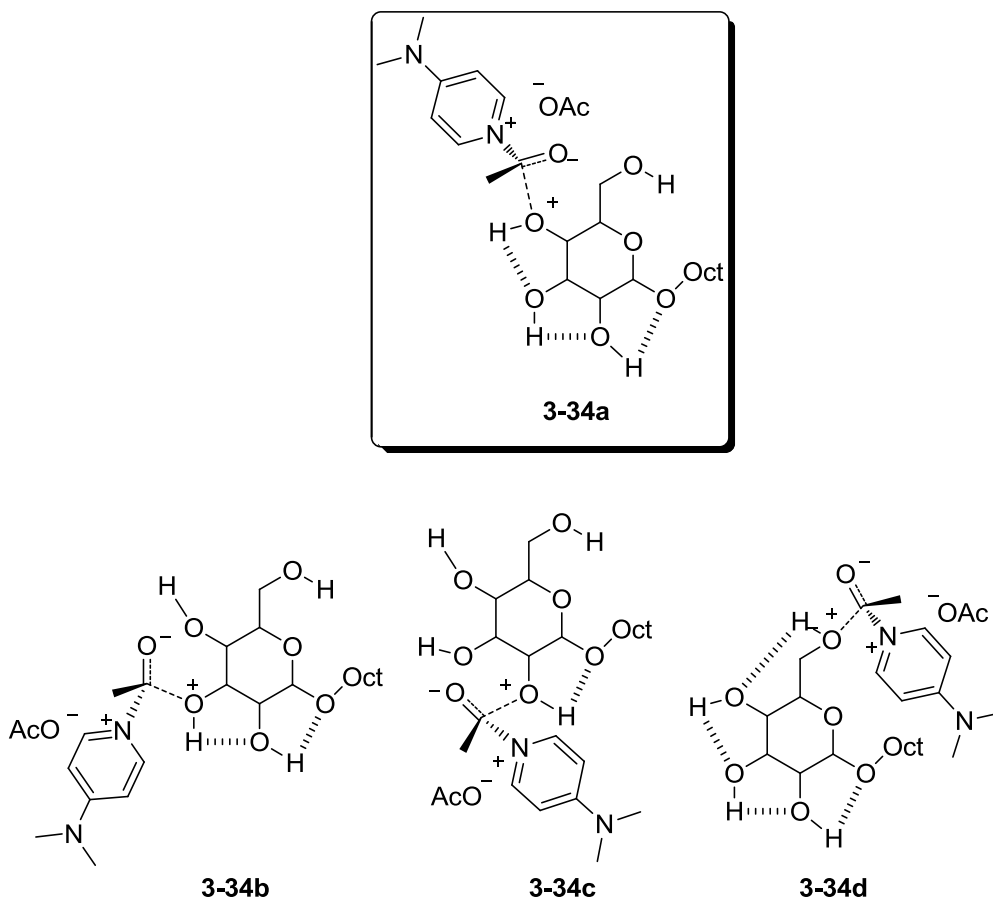
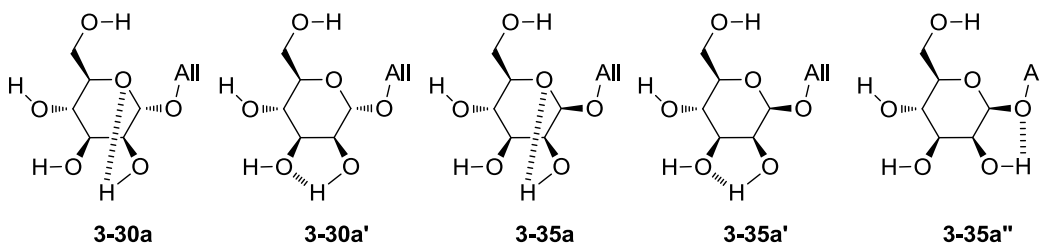


Figure 3.4 Kurahashi Muzutani and Yoshida proposed the hydrogen bond network of octyl- α -D-glucopyranoside supports DMAP-catalyzed acylation of the 4-OH (3-34a) over the 3-OH (3-34b), the 2-OH (3-34c) and the 6-OH (3-34d).

For example, even though position 6 is the most accessible position from a steric point of view, the 6-OH is the least acylated position because this flexible primary hydroxyl does not hydrogen bond well (3-34d). On the other hand, position 4 is preferentially acylated because the positive charge can be thoroughly delocalized through the hydrogen bond network (as in 3-34a). Kurahashi, Mizutani and Yoshida also performed semi-empirical calculations (PM3) to quantify the proton

affinities of the hydroxyl groups of monosaccharides, finding that the reactivity trend parallels the proton affinities, in other words, position 4 has a higher proton affinity than the 3-OH and 2-OH. The measured proton affinities mirror the hydroxy-nucleophilicities in this case.

Pakulski attributed the results from the mannosylation experiments to the hydrogen bond network of the mannopyranosides used (**3-30a-a'** and **3-35a-a''** in Scheme 3.13).²⁶



Scheme 3.13 Some possible hydrogen bonds that could explain why the 2-OH of allyl 6-*O*-TBDPS β -D-mannopyranoside (shown in **3-35a-a''**) reacts more than in the α -form (shown in **3-3-a'**).

In fact, allyl 6-*O*-TBDPS β -D-mannopyranoside should be capable of an extra hydrogen bond, between the 2-OH and the anomeric O-allyl (**3-35a''**) because they are in a cis-configuration of the sugar, and therefore close enough to interact. The 2-OH could therefore have a slightly more negative charge in the β -form than in the α -form, rendering it slightly more nucleophilic in the β -form. Thus, mixtures containing predominantly products mannosylated at position 3, but also at position 2 are observed.

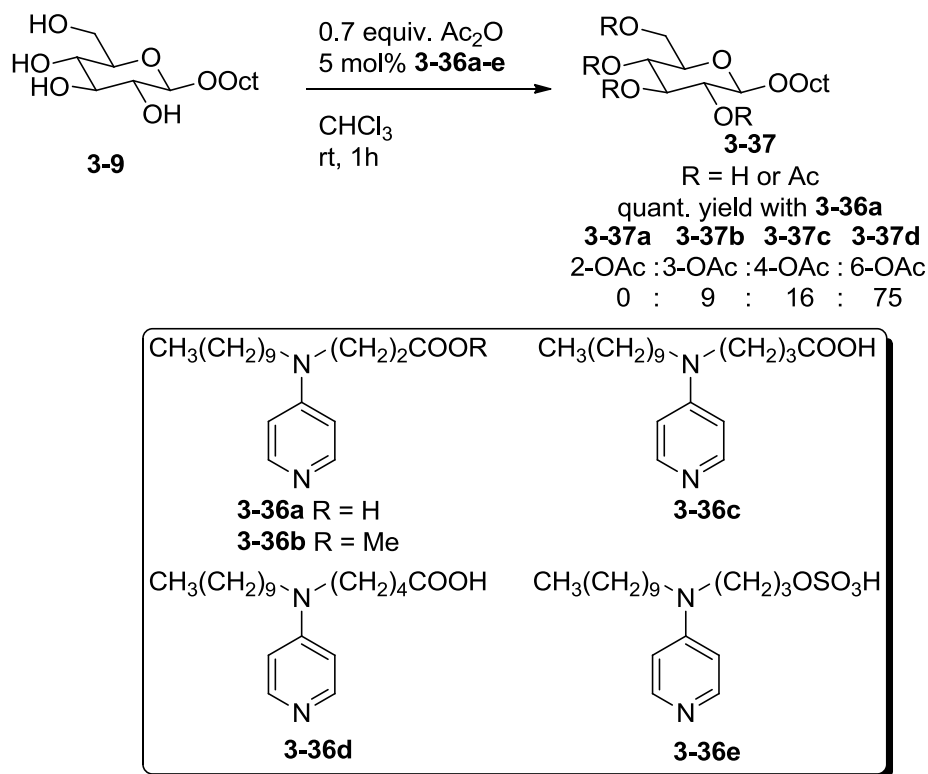
From these efforts, we can clearly see that the hydrogen bond network influences reactions (whether simple acylation reactions or more complex glycosylations) performed on unprotected or partially protected sugars.

3.4 Extrinsic methods which internally deliver the reagent

Some researchers have chosen to replicate enzyme active sites creating compounds or peptides capable of hydrogen-bonding with the substrate, reacting with the reagent and internally delivering the reagent to a specific position.

3.4.1 DMAP-based catalysts

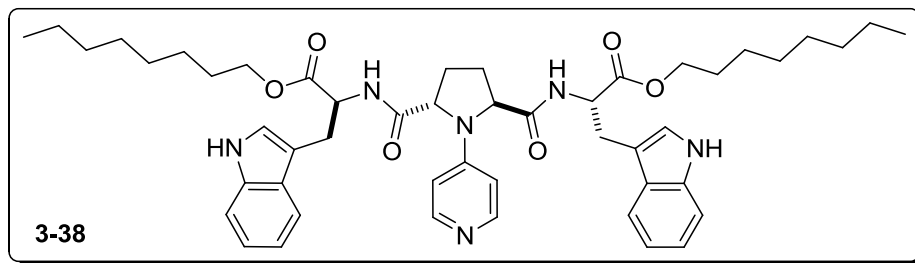
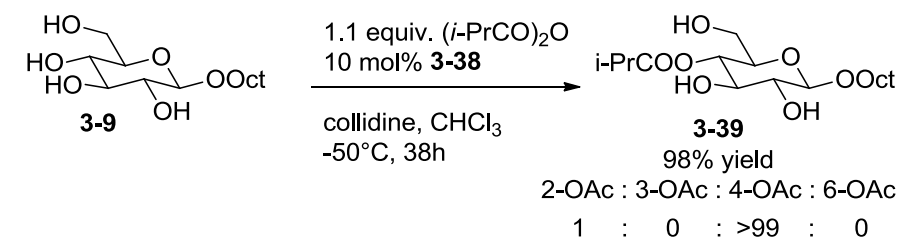
Kurahashi, Mizutani and Yoshida continued their work on DMAP-catalyzed acylation, using DMAP analogues with acid moieties (**3-36a-e**) capable of hydrogen bonding with the sugars (Scheme 3.14). In this case, they found that the 6-OH is the most reactive for the octyl- α - and octyl- β -D-glucopyranosides and galactopyranosides. The 4- and 6-OH positions of the mannopyranosides reacted equally. Interestingly, while di-acylation was previously inevitable, as in Scheme 3.1, Kurahashi, Mizutani and Yoshida have developed a method which avoids this issue.³³



Scheme 3.14 Acetylation catalyzed by DMAP analogues.

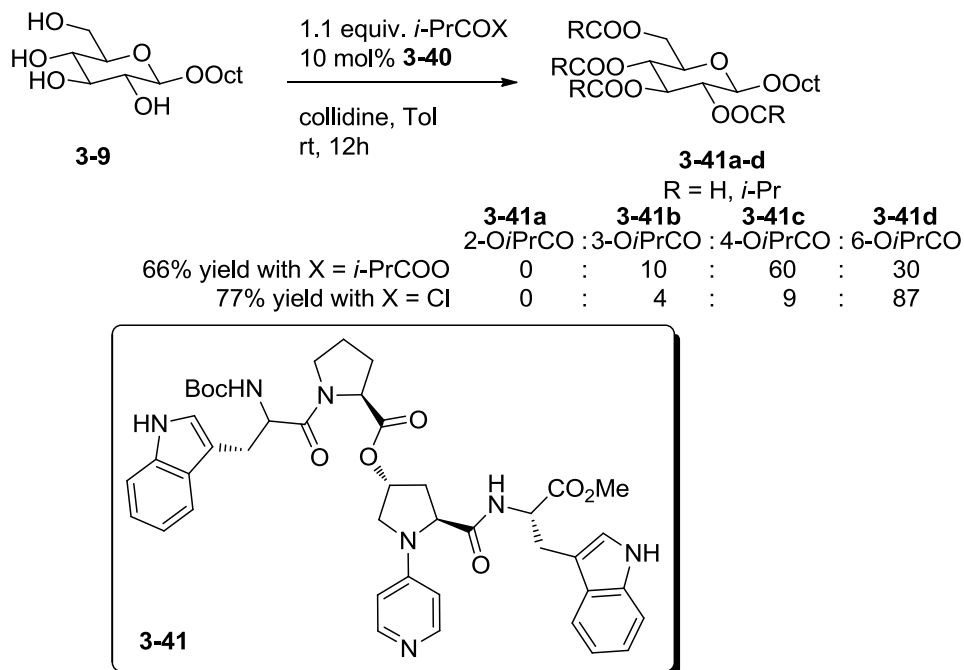
In the quest for more efficient catalysts for acylation of sugars, Kawabata and colleagues incorporated DMAP analogues into short di- and tri-peptides (such as **3-37**). Initially, the catalysts were used to enantioselectively acylate meso-1,2- and 1,3-diols.^{34,35} These catalysts and others were also applied to selective acylation of sugars. Kawabata hypothesized that the catalysts can wrap around the

sugar being acylated, directly delivering the acyl group to a specific position: only the 4-OH is selectively acylated (Scheme 3.15). Once again, the intrinsic reactivity of the sugar has been manipulated, and the usual the reactivity (or rather the accessibility) of position-6 is quenched and the acyl group is delivered very specifically.^{36,37}



Scheme 3.15 Acylation catalyzed by tri-peptide containing DMAP.

Recently, the Kawabata group used this same catalyst with other anhydrides, for example bearing an amino acid, successfully installing a N-Cbz-phenylalanine at position 4 of octyl β-D-glucopyranoside (**3-9**).³⁸

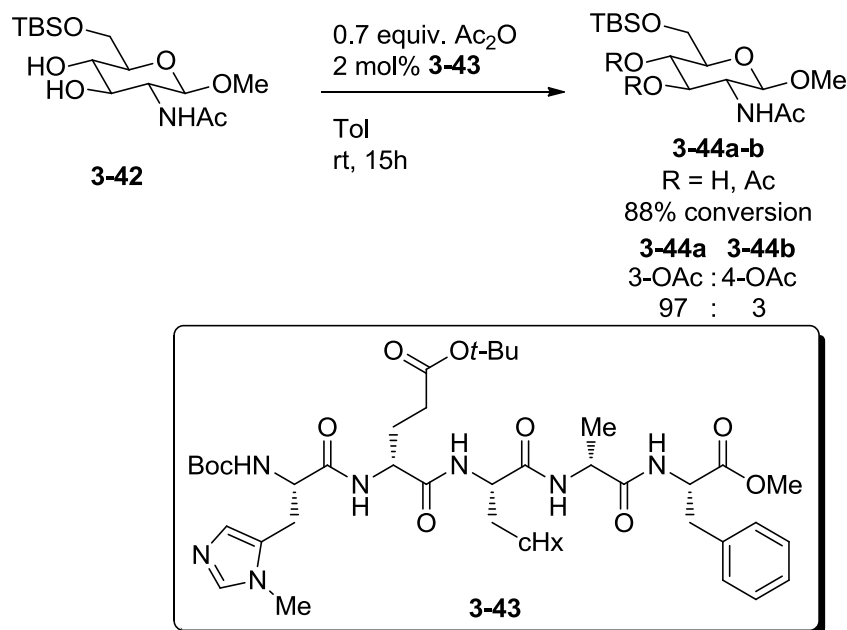


Scheme 3.16 Acylation catalyzed by tetra-peptide containing DMAP.

The Kawabata group also developed other catalysts still featuring DMAP (like **3-40** of Scheme 3.16), also showing that changing the acylating agent from the anhydride to the acyl chloride allows them to switch from acylating the position 4-OH to the position 6-OH.³⁹

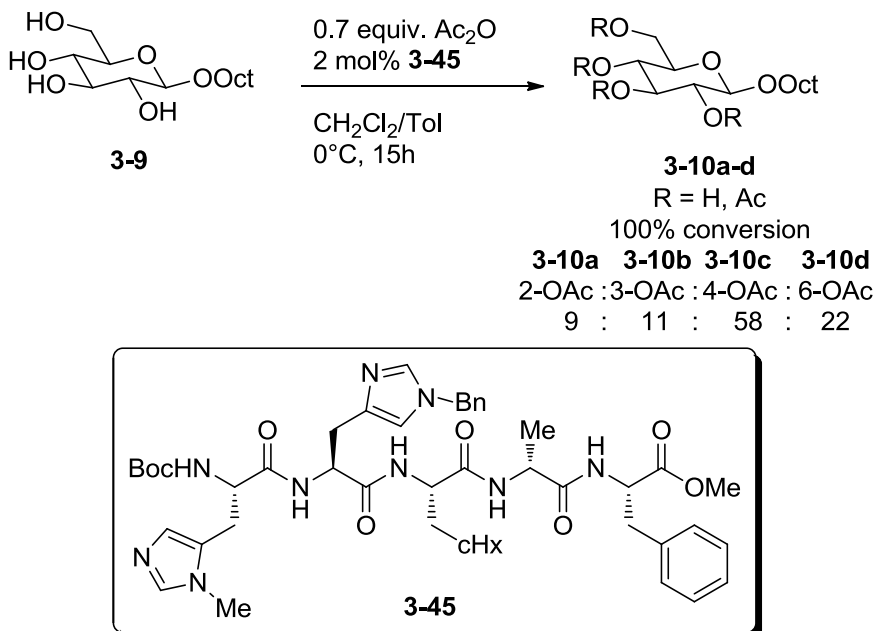
3.4.2 Peptidic catalysts

The Kawabata group was not the only group to develop peptidic catalysts to perform selective acylation reactions. Miller constructed and screened a series of longer peptides to catalyze acetylation reactions.⁴⁰ Of the series, peptide **3-43** was particularly noteworthy as it favoured acetylation at position 3 over position 4 (97:3) of a glucosamine substrate (**3-42**), whereas the same substrate was acetylated at position 4 in the absence of the peptide catalyst (Scheme 3.17). Furthermore, when the catalyst was absent, a significant portion of di-acetylated product was recovered, while in the presence of the catalyst, di-acetylation did not occur.



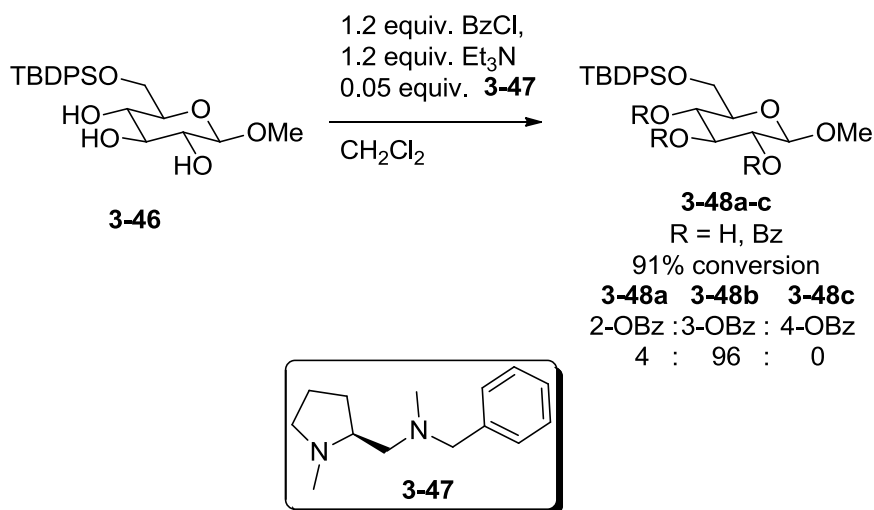
Scheme 3.17 Selective acetylation of position 3 over position 4 of a glucosamine substrate **3-42**, catalyzed by peptide **3-43**.

On the other hand, when peptide **3-45** catalyzes the reaction, the secondary hydroxyl at position 4 is acetylated predominantly, while the primary hydroxyl reacts to a lesser extent, and finally positions 3 and 2 react about equally (Scheme 3.18).



Scheme 3.18 Optimized acylation catalyzed by a short peptide.

Instead of using peptides, the Vasella group selectively benzoylated methyl 6-*O*-TBDPS- β -D-glucopyranoside (**3-46**), in the presence of a chiral diamine (**3-47**).⁴¹ Although they give little explanation to the regioselectivity they observe, they infer that the hydrogen bond network of the sugar may influence the outcome of the reaction.⁴²



Scheme 3.19 Chiral diamine (**3-47**) catalyzed acylation of methyl-6-*O*-TBDPS- β -D-glucopyranoside (**3-46**).

3.5 Extrinsic methods which pre-functionalize the sugar

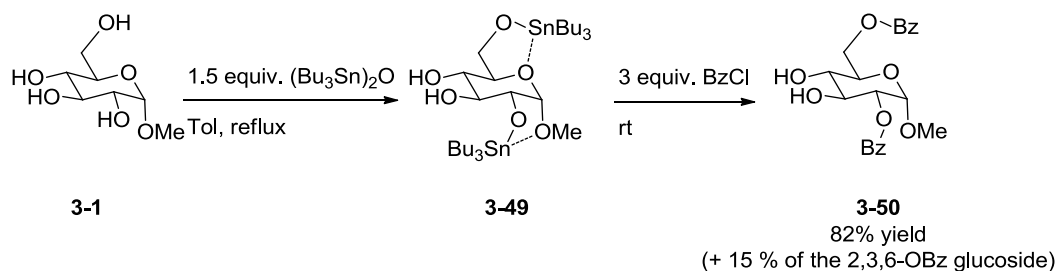
Researchers have developed many methods to pre-functionalize sugars with tin or boron derivatives, or salts, prior to performing the reaction of interest.

3.5.1 Organotin derivatives

Although Hanessian reviewed many of the applications of organotin derivatives of various sugars,⁴³ a few among them are worth mentioning here.

Acylation via stannyl ether derivatives

Ogawa and Matsui prepared stannyl ethers of methyl α -D-glucopyranoside (**3-1**), mannopyranoside (**3-2**) and galactopyranoside (**3-3**), as well as methyl β -D-galactopyranoside which they benzoylated.^{44,45}

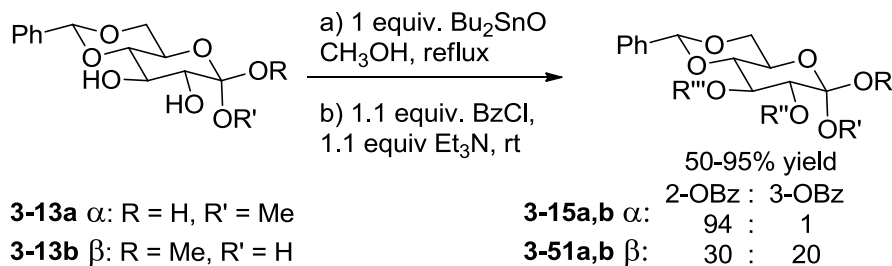


Scheme 3.20 Stannyl ethers promote regioselective acylations.

Interestingly, when the methyl α -D-glucopyranoside (**3-1**) was treated with bis(tributyltin) oxide, Ogawa and Matsui hypothesized that stannyl ethers formed at positions 2 and 6 (**3-49** in Scheme 3.20). Subsequent benzylation therefore occurred at positions 2 and 6 of methyl α -D-glucopyranoside (**3-50**, 81% yield). When treated in the same way, benzylation occurred at positions 3 and 6 of methyl α -D-mannopyranoside (**3-2**) (90% yield) and methyl β -D-galactopyranoside (95% yield). On the other hand, benzylation of methyl α -D-galactopyranoside (**3-3**) actually yielded four products, the product mono-benzoylated at position 6, di-benzoylated at positions 2 and 6, and positions 3 and 6, and finally the tri-benzoylated product at positions 2, 3, and 6 (yields of 21, 10, 20, and 41% respectively).

Acylation via stannylene acetals

When conventional acylation methods failed to be regioselective and following preliminary work on regioselective tosylation of nucleosides using tin,^{46,47} Munavu and Szmant turned to dibutylstannylene acetals to selectively functionalize partially-protected methyl α/β -D-hexopyranoside sugars.⁴⁸ Acylation occurred exclusively at position 2 for the α -D-glucopyranoside, but was non selective for the β -anomer (**3-13b**) (Scheme 3.21).



Scheme 3.21 Selective benzoylation via a stannylene acetal intermediate.

The stannylene acetal of 4,6-*O*-benzylidene methyl α -D-glucopyranoside formed at positions 2 and 3, most likely because the anomeric methoxy could stabilize the tin acetal (Figure 3.5). On the other hand, when the stereochemistry of the starting sugar does not allow for stabilization of the stannylene acetal, acylation was non-selective, as for the 4,6-*O*-benzylidene of methyl β -D-glucopyranoside (**3-52**) and methyl α -D-mannopyranoside (**3-53**).

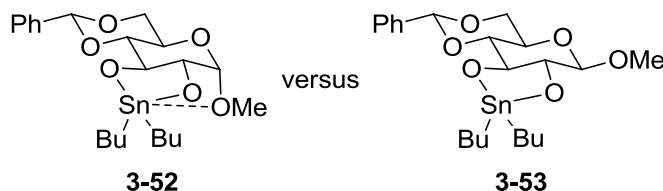
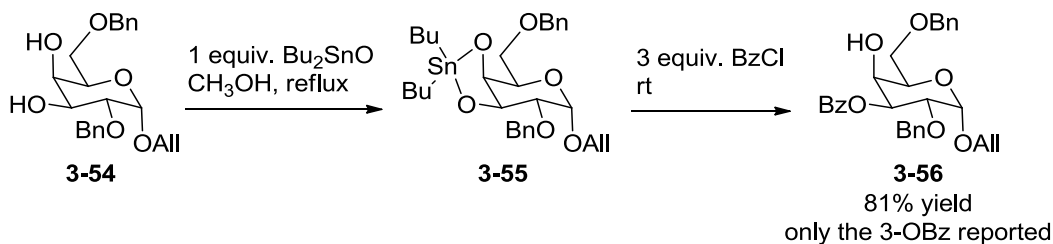


Figure 3.5 Stannylene acetal of methyl α -D-glucopyranoside (3-52) compared to methyl β -D-glucopyranoside (3-53).

The importance of the anomeric center was further demonstrated when Munavu and Szmant acylated the unprotected methyl α - and β -D-glucopyranosides under the same conditions: the α -isomer was acylated at position 2 (as expected from the previous experiments), while the β -isomer, lacking the possible anomeric stabilization of the 2,3-stannylene acetal, reacted at position 6, the primary alcohol (80% yield of 6-*O* benzoylated product).

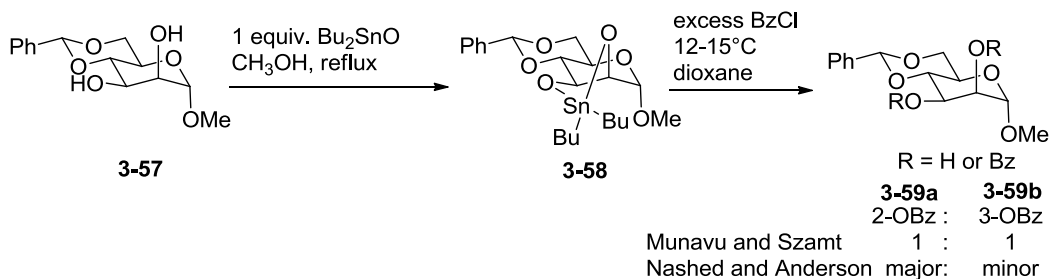
In a further exploration of stannylene acetals, Nashed and Anderson⁴⁹ compared the reactivity of axial hydroxyls with equatorial hydroxyls of stannylene acetals of a partially protected galactopyranoside and mannopyranoside. As expected, they found that the equatorial hydroxyls were more reactive: the 3-*O* of the galactopyranoside **3-54** reacted selectively to

benzoylation (as in Scheme 3.22), and the equatorial 3-O of the mannopyranoside was most reactive and predominantly alkylated over the axial 2-O position.^{49,50}



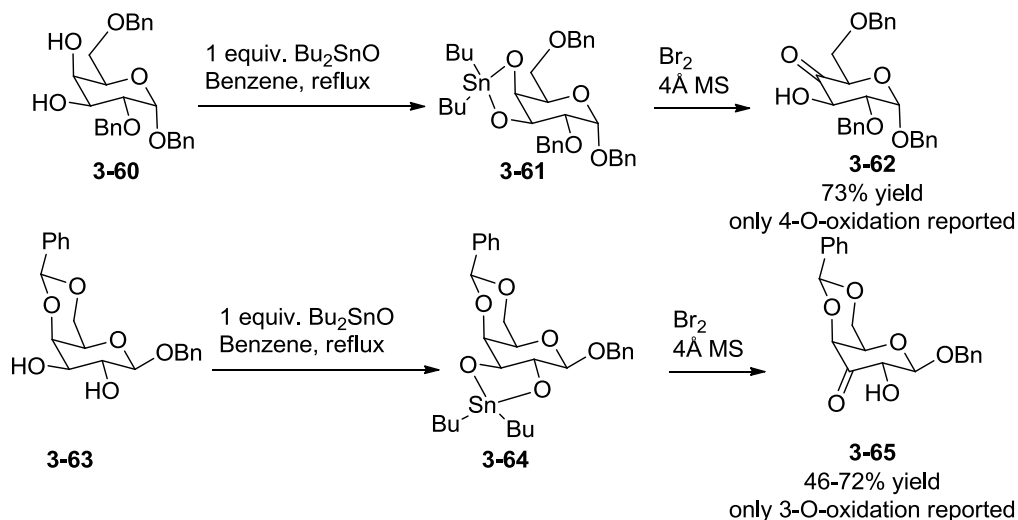
Scheme 3.22 Stannylene acetal **3-55** for regioselective acylation of a partially protected galactopyranoside **3-54**.

Nashed and Anderson found that the conditions developed to benzoylate the equatorial position of the galactopyranoside actually yielded the mannopyranoside benzoylated selectively at the axial position 2 (**3-59a**). They also developed conditions to selectively benzylate the equatorial hydroxyl, position 3. Thus, unlike Munavu and Szmant, Nashed and Anderson found optimal conditions for functionalizing either the equatorial hydroxyl at position 3 or the axial hydroxyl, at position 2 (as shown in Scheme 3.23).



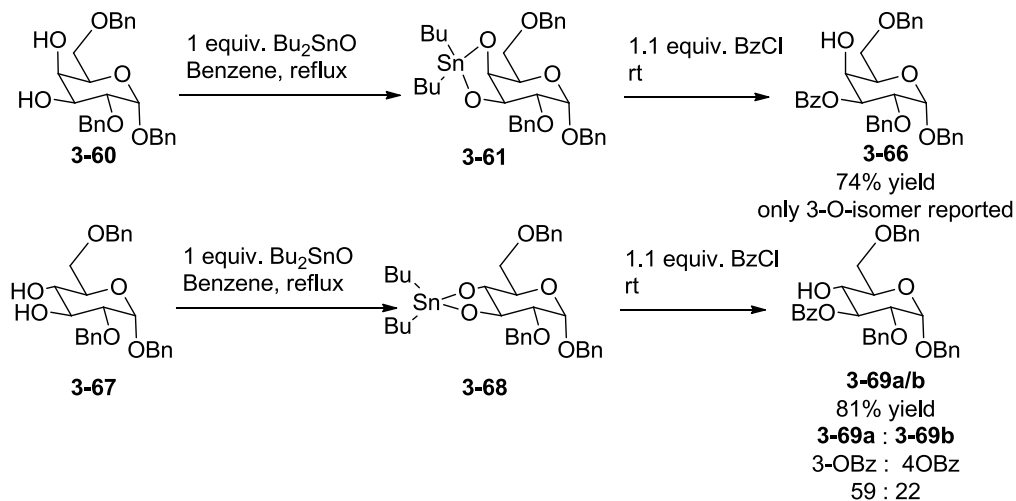
Scheme 3.23 Stannylene acetal for regioselective acylation of a partially protected mannopyranoside.

David and Thieffry⁵¹ also successfully used stannylene acetals not only to selectively acylate sugars, but also to oxidize a 4,6-*O*-benzylidene- β -D-galactopyranoside (**3-63**) at position 3 and a 2,6-*O*-di-benzoyl- α -D-galactopyranoside (**3-60**) at position 4 (Scheme 3.24).



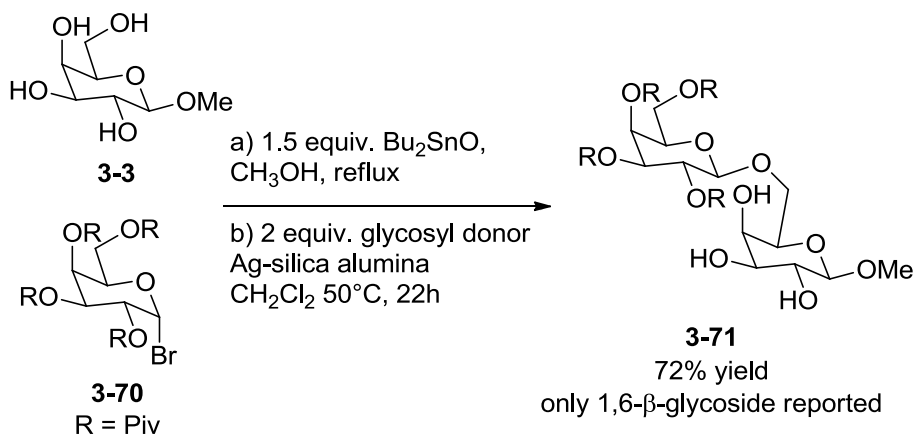
Scheme 3.24 Selective oxidation at position 3 of a 3,4-stannylene acetal of a galactopyranoside.

Benzoylation conditions were also applied to galacto- and glucopyranosides protected at positions 2 and 6 (**3-60** and **3-67**, respectively). In both cases, although position 4 should be activated by the stannylene acetal, position 4 was unreactive and thus position 3 was selectively benzoylated (Scheme 3.25).



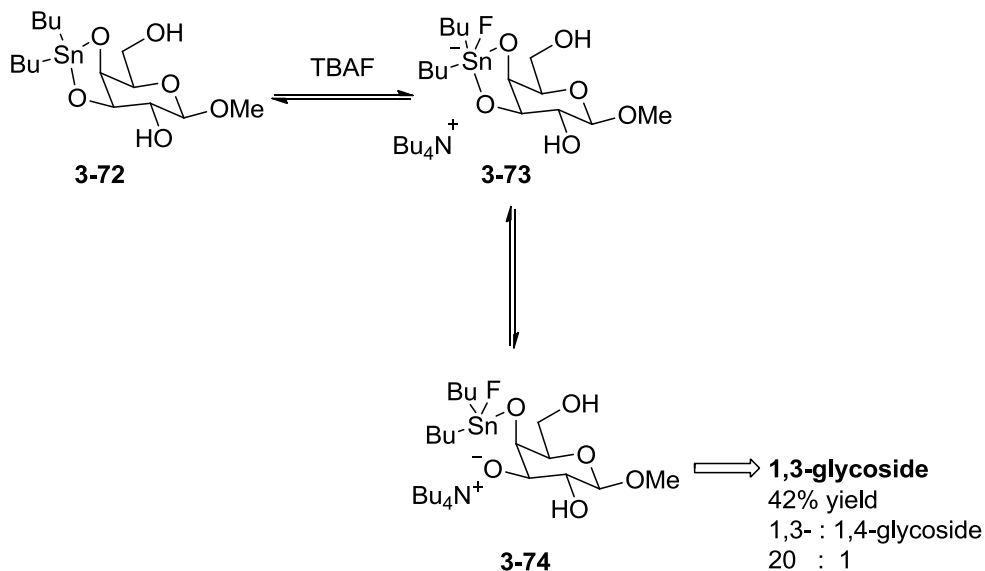
Scheme 3.25 Selective benzoylation of position 3 of a galactopyranoside and a glucopyranoside.

Several groups have also used this type of chemistry to perform regioselective glycosylations.⁵²⁻⁵⁴



Scheme 3.26 Glycosylation of a galactopyranoside acceptor via a stannylene acetal intermediate.

The Kaji group examined using stannylene acetals to selectively glycosylate sugars. In fact, starting with a sugar protected at position 6 (either with a trityl or TBDMS group), glycosylation occurred at position 3. On the other hand, for sugars with a free primary hydroxyl at position 6 (as in **3-3**), the acetal formed between positions 4 and 6, and glycosylation occurred selectively at position 6 (**3-71** of Scheme 3.26).⁵⁵



Scheme 3.27 TBAF mediated glycosylation of a 3,4-O-stannylene acetal yields a 3-O-glycoside.

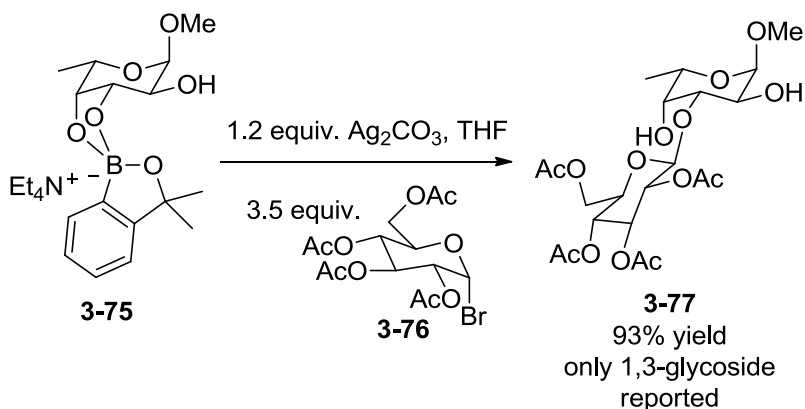
The Kaji group later developed a new method to switch from glycosylation at position 6 to position 3 of the glycosyl acceptor, without protecting position 6

prior to glycosylation of the glycosyl acceptor.⁵⁶ Simply using TBAF as an additive to the glycosylation reaction, they are able to glycosylate at position 3 of the glycosyl acceptor (**3-72**). Most likely, the 3,4-stannylene acetal, formed initially, quickly reacts with the fluoride source forming **3-73**, releasing the position 3 alkoxide (**3-74**) which is more reactive and easily glycosylated (Scheme 3.27). Thus, without TBAF, glycosylation occurs at position 6 of the acceptor, but with TBAF, glycosylation occurs at position 3.

More recently, Namazi and Sharifzadeh⁵⁷ this organotin-based chemistry to install an acrylate and a methacrylate at position 2 of methyl 4,6-*O*-benzylidene- α -D-glucopyranoside (49% yield with acryloyl chloride and 45% with methacryloyl chloride) and of methyl 4,6-*O*-benzylidene- α -D-galactopyranoside (45% yield with acryloyl chloride and 58% with methacryloyl chloride). Heidecke and Lindhorst⁵⁸ applied the same stannylene acetal chemistry to selectively install a phthalimidopropyl group at position 3 of methyl- α -D-galactopyranoside (77% yield).

3.5.2 Organoboron derivatives

Given that sugars readily complex to boronates,⁵⁹⁻⁶¹ the Aoyama group investigated how to utilize those complexes to selectively alkylate⁶² and glycosylate⁶³ sugars. In their initial studies, the Aoyama group selectively alkylated fucopyranosides at position 3, going through a 3,4-boronate intermediate. More recently, they applied these same boronate intermediates to glycosylations (Scheme 3.28).

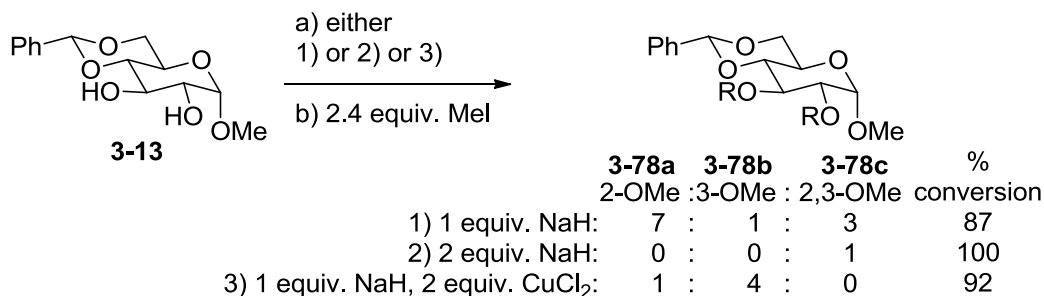


Scheme 3.28 A peracetylated bromide glycosyl donor reacts with an activated 3,4-boronate of a fucopyranoside.

From the boronic activation of various sugars, they observe that some sugars are glycosylated at position 3 (such as methyl 6-*O*-trityl- α -D-galactopyranoside in a 91% yield, methyl α -D-mannopyranoside in a 32% yield, and methyl α -L-fucoside **3-75** in a 93% yield of **3-77**). Unfortunately, this method was hardly applicable to other sugars, which were glycosylated at position 6 (like both methyl α - and octyl β -D-glucopyranosides in 24% and 35% yields respectively). In most cases, yields are lower because trisaccharides are formed, when both positions 3 and 6 are glycosylated. In fact, the only instances of high yields are with fucose **3-75** (Scheme 3.28), which lacks a hydroxyl at position 6, and the galactopyranoside they used, in which the hydroxyl at position 6 is protected.⁶²

3.5.3 Salt additives

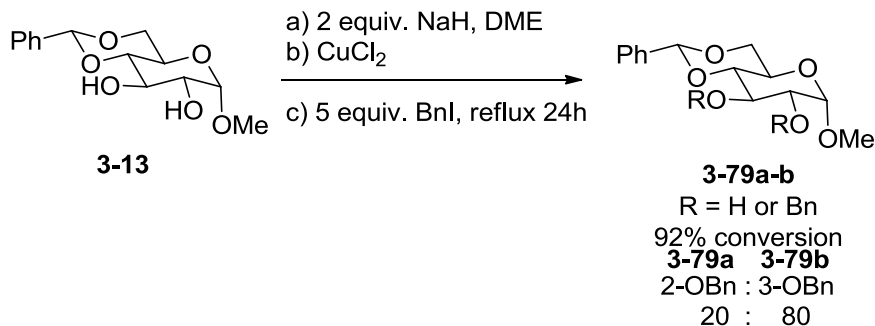
Many researchers have selectively functionalized sugars by first adding salts to the reaction mixture, prior to adding the functionalizing agent. Initially, Avela, Melander and Holmbom formed copper(II) chelates of various sugars to observe if the chelate would influence the outcome of alkylation.^{64,65}



Scheme 3.29 Avela compare sodium hydride the reactivity of 4,6-*O*-benzylidene-methyl- α -D-glucopyranoside to copper(II) chloride used following treatment with sodium hydride.

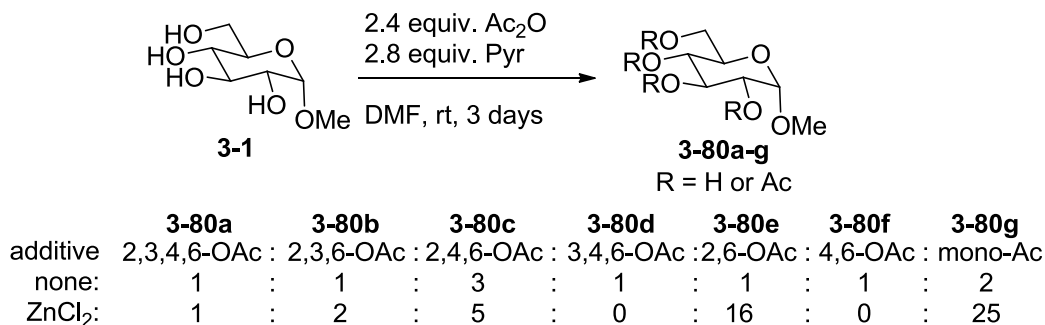
In fact, if only one equivalent of sodium hydride was used, Avela found that position 2 reacted to alkylation, yielding mainly **3-78a**. If an excess of sodium hydride was used, Avela found that the sugar would react at positions 2 and 3, yielding **3-78c**. On the other hand, if the mono-sodium alkoxide reacted with copper(II) chloride prior to functionalization, Avela noted that position 3 reacted predominantly, yielding **3-78b**, not position 2, the reason being that the copper sticks to the first site of deprotonation (position 2) and therefore alkylation can only occur at position 3 (Scheme 3.29). Although the authors do not infer this from their results, perhaps the hydrogen bond network of the sugar may play a role in that position 2 seems to be the most acidic, leading to copper blocking the 2-O from alkylation.

Eby and Schuerch⁶⁶ formed dianions of various α -D-hexopyranoside starting materials with two equivalents of sodium hydride and used copper(II) salt, namely copper(II) chloride to chelate the dianion, deactivating it prior to alkylation (using either methyl, benzyl, or allyl iodide). In this way, Eby and Schuerch alkylated a number of different sugars, protected at various positions.



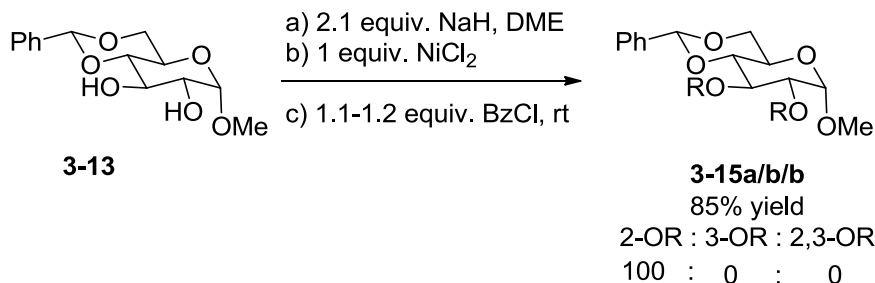
Scheme 3.30 Selective alkylation in the presence of copper(II) chloride.

For example, when positions 4 and 6 were protected as a benzylidene (as in Scheme 3.30), alkylation occurred at position 3 of the sugar (66-95% yield of mainly **3-79b**), confirming Avela's results. When positions 2 and 3 were benzylated, alkylation occurred at position 4 (51-100% yield). They later continued with selective alkylation and acylations, finding that copper salts (as opposed to mercury salts) eliminated any disubstitution reactions, favouring mono-functionalization of the starting materials.⁶⁷



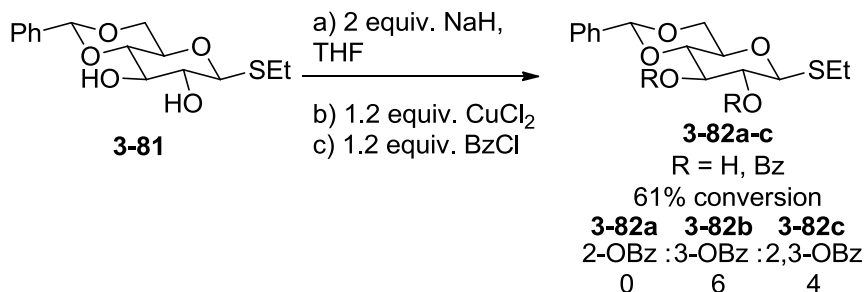
Scheme 3.31 Acetylation using zinc(II) chloride.

In 1990, Hanessian and Kagotani⁶⁸ acetylated various methyl α-D-hexopyranosides (including **3-1**). The selectivity observed was highly dependent on the presence of zinc(II) chloride in their experiments (Scheme 3.31).

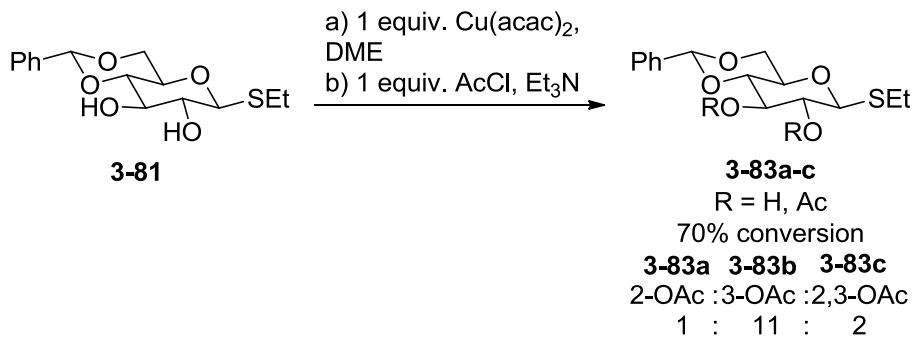


Scheme 3.32 Selective benzoylation in the presence of nickel(II) chloride.

More recently, Gangadharmath and Demchenko⁶⁹ compared chloride salts of zinc, platinum and nickel to observe their effect on benzoylation of sugars, finding that the nickel(II) chloride salt yielded the most selective benzoylation of **3-13** (Scheme 3.32) and benzylation.



Scheme 3.33 Selective benzoylation in the presence of copper(II) chloride.

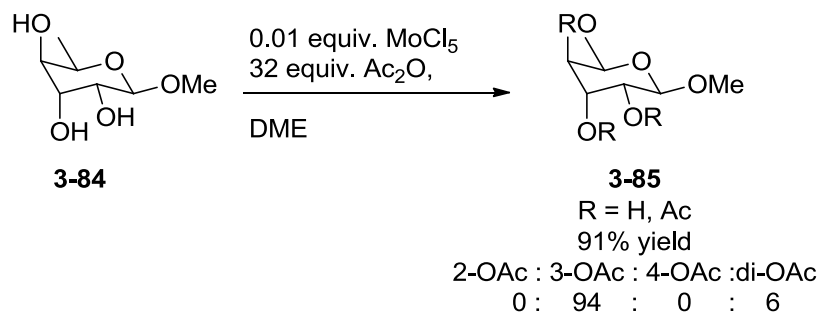


Scheme 3.34 Optimized conditions to acylate a sugar using copper(II) acetylacetonate.

Osborn also selectively acylated and alkylated 4,6-*O*-benzylidene- α - and β -D-glucopyranosides (such as **3-81**) at position 3, first forming the copper(II) chelate prior to further functionalization (Scheme 3.33).⁷⁰ The Osborn

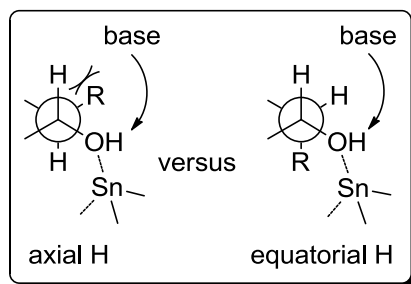
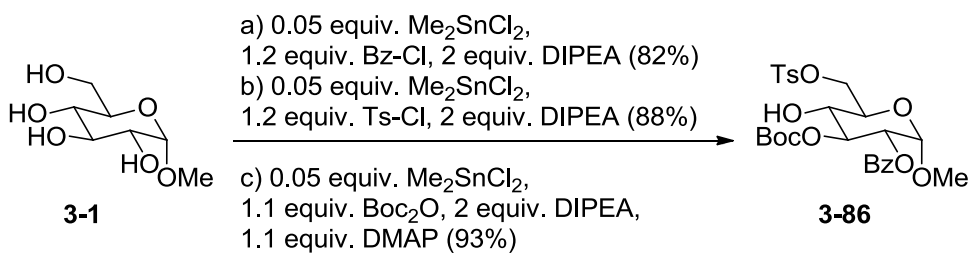
group also successfully applied this chemistry to glycosylate these sugars, also selectively at position 3.⁷¹

The Osborn group continued to optimize the conditions to functionalize sugars in the presence of copper(II), screening other copper sources. In fact, while copper(II) chloride requires a first step deprotonating the sugar in order to strongly interact with the sugar, other copper sources like copper(II) acetylacetonate ($\text{Cu}(\text{acac})_2$) interact strongly with the sugar without the need for deprotonating. Thus, they optimized conditions to acetylate **3-81** (Scheme 3.34)⁷²



Scheme 3.35 Selective functionalization of methyl α -L-rhamnopyranoside with molybdenum(V) chloride.

Evtushenko⁷³ investigated molybdenum(V) chloride as catalyst for selective acylation of deoxyhexoses such as **3-84** (Scheme 3.35).

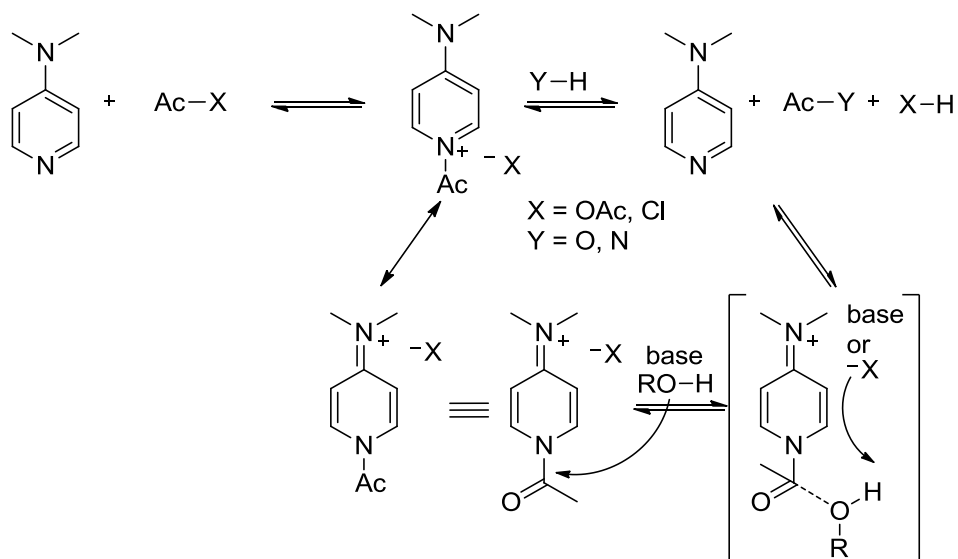


Scheme 3.36 Stepwise protection of methyl α -D-glucopyranoside (**3-1**) with catalytic dimethyl tin(IV) chloride.

The Onomura group⁷⁴ used catalytic amounts of dimethyl tin(IV) chloride to selectively mono-benzoylate various methyl α - and β -D-hexopyranosides such as **3-1** (72-91% yield). In fact, they used dimethyl tin(IV) chloride at each step to protect methyl α -D-glucopyranoside, leaving, in the end, only position 4 of **3-86** free for further selective functionalization. Deprotonation and subsequent functionalization in the first step of the synthesis occurs at position 2 which is the most open position, having one equatorial hydrogen nearby as opposed to a bulkier equatorial hydroxyl (position 3), hydroxymethyl (of position 6) (Scheme 3.36).

3.6 The role of the acylating agent

Many of the methods presented thus far differ, not only through the use of a variety of catalysts or additives, but also through the acylating agent used. In fact, only a few research groups addressed the role of the acylating agent when selectively protecting sugars, and yet the following examples clearly illustrate that the acylating agent used influences the selectivity of the reaction and therefore the products formed. Kattnig and Albert researched the mechanism of DMAP-catalysis, investigating specifically the influence of different acylating agents and bases on DMAP catalyzed acylation reactions.⁷⁵



Scheme 3.37 Detailed mechanism of DMAP-catalyzed acylations illustrating the role of the counterion (X^-) or base.

Homogeneous acylations with acetyl chloride, pyridine (as a base) and DMAP (as a catalyst) are faster than those with acetic anhydride under the same conditions. The reverse is true for heterogeneous acylations with acetic anhydride and potassium carbonate (as a base) which are faster than those using acetyl chloride under the same conditions. Updating Scheme 3.3, which illustrated the proposed mechanism for DMAP-catalyzed acylations, to include the base used for these reactions and the deprotonation step, we obtain Scheme 3.37.

Kattnig and Albert further investigated the influence of pyridinium ion pair formed, which Guibe-Jampel, Le Corre and Wakselman began to examine in 1979.⁷⁶

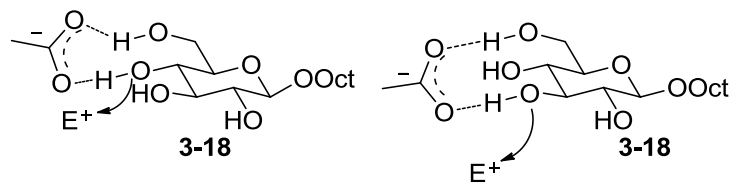
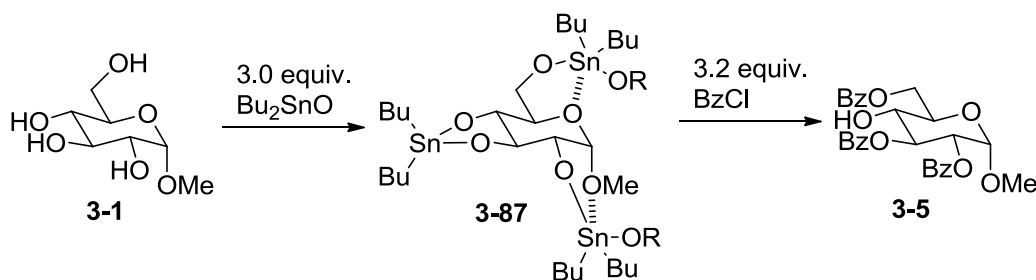


Figure 3.6 Acetate counterion can direct acylation to secondary hydroxyls.

If the base is “unavailable” to deprotonate the nucleophile $Y-H$, like when using insoluble potassium carbonate, the counterion (either acetate or chloride provided by the acylating agent) may act as the base. If the counterion is a

chloride or a cyanide, deprotonation can only occur at one position, most likely the most accessible position 6. On the other hand, if the counterion is an acetate ion, the acetate oxygens can hydrogen bond to position 6 and position 3 or 4. In this way, deprotonating a secondary hydroxyl, at either position 3 or 4, is possible and the electrophile can add onto a secondary hydroxyl, while acylation of the primary position is suppressed (Figure 3.6).

In fact, the acylating agent affects the position acylated even when acylating stannylene acetal intermediates. In their paper on benzoyl migration, Zhang and Wong form several multi-acylated sugars using an excess of BzCl and Bu₂SnO at higher temperatures (70-100°C) hypothesizing that the stannylene acetals of **3-87** at position 2 may coordinated with the anomeric methoxy, while the acetal at position 6 may coordinate to the ring oxygen (depicted in Scheme 3.38). From their experiments, Zhang and Wong were able to confirm the order of reactivity of the hydroxyls as 6-OH > 2-OH > 3-OH > 4-OH.



Scheme 3.38 Multi-benzoylation of methyl α-D-glucopyranoside.

With this in mind, the Ramström group⁷⁷ investigated how to manipulate stannylene acetals and generate sugars acylated at multiple, specific positions of methyl β-D-galactopyranoside. The Ramström group found that benzoylation of methyl β-D-galactopyranoside at low temperatures yielded the 3,6-dibenzoylated sugar, but at high temperatures, the 4,6-dibenzoylated product was observed, indicating that benzoyl migration most likely occurred with heat. Knowing also that acetyls migrate much more readily at room temperature, the acetylating agent and the number of equivalents of reagents were varied to better understand how to specifically multi-acetylate the sugar. With 2.2 equivalents of dibutyltin oxide and

acetyl chloride, acetylation occurred at positions 4 and 6 (35% yield), while when 3.3 equivalents of dibutyltin oxide were used, acetylation occurred at positions 3, 4 and 6 with acetyl chloride (57% yield). Given the reactivity observed for benzylation, the 3,6-di-acetylated product was most likely formed first but one of the acetyls migrated from position 3 to position 4. On the other hand, when acetylation was performed using acetic anhydride, methyl β -D-galactopyranoside was acetylated at positions 3 and 6 with 2.2 equivalents of dibutyltin oxide and at positions 2, 3 and 6 with 3.3 equivalents of dibutyltin oxide. Interestingly, no migration was observed with acetic anhydride.

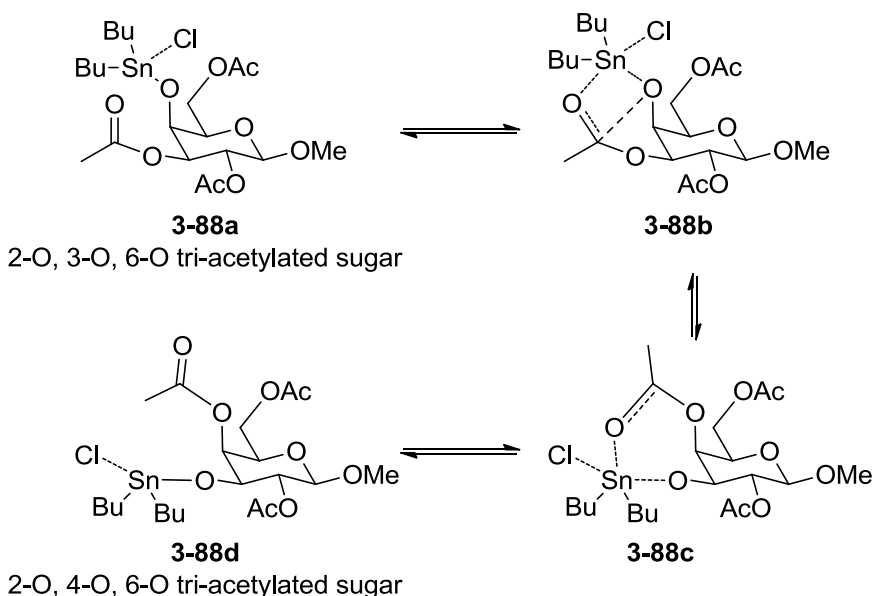


Figure 3.7 Mechanism for acetate-facilitated acetyl migration.

Ramström hypothesizes that the chloride counterion can coordinate to the organotin at position 4 (**3-88b**), which in turn can also coordinate with the acetyl oxygen at position 3 (**3-88c**), thereby promoting migration of the tin to position 3 and the acetyl to position 4 (**3-88d**) (Figure 3.7). On the other hand, in the presence of the acetate counterion, the tin at position 3 can only coordinate with the acetate which reduces the reactivity of the tin, which in turn can no longer coordinate with the acetyl at position 3. Thus, more factors than just the additive or catalyst used affect the products formed during regioselective functionalization of sugars.

3.7 Tethering

Many groups formed disaccharides from sugars that were first tethered together with different linkers, prior to glycosylation.

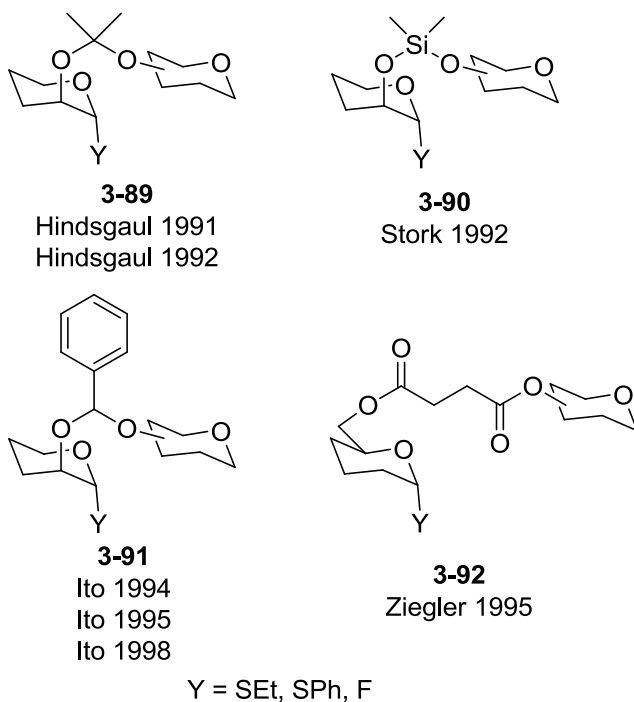
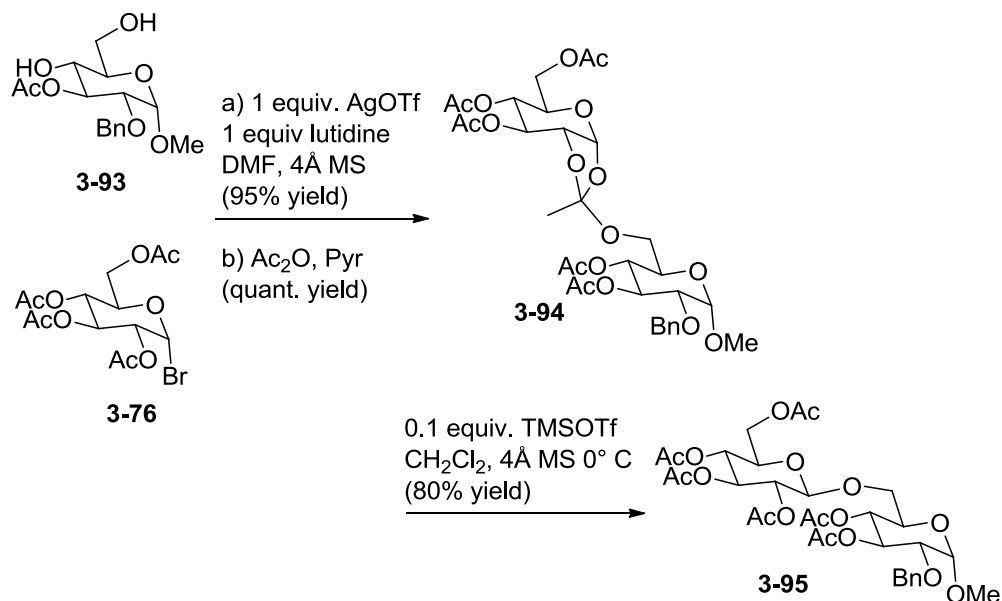


Figure 3.8 Some examples of linkers which researchers use to tether the glycosyl donor to the acceptor.

The Hindsgaul group^{78,79} used methylene tethers (**3-89**), while Stork tethered the glycosyl donor to the acceptor using a silicon linker (as in **3-90** of Figure 3.8).⁸⁰ The Ito group⁸¹⁻⁸³ used benzylidene tethers (**3-91**). Others⁸⁴⁻⁸⁷ tether donor and acceptor with a succinic acid linker (or other diacid moieties as in **3-92**).

3.7.1 Orthoesters

Wang and Kong form ortho esters from their glycosyl donors for glycosylation of almost fully protected glycosyl acceptors.^{88,89}



Scheme 3.39 Selective glycosylations through ortho esters.

Applied to sugars where positions 4 and 6 are the only free positions, glycosylation occurs at position 6 of **3-93** (Scheme 3.39), while if positions 3 and 4 are available, only position 3 reacts.^{88,90} Wang and Kong later applied this same chemistry to form trisaccharides.⁸⁹ More recently, Kong reviewed all of the available orthoester methods for selective glycosylations (including this one).⁹¹

3.7.2 Peptidic tethers

More recently, the Fairbanks group⁹² tethered a glycosyl donor to a peptide, which in turn was tethered to a mostly unprotected glycosyl acceptor (**3-96**).

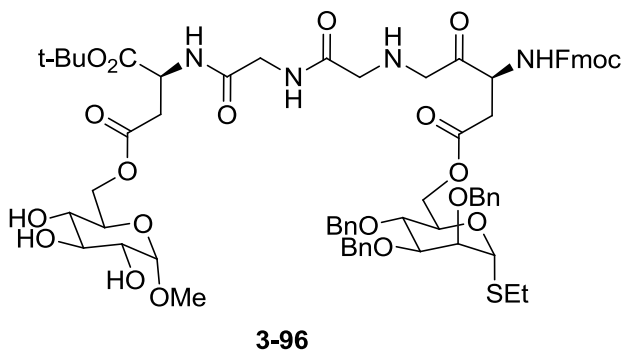


Figure 3.9 Peptide tethering glycosyl acceptor and donor for glycosylation.

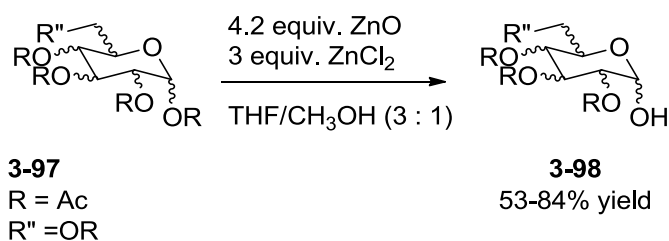
Subsequent glycosylation revealed that the peptide used to tether joining the donor and acceptor actually influences the position of glycosylation on the acceptor. For example, the acceptor of **3-96** (shown in Figure 3.9) was glycosylated exclusively at position 3 (56% yield), while if the two glycines of the peptide were replaced with one proline, glycosylation occurred mainly at position 2.

3.8 Methods for selective deprotection of sugars

In further attempts to selectively manipulate one hydroxyl among so many on a sugar, a few researchers have opted to selectively remove a protecting group, rather than selectively install one.

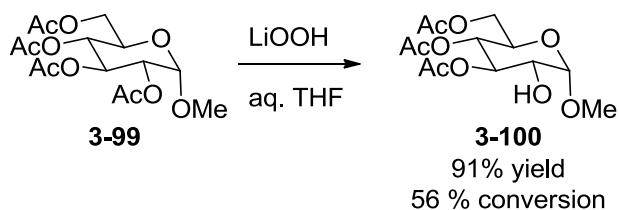
3.8.1 Selective removal of an acyl group

Several groups have investigated how to selectively transesterify an acetate from per-acylated sugars, using such reagents as sodium methoxide,⁹³ ammonium carbonate,⁹⁴ and more recently methylamine.⁹⁵



Scheme 3.40 Wang's method for selective removal of the anomeric acyl group of various peracylated glycopyranosides.

Wang and co-workers⁹⁶ worked on selective de-acylation of the anomeric position of various peracylated sugars, using a combination of zinc chloride and zinc oxide (Scheme 3.40).



Scheme 3.41 Selective deacetylation with lithium hydroperoxide.

Hanessian and Kagotani⁶⁸ found that lithium hydroperoxide could be used to selectively remove one acetyl, at position 2 (50% isolated yield of tri-acetylated product), from methyl 2,3,4,6-tetra-*O*-acetyl- α -D-glucopyranoside (**3-99**), most likely through selective chelation of the *cis* protected diol at positions 1 and 2. In fact, this method was also applicable on substrates having a benzylidene between positions 4 and 6, once again, only the acetyl at position 2 was removed (44% yield). Of course, if the anomeric position was also acetylated as in the penta-acetylated methyl α -D-glucopyranoside, lithium hydroperoxide removed the acetyls at position 2, as well as the anomeric position.

3.8.2 Selective cleavage of 4,6-*O*-benzylidenes

Researchers have developed many methods to open the 4,6-*O*-benzylidene ring, yielding either the 4-*O*-benzylated sugar or the 6-*O*-benzylated sugar depending on the reagents and the conditions used (Figure 3.10).

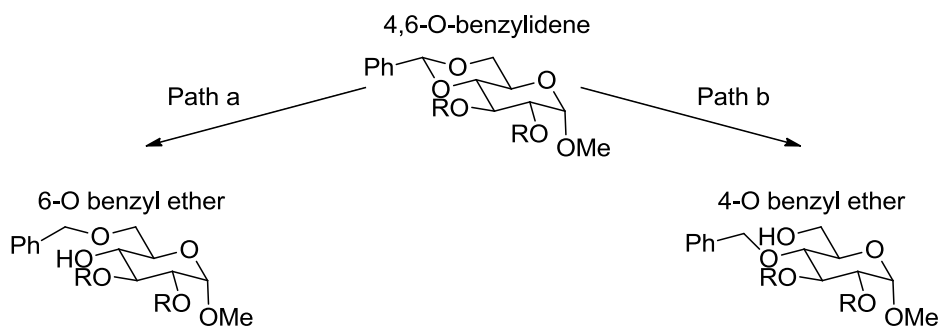
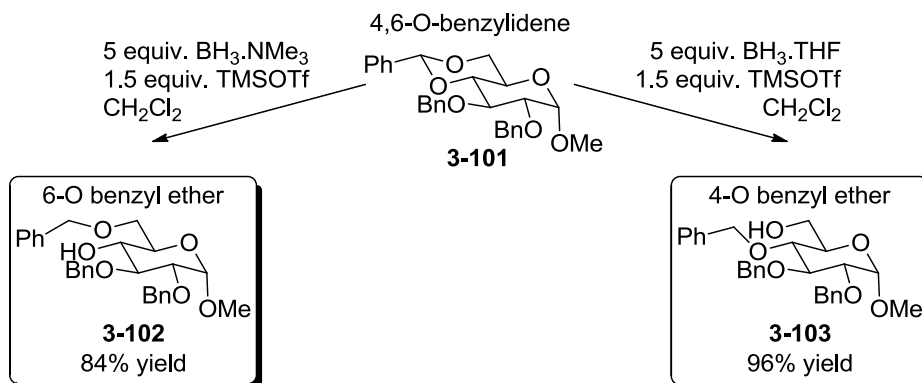


Figure 3.10 Two possible paths for cleavage of 4,6-*O*-benzylidene, either by Path a, leading to a 6-*O* benzyl ether or, by Path b, leading to a 4-*O* benzyl ether.

Recently, Daragics and Fügedi⁹⁷ listed most of these methods, noting that the ring opening reaction, although seemingly easy, is actually quite challenging because many of the reaction conditions are incompatible with other protecting

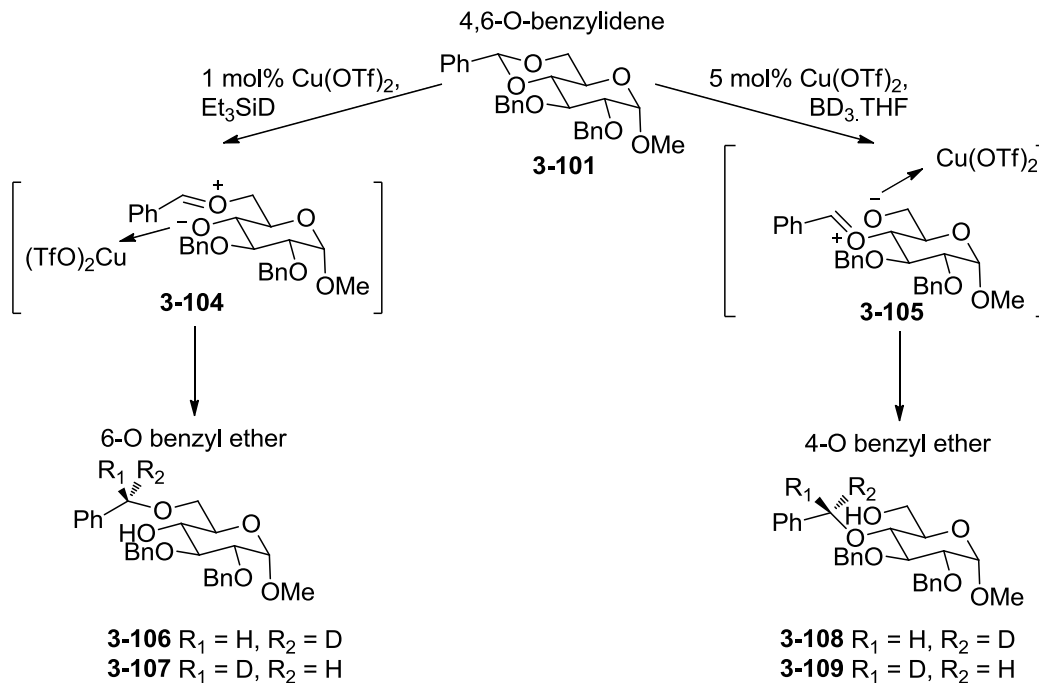
groups bound to the starting material sugar, are sensitive to temperature and humidity, etc. In fact, most of the methods are hazardous, expensive and may not be applicable for more complex, bulkier sugars, thus limiting their utility.

In search of a clean, easier method to form 4-O benzyl ethers from 4,6-O benzylidenes (**3-101**), Daragics and Fügedi screened different borane complexes ($\text{BH}_3\cdot\text{THF}$, $\text{BH}_3\cdot\text{SMe}_2$, $\text{BH}_3\cdot\text{NMe}_3$) as hydride donors, all used in conjunction with TMSOTf (Scheme 3.42). While $\text{BH}_3\cdot\text{SMe}_2$ seemed to be non-selective, yielding equal amounts of the 4-O and 6-O benzyl ether products, $\text{BH}_3\cdot\text{NMe}_3$ specifically cleaved the benzylidene from position 4, yielding the 6-O benzyl ether (**3-102**, 84% yield), while $\text{BH}_3\cdot\text{THF}$ yielded exclusively the 4-O-benzyl ether (**3-103**, 96% yield).



Scheme 3.42 Two methods to cleave 4,6-O-benzylidenes using borane, yielding either the 4-O or the 6-O benzyl ether.

Various Lewis acids (TMSOTf , $\text{Sc}(\text{OTf})_3$, ZnI_2 , AlCl_3 , $\text{BF}_3\cdot\text{OEt}_2$) were also screened, but TMSOTf yielded the fastest reaction, complete in only one hour. The reaction conditions developed were not only compatible with different types of benzylidenes, but also safe to use with substrates having other types of protecting groups. Unfortunately, Daragics and Fügedi gave no explanation for the observed regioselectivity. On the other hand, in 2005, the Hung group performed NMR studies of the benzylidene ring opening reaction of **3-104** with either $\text{BD}_3\cdot\text{THF}$ or Et_3SiD (Scheme 3.43).

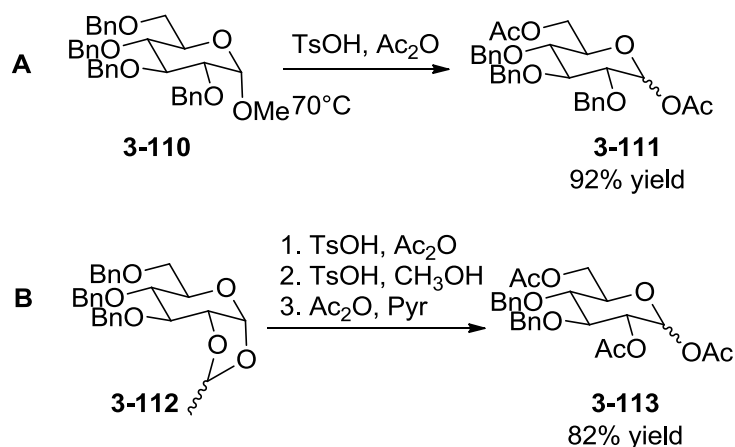


Scheme 3.43 First experimental evidence on mechanism of benzylidene ring opening reaction using either a borane or a silane reducing agent.

They found that given the bulk surrounding the 4-*O*-position of the sugar, a larger, hindered reagent, such as triethylsilane cannot reduce the 4-*O*-benzyl cation **3-105**, therefore, reducing with triethylsilane yields the 6-*O* benzyl ether (**3-106** and **3-107**). On the other hand, the borane reagent is small enough to access and reduce the 4-*O* benzyl cation and therefore reducing with this reagent yields the 4-*O* benzyl ether.⁹⁸

3.8.3 Selective removal of benzyls

Several groups have reported selective removal of benzyl groups under acidic conditions, leading to sugars acetylated at the de-benzylated positions (in a process known as “acetolysis”).⁹⁹⁻¹⁰⁴ More recently, the Yamada group^{105,106} focused on a newer method for the selective removal of benzyls at positions 1 and 6 of **3-110**, followed by acetylation of these positions (Scheme 3.44).

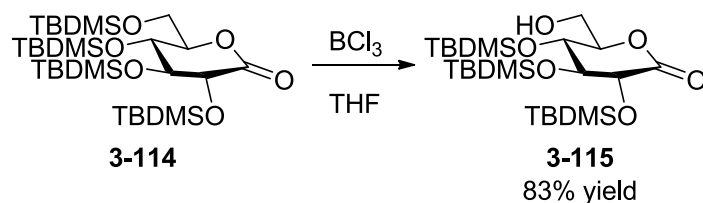


Scheme 3.44 Selective de-benzylation.

Given the methods for selective removal of the 1-O acetyl, one can imagine that the pyranose **3-113** could then be transformed into a glycosyl donor. Furthermore, if the perbenzylated starting material had a 1,2-acetylidene, their benzyl cleavage method led to the formation of the 1,2,6-tri-*O*-acetylated product, which could in turn be transformed to a glycosyl donor leading to more selective glycosylations courtesy of neighbouring group participation.

3.8.4 Selective deprotection of silyl groups

Only a few papers focus on selectively removing silyl protecting groups from persilylated sugars.



Scheme 3.45 Selective removal of TBDMS groups from a persilylated D-gluconolactone using BCl_3 .

For example, the Lin group¹⁰⁷ developed a method to selectively removal the TBDMS protection of **3-114** from primary alcohols in the presence of secondary TBDMS protected sites, using boron trichloride (BCl_3) (Scheme 3.45). They found that their method was also applicable to benzyl 2,3,4,6-*O*-TBDMS α -D-

manno- and galactopyranosides, but they did not apply their method to a glucopyranoside.

3.9 Summary

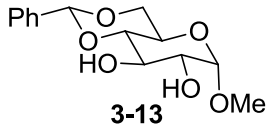
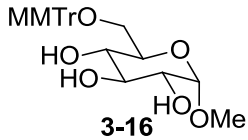
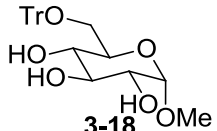
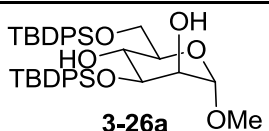
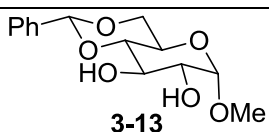
We have summarized the results of this review in Table 3.1 which can serve as a useful reference tool for researchers seeking to perform a selective reaction on a hexopyranoside.

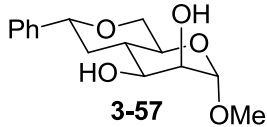
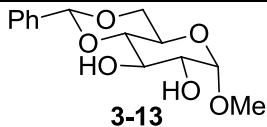
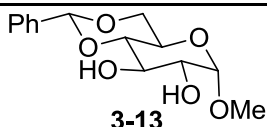
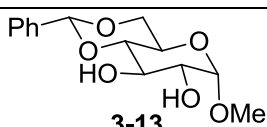
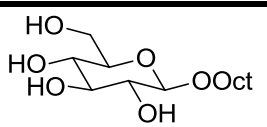
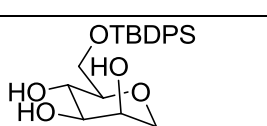
3.10 Conclusion and outlook

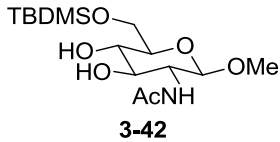
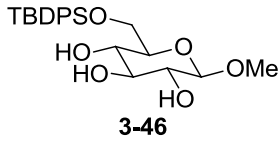
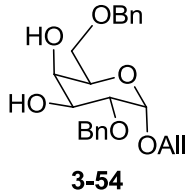
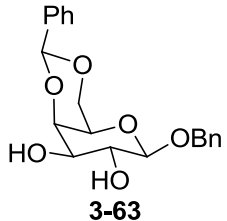
From the many methods presented above to selectively protect and deprotect a variety of sugars, we find that performing any type of reaction selectively on a sugar presents many issues, from the type of reagent used, to the general conditions, to the substrate's orthogonal protections, stereochemistry, etc. These issues are even more apparent when researchers look into how to perform regioselective glycosylations. Levy and Fügedi wrote in 2006 that “The *holy grail* of glycosylations – the generally applicable, stereoselective and technically simple glycosylation method – has yet to be found.”¹⁰⁸ However, considering that we see regioselective glycosylations as the “holy grail” of carbohydrate chemistry, we find that there are significantly fewer groups publishing research on regioselective glycosylation. Perhaps, few embark on this quest for reasons such as the sheer number of possible products that can form during a single glycosylation experiment between a glycosyl donor and a glycosyl acceptor, leading to complicated separation and identification of products. And, while in the case of simpler acylation chemistry experiments, we envision that one main difficulty researchers face when attempting to characterize the possible products is determining the modified position, for glycosylation products, we see that not only does the position of glycosylation need to be determined, but also the stereochemistry, whether alpha or beta. Indeed, the quest for a simple, selective glycosylation method is intimidating.

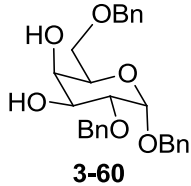
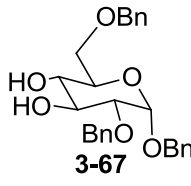
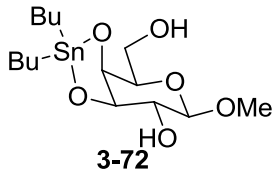
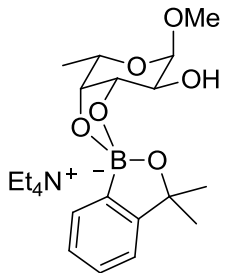
Researchers have followed a few impressive paths in a quest to find this “holy grail” in carbohydrate chemistry. However, most researchers seem to report end results from the path they have chosen, rather than explaining why they chose that path. Methods are applied and products are analyzed, and, only a few research groups provided some rationale for their results. Furthermore, few have designed methods which they predict and prove to form a specific product. In many cases, the hydrogen bond network of the sugar substrate is mentioned, as an after-fact, rather than in the forefront of the research, considering that this network seems to influence so many of the reactions performed on sugars. In fact, none of these methods truly seek to manipulate the hydrogen bond network to their advantage with a goal in mind. If in fact the hydrogen bond network is the key to many of these methods, much more work needs to be done to seek how to use this network to form the desired product in a few steps. In the next chapters, we will explore the path which the Moitessier group has chosen to explore, attempting to manipulate the hydrogen-bond network of sugars in order to perform regioselective functionalizations and glycosylations on minimally protected sugars.

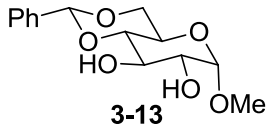
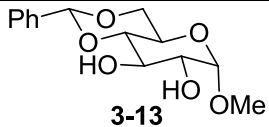
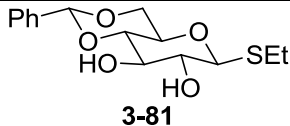
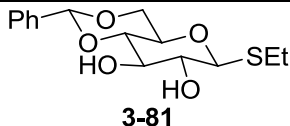
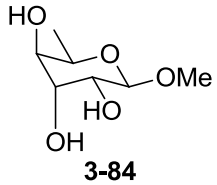
Table 3.1 Summary of the available methods to selectively functionalize position 2, 3 or 4 of hexopyranosides.

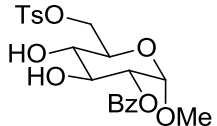
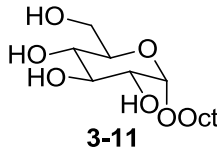
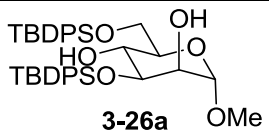
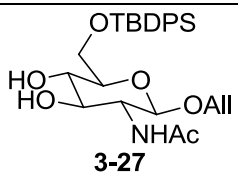
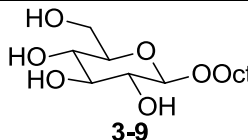
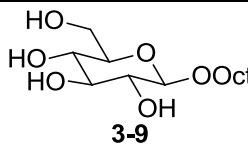
Goal	Starting material	Conditions	yield or conversion and ratios of products	Scheme	Ref
2-OAc or 2-OBz	 3-13	9 equiv Et ₃ N, 1.4 equiv. Ac ₂ O or Bz ₂ O, CH ₂ Cl ₂	80% yield (Ac ₂ O) 93% yield (Bz ₂ O) only the 2-O-isomer reported	3.6	18
2-OCbz	 3-16	4.0 equiv. CbzCl, 0.7 equiv. DMAP, 2.5 equiv. DABCO, CH ₂ Cl ₂ , 0°C, 15 min	80% yield only the 2-O-isomer reported	3.7	19
2-OBz	 3-18	1.2 equiv. PhCOOH, 1.2 equiv. DMAP, 2.4 equiv. BOP-Cl, Pyr., R.T., 15h	88.9% yield of 2-OBz : 3-OBz : 4-OBz 72.6 : 2.5 : 13.8	3.8	20
2-OTBDPS	 3-26a	3,2-TBDPS shift higher temperature, mild base, long reaction time	3,6-OR : 2,6-OR : 4,6-OR 20 : 69 : 11 R = TBDPS	3.10	24
2-OBz	 3-13	a) 1 equiv. Bu ₂ SnO, CH ₃ OH, reflux b) 1.1 equiv. BzCl, 1.1 equiv Et ₃ N, rt	95% yield 2-OBz : 3-OBz 94 : 1	3.21	48

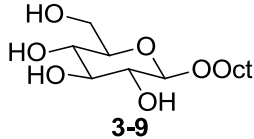
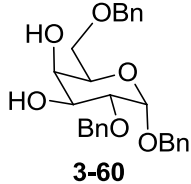
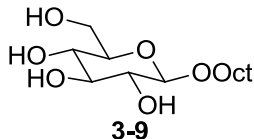
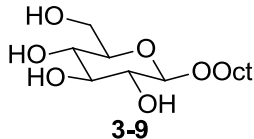
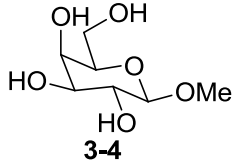
2-OBz		a) 1 equiv. Bu_2SnO , CH_3OH , reflux b) excess BzCl , $12-15^\circ\text{C}$, dioxane	2-OBz : 3-OBz major : minor	3.23	49
2-OMe		a) 1 equiv. NaH b) 2.4 equiv. MeI	87% conversion 2-OBz : 3-OBz : 2,3-OBz 7: 1 : 3	3.29	64
2-OBz		a) 2.1 equiv. NaH b) 1 equiv. NiCl_2 c) 1.2 equiv. BzCl	85% yield 2-OBz : 3-OBz : 2,3-OBz 100: 0 : 0	3.32	69
2-OBz		0.05 equiv. Me_2SnCl_2 , 1.2 equiv. BzCl , 2 equiv. DIPEA	82% yield only the 2-O-isomer reported	3.36	74
3-OAc		0.7 equiv. Ac_2O , 0.05 equiv. DMAP , K_2CO_3 , CHCl_3 , rt., 1h	quant. yield 2-OAc : 3-OAc : 4-OAc : 6-OAc 2 : 42 : 37 : 19	3.4	17
1,3-glycosidic linkage		0.2 equiv. TMSOTf , trichloroacetimidate 3-31 , CH_2Cl_2 , -40°C , 40 min	56% yield 1,2 : 1,3 : 1,4 glycosidic linkage 0 : 100 : 0	3.12	26

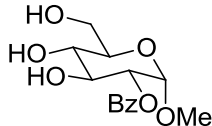
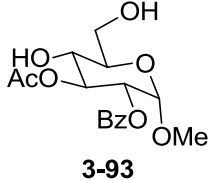
3-OAc	 3-42	0.7 equiv. Ac ₂ O, 2 mol% peptidic catalyst 3-43 , Tol, rt	88% conversion 3-OAc : 4-OAc 97 : 3	3.17	40
3-OBz	 3-46	1.2 equiv. BzCl, 1.2 equiv. Et ₃ N, 0.05 equiv. chiral diamine 3-47 , CH ₂ Cl ₂	91% conversion 2-OBz : 3-OBz : 4-OBz 4 : 96 : 0	3.19	41
3-OBz	 3-54	a) 1 equiv. Bu ₂ SnO, CH ₃ OH, reflux b) 3 equiv. BzCl, rt	81% yield only the 3-O-isomer reported	3.22	49
3-O oxidation	 3-63	a) 1 equiv. Bu ₂ SnO, benzene, reflux b) Br ₂ , 4 Å MS, benzene	46-72% yield only 3-O-oxidation reported	3.24	51

3-OBz	 3-60	a) 1 equiv. Bu_2SnO , benzene, reflux b) 1.1 equiv. BzCl , rt	74% yield only 3-O-isomer reported	3.25	51
3-OBz	 3-67	a) 1 equiv. Bu_2SnO , benzene, reflux b) 1.1 equiv. BzCl , rt	81% yield 3-OBz : 4OBz 59 : 22	3.25	51
1,3-glycosidic linkage	 3-72	a) Bu_4NF , CH_3CN b) glycosyl bromide 3-70	42% yield 1,3 : 1,6-glycosidic linkage 20 : 1	3.27	55
1,3-glycosidic linkage	 3-75	1.2 equiv. Ag_2CO_3 , glycosyl bromide 3-76 , THF	93% yield only 1,3-glycoside reported	3.28	63

3-OMe		a) 1 equiv. NaH, 2 equiv. CuCl ₂ b) 2.4 equiv. MeI	92% conversion 2-OMe : 3-OMe : 2,3-OMe 1 : 4 : 0	3.29	64
3-OBn		a) 2 equiv. NaH, CuCl ₂ b) 5 equiv. BnI	92% conversion 2-OBn : 3-OBn 20 : 80	3.30	66
3-OAc		a) 1 equiv. CuCl ₂ , DME b) 1 equiv. AcCl, Et ₃ N	61% conversion 2OAc : 3OAc : 2,3OAc 0 : 6 : 4	3.33	70
3-OAc		a) 1 equiv. Cu(OAc) ₂ , DME b) 1 equiv. AcCl, Et ₃ N	70% conversion 2-OAc : 3-OAc : 2,3-OAc 1 : 11 : 2	3.34	72
3-OAc		a) 0.01 equiv. MoCl ₅ , DME b) 32 equiv. Ac ₂ O	91% yield 2-OAc : 3-OAc : 4-OAc : di-OAc 0 : 94 : 0 : 6	3.35	73

3-OBoc		0.05 equiv. Me ₂ SnCl ₂ , 1.1 equiv. Boc ₂ O, 2 equiv. DIPEA, 1.1 equiv. DMAP	88% yield only 2-O-isomer reported	3.36	74
4-OAc		0.7 equiv. Ac ₂ O, 0.05 equiv. DMAP, K ₂ CO ₃ , CHCl ₃ , rt., 1h	98% yield 2-OAc : 3-OAc : 4-OAc : 6-OAc 0 : 25 : 61 : 14	3.5	17
4-OTBDPS		low temperature, strong base	3,6-OR : 2,6-OR : 4,6-OR 6 : 20 : 73 R = TBDPS		24
1,4- glycosidic linkage		1 equiv. BF ₃ .Et ₂ O, trichloroacetimidate 3-28 , CH ₂ Cl ₂ , -45°C, 1 h	68% yield only 1,4-glycoside reported	3.11	25
4-OAc		0.7 equiv. (<i>i</i> -PrCO) ₂ O, 10 mol% peptidic DMAP-based catalyst 3-38 , collidine, CHCl ₃ , -50°C, 1h	98% yield 2-OAc : 3-OAc : 4-OAc : 6-OAc 1 : 0 : >99 : 0	3.15	36 37
4-O <i>i</i> -Pr		1.1 equiv. (<i>i</i> -PrCO) ₂ O, 10 mol% peptidic DMAP-based catalyst 3-42 , collidine, Tol, rt, 12h	66% yield, R = <i>i</i> PrCO 2-OR : 3-OR : 4-OR : 6-OR 0 : 10 : 60 : 30	3.16	39

4-OAc		0.7 equiv. Ac ₂ O, 2 mol% peptidic catalyst 3-45 , CH ₂ Cl ₂ /Tol, 0°C, 15 h	100% conversion 2-OAc : 3-OAc : 4-OAc : 6-OAc 9:11:58:22	3.18	40
4-O oxidation		a) 1 equiv. Bu ₂ SnO, benzene, reflux b) Br ₂ , 4Å MS, benzene	73% yield only 4-O-oxidation reported	3.24	51
6-OAc		0.7 equiv. Ac ₂ O, 2 mol% DMAP-based catalyst 3-36a , CH ₂ Cl ₂ /Tol, 0°C, 15h	quant. 2-OAc : 3-OAc : 4-OAc : 6-OAc 0 : 9 : 16 : 75	3.14	33
6-O <i>i</i> -Pr		1.1 equiv. <i>i</i> -PrCOCl, 10 mol% peptidic DMAP-based catalyst 3-40 , collidine, Tol rt, 12h	77% yield 2-OR : 3-OR : 4-OR : 6-OR 0 : 4 : 9 : 87 R = <i>i</i> -PrCO	3.16	39
1,6- glycosidic linkage		a) 1.5 equiv. Bu ₂ SnO, MeOH reflux b) 2 equiv. glycosyl bromide 3-70 , Ag-silica alumina CH ₂ Cl ₂ 50°C, 22h	73% yield only 1,6-β-glycoside reported	3.26	55

6-OTs		0.05 equiv. Me ₂ SnCl ₂ , 1.2 equiv. TsCl, 2 equiv. DIPEA	93% yield only 6-OTs reported	3.36	74
1,6-glycosidic linkage	 3-93	a) 1 equiv. AgOTf, glycosyl bromide 3-76 , 1 equiv lutidine, DMF, 4Å MS b) Ac ₂ O, Pyr c) 0.1 equiv. TMSOTf, CH ₂ Cl ₂ , 4Å MS, 0° C	76% yield only 1,6-glycoside reported	3.39	88 90

3.11 References

1. Richardson, A. C.; Williams, J. M. Selective O-acylation of pyranosides. *Chem. Commun. (London)* **1965**, 104-105.
2. Williams, J. M.; Richardson, A. C. Selective acylation of pyranoside--I. : Benzoylation of methyl α -D-glycopyranosides of mannose, glucose and galactose. *Tetrahedron* **1967**, 23, 1369-1378.
3. Richardson, A. C.; Williams, J. M. Selective acylation of pyranosides-II. Benzoylation of methyl 6-deoxy- α -L-galactopyranoside and methyl 6-deoxy- α -L-mannopyranoside. *Tetrahedron* **1967**, 23, 1641-1646.
4. Kondo, Y.; Miyahara, K.; Kashimura, N. Selective benzoylation of methyl 6-deoxy- α - and β -D-glucopyranosides. *Can. J. Chem.* **1973**, 51, 3272-3276.
5. Wang, S. S.; Tam, J. P.; Wang, B. S. H.; Merripield, R. B. Enhancement of peptide coupling reactions by 4-dimethylaminopyridine. *Int. J. Pept. Protein Res.* **1981**, 18, 459-467.
6. Bugarin, A.; Connell, B. T. Acceleration of the Morita-Baylis-Hillman reaction by a simple mixed catalyst system. *J. Org. Chem.* **2009**, 74, 4638-41.
7. Wurz, R. P. Chiral dialkylaminopyridine catalysts in asymmetric synthesis. *Chem Rev* **2007**, 107, 5570-95.
8. Verley, A.; Bölsing, F. Ueber quantitative Esterbildung und Bestimmung von Alkoholen resp. Phenolen. *Ber. Dtsch. Chem. Ges.* **1901**, 34, 3354-3358.
9. Steglich, W.; Höfle, G. N,N-Dimethyl-4-pyridinamine, a Very Effective Acylation Catalyst. *Angew. Chem. Int. Ed.* **1969**, 8, 981.
10. Fersht, A. R.; Jencks, W. P. The acetylpyridinium ion intermediate in pyridine-catalyzed hydrolysis and acyl transfer reactions of acetic anhydride. Observation, kinetics, structure-reactivity correlations, and effects of concentrated salt solutions. *J. Am. Chem. Soc.* **1970**, 92, 5432-5442.
11. Gold, V. The hydrolysis of acetic anhydride. *Trans. Faraday Soc.* **1948**, 44, 506-518.

12. Bafna, S. L.; Gold, V. The hydrolysis of acetic anhydride. Part II. Catalysis by pyridine. *J. Chem. Soc. (Resumed)* **1953**, 1406-1409.
13. Gold, V.; Jefferson, E. G. The hydrolysis of acetic anhydride. Part III. The catalytic efficiency of a series of tertiary amines. *J. Chem. Soc. (Resumed)* **1953**, 1409-1415.
14. Höfle, G.; Steglich, W.; Vorbrüggen, H. 4-Dialkylaminopyridines as highly active acylation catalysts. [New synthetic method (25)]. *Angew. Chem. Int. Ed.* **1978**, 17, 569-583.
15. Hierl, M. A.; Gamson, E. P.; Klotz, I. M. Nucleophilic catalysis by polyethylenimines with covalently attached 4-dialkylaminopyridine. *J. Am. Chem. Soc.* **1979**, 101, 6020-6022.
16. Xu, S.; Held, I.; Kempf, B.; Mayr, H.; Steglich, W.; Zipse, H. The DMAP-catalyzed acetylation of alcohols - A mechanistic study. *Chem. Eur. J.* **2005**, 11, 4751-4757.
17. Kurahashi, T.; Mizutani, T.; Yoshida, J. I. Effect of intramolecular hydrogen-bonding network on the relative reactivities of carbohydrate OH groups. *J. Chem. Soc., Perkin Trans. I* **1999**, 465-473.
18. Lu, X. A.; Chou, C. H.; Wang, C. C.; Hung, S. C. Regioselective esterification of various D-glucopyranosides: Synthesis of a fully protected disaccharide unit of hyaluronic acid. *Synlett* **2003**, 1364-1366.
19. Morère, A.; Mouffouk, F.; Jeanjean, A.; Leydet, A.; Montero, J. L. High yield regioselective monobenzyloxycarbonylation of secondary alcohols in glycopyranoside series. *Carbohydr. Res.* **2003**, 338, 2409-2412.
20. Dalpozzo, R.; De Nino, A.; Maiuolo, L.; Procopio, A.; Sindona, G.; Tagarelli, A. Regioselective acylation of secondary hydroxyl groups by means BOP-Cl. *Synth. Commun.* **2004**, 34, 4207-4217.
21. Wuts, P. G. M.; Greene, T. W. *Greene's Protective Groups in Organic Synthesis*. 4th ed.; Wiley-Interscience: Hoboken, NJ, 2007.

22. Corey, E. J.; Hopkins, P. B. Diisopropylsilyl ditriflate and di-tert-butylsilyl ditriflate: new reagents for the protection of diols. *Tetrahedron Lett.* **1982**, 23, 4871-4874.
23. Flemming, A.; Mamat, C.; Köckerling, M.; Krempner, C.; Miethchen, R. Novel carbohydrate-based mono- and bidentate oligosilyl ethers. *Synthesis* **2006**, 2685-2692.
24. Arias-Pérez, M. S.; Santos, M. J. An efficient approach to partially O-methylated α -D-mannopyranosides using bis-tert-butyldiphenylsilyl ethers as intermediates. *Tetrahedron* **1996**, 52, 10785-10798.
25. Gan, Z.; Cao, S.; Wu, Q.; Roy, R. Regiospecific syntheses of N-acetyllactosamine derivatives and application toward a highly practical synthesis of Lewis X trisaccharide. *J. Carbohydr. Chem.* **1999**, 18, 755-773.
26. Cmoch, P.; Pakulski, Z. Comparative investigations on the regioselective mannosylation of 2,3,4-triols of mannose. *Tetrahedron: Asymmetry* **2008**, 19, 1494-1503.
27. Christofides, J. C.; Davies, D. B. Co-operative intramolecular hydrogen bonding in glucose and maltose. *J. Chem. Soc., Perkin Trans. 2* **1987**, 97-102.
28. Brewster, M. E.; Huang, M.; Pop, E.; Pitha, J.; Dewar, M. J. S.; Kaminski, J. J.; Bodor, N. An AM1 molecular orbital study of α -D-glucopyranose and β -maltose: Evaluation and implications. *Carbohydr. Res.* **1993**, 242, 53-67.
29. Vasquez Jr, T. E.; Bergset, J. M.; Fierman, M. B.; Nelson, A.; Roth, J.; Khan, S. I.; O'Leary, D. J. Using equilibrium isotope effects to detect intramolecular OH/OH hydrogen bonds: Structural and solvent effects. *J. Am. Chem. Soc.* **2002**, 124, 2931-2938.
30. Vicente, V.; Martin, J.; Jiménez-Barbero, J.; Chiara, J. L.; Vicent, C. Hydrogen-bonding cooperativity: Using an intramolecular hydrogen bond to design a carbohydrate derivative with a cooperative hydrogen-bond donor centre. *Chem. Eur. J.* **2004**, 10, 4240-4251.
31. Ko, H.; Shim, G.; Kim, Y. Evidences that β -lactose forms hydrogen bonds in DMSO. *Bull. Korean Chem. Soc.* **2005**, 26, 2001-2006.

32. Gonzalez-Outeiriño, J.; Kirschner, K. N.; Thobhani, S.; Woods, R. J. Reconciling solvent effects on rotamer populations in carbohydrates - A joint MD and NMR analysis. *Can. J. Chem.* **2006**, 84, 569-579.
33. Kurahashi, T.; Mizutani, T.; Yoshida, J. Functionalized DMAP catalysts for regioselective acetylation of carbohydrates. *Tetrahedron* **2002**, 58, 8669-8677.
34. Kawabata, T.; Stragies, R.; Fukaya, T.; Nagaoka, Y.; Schedel, H.; Fuji, K. Preparation and properties of chiral 4-pyrrolidinopyridine (PPY) analogues with dual functional side chains. *Tetrahedron Lett.* **2003**, 44, 1545-1548.
35. Kawabata, T.; Stragies, R.; Fukaya, T.; Fuji, K. Remote chirality transfer in nucleophilic catalysis with N-(4-pyridinyl)-L-proline derivatives. *Chirality* **2003**, 15, 71-76.
36. Kawabata, T.; Muramatsu, W.; Nishio, T.; Shibata, T.; Schedel, H. A catalytic one-step process for the chemo- and regioselective acylation of monosaccharides. *J. Am. Chem. Soc.* **2007**, 129, 12890-12895.
37. Kawabata, T.; Furuta, T. Nonenzymatic regioselective acylation of carbohydrates. *Chem. Lett.* **2009**, 38, 640-647.
38. Ueda, Y.; Muramatsu, W.; Mishiro, K.; Furuta, T.; Kawabata, T. Functional group tolerance in organocatalytic regioselective acylation of carbohydrates. *J. Org. Chem.* **2009**, 74, 8802-8805.
39. Kawabata, T.; Muramatsu, W.; Nishio, T.; Shibata, T.; Uruno, Y.; Stragies, R. Regioselective acylation of octyl β -D-glucopyranoside by chiral 4-pyrrolidinopyridine analogues. *Synthesis* **2008**, 747-753.
40. Griswold, K. S.; Miller, S. J. A peptide-based catalyst approach to regioselective functionalization of carbohydrates. *Tetrahedron* **2003**, 59, 8869-8875.
41. Hu, G. X.; Vasella, A. Regioselective benzylation of 6-O-protected and 4,6-O-diprotected hexopyranosides as promoted by chiral and achiral ditertiary 1,2-diamines. *Helv. Chim. Acta* **2002**, 85, 4369-4391.

42. Oriyama, T.; Hori, Y.; Imai, K.; Sasaki, R. Nonenzymatic enantioselective acylation of racemic secondary alcohols catalyzed by a SnX₂-chiral diamine complex. *Tetrahedron Lett.* **1996**, 37, 8543-8546.
43. David, S.; Hanessian, S. Regioselective manipulation of hydroxyl-groups via organotin derivatives. *Tetrahedron* **1985**, 41, 643-663.
44. Ogawa, T.; Matsui, M. A new approach to regioselective acylation of polyhydroxy compounds. *Carbohydr. Res.* **1977**, 56, c1-c6.
45. Ogawa, T.; Matsui, M. Regioselective stannylation. Acylation of carbohydrates: coordination control 1 For Preliminary communication see T. Ogawa and M. Matsui, *Carbohydr. Res.* 56, C1 (1977). *Tetrahedron* **1981**, 37, 2363-2369.
46. Wagner, D.; Verheyden, J. P. H.; Moffatt, J. G. Preparation and synthetic utility of some organotin derivatives of nucleosides. *J. Org. Chem.* **1974**, 39, 24-30.
47. Ikehara, M.; Maruyama, T. Studies of nucleosides and nucleotides. LXV. Purine cyclonucleosides 26, a versatile method for the synthesis of purine O cyclo nucleosides. The first synthesis of 8,2' anhydro 8 oxy 9 β D arabinofuranosylguanine. *Tetrahedron* **1975**, 31, 1369-1372.
48. Munavu, R. M.; Szmant, H. H. Selective formation of 2 esters of some methyl α -D-hexopyranosides via dibutylstannylene derivatives. *J. Org. Chem.* **1976**, 41, 1832-1836.
49. Nashed, M. A.; Anderson, L. Organotin derivatives and the selective acylation and alkylation of the equatorial hydroxy group in a vicinal, equatorial-axial pair. *Tetrahedron Lett.* **1976**, 17, 3503-3506.
50. Nashed, M. A. An improved method for selective substitution on O-3 of -mannose. Application to the synthesis of methyl 3-O-methyl-and 2-O- α -mannopyranosides. *Carbohydr. Res.* **1978**, 60, 200-205.
51. David, S.; Thieffry, A. The brominolysis reaction of stannylene derivatives: A regiospecific synthesis of carbohydrate-derived hydroxy-ketones. *J. Chem. Soc., Perkin Trans. I* **1979**, 1568-1573.

52. Cruzado, C.; Bernabe, M.; Martin-Lomas, M. Regioselective glycosylation of mono- and di-saccharides via organotin derivatives. *Carbohydr. Res.* **1990**, 203, 296-301.
53. Garegg, P. J.; Maloisel, J. L.; Oscarson, S. Stannylene activation in glycoside synthesis: Regioselective glycosidations at the primary position of galactopyranosides unprotected in the 2-, 3-, 4-, and 6-positions. *Synthesis* **1995**, 409-414.
54. Kartha, R. K. P.; Kiso, M.; Hasegawa, A.; Jennings, H. J. Simple and efficient strategy for making β -(1 \rightarrow 6)-linked galactooligosaccharides using 'naked' galactopyranosides as acceptors. *J. Chem. Soc., Perkin Trans. I* **1995**, 3023-3026.
55. Kaji, E.; Harita, N. Stannylene acetal-mediated regioselective open glycosylation of methyl β -D-galactopyranoside and methyl α -L-rhamnopyranoside. *Tetrahedron Lett.* **2000**, 41, 53-56.
56. Kaji, E.; Shibayama, K.; In, K. Regioselectivity shift from β -(1 \rightarrow 6)- to β -(1 \rightarrow 3)-glycosylation of non-protected methyl β -D-galactopyranosides using the stannylene activation method. *Tetrahedron Lett.* **2003**, 44, 4881-4885.
57. Namazi, H.; Sharifzadeh, R. Regioselective synthesis of vinylic derivatives of common monosaccharides through their activated stannylene acetal intermediates. *Molecules* **2005**, 10, 772-782.
58. Heidecke, C. D.; Lindhorst, T. K. Regioselective phthalimidopropyl-modification of carbohydrates in one step. *Synthesis* **2006**, 161-165.
59. Ferrier, R. J. The interaction of phenylboronic acid with hexosides. *J. Chem. Soc.* **1961**, 2325-2330.
60. Ferrier, R. J.; Prasad, D. Boric acid derivatives as reagents in carbohydrate chemistry. Part VI. Phenylboronic acid as a protecting group in disaccharide synthesis. *J. Chem. Soc.* **1965**, 7429-7432.
61. Verchere, J. F.; Hlaibi, M. Stability constants of borate complexes of oligosaccharides. *Polyhedron* **1987**, 6, 1415-1420.

62. Oshima, K.; Kitazono, E.-i.; Aoyama, Y. Complexation-induced activation of sugar OH groups. Regioselective alkylation of methyl fucopyranoside via cyclic phenylboronate in the presence of amine. *Tetrahedron Lett.* **1997**, 38, 5001-5004.
63. Oshima, K.; Aoyama, Y. Regiospecific glycosidation of unprotected sugars via arylboronic activation. *J. Am. Chem. Soc.* **1999**, 121, 2315-2316.
64. Avela, E.; Holmbom, B. Reactions of metal chelates of hydroxyl compounds in anhydrous conditions I. *Acta. Acad. Ab., Ser. B* **1971**, 31, 1-14.
65. Avela, E.; Melander, B.; Holmbom, B. Reactions of metal chelates of hydroxyl compounds in anhydrous conditions II. *Acta. Acad. Ab., Ser. B* **1971**, 31, 1-13.
66. Eby, R.; Schuerch, C. Regioselective alkylation of carbohydrates in metal complexes. *Carbohydr. Res.* **1982**, 100.
67. Eby, R.; Webster, K. T.; Schuerch, C. Regioselective alkylation and acylation of carbohydrates engaged in metal complexes. *Carbohydr. Res.* **1984**, 129, 111-120.
68. Hanessian, S.; Kagotani, M. Novel methods for the preparation of partially acetylated carbohydrates. *Carbohydr. Res.* **1990**, 202, 67-79.
69. Gangadharmath, U. B.; Demchenko, A. V. Nickel(II) chloride-mediated regioselective benzylation and benzylation of diequatorial vicinal diols. *Synlett* **2004**, 2191-2193.
70. Gridley, J. J.; Osborn, H. M. I.; Suthers, W. G. Regioselective C-3-O-acylation and O-alkylation of 4,6-O-benzylidene- β -D-glucopyranoside derivatives displaying a range of anomeric substituents. *Tetrahedron Lett.* **1999**, 40, 6991-6994.
71. Evans, P. G.; Osborn, H. M. I.; Suthers, W. G. The utility of glycoside copper chelates for effecting regioselective glycosidation. *Tetrahedron Lett.* **2002**, 43, 7855-7857.
72. Osborn, H. M. I.; Brome, V. A.; Harwood, L. M.; Suthers, W. G. Regioselective C-3-O-acylation and O-methylation of 4,6-O-benzylidene- β -D-

gluco- and galactopyranosides displaying a range of anomeric substituents. *Carbohydr. Res.* **2001**, 332, 157-166.

73. Evtushenko, E. V. Regioselective monoacetylation of methyl pyranosides of pentoses and 6-deoxyhexoses by acetic anhydride in the presence of MoCl₅. *Synth. Commun.* **2006**, 36, 1593-1599.

74. Demizu, Y.; Kubo, Y.; Miyoshi, H.; Maki, T.; Matsumura, Y.; Moriyama, N.; Onomura, O. Regioselective protection of sugars catalyzed by dimethyltin dichloride. *Org. Lett.* **2008**, 10, 5075-5077.

75. Kattinig, E.; Albert, M. Counterion-directed regioselective acetylation of octyl β -D-glucopyranoside. *Org. Lett.* **2004**, 6, 945-948.

76. Guibe-Jampel, E.; Le Corre, G.; Wakselman, M. Is 1-acetyl-4-dimethylaminopyridinium acetate an intermediate in the DMAP-catalyzed acetylation of tertiary alcohols? *Tetrahedron Lett.* **1979**, 20, 1157-1160.

77. Dong, H.; Pei, Z.; Bystrom, S.; Ramstrom, O. Reagent-dependent regioselective control in multiple carbohydrate esterifications. *J. Org. Chem.* **2007**, 72, 1499-502.

78. Barresi, F.; Hindsgaul, O. Synthesis of β -mannopyranosides by intramolecular aglycon delivery. *J. Am. Chem. Soc.* **1991**, 113, 9376-9377.

79. Barresi, F.; Hindsgaul, O. Improved synthesis of β -mannopyranosides by intramolecular aglycon delivery. *Synlett* **1992**, 1992, 759-761.

80. Stork, G.; Kim, G. Stereocontrolled synthesis of disaccharides via the temporary silicon connection. *J. Am. Chem. Soc.* **2002**, 124, 1087-1088.

81. Ito, Y.; Ohnishi, Y.; Ogawa, T.; Nakahara, Y. Highly optimized β -mannosylation via p-methoxybenzyl assisted intramolecular aglycon delivery. *Synlett* **1998**, 1102-1104.

82. Dan, A.; Ito, Y.; Ogawa, T. A convergent and stereocontrolled synthetic route to the core pentasaccharide structure of asparagine-linked glycoproteins. *J. Org. Chem.* **1995**, 60, 4680-4681.

83. Ito, Y.; Ogawa, T. A novel approach to the stereoselective synthesis of β -mannosides. *Angew. Chem. Int. Ed.* **1994**, 33, 1765-1767.

84. Ito, Y.; Ogawa, T. A novel approach to the stereoselective synthesis of β -mannosides. *Angew. Chem. Int. Ed.* **1994**, 33, 1765-1767.
85. Ziegler, T.; Lau, R. Intramolecular glycosylation of prearranged glycosides. A novel tool for controlling the reactivity and anomeric selectivity of glycosylations. *Tetrahedron Lett.* **1995**, 36, 1417-1420.
86. Ziegler, T.; Lemanski, G.; Rakoczy, A. Anomeric selectivity during intramolecular mannosylation of succinyl bridged glycosides 1. *Tetrahedron Lett.* **1995**, 36, 8973-8976.
87. Yamada, H.; Imamura, K.; Takahashi, T. Synthesis of a branched oligosaccharide by remote glycosidation. *Tetrahedron Lett.* **1997**, 38, 391-394.
88. Wang, W.; Kong, F. New synthetic methodology for regio- and stereoselective synthesis of oligosaccharides via sugar ortho ester intermediates. *J. Org. Chem.* **1998**, 63, 5744-5745.
89. Wang, W.; Kong, F. Z. Highly regio- and stereoselective synthesis of bioactive oligosaccharides using 1,2-*O*-ethylidene- α -D-glucopyranose and - β -D-mannopyranose as the acceptors and acetobromosugars as the donors via ortho ester intermediates. *J. Org. Chem.* **1999**, 64, 5091-5095.
90. Zeng, Y.; Kong, F. Regioselective glycosylation of 4,6-*O*-benzylidenated glucopyranosides. *Carbohydr. Res.* **2003**, 338, 843-849.
91. Kong, F. Recent studies on reaction pathways and applications of sugar orthoesters in synthesis of oligosaccharides. *Carbohydr. Res.* **2007**, 342, 345-373.
92. Tennant-Eyles, R. J.; Davis, B. G.; Fairbanks, A. J. Peptide templated glycosylation reactions. *Tetrahedron: Asymmetry* **2000**, 11, 231-243.
93. Itoh, T.; Takamura, H.; Watanabe, K.; Araki, Y.; Ishido, Y. A facile procedure for regioselective 1-*O*-deacylation of fully acylated sugars with sodium methoxide. *Carbohydr. Res.* **1986**, 156, 241-246.
94. Mikamo, M. Facile 1-*O*-deacylation of per-*O*-acylaldoses. *Carbohydr. Res.* **1989**, 191, 150-153.
95. Egusa, K.; Kusumoto, S.; Fukase, K. Solid-phase synthesis of a phytoalexin elicitor pentasaccharide using a 4-azido-3-chlorobenzyl group as the

- key for temporary protection and catch-and-release purification. *Eur. J. Org. Chem.* **2003**, 3435-3445.
96. Dong, J. Q.; Zhang, S. J.; Wang, Y. G. A facile approach to regioselective 1-*O*-deacylation of peracylated glycopyranoses. *Chin. Chem. Lett.* **2003**, 14, 233-234.
97. Daragics, K.; Fügedi, P. Regio- and chemoselective reductive cleavage of 4,6-*O*-benzylidene-type acetals of hexopyranosides using BH₃·THF-TMSOTf. *Tetrahedron Lett.* **2009**, 50, 2914-2916.
98. Shie, C. R.; Tzeng, Z. H.; Kulkarni, S. S.; Uang, B. J.; Hsu, C. Y.; Hung, S. C. Cu(OTf)₂ as an efficient and dual-purpose catalyst in the regioselective reductive ring opening of benzylidene acetals. *Angew. Chem. Int. Ed.* **2005**, 44, 1665-1668.
99. Ponpipom, M. M. Synthesis of 3-*O* substituted D-mannoses. *Carbohydr. Res.* **1977**, 59, 311-317.
100. Eby, R.; J. Sondheimer, S.; Schuerch, C. Selective acetolysis of primary benzyl ethers. *Carbohydr. Res.* **1979**, 73, 273-276.
101. Yang, G.; Ding, X.; Kong, F. Selective 6-*O*-debenzylation of mono- and disaccharide derivatives using ZnCl₂-Ac₂O-HOAc. *Tetrahedron Lett.* **1997**, 38, 6725-6728.
102. Zhang, G.-t.; Guo, Z.-w.; Hui, Y.-z. A facile regioselective 1,6-*O*-diacetylation method of methyl-glycopyranosides and their dimethyl phosphonates. *Synth. Commun.* **1997**, 27, 1907 - 1917.
103. Lam, S. N.; Gervay-Hague, J. Solution- and solid-phase oligosaccharide synthesis using glucosyl iodides: a comparative study. *Carbohydr. Res.* **2002**, 337, 1953-1965.
104. Lu, W.; Navidpour, L.; Taylor, S. D. An expedient synthesis of benzyl 2,3,4-tri-*O*-benzyl-β-D-glucopyranoside and benzyl 2,3,4-tri-*O*-benzyl-β-D-mannopyranoside. *Carbohydr. Res.* **2005**, 340, 1213-1217.

105. Cao, Y.; Okada, Y.; Yamada, H. Facile and regioselective preparation of partly O-benzylated D-glucopyranose acetates via acid-mediated simultaneous debenzylation-acetolysis. *Carbohydr. Res.* **2006**, 341, 2219-2223.
106. Cao, Y.; Yamada, H. Corrected order in the simultaneous debenzylation-acetolysis of methyl 2,3,4,6-tetra-O-benzyl- α -D-glucopyranoside. *Carbohydr. Res.* **2006**, 341, 909-911.
107. Yang, Y. Y.; Yang, W. B.; Teo, C. F.; Lin, C. H. Regioselective deprotection of tert-butyldimethylsilyl ethers by boron trichloride. *Synlett* **2000**, 1634-1636.
108. Levy, D. E.; Fügedi, P. The organic chemistry of sugars. In Taylor & Francis: Boca Raton, 2006; pp 150-151.

Chapter 4 Regioselective glycosylation of position 2 of sugars using directing-protecting groups

Contrary to the methods reviewed in Chapter 3, in Chapter 4 we selectively protect the most easily accessed position of a carbohydrate (the primary hydroxyl) with a group that can actually modify and manipulate the accessibility and reactivity of the other hydroxyls of the substrate. Herein, we will demonstrate that this protecting group can actually be applied to the most complex of reactions in carbohydrate chemistry: the glycosylation reaction with a benzylated glucosyl donor.

4.1 Abstract

Performing reactions on free sugars is daunting because all sugars, like D-glucose, bear multiple hydroxyls which are difficult to chemically differentiate. We hypothesize that a dipyridyl-based protecting group installed at position 6 of a glucopyranoside, which can hydrogen bond to positions 3 and 4 and provide enough bulk around these positions. This group would direct glycosylation to the 2-OH. To test this approach of using directing-protecting groups, we glycosylated a series of 6-*O*-protected methyl α -D-glucopyranoside acceptors, protected at position 6, with a 2,3,4,6-tetra-benzylated glucopyranose trichloroacetimidate donor. A variety of commonly used protecting groups, as well as pyridyl-based protecting groups, were screened. We found that while most of the 6-*O*-protected sugars were glycosylated mainly at position 3, the 6-*O*-protected sugar bearing two pyridyl rings was mainly glycosylated at position 2 (57-61 % yield, 1:1.8 mixture of α/β). This method proves that a hydrogen-bond accepting protecting group, such as our directing-protecting group, installed at position 6 can significantly influence which position of the glucopyranoside acceptor is glycosylated.

4.2 Introduction

4.2.1 Background

One of Nature's vital building blocks is D-glucose. Chemists seek to use this building block as efficiently as Nature does, but working with the polyol that is glucose seems to be more intimidating and challenging for chemists than for Nature. Unlike Nature, chemists must perform several chemical transformations, such as protection and deprotection steps on the multiple hydroxyls of glucose and other sugars, in order to selectively react at one position. The question that remains unanswered is how can a chemist possibly perform a reaction as difficult as a glycosylation selectively and efficiently when glucose has so many hydroxyls that are seemingly identical? In the quest for an easy, regioselective and

stereoselective glycosylation method, researchers have yet to come up with a high yielding, selective method to glycosylate sugars, more specifically to form a specific disaccharide between two glucose molecules, in a high yield and with minimal side products. A few researchers have faced the challenge of performing regioselective reactions on sugars, proposing a number of methods: for example, several groups utilized tin to form sugar-tin intermediates prior to functionalizing the sugar,¹ while others tethered the glycosyl acceptor to the glycosyl donor with a short peptide linker,² among many other methods reviewed in Chapter 3. Unfortunately, most of these methods are hardly practical and often not green, especially on a large scale: tin is highly toxic, short peptides still need to be synthesized and coupled to the carbohydrates prior to performing the desired reaction.

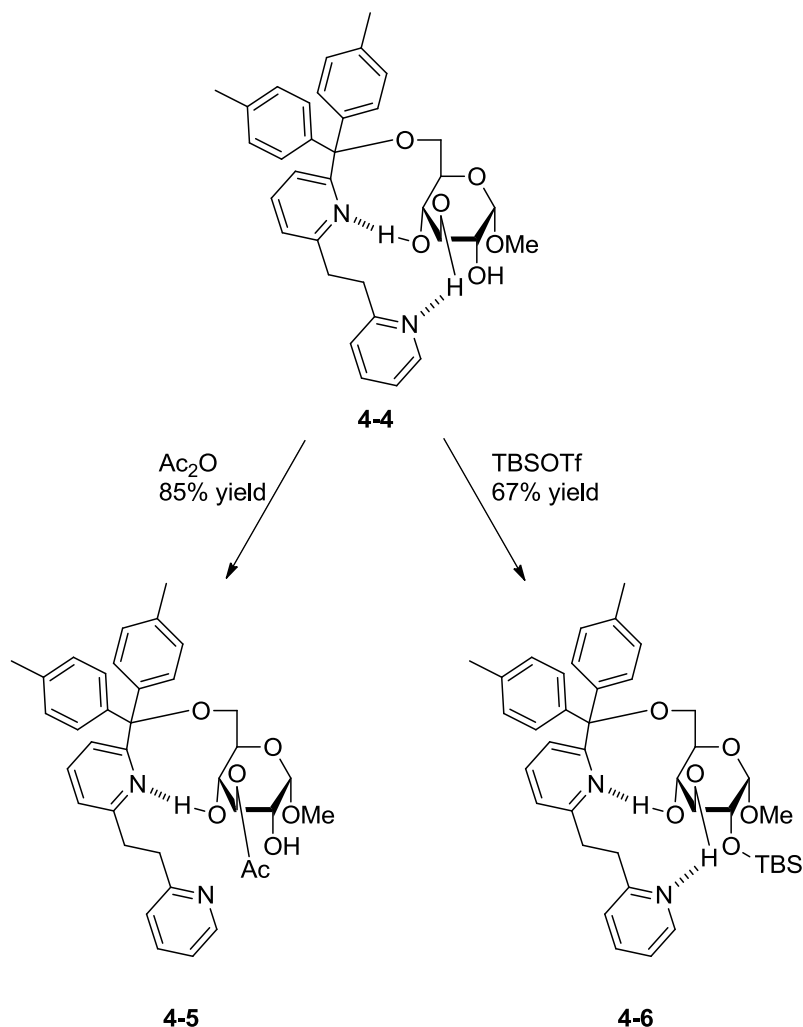
In an effort to minimize the number of steps and protecting groups in a glycosylation reaction, the CmoCh group proposed that the hydrogen bond network of allyl 6-*O*-TBDPS- α -D-mannopyranoside (**4-1**) rendered position 3 the most reactive position towards glycosylation with a tetra-benzoylated mannose trichloroacetimidate (**4-2**). (Scheme 4.1).³ In fact, the CmoCh group obtained a 56% yield of one product, the 3-*O*-glycoside (**4-3**).



Scheme 4.1 Regioselective mannosylation at position 3 of 6-*O*-TBDPS-allyl- α -mannopyranoside (**4-1**).

Of course, position 2 is axial in mannose and less reactive, and the two positions left to react are positions 3 and 4. Based on prior work from Williams and Richardson,⁴ we know that position 3 should be the most accessible and reactive. Unfortunately, this method applies only to mannose and the authors do not test their conditions on other sugars, and most importantly, on glucose.

In 1965, Williams and Richardson proposed that the internal hydrogen bond network of each sugar may influence the reactivity of the hydroxyls.⁴ With this in mind, we have chosen a different path to attack the issue of performing a reaction selectively on a sugar: we aim to manipulate the hydrogen bond network innate in a sugar, thereby influencing the reactivity of the hydroxyls of the sugar under investigation.



Scheme 4.2 Manipulation of the hydrogen bond network renders position 3 more nucleophilic, but also hindered and position 2, less hindered, but also less nucleophilic.

In 2005, our group reported that a judiciously-designed trityl-like protecting group containing two pyridine rings separated by a short linker, could be easily installed at position 6 and hydrogen bond with the 3- and 4-OHs of the 6-*O*-

protected methyl α -D-glucopyranoside (as in **4-4** of Scheme 4.2).⁵ This directing-protecting group modifies the internal hydrogen bond network and influences the reactivity of the sugar, rendering the 3-OH more reactive to small electrophiles (like acetic anhydride) and the 2-OH more accessible to larger electrophiles (like pivaloyl chloride or TBSOTf).

This directing-protecting group was never applied to glycosylations, a reaction known to be more challenging than the esterifications and silyl ether formations listed above. If researchers could use such a protecting group to direct and control which hydroxyl would react during a glycosylation experiment, this would represent a milestone towards a method that is regioselective, but also user-friendly. In fact, many fields could benefit from such an easy method to regioselectively glycosylate sugars: in medicinal chemistry, sugars can be attached to drugs in order for cells to uptake the drug (drug addressing) and carbohydrate-based drugs would also be more feasible; in any field involving nucleic acid synthesis, where reactions need to be performed selectively on the sugar ribose; in materials science, where sugars could be used as building blocks.

In this chapter, we seek to apply the di-pyridyl directing-protecting group to glycosylation chemistry and to develop a method to react a glucopyranoside acceptor with a glucopyranose donor and form disaccharides regioselectively. We found that, with the di-pyridyl directing-protecting group at position 6, we could selectively glycosylate the 2-OH of the 6-*O*-protected sugar with a tetra-benzylated glucopyranose trichloroacetimidate (40-60% yield of a mixture of α - and β -anomers). We also determined that this directing-protecting group worked well with methyl α -D-mannopyranoside and octyl β -D-glucopyranoside.

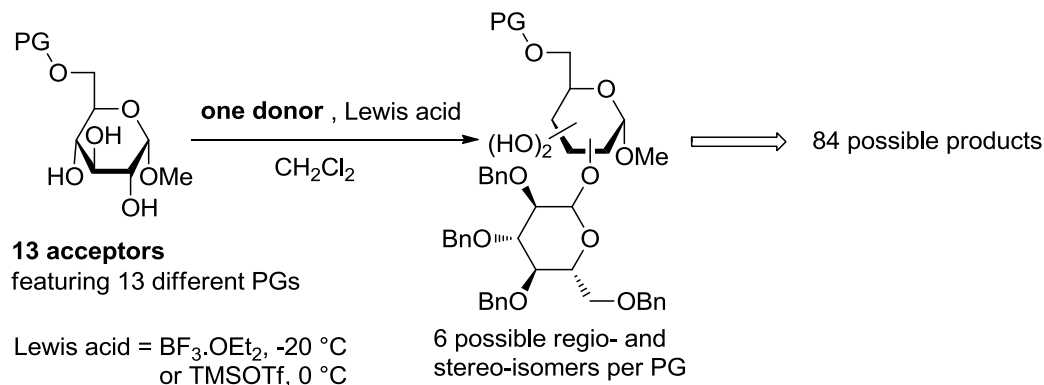
4.2.2 Challenges of regioselective glycosylations

The challenges of regioselective glycosylations which we expected to encounter and aimed to overcome in this study are as follows:

- Regioselectivity: we are looking for conditions that will allow us to selectively react at one hydroxyl over all the hydroxyls of minimally protected sugars.
- Stereoselectivity: the glycosidic linkage that is set can be either α or β , therefore we need to find a method that can allow us to form one stereoisomer or the other.
- Synthetic efficiency: we need to find a method that is less wasteful, less time-consuming and more user-friendly than a series of protections and deprotections prior to glycosylation.
- Polyglycosylation: we are aiming for conditions that will maximize the yield of the desired disaccharide, while minimizing the over-glycosylation of the starting material, leading to unwanted trisaccharides.

4.2.3 Objectives and methods

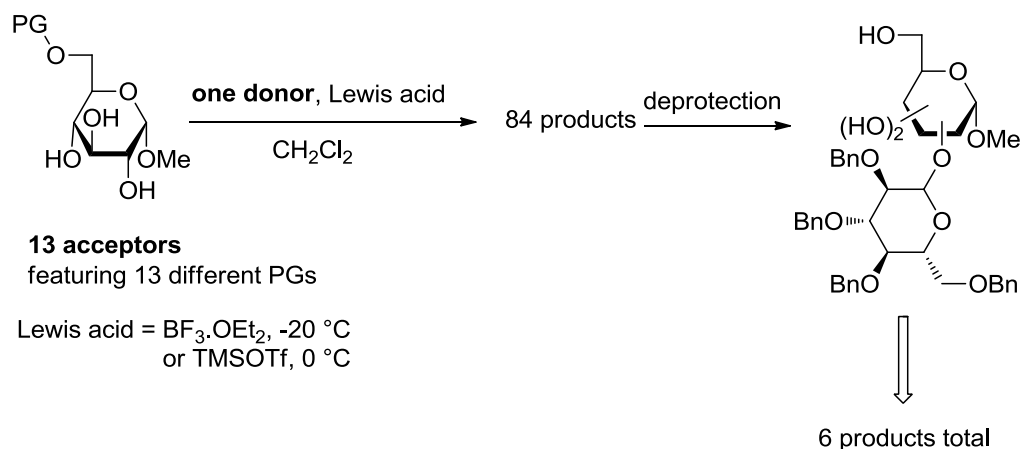
In the first part of our research to find the best method to overcome these challenges, we wanted to screen a number of protecting groups (13 total), installed at position 6 of methyl α -D-glucopyranosides, to determine which of the 6-*O*- and 4,6-*O*-protected sugars could be regioselectively glycosylated with a tetra-benzylated glucopyranose trichloroacetimidate (Scheme 4.3).



Scheme 4.3 General glycosylation reaction between 13 different glycosyl acceptors and one glycosyl donor which would lead to the formation of 84 possible disaccharides.

To this end, we prepared two series of glycosyl acceptors featuring a variety of protecting groups, installed at position 6, so that we could see the influence of these groups on subsequent glycosylation reactions. The preparation of these 6-*O*-protected glucopyranosides is described in section 4.3.1. Given that we aimed to glycosylate a total of 13 different acceptors with one donor, we expected up to 84 possible products (6 per acceptor starting material). We would then have to purify each of these products and characterize them individually. Time-wise, this was not feasible. Furthermore, the ^1H -NMR spectrum of the sugar backbone and the benzylic protons of 2,3,4,6-tetrabenzyl glucopyranose trichloroacetimidate overlap the region of the ^1H -NMR spectra of the sugar backbone of all of the 6-*O*-protected glucopyranosides which we prepared. Therefore, we could not characterize the products using 2-D NMR studies as it would be impossible for us to attribute a signal to each proton of the disaccharide with a high degree of certainty. We needed to find an efficient method to analyze all the possible products.

We devised an alternate route (Scheme 4.4) to analyze all the products of our glycosylation reactions: if, after glycosylating each of the 13 6-*O*-protected glucopyranosides, we remove the protecting groups at position 6 from the crude mixtures, we technically would be left with only 6 possible products, identical for all 13 protecting groups initially installed on the 13 acceptors.



Scheme 4.4 Revised method to screen different 6-*O*-protected glucopyranosides, first glycosylating to form potentially 84 products, then deprotecting position 6 of these to obtain only 6 possible products identical for all the reactions and which can easily be analyzed using HPLC.

These products could be analyzed using analytical HPLC, which would also allow us to determine the ratios of the 6 products in each sample of the crude mixtures. Furthermore, preparing each of the 6 possible products using typical protection and deprotection chemistry and analyzing these using analytical HPLC would allow us to also identify each of the products formed for each of our glycosylation reactions. The preparation of these 6 reference disaccharides is described in section 4.3.2.

In section 4.3.3, we explore the application and results of the strategy shown in Scheme 4.4.

4.3 Results and discussion

4.3.1 Preparation of the 6-*O*-protected glucopyranosides

We prepared the first series (4-7 to 4-14) of 6-*O*-protected methyl α -D-glucopyranosides (depicted in Figure 4.1) from commercially available reagents and using reported methods (detailed in the Experimental Section).

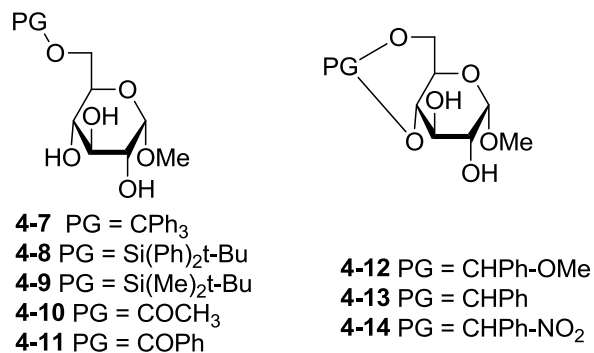


Figure 4.1 First series of 6-*O* and 4,6-*O*-protected methyl α -D-glucopyranosides. Protecting groups selected are those which carbohydrate chemists typically use.

The second series (**4-4**, **4-15** to **4-18**) included the directing-protecting groups initially designed to influence and direct functionalization reactions to either position 2 or 3 depending on the bulkiness of the reagent. This second series of 6-*O*-protected sugars featuring hydrogen-bond acceptors are shown in Figure 4.2. Each protecting group of the second series features one or two pyridyl rings able to hydrogen bond with the sugar hydroxyl at position 4, as well as at position 3 (for the di-pyridyl-based protecting group).

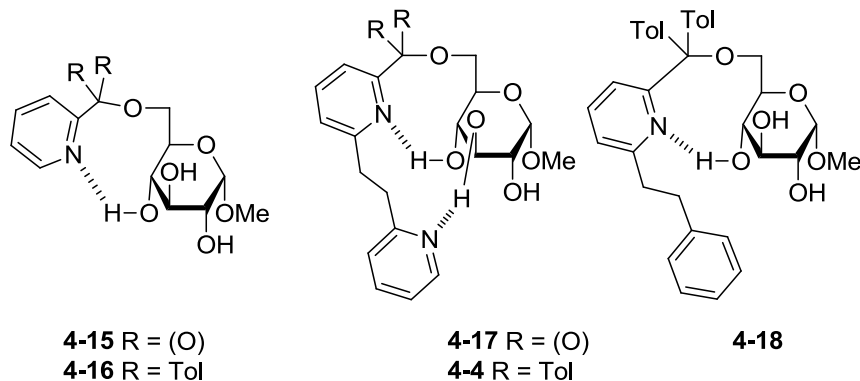
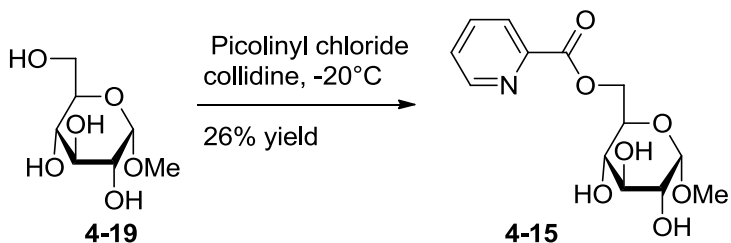
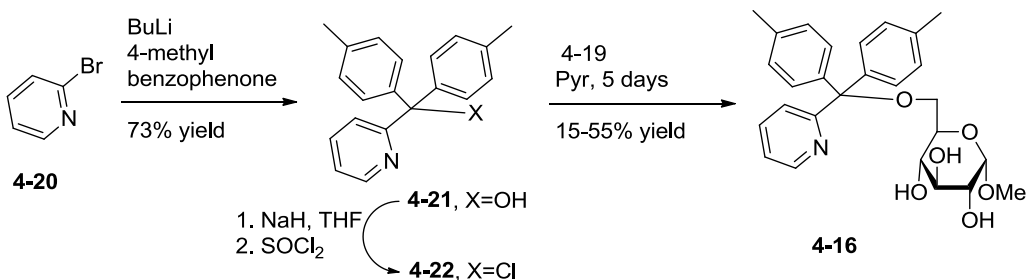


Figure 4.2 Second series of 6-*O*-protected methyl α -D-glucopyranosides. Protecting groups chosen feature one or two pyridyl ring which has been shown to hydrogen-bond with the sugar.

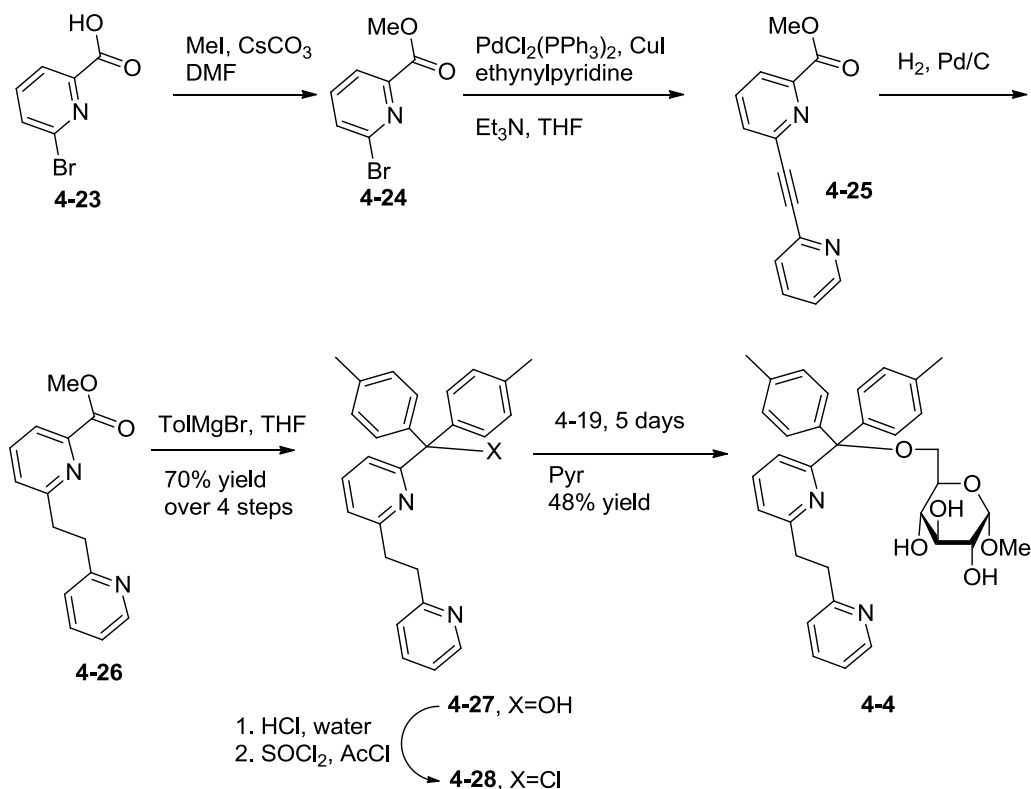
Contrary to the first series, we had to synthesize the protecting groups of the second series prior to installing them at position 6 of methyl- α -D-glucopyranoside (**4-19**).

**Scheme 4.5 Synthesis of 4-15.**

We prepared **4-15** by reacting methyl α -D-glucopyranoside (**4-19**) with commercially available picolinyl chloride (Scheme 4.5).

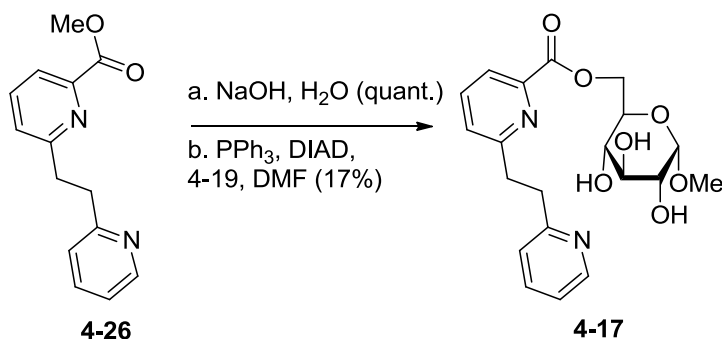
**Scheme 4.6 Synthesis of 4-16.**

To prepare **4-16**, we performed a lithium-halogen exchange between 2-bromopyridine (**4-20**) and butyllithium, rendering position 2 of the pyridine ring more nucleophilic. Then we added the corresponding lithium salt to 4,4'-dimethylbenzophenone, yielding this trityl alcohol-like group (**4-21**). We then substituted the alcohol for a chloride (**4-22**) and this trityl chloride-like group could be coupled to the sugar yielding **4-16** (15-55% yield) (Scheme 4.6).



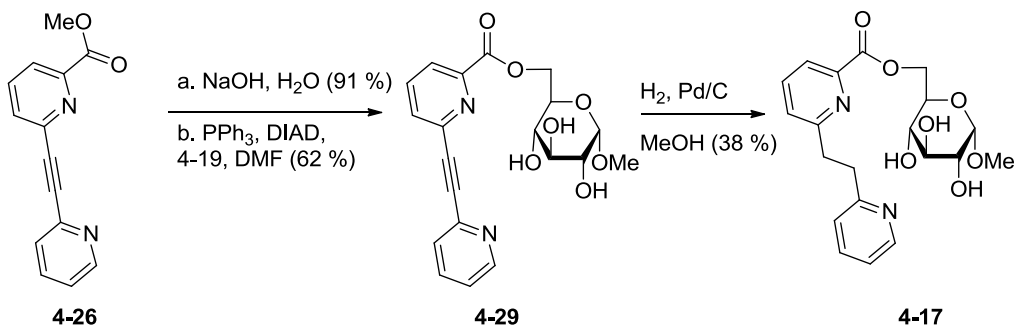
Scheme 4.7 Synthesis of 4-4.

The di-pyridyl protecting group (**4-27**) was prepared from 2-bromo-6-picolinic acid (**4-23**). We first esterified **4-23**, then performed a Sonogashira coupling to substitute the bromide with 2-ethynyl-pyridine yielding **4-25**. Then, hydrogenation of the triple bond reduced it to a flexible alkyl linker (as in **4-26**), which is necessary for the terminal pyridine to be able to interact with position 3 of the sugar. A double Grignard addition of *p*-tolylmagnesium bromide on the ester renders the protecting group (**4-27**) bulkier and more trityl-like. Finally we substituted the alcohol for a chloride which enabled us to couple it to the sugar, forming **4-4** (Scheme 4.7).



Scheme 4.8 Preparation of **4-17** via saponification of **4-26**, followed by Mitsunobu coupling to **4-19**.

Alternatively, instead of performing the double Grignard addition to yield the bulky, “trityl-like” protecting group **4-27**, we also saponified **4-26** to the corresponding acid which was then coupled to **4-19** via a Mitsunobu reaction (Scheme 4.8). However, we found that the 6-*O*-protected glucopyranoside **4-17** was not easily separated from the starting material **4-19** as both are very polar. On the other hand, separating **4-19** from **4-29** (Scheme 4.9) was easier, at which point we could reduce the alkyne of **4-29** to the corresponding flexible linker, yielding **4-17** (38% yield).

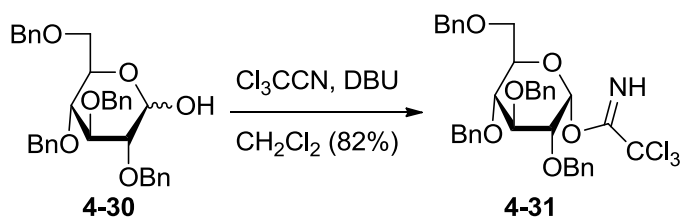


Scheme 4.9 Alternate route to **4-17**, coupling saponified **4-26** prior to reduction.

The glucopyranoside **4-18** was synthesized using the same route which we previously reported.⁵

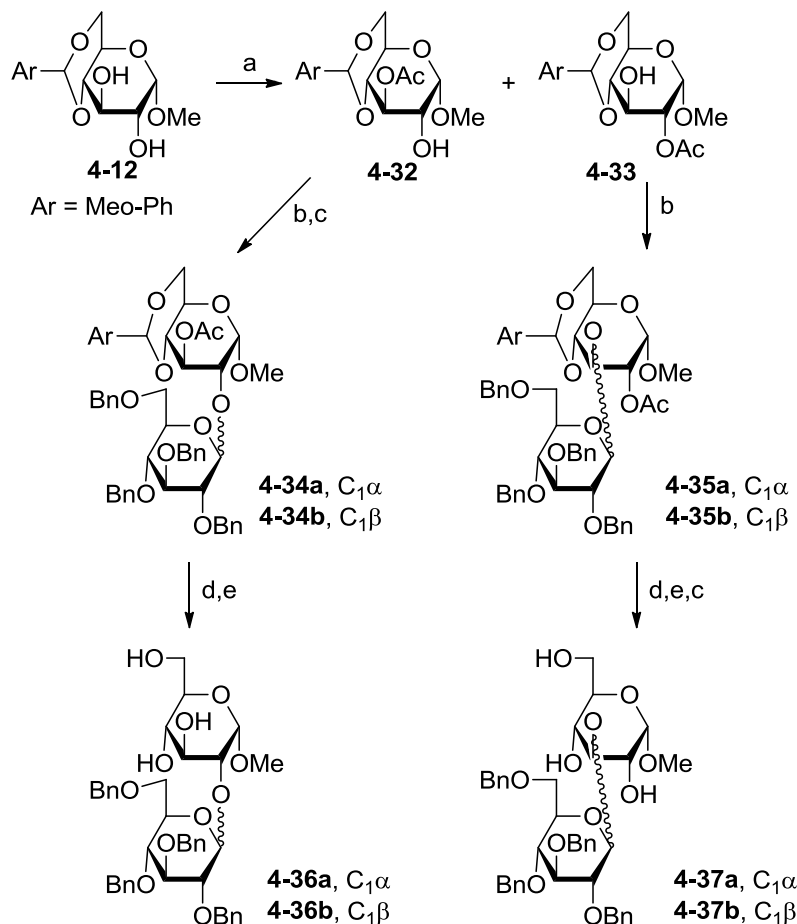
4.3.2 Preparation of the glycosyl donor and reference compounds for glycosylation

Prior to evaluating how the protecting group at position 6 influences the glycosylation reaction of these acceptors, we needed to prepare the glycosyl donor (**4-31**, Scheme 4.10) using standard procedures.⁶ We also prepared the six possible regio- and stereoisomers **4-36a/b**, **4-37a/b** and **4-41a/b**, which were needed as HPLC reference compounds (Scheme 4.11 and Scheme 4.12).



Scheme 4.10 Formation of 2,3,4,6-tetra-benzylated glucopyranose trichloroacetimidate **4-31**.

We began by first differentiating the two hydroxyl groups of **4-12** (Scheme 4.11). Mono-acetylation of **4-12** with acetic anhydride led to regioisomers **4-32** and **4-33** which we could separate by column chromatography. We then glycosylated **4-32** and **4-33** using the trichloroacetimidate donor **4-31**, yielding separable disaccharides **4-34a** and **4-34b** and non-separable disaccharides **4-35a** and **4-35b** (Scheme 4.11). Both anomers **4-34a** and **4-34b** were sequentially deprotected by hydrolysis in acidic medium and Zemplén deacetylation to give target compounds **4-36a** and **4-36b** in good yields. Similarly, the benzyldiene and the acetals of compounds **4-35a** and **4-35b** were removed yielding the corresponding separable mixture of anomers **4-37a** and **4-37b**.

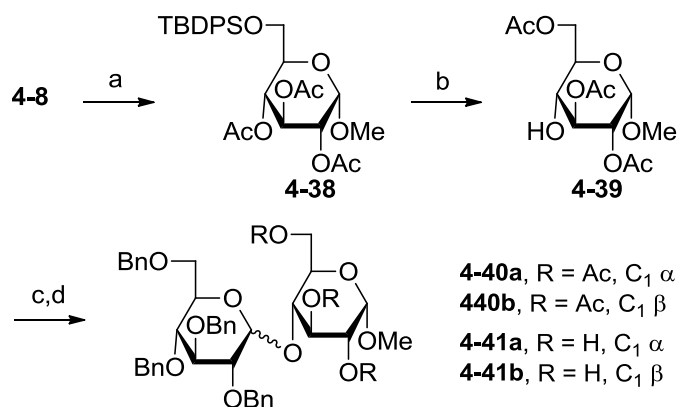


Scheme 4.11 Preparation of reference compounds 4-36a, 4-36b, 4-37a and 4-37b.

a) Ac₂O (1.1 eq.), DMAP, K₂CO₃, CH₂Cl₂, 47% (4-32), 40% (4-33); b) 2,3,4,6-tetra-*O*-benzyl glucopyranosyl trichloroacetimidate 4-31, TMSOTf, 4Å MS, CH₂Cl₂, 84% (4-34a/4-34b = 2:1), 72% (4-35a/4-35b = 2:1); c) preparative HPLC separation; d) AcOH / THF / H₂O, 1:1:1, 40°C; e) MeONa, CH₃OH, 90% (4-36a), 93% (4-36b), 93% (4-37a + 4-37b).

The last two reference compounds were prepared from readily available triacetylated glucopyranoside 4-39. As illustrated in Scheme 4.12, we peracetylated triol 4-8, reacting 4-8 with acetic anhydride in presence of DMAP yielding the fully protected monosaccharide 4-38. Triacetylated compound 4-38 was subsequently treated with a fluoride source to generate 4-39 which forms after the acetyl at position 4 migrates to position 6 (Passacantilli and co-workers' procedure⁷). Both glycosylation partners (4-31 and 4-39) were next reacted to give disaccharides 4-40a and 4-40b which were inseparable. These two fully protected compounds were subjected to Zemplén deacetylation, forming the target

disaccharides **4-41a** and **4-41b**, which unfortunately remained inseparable even after extensive chromatographic work.



Scheme 4.12 Preparation of reference compounds **4-41a** and **4-41b**.

a) Ac₂O (10 eq.), DMAP, Et₃N, CH₂Cl₂, 100%; b) TBAF, THF, 0°C then rt, 84% ; c) **4-31**, TMSOTf, 4Å MS, CH₂Cl₂, 79%; d) MeONa, CH₃OH, 91%.

Analytical HPLC conditions were found where 2, 3 and 4-glycosylated isomers (**4-36a**, **4-36b**, **4-37a**, **4-37b**, **4-41a** and **4-41b**) were clearly identified on chromatograms. In addition, the ratios of model mixtures of known composition were accurately reproduced on chromatograms with an accuracy of 0.5%. However, even if the isomers **4-36a**, **4-36b**, **4-37a** and **4-37b** were separated, the epimers **4-41a** and **4-41b** eluted with identical retention times on silica gel and reversed phase HPLC columns. Therefore, the ratio of the stereoisomers **4-41a** to **4-41b** could not be determined.

4.3.3 Regioselectivity of the glycosylation reaction with a benzylated glycosyl donor

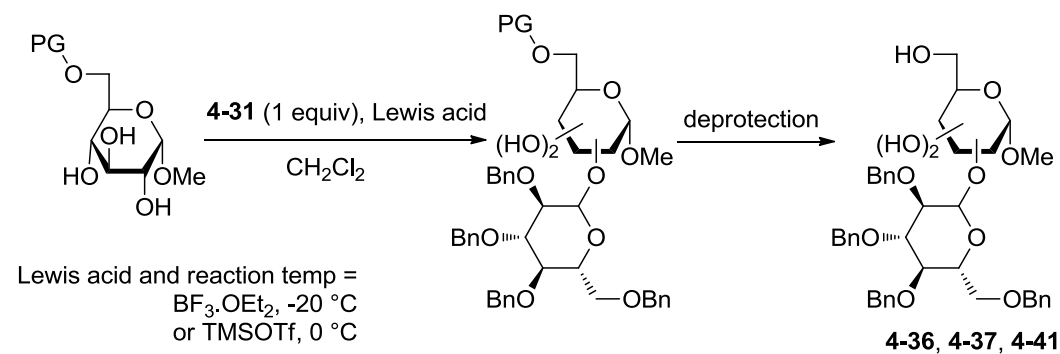
With the 13 protected glucopyranosides and the 6 reference disaccharides prepared, we were ready to investigate the influence of the protecting groups on the regioselectivity of the glycosylation reaction (Table 4.1). All the following glycosylation reactions were performed in dichloromethane, a solvent which favours hydrogen bonding and therefore may enhance the influence of the pyridyl-containing protecting groups on the regioselectivity of the reactions.

These partially protected glucopyranoside acceptors were reacted with one equivalent of glycosyl donor in presence of TMSOTf and yielded many, if not all, of the 6 possible isomers **4-36a/b**, **4-37a/b** and **4-41a/b** after deprotection (Table 4.1). Quick filtration on a silica gel pad enabled the isolation of the six expected disaccharides in combined yields of 30 to 55%. The use of a single equivalent of donor reduced the amount of trisaccharides and made our evaluation more reliable because we eliminated the formation of compounds which may interfere with our analysis. In fact, at this stage, we were looking for a regioselective reaction, and not necessarily a high yielding reaction.

As expected, we detected no trisaccharides in the reaction mixture which could have formed from di-glycosylation of the acceptors. The conversion (calculated from the amount of remaining starting material) and yields of disaccharides were equivalent, indicating that all the starting material which was consumed was transformed into disaccharides and that the steps of deprotection and filtration did not alter the ratio of regioisomers. We also observed that the benzylidene groups and the second series of hydrogen bond accepting protecting groups reduced the reactivity of the hydroxyl groups leading to the lowest conversions (**4-4** ~ 30%, **4-12-4-14** ~ 30-40%). These results are consistent with the data obtained previously with the acetylation of these protected glucopyranoside derivatives.⁵ Unfortunately, we could not use **4-17** in this experiment because it was insoluble in the reaction solvent. In fact, from some preliminary acylation experiments (unpublished work), we found that, in this same solvent, the product from mono-acetylation of **4-17** was soluble and then reacted again with the reagents used, leading to a mixture of polyacylated products and insoluble **4-17**. Given that we are trying to avoid polyglycosylation of our starting material, **4-17** was not used in this study.

We summarize the results of our first batch of experiments in Table 4.1.

Table 4.1 Regioselectivity of the glycosylation of the secondary hydroxyl groups of 4-4, 4-8-4-18.



Entry	Starting material	Protecting Group	2-OGlu 4-36a/b (%) ^{a)}	3-OGlu 4-37a/b (%) ^{a)}	4-OGlu 4-41a/b (%) ^{a)}
1	4-7	Tr	39 (1:1.1)	53 (1:4.2)	8
2	4-8	TBDPS	39 (1.0:1)	57 (1:1.4)	4
3	4-9	TBDMS	40 (1.3:1)	56 (1.1:1)	4
4	4-10	Ac	24 (1.6:1)	60 (1:1.2)	16
5	4-11	Bz	27 (1.5:1)	69 (1:1.2)	4
6	4-12	MeOPhCH	41 (1.4:1)	59 (1:1.6)	-
7	4-13	PhCH	45 (1.8:1)	55 (1:7.9)	-
8	4-14	NO_2PhCH	45 (2.2:1)	55 (1:2.1)	-
9	4-15	PyrC(O)	35 (1.1:1)	53 (1:1.2)	12
10	4-16	Pyr(Tol) ₂ C	40 (1:1.1)	56 (1:1.4)	4
11	4-4	Pyr-(CH ₂) ₂ - Pyr(Tol) ₂ C	65 (1.6:1)	33 (1.6:1)	2
12	4-18	Ph-(CH ₂) ₂ - Pyr(Tol) ₂ C	45 (1:1)	51 (2.2:1)	4

^{a)}HPLC analysis of the mixtures after filtration on a silica gel pad, α : β ratios are given in brackets.

We next analyzed the observed regioselectivities and the effect of protecting groups. In agreement with the amount of acetylation at position 2 of **4-4**, **4-7-4-18** previously reported (6 to 19%),⁵ we observed that a significant amount of glycosylation of the bulky donor **4-31** occurred at position 2 of the acceptors especially of **4-4**, forming compounds **4-36a** and **4-36b** (24 to 45%, entries 1-8) after deprotection. Furthermore, for the reaction of **4-31** with the bulky TBDPS or trityl group containing derivatives **4-7** and **4-8**, we observed 4-8% of 4-O glycosylated products **4-41a** and **4-41b**, while the small acetylated derivative **4-10** gave larger amounts of **4-41a/b** (16%, entry 4). As expected, steric effects were more prominent in the glycosylation than in the acetylation reaction. The glycosylation of the bulky donor led to increased amounts of 2-O glycosylated compounds **4-36a/4-36b** (24 to 41%, entries 1-10) relatively to the acetylation reaction (6 to 19%). Furthermore, 4-O glycosylated products were favoured when we switched from ethers (entries 1-4) to esters (entries 5, 6 and 11). The electron-donating or withdrawing groups on the benzyldiene ring also induced effects on the regioselectivity (entries 6-8) of glycosylation (**4-14** vs. **4-12**).

We were also pleased to observe the influence of the pyridyl ring of **4-16** which reduced glycosylation at position 4 (**4-7** vs. **4-16**, **4-18** and **4-4**, entries 1 and 10 to 12) while apparently not interfering with the Lewis acidic conditions required for glycosylation. This is additional proof demonstrating the strong hydrogen bond between the directing/protecting group and the hydroxyl at position 4. Even more gratifying was the reversal of selectivity observed with **4-4** (**4-36/4-37**: 65:33, entry 11) as compared to **4-16** (**4-36/4-37**: 40:56, entry 10). Position 3 is more reactive, and yet we observed glycosylation at position 2, most likely due to the hindrance of the second pyridine ring that hydrogen bonds to the hydroxyl of position 3. To prove the importance of the terminal pyridyl ring of **4-4**, the terminal phenyl analogue **4-18** was reacted under the same conditions. We expected that, in the absence of this second critical hydrogen bond, the selectivity of glycosylation of **4-18** compared to **4-4** would be affected. Indeed, once this hydrogen bond interaction was removed (entries 10 and 12), the selectivity of

glycosylation returned to a level consistent with the earlier single hydrogen bond-controlled reactions (entries 10 and 12 vs. 11). This observation demonstrates the critical role of the nitrogen of the terminal pyridyl group of **4-4** which indeed may provide bulk and block position 3 from being glycosylated.

4.3.4 Optimization of the glycosylation methodology with a benzylated glycosyl donor

Unlike other reported methods, our strategy favours glycosylation of position 2 over positions 3 and 4. To probe the applicability of this methodology towards the synthesis of large amounts of disaccharides, we further optimized the conditions to improve the regioselectivity and conversion rate of the reaction. The optimized procedure requires portionwise addition of **4-31** and TMSOTf at -50°C . Under these conditions, glycosylation of **4-4** led to 40-60% (isolated yield) of the 2-*O* glycosylated products **4-36a/b**, 8-11% of the other four possible isomers and recovered starting material. Complete conversion may have resulted in the formation of trisaccharides (uncharacterized). Interestingly, **4-16** exhibited higher di-glycosylation rates, further demonstrating the role of the terminal pyridyl ring to block positions 3 and 4 from reacting (entry 10).

We next expanded the scope of our study to other hexopyranosides having different hydrogen bond patterns, such as a β -D-glucopyranoside (**4-42**), an α -D-mannopyranoside (**4-43**) and an α -D-galactopyranoside (**4-44**) (Figure 4.3). With these extra acceptors, we also aimed to further elucidate the role of hydrogen bonds in the regioselectivity of this reaction. The derivatives **4-43** and **4-44** were prepared in one step from methyl α -D-mannopyranoside and methyl α -D-galactopyranoside.

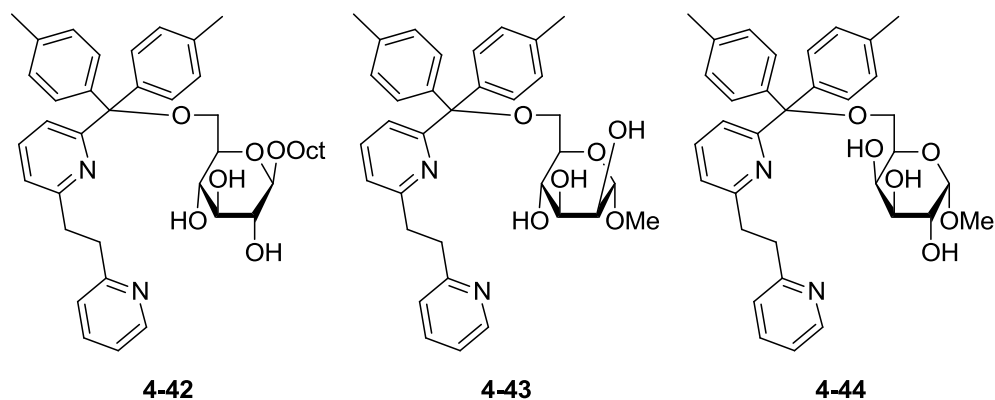
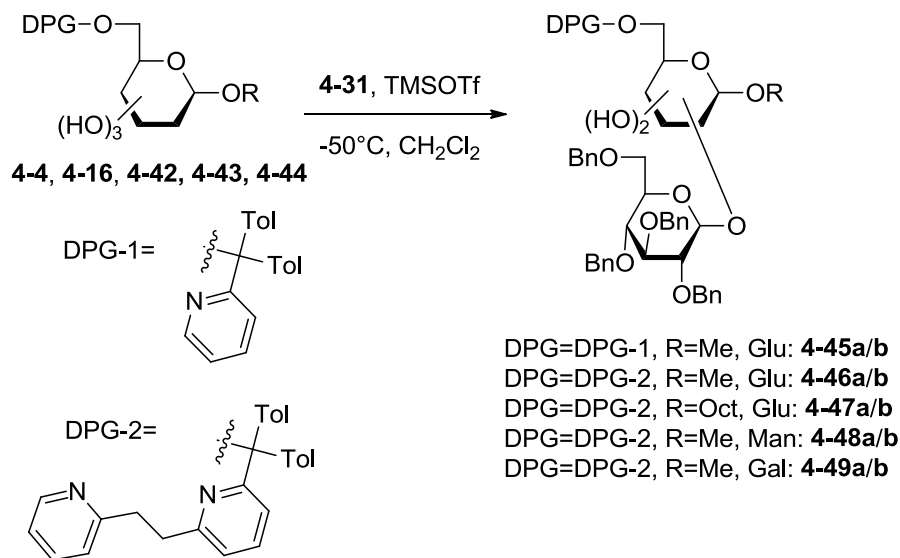


Figure 4.3 More 6-O-protected hexopyranosides to verify the scope of our method

As for the methyl α -D-glucopyranoside, the octyl- β -glucopyranoside **4-32** was glycosylated with good regioselectivity although with lower yields and conversions due to the presence of the bulky octyl group (entry 4).

As mentioned in the introduction, the Cmoch group demonstrated that they could selectively glycosylate 6-O TBDPS-protected mannopyranosides at position 3 over position 2.³ However, we expected that, as observed for the glucopyranoside derivative **4-4**, our di-pyridyl protecting group could shut down the reactivity of **4-43** leading to lower conversions (entry 5, Table 4.2). As expected, when **4-43** was reacted with an excess of **4-31** and Lewis acid, we isolated a mixture of disaccharides (41% yield), glycosylated at position 3 (entry 6), consistent with Cmoch's results. In fact, we were expecting that **4-43** would be glycosylated at position 3 over position 2 as position 2 is much less accessible for α -D-mannopyranosides.

Table 4.2 Regioselectivity of glycosylation of the secondary hydroxyl groups of 4-4, 4-16, 4-42, 4-43 and 4-44. *

Entry	Starting material	2-O	% 2-O ^a)	% 3-O ^a)	% SM
1	4-16^c	4-45a/b	13-28 (1:7.7)	28-37 (1:5.1)	0-34
2	4-4	4-46a/b	47 (1:1.5)	8 (1:1.8)	41
3	4-4	4-46a/b	57-61 (1:1.5-1.8)	9-11 (1:1.4-1.9)	0-8
4	4-42	4-47a/b	28 (1.5:1)	nd ^b)	50
5	4-43^d	4-48a/b	-	-	>90
6	4-43	4-48a/b	nd ^b)	41 (1.2:1)	52
7	4-44	4-49a/b	Complex mixture		

^a α:β ratios are given in brackets. ^b not determined (<10%). ^c ran at -70°C. ^d reacted with one equivalent of **4-31**. * 1,4-glycosylation products were not determined in any of the entries.

While the hydrogen bond network observed in the mannose derivative **4-43** is similar enough to that of the glucopyranoside derivatives **4-16**, **4-4** and **4-42**, experimental evidence indicate that the hydroxyl at position 3 of the galactose derivative **4-44** is not hydrogen bonding with the di-pyridyl protecting group. As a result, the regioselectivity drops with **4-44** and a complex mixture of isomers

(recovered **4-44** and disaccharides) is produced (i.e., lower regioselectivity) (entry 7).

4.4 Postulated mechanism

With our mono-pyridyl-based protecting groups, which can be selectively installed at position 6, we have observed that the 4-OH is less reactive, while the adjacent 3-OH is more reactive. Glycosylation is directed to position 3. We can also seek out position 2 by using a protecting group with two pyridine rings, one to hydrogen-bond to the 4-OH and the other to the 3-OH. With this di-pyridyl protecting group, glycosylation at the position 2-OH is now favoured. Our hydrogen bond-accepting protecting groups operate by modifying the intramolecular hydrogen bond network observed in non protected carbohydrates. Clearly, we observed preference for the two 2-O glycosylated isomeric disaccharides (more than 80% of the 6 possible isolated isomers) when a bulky glycosyl donor was used, while 3-O isomers were predominant when using a smaller reagent (like with acetylating reagents as previously reported).

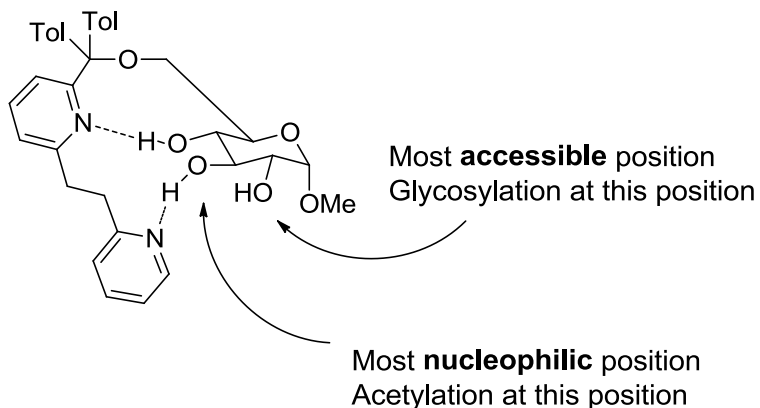
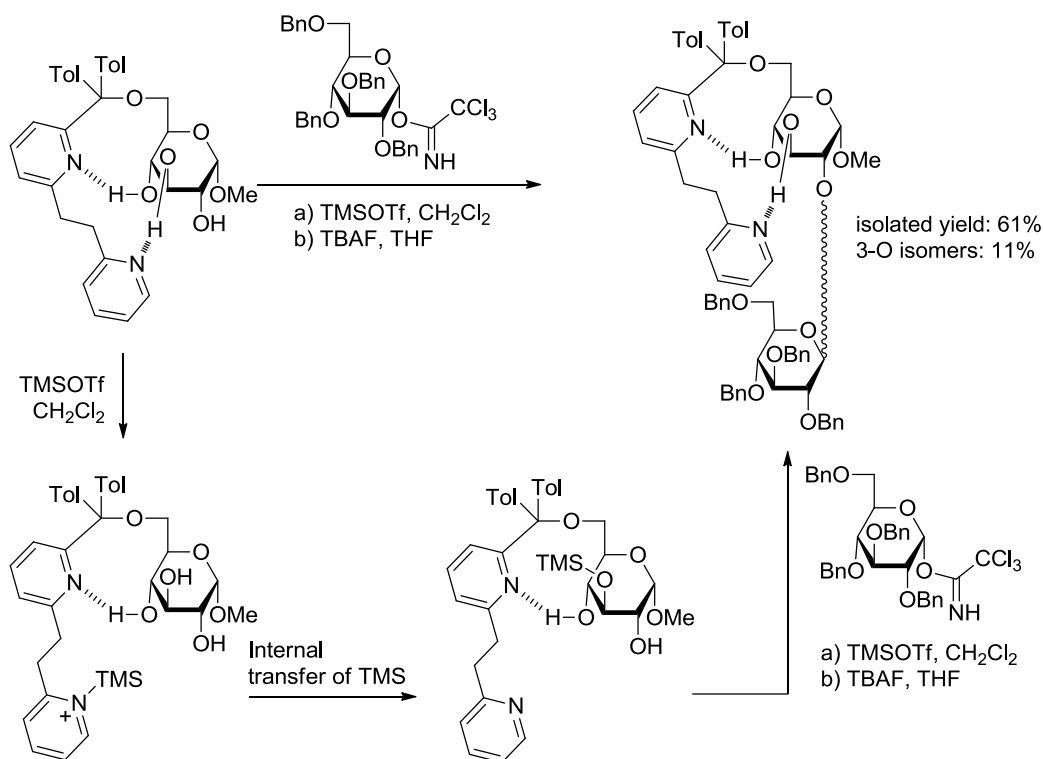


Figure 4.4 The influence of the di-pyridyl-based protecting group on the regioselectivity of reactions.

This study demonstrates that these pyridyl-based protecting groups can be used in different ways (Figure 4.4) as they enhance the nucleophilicity of hydroxyl groups (increase selectivity for the acetylation at position 3) but also the steric hindrance around selected hydroxyls (increased steric bulk around the 3-OH

reduces its accessibility to bulky reagents such as glycosyl donors, while position 2 is free to react with bulky reagents).

Interestingly, unlike for all the 6-*O*-protected glucopyranosides from our first series (**4-7** to **4-14**), we found that we had to treat the crude mixtures with TBAF after glycosylating the 6-*O*-pyridyl-protected glucopyranosides because a fraction of the products seemed to bear TMS protections (based on NMR analysis of the crude mixtures). Therefore, we propose two possible mechanisms for the glycosylation reaction which could explain why glycosylation at position 2 is favoured (Scheme 4.13).



Scheme 4.13 Postulated mechanisms.

The first possibility is that the TMSOTf activation of the trichloroacetimidate is slow and therefore, prior to this, the terminal-pyridyl reacts with the TMSOTf. This TMS-pyridine can therefore transfer its TMS group to the sugar, most likely at position 3, thereby blocking the 3-OH from reacting further. The only available position at this point would be position 2. Alternately, if activation of the trichloroacetimidate donor is fast enough, this step will occur first, and this

activated donor will quickly react at the most accessible position, in other words position 2. The remainder of the TMSOTf could react with the disaccharide. In both cases, the products would bear one or more TMS groups, requiring an extra step of TBAF-mediated deprotection to remove them. From this work, we cannot confirm which of these two mechanisms actually occurs. Furthermore, although our method is regioselective as our starting materials are mainly glycosylated at position 2 (or 3 in the case of the mannopyranoside used), our method is not yet stereoselective, in that we obtain a mixture of α - and β -linked disaccharides. We could improve this method by switching the glycosyl donor from a 2,3,4,6-tetra-benzylated donor to a 2,3,4,6-tetra-benzoylated group of which the stereochemistry at position 2 of the donor has been shown to influence the stereochemistry of the glycosidic linkage formed.

In this Chapter, our major goal was to assess the effects of protecting groups on the regioselectivity of glycosylation reactions. Our strategy relied on a deprotection step prior to the analysis of the regioisomer mixtures. This deprotection was intended to remove the protecting group at position 6 while not removing the protecting groups (benzyl ethers) of the donor. This strategy could not be applied to benzoylated donors as benzoyl groups would have been cleaved while removing the protecting groups at position 6 of the 13 acceptors. At this stage, as the effect of pyridyl-containing protecting groups is demonstrated and regioselectivity is achieved, we turned our attention to a more efficient and stereoselective approach. In Chapter 5, we will present our results for the glycosylation of a small series of sugar acceptors with a 2,3,4,6-tetra-benzoylated glucopyranose trichloroacetimidate.

4.5 Conclusion

With the goal of rendering sugars more accessible as starting materials for chemists, we developed a protecting group that can be installed at position 6 of a variety of sugars and that bears two pyridyl rings. Through its ability to hydrogen bond with positions 3 and 4 of the sugar it is attached to, this protecting group

renders position 3 more nucleophilic, but also less accessible to larger reagents. For this reason, with small reagents, position 3 is functionalized, while with larger reagents, such as a glycosyl donor, position 2 is functionalized. This protecting group allowed us to regioselectively glycosylate methyl 6-*O*-protected- α -d-glucopyranoside at position 2 (58-61% yield), producing a mixture of α and β anomers (1:1.5-1.8). To our knowledge none of the other reported method can so easily favour position 2 of glucopyranosides over position 3. The results of this chapter present another line of evidence that protecting-directing groups are a valuable tool for regioselective functionalization of sugars.

4.6 Experimental section

4.6.1 General remarks

Solvents were distilled and dried by standard methods; THF and ether, from Na/benzophenone; and CH₂Cl₂ from P₂O₅. All commercially available reagents were used without further purification. 4 Å molecular sieves were dried at 100°C prior to use. Melting points are uncorrected and recorded with a Büchi capillary tube melting-point apparatus. Optical rotations were measured on a Perkin Elmer 141 polarimeter in a 1 dm cell at 20°C or a JASCO DIP 140 in a 1dm cell at 20°C. FTIR spectra were recorded on a Perkin Elmer Spectrum 1000 on NaCl windows or KBr pellets or using a Perkin Elmer Spectrum One FT-IR. ¹H and ¹³C NMR spectra were recorded on Bruker AC 250 (250 MHz) or DRX 400 (400 MHz) and Varian mercury 400 MHz, 300 MHz or Unity 500 spectrometers. Chemical shifts are reported in ppm using the residual of chloroform as internal standard (7.260 ppm for ¹H and 77.16 ppm for ¹³C). Mass spectra were recorded on either a Trio 1000 Thermo Quest spectrometer in the electron impact mode or a Platform Micromass in the electrospray mode or EI Peak matching (70 eV) on a Kratos MS25 RFA Double focusing mass spectrometer or by ESI on a IonSpec 7.0 tesla FTMS at McGill University. Elemental analyses were obtained on a Perkin Elmer 240C microanalyser. Analytical thin-layer chromatography was

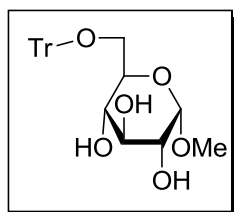
performed on Merck 60F254 pre-coated silica gel plates. TLC visualization was performed by UV or by development using KMnO_4 , $\text{H}_2\text{SO}_4/\text{MeOH}$ or Mo/Ce solutions. Chromatography was performed on silica gel 60 (230-40 mesh). Analytic reverse phase HPLC was performed on two C18 columns: Kromasyl C18 10 μm , from A.I.T. Chromato (Le Mesnil le Roi, France) and Platinum C18 10 μm , from Alltech (Laarne, Belgium). A flow rate of 1.0 mL min^{-1} was used with a mobile phase of $\text{CH}_3\text{CN}/\text{H}_2\text{O}$ (gradient A: 50%-70% within 45 min., gradient B: 70-90% within 40 min.). UV detection was monitored at 254 nm.

4.6.2 Synthesis

Synthesis of the first series of 6-*O*-monoprotected carbohydrates⁵

Methyl 6-*O*-trityl- α -D-glucopyranoside (4-7)

To a solution of glucopyranoside **4-19** (5.1 g, 0.026 mol) in pyridine (50 mL), was added DMAP (30 mg, 0.25 mmol) and trityl chloride (7.2 g, 0.026 mol). The resulting mixture was stirred for 3 days, then concentrated *in vacuo*, redissolved in CH_2Cl_2 , washed with water and brine, dried over Na_2SO_4 , filtered and concentrated *in vacuo*. The residue was purified by column chromatography (CH_2Cl_2 , then $\text{CH}_2\text{Cl}_2/\text{MeOH}$, 19:1) to give **4-7** as a white solid (7 g, 61 %).



$\text{C}_{26}\text{H}_{28}\text{O}_6$; Mol. Wt. = 436.50

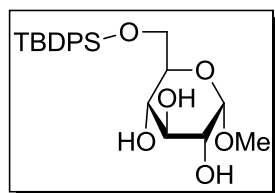
$R_f = 0.3$ ($\text{CH}_2\text{Cl}_2/\text{CH}_3\text{OH}$, 9:1)

^1H NMR (300 MHz, CDCl_3) δ 7.48-7.20 (m, 20H), 4.77 (d, $J = 3.8$, 1H), 3.67 (dt, $J = 6.7, 7.6$, 2H), 3.50 (ddd, $J = 5.3, 8.8, 13.3$, 3H), 3.42 (d, $J = 2.7$, 3H), 3.41-3.31 (m, 2H).

Methyl 6-*O*-*t*-butyl-diphenylsilyl- α -D-glucopyranoside (4-8)

To a solution of glucopyranoside **4-19** (2.0 g, 0.01 mol) in DMF (20 mL) was added TBDPSCl (2.7 mL, 0.01 mol) and imidazole (2.25 g, 0.03 mol). After

stirring overnight, the solution was concentrated *in vacuo*. The residue was redissolved in CH₂Cl₂, washed with water, brine, dried over Na₂SO₄, filtered, concentrated *in vacuo* to give **4-8** as a white solid after washing with hexanes (3.6 g, 80% yield).



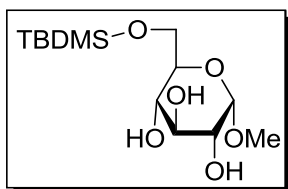
C₂₃H₃₂O₆ ; Mol. Wt. = 432.58

R_f = 0.7 (CH₂Cl₂/CH₃OH, 9:1)

¹H NMR (400 MHz, CDCl₃) δ 7.69 (ddd, *J* = 1.6, 6.2, 7.9, 4H), 7.50-7.35 (m, 6H), 4.74 (d, *J* = 3.8, 1H), 3.88 (d, *J* = 4.5, 2H), 3.72 (t, *J* = 8.9, 1H), 3.66-3.55 (m, 2H), 3.51 (dd, *J* = 3.9, 9.5, 1H), 3.43-3.34 (m, 3H), 1.10-1.01 (s, 9H).

Methyl 6-*O*-*t*-butyl-dimethylsilyl-α-D-glucopyranoside (**4-9**)

To a solution of glucopyranoside **4-19** (5.0 g, 0.024 mol) in DMF was added DMAP (30 mg, 0.25 mmol), Et₃N (4.3 mL, 0.03 mol) and TBDMSCl (4.3 g, 0.029 mol) at 0 °C. The solution was stirred for 3 days, then concentrated *in vacuo*, washed with water and brine, dried over Na₂SO₄, filtered and concentrated *in vacuo*. The residue was purified by column chromatography (CH₂Cl₂, then CH₂Cl₂/MeOH, 19:1) to yield **4-9** as a white powder (2.8 g, 38 % yield).



C₁₃H₂₈O₆Si ; Mol. Wt. = 308.44

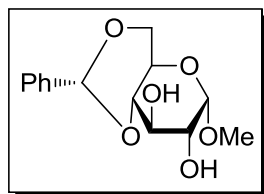
R_f = 0.5 (CH₂Cl₂/CH₃OH, 9:1)

¹H NMR (400 MHz, CDCl₃) δ 4.75 (d, *J* = 3.8, 1H), 3.85 (qd, *J* = 4.9, 10.6, 2H), 3.74 (t, *J* = 9.1, 1H), 3.60 (dt, *J* = 4.8, 9.8, 1H), 3.53 (t, *J* = 9.1, 2H), 3.42 (s, 3H), 0.90 (s, 9H).

Methyl 4,6-*O*-benzylidene-α-D-glucopyranoside (**4-13**)

To a solution of glucopyranoside **4-19** (5.0 g, 0.026 mol) in DMF (40 mL) was added benzaldehyde dimethyl acetal (4.6 mL, 0.031 mol) and CSA (0.6 g, 2.6

mmol). The solution was stirred at rt for 2 days, then concentrated *in vacuo* to yield **4-13** (quant. yield).



$C_{14}H_{18}O_6$; Mol. Wt. = 282.29

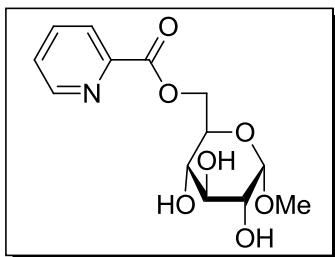
$R_f = 0.2$ (H/Ea, 3:7)

1H NMR (400 MHz, $CDCl_3$) δ 4.75 (d, $J = 3.8$, 1H), 3.85 (qd, $J = 4.9, 10.6$, 2H), 3.74 (t, $J = 9.1$, 1H), 3.60 (dt, $J = 4.8, 9.8$, 1H), 3.53 (t, $J = 9.1$, 2H), 3.42 (s, 3H), 0.90 (s, 9H).

Synthesis of the second series of 6-O-monoprotected carbohydrates⁵

Methyl 6-O-picolinyl α -D-glucopyranoside (4-15)

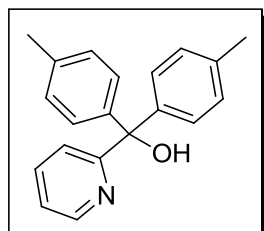
Following the same procedure as reported.



$C_{25}H_{27}NO_6$; Mol. Wt. = 437.48

Methyl 6-O-(di-*p*-tolyl-(2-pyridyl)methanol) (4-21)

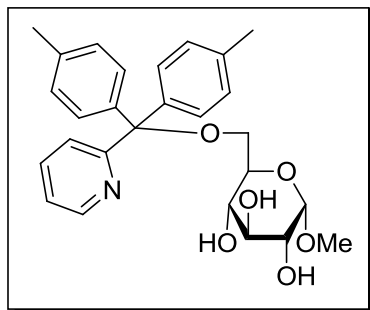
Following the same procedure as reported, from **4-20** and 4,4'-dimethylbenzoylphenone.



$C_{20}H_{19}NO$; Mol. Wt. = 289.37

Methyl 6-O-(ditolyl-(2-pyridyl)methyl) α -D glucopyranoside (4-16)

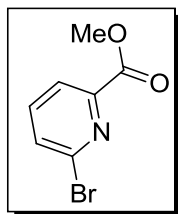
Following the same procedure as reported, from **4-21** and **4-19**.



$C_{13}H_{12}N_2O_2$; Mol. Wt. = 228.25

2-bromopicolinic acid methyl ester (**4-24**)

To a solution of 6-bromopicolinic acid (5.3 g, 0.026 mol) in DMF was added $CsCO_3$ (16 g, 0.05 mol) and iodomethane (2 mL, 0.045 mol). The resulting solution was stirred at rt, overnight, then filtered through Celite and concentrated *in vacuo*. The resulting residue was redissolved in EtOAc and washed with water and brine, dried over Na_2SO_4 , filtered, concentrated *in vacuo* to yield **4-24** as a white solid used directly in the next step.



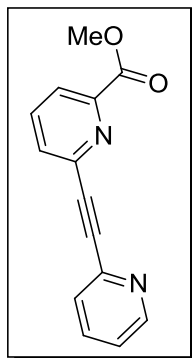
$C_7H_6BrNO_2$; Mol. Wt. = 216.03

$R_f = 0.8$ (EA)

1H NMR (200 MHz, $CDCl_3$) δ 8.09 (d, $J = 4.0, 8.0$, 1H), 7.78- 7.60 (m, 2H), 3.96 (s, $J = 18.3$, 3H).

6-Pyridin-2-yl-ethynyl-pyridine-2-carboxylic acid methyl ester (**4-25**)

To a solution of bromopicolinic acid methyl ester **4-24** (0.026 mol) and 2-ethynylpyridine (3.09 g) in Et_3N /THF (1:1, 120 mL) were added copper iodide (35 mg, 0.17 mmol) and $PdCl_2(PPh_3)_2$ (702 mg, 1.0 mmol). The resulting mixture was heated to 60 °C and stirred for 2 h. The solid suspension was filtered through Celite, concentrated *in vacuo* to yield **4-25** as a brown oil used directly in the next step.



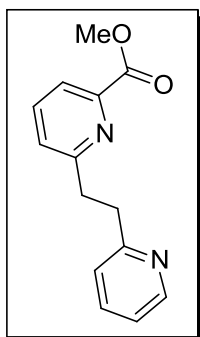
$C_{14}H_{10}N_2O_2$; Mol. Wt. = 238.24

$R_f = 0.25$ (EA)

1H NMR (400 MHz, $CDCl_3$) δ 8.71-8.60 (m, $J = 5.1, 10.3$, 1H), 8.12 (dd, $J = 1.0, 7.8$, 1H), 7.87 (t, $J = 7.8$, 1H), 7.83-7.76 (m, 1H), 7.74-7.60 (m, 2H), 7.34-7.28 (m, 1H), 4.02 (s, 3H).

6-Pyridin-2-yl-ethyl-pyridine-2-carboxylic acid methyl ester (4-26)

A suspension of the ester **4-25** (0.026 mol) and 10% Pd/C (10 g) in methanol was stirred for 24 h under hydrogen. Argon was bubbled through the solution, which was then diluted with CH_2Cl_2 , filtered through Celite and concentrated *in vacuo* to yield **4-26** which was used in the next step without further purification.



$C_{14}H_{14}N_2O_2$; Mol. Wt. = 242.27

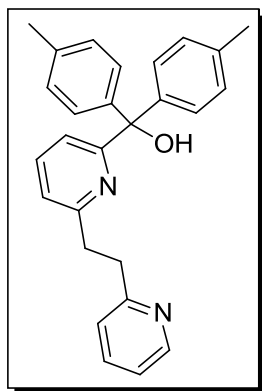
$R_f = 0.4$ (EA)

1H NMR (200 MHz, $CDCl_3$) δ 8.55 (d, $J = 4.9$, 1H), 7.96 (d, $J = 7.7$, 1H), 7.79-7.38 (m, 3H), 7.21-7.02 (m, 2H), 4.01 (s, 3H), 3.31 (dd, $J = 7.2, 16.2$, 4H).

Methyl 6-O-[6-(2-pyridin-2-yl-ethyl)-pyridin-2-yl]-di-*p*-tolyl-methanol (4-27)

To a solution of **4-26** in THF (0.026 mol) was added dropwise *p*-tolylmagnesium bromide (57 mL, 1M in THF) at 0 °C.. The solution was slowly warmed to rt and stirred overnight, then quenched with saturated NH_4Cl , diluted with $CHCl_3$, and

washed with saturated NaHCO_3 , water and brine. The organic extracts were dried over Na_2SO_4 , filtered, concentrated *in vacuo*. The residue was purified by column chromatography (H/EA, 7:3) to yield **4-27** as a brown oil (7.0 g, 70% yield over 4 steps).



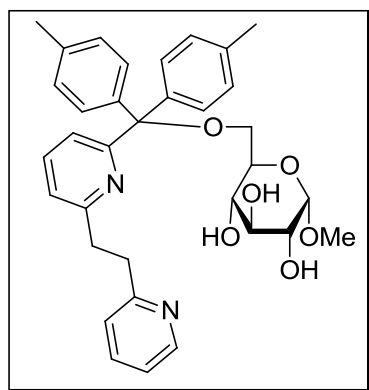
$\text{C}_{27}\text{H}_{26}\text{N}_2\text{O}$; Mol. Wt. = 394.51

$R_f = 0.74$ (H/EA, 1:1)

^1H NMR (200 MHz, CDCl_3) δ 8.53 (d, $J = 4.6$, 1H), 7.50 (t, $J = 7.7$, 2H), 7.21-7.00 (m, 14H), 2.34 (s, 6H).

Methyl 6-*O*-[6-(2-pyridin-2-yl-ethyl)-pyridin-2-yl]-di-*p*-tolyl-methyl- α -D-glucopyranoside (4-4)

A solution of **4-27** in water (32 mL) and HCl (3.6 mL) was heated at 100 °C for 1 h, then concentrated *in vacuo*, rinsed with toluene and concentrated again. The resulting brown residue (**4-28**) was redissolved in AcCl (7.2 mL) and SOCl_2 (10.8 mL) and stirred for 2 days at rt, then concentrated *in vacuo*, rinsed with toluene and concentrated again to yield a beige foam. To this foam was added a solution of glucopyranoside **4-19** (3.1 g, 0.016 mol) in pyridine (70 mL). The resulting mixture was stirred for 5 days, then concentrated *in vacuo*, redissolved in CH_2Cl_2 and washed with water and brine, dried over Na_2SO_4 , filtered, concentrated *in vacuo*. The residue was purified by column chromatography to yield **4-4** as a beige foam (1.1 g, 48% yield).



$C_{34}H_{38}N_2O_6$; Mol. Wt. = 570.68

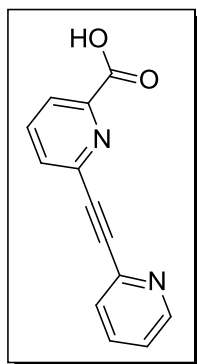
$R_f = 0.4$ (CH_2Cl_2/CH_3OH , 9:1)

1H NMR (500 MHz, $CDCl_3$) δ 8.59-8.53 (m, 1H), 7.54 (ddd, $J = 3.4, 7.2, 12.6$, 2H), 7.37 (d, $J = 8.3$, 2H), 7.27 (s, 1H), 7.24 (d, $J = 8.1$, 1H), 7.11 (dd, $J = 8.5, 16.0$, 7H), 7.04 (d, $J = 7.5$, 1H), 4.70 (d, $J = 3.9$, 1H), 3.92 (t, $J = 9.0$, 1H), 3.88-3.79 (m, 2H), 3.64 (dd, $J = 3.8, 9.1$, 1H), 3.35 (s, 3H), 3.30-3.22 (m, 2H), 3.23-3.12 (m, 2H), 2.35 (s, 3H), 2.32 (s, 3H).



6-Pyridin-2-yl-ethyl-pyridine-2-carboxylic acid

To a solution of NaOH (0.457 g, 11.4 mmol) in $H_2O/MeOH$ (2.5:1, 43 mL,) was added 6-Pyridin-2-ylethynyl-pyridine-2-carboxylic acid methyl ester (0.908 g, 3.81 mmol) at 0 °C. The solution was stirred for 2h and then the product was precipitated from solution by acidifying to pH 2 with 5% HCl aqueous. The precipitate is vacuum filtered, washed with H_2O and co evaporated with toluene to give a yellow powder (90.4% yield).



$C_{13}H_8N_2O_2$; Mol. Wt. = 228.25

$R_f = 0.0$ (EA)

IR (cm^{-1}): 1683

^1H NMR (400 MHz, CDCl_3) δ 8.68 (d, $J=4.8$, 1H), 8.21 (d, $J=7.8$, 1H), 7.97 (t, $J=7.8$, 1H), 7.84 (d, $J=7.8$, 1H), 7.76 (t, $J=7.7$, 1H), 7.64 (d, $J=7.1$, 1H), 7.37 – 7.32 (m, 1H).

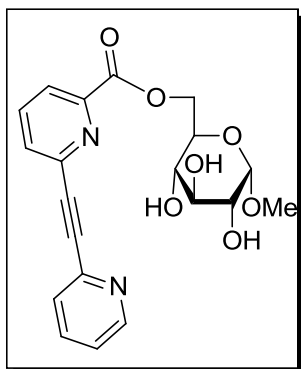
^{13}C NMR (500MHz, DMSO) δ 165.50, 150.47, 150.38, 149.20, 141.35, 141.24, 138.36, 136.96, 130.40, 127.81, 124.63, 124.28.

HRMS (EI+) calc'd for $[\text{C}_{13}\text{H}_8\text{N}_2\text{O}_2 + \text{H}]^+$: 225.06585. Found: 225.06551.



Methyl 6-O [6-pyridin-2-yl-ethynyl-pyridine-2-carboxylate] α -D-glucopyranoside (4-29)

To a solution containing 6-Pyridin-2-ylethynyl-pyridine-2-carboxylic acid (0.156 g, 0.696 mmol), **4-19** (0.135 g, 0.696 mmol) and PPh_3 (0.365 g, 1.392 mmol) in DMF (11 mL) at 0°C was added DIAD (0.273 mL, 1.392 mmol). The mixture was slowly warmed to rt, stirred for 3 days, then concentrated *in vacuo*. The residue is purified by chromatography to yield **4-29** as a light yellow foam (5% MeOH in DCM then 6%) (61.7% yield).



$\text{C}_{20}\text{H}_{24}\text{N}_2\text{O}_7$; Mol. Wt. = 404.41

R_f = 0.45 ($\text{CH}_2\text{Cl}_2/\text{CH}_3\text{OH}$, 9:1)

IR (cm^{-1}): 3403 (broad), 1732

$[\alpha]_D = +69.2$ (c 0.11, CH_3OH)

^1H NMR (400 MHz, CDCl_3) δ 8.64 (s, 1H), 8.06 (d, $J=7.6$, 1H), 7.86 (t, $J=7.6$, 1H), 7.74 (dd, $J=7.6$, 15.3, 2H), 7.63 (d, $J=7.6$, 1H), 7.34-7.28 (m, 1H), 4.75 (s, 1H), 4.66 (s, 2H), 4.59 (s, 1H), 3.89 (s, 2H), 3.63 (s, 3H), 3.39 (s, 3H).

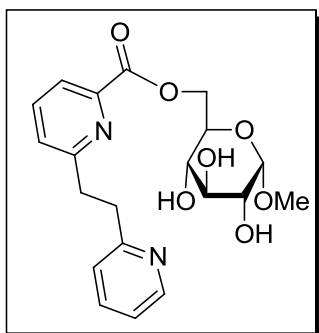
^{13}C NMR (300MHz, CDCl_3) δ 164.15, 150.04, 148.16, 142.64, 141.82, 137.68, 136.65, 130.89, 127.97, 124.82, 123.86, 99.61, 88.71, 87.29, 74.04, 71.97, 70.344, 69.57, 65.15, 55.16.

HRMS (EI+) calc'd for $[\text{C}_{20}\text{H}_{20}\text{N}_2\text{O}_7 + \text{Na}]^+$: 423.11627. Found: 423.11664.



Methyl 6-O [6-pyridin-2-yl-ethyl-pyridine-2-carboxylate] α -D-glucopyranoside (4-17)

To a solution of **4-29** (1.08 g, 2.70 mmol) in MeOH (50mL) was added Pd 10wt% on activated carbon (1.031 g) and H₂ for 6h. The solution was quenched with CH₂Cl₂ and filtered through Celite. The residue was purified by column chromatography (CH₂Cl₂/CH₃OH, 95:5 to 94:6) to yield **4-17** as a white powder (0.421 g, 38.7%)



C₂₀H₂₄N₂O₇ ; Mol. Wt. = 404.41

R_f = 0.2 (CH₂Cl₂/CH₃OH, 9:1)

IR (cm⁻¹): 3369 (broad), 1732

[α]_D = +75.9 (c 0.11, CH₃OH)

¹H NMR (400 MHz, CDCl₃) δ 8.49 (s, 1H), 7.87 (d, *J*=7.6, 1H), 7.70-7.56 (m, 2H), 7.51 (s, 1H), 7.44 (s, 1H), 7.10 (dd, *J*=7.3, 11.4, 1H), 4.73 (s, 1H), 4.67-4.49 (m, 2H), 3.93-3.77 (m, 2H), 3.55 (s, 2H), 3.37 (s, 3H), 3.31-3.13 (m, 4H)

¹³C NMR (300MHz, CDCl₃) δ 164.95, 161.46, 160.29, 148.81, 147.08, 137.39, 136.80, 126.58, 123.20, 122.84, 121.40, 99.53, 73.89, 71.86, 70.30, 69.53, 64.82, 55.02, 49.95, 37.67, 37.58.

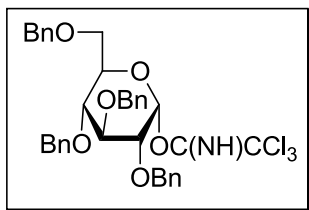
HRMS (EI⁺) calc'd for [C₂₀H₂₄N₂O₇ + H]⁺: 405.16563. Found: 405.16564.



Synthesis of the glycosyl donor

2,3,4,6-tetra-*O*-benzyl α -D-glucopyranosyl trichloroacetimidate(**4-31**)⁶

To a solution of 2,3,4,6-tetra-*O*-benzyl α/β -D-glucopyranose **4-30** (2.02 g, 0.0037 mol) in CH₂Cl₂ (60 mL) was added trichloroacetonitrile (3.2 mL, 0.032 mol) and DBU (16 drops). The resulting yellow solution was stirred at room temperature overnight, then concentrated *in vacuo*. The residue was purified by column chromatography (Tol/EA/Et₃N, 200:5:2) to yield the trichloroacetimidate as a colorless oil (2.12 g, 82% yield).



$C_{36}H_{36}Cl_3NO_6$, Mol. Wt. = 685.03

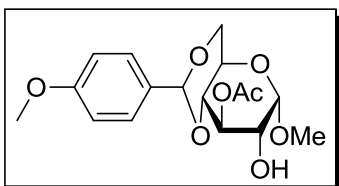
$R_f = 0.8$ (Tol/EA, 9:1)

1H NMR (400 MHz, $CDCl_3$) δ 8.61 (s, 1H), 7.39-7.28 (m, $J = 5.1, 13.4$, 22H), 7.24-7.14 (m, 3H), 6.57 (d, $J = 3.3$, 1H), 4.98 (t, $J = 8.6$, 1H), 4.89 (q, $J = 11.2$, 3H), 4.81-4.67 (m, 2H), 4.58 (dt, $J = 12.2, 15.4$, 4H), 4.13-3.97 (m, 2H), 3.88-3.74 (m, 4H), 3.70 (d, $J = 10.8$, 2H).

Synthesis of reference compounds

Methyl 3-*O*-acetyl-para-methoxy-4,6-*O*-benzylidene α -D glucopyranoside (4-32) and Methyl 2-*O*-acetyl-para-methoxy-4,6-*O*-benzylidene α -D glucopyranoside (4-33)

To a suspension of **4-12** (2.15 g, 6.9 mmol) and K_2CO_3 (4.4 g, 32 mmol) in CH_2Cl_2 (400 mL) was added acetic anhydride (0.78 mL, 8.3 mmol) and DMAP (77 mg, 1.4 mmol). After stirring for 5 h, the reaction mixture was concentrated and the resulting mono- and diacetylated compounds were separated (silica gel, H/EA, 4:1 then 3:2) to afford isomers **4-32** (1.15 mg, 47%, white crystals) and **4-33** (991 mg, 40%, white powder) along with the diacetylated compound (344 mg, 12%).



$C_{11}H_{19}NO_4$; Mol. Wt. = 229.27

$R_f = 0.24$ (H/EA, 1:1)

$[\alpha]_D = +92.8$ (c 0.9, $CHCl_3$)

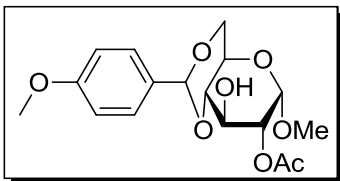
mp: 175°C

IR (neat/NaCl): 3474, 1741 cm^{-1}

Data for **4-32**: 1H NMR (250 MHz, $CDCl_3$) δ 7.39 (d, 2H, $J = 8.9$ Hz), 6.88 (d, 2H, $J = 8.9$ Hz), 5.45 (s, 1H), 5.22 (dd, 1H, $J = 9.5, 9.5$ Hz), 4.80 (d, 1H, $J = 3.5$ Hz), 4.29 (dd, 1H, $J = 3.5, 9.5$ Hz), 3.87 (m, 1H), 3.81 (s, 3H), 3.75 (dd, 1H, $J =$

9.5, 9.5 Hz), 3.65 (m, 1H), 3.56 (dd, 1H, $J = 9.5, 9.5$ Hz), 3.47 (s, 3H), 2.29 (d, 1H, $J = 11.0$ Hz), 2.12 (s, 3H)

^{13}C NMR (65 MHz, CDCl_3) δ 170.9, 159.9, 129.4, 127.4, 113.4, 101.3, 100.0, 78.5, 72.1, 71.6, 68.6, 62.6, 55.4, 55.1, 20.9.



$\text{C}_{17}\text{H}_{22}\text{O}_8$, Mol. Wt. = 354.35

$R_f = 0.34$ (H/EA, 1:1)

$[\alpha]_D = +93.6$ (c 0.8, CHCl_3)

mp: 123°C

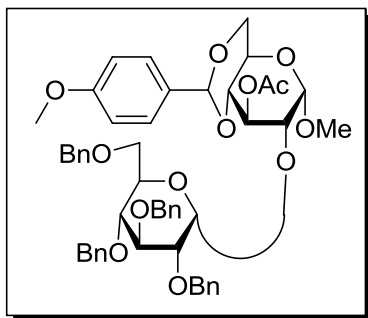
IR (neat/ NaCl): 3480, 1741 cm^{-1}

Data for **4-33**: ^1H NMR (250 MHz, CDCl_3) δ 7.43 (d, 2H, $J = 8.9$ Hz), 6.90 (d, 2H, $J = 8.9$ Hz), 5.51 (s, 1H), 4.96 (d, 1H, $J = 4.5$ Hz), 4.81 (dd, 1H, $J = 4.5, 9.5$ Hz), 4.29 (dd, 1H, $J = 3.5, 9.5$ Hz), 4.18 (ddd, 1H, $J = 2.0, 9.5, 9.5$ Hz), 3.82 (m, 1H), 3.81 (s, 3H), 3.75 (dd, 1H, $J = 9.5, 9.5$ Hz), 3.54 (dd, 1H, $J = 9.5, 9.5$ Hz), 3.41 (s, 3H), 2.57 (bs, 1H), 2.17 (s, 3H)

^{13}C NMR (65 MHz, CDCl_3) δ 170.6, 159.9, 129.3, 127.4, 113.4, 101.6, 97.2, 81.0, 73.3, 68.5, 68.1, 61.8, 55.1, 55.0, 20.6.

Methyl 3-*O*-acetyl-para-methoxy-4,6-*O*-benzylidene-2-*O*-(2',3',4',6'-tetra-*O*-benzyl- α -D-glucopyranosyl)- α -D-glucopyranoside (4-34a) and methyl 3-*O*-acetyl-para-methoxy-4,6-*O*-benzylidene-2-*O*-(2',3',4',6'-tetra-*O*-benzyl- β -D-glucopyranosyl)- α -D-glucopyranoside (4-34b)

To a solution of pyranoside **4-32** (307 mg, 0.87 mmol), glucopyranosyl trichloroacetimidate **4-31** (652 mg, 0.95 mmol) and 4Å MS in dry CH_2Cl_2 (25 mL) was added a freshly prepared 0.1 M solution of TMSOTf in CH_2Cl_2 . The resulting mixture was stirred for 1 h then quenched with a drop of Et_3N , diluted with CH_2Cl_2 , washed with 1M NaHCO_3 and brine, dried over MgSO_4 and concentrated *in vacuo*. The isomers were separated by chromatography (H/EA, 4:1) to afford regioisomers **4-34a** (425 mg, 56%, colorless oil) and **4-34b** (215 mg, 28%, white crystals).



$C_{51}H_{56}O_{13}$, Mol. Wt. = 876.98

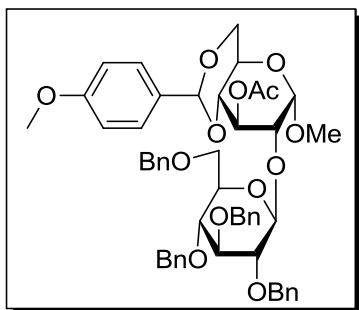
$R_f = 0.43$ (H/EA, 7:3)

$[\alpha]_D = +48.5$ (c 1.1, $CHCl_3$)

IR (neat/NaCl, cm^{-1}): 1755

Data for **4-34a**: 1H NMR (250 MHz, $CDCl_3$) δ 7.40 (d, 2H, $J = 8.9$ Hz), 7.32 (m, 20H), 6.88 (d, 2H, $J = 8.9$ Hz), 5.62 (dd, 1H, $J = 9.5, 9.5$ Hz), 5.43 (s, 1H), 4.96 (d, 1H, $J = 11.5$ Hz), 4.91 (d, 1H, $J = 3.5$ Hz), 4.86 (d, 1H, $J = 3.5$ Hz), 4.84 (d, 1H, $J = 11.5$ Hz), 4.82 (2d, 2H, $J = 11.5$ Hz), 4.65 (d, 1H, $J = 11.5$ Hz), 4.59 (d, 1H, $J = 11.5$ Hz), 4.46 (2d, 2H, $J = 11.5$ Hz), 4.28 (dd, 1H, $J = 4.5, 9.5$ Hz), 3.96 (dd, 1H, $J = 9.5, 9.5$ Hz), 3.92 (m, 1H), 3.88 (m, 1H), 3.81 (s, 3H), 3.79 (dd, 1H, $J = 3.5, 9.5$ Hz), 3.74-3.60 (m, 3H), 3.53 (dd, 1H, $J = 9.5, 9.5$ Hz), 3.54 (dd, 1H, $J = 3.5, 9.5$ Hz), 3.51 (dd, 1H, $J = 9.5, 9.5$ Hz), 3.43 (s, 3H), 2.02 (s, 3H)

^{13}C NMR (65 MHz, $CDCl_3$) δ 169.4, 159.9, 138.6, 138.3, 138.2, 137.7, 129.4, 128.3-127.3, 113.4, 101.3, 97.5, 95.8, 81.4, 79.3, 79.2, 77.2, 75.4, 74.7, 74.6, 73.2, 72.9, 70.6, 69.8, 68.7, 68.1, 62.2, 55.1, 55.0, 20.9.



$C_{51}H_{56}O_{13}$, Mol. Wt. = 876.98

$R_f = 0.30$ (H/EA, 7:3)

$[\alpha]_D = +35.7$ (c 0.7, $CHCl_3$)

IR (neat/NaCl, cm^{-1}): 1755

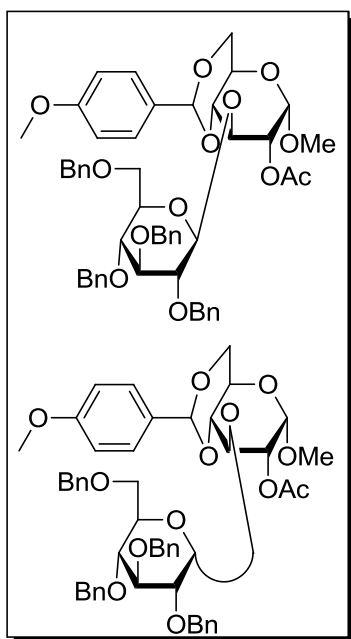
Data for **4-34b**: 1H NMR (250 MHz, $CDCl_3$) δ 7.40 (d, 2H, $J = 8.9$ Hz), 7.32 (m, 18H), 7.19 (m, 2H), 6.88 (d, 2H, $J = 8.9$ Hz), 5.65 (dd, 1H, $J = 9.5, 9.5$ Hz), 5.45 (s, 1H), 5.07 (d, 1H, $J = 3.5$ Hz), 4.94 (d, 1H, $J = 11.5$ Hz), 4.92 (d, 1H, $J = 11.5$ Hz), 4.82 (d, 1H, $J = 11.5$ Hz), 4.78 (d, 1H, $J = 11.5$ Hz), 4.70 (d, 1H, $J = 11.5$ Hz), 4.57 (d, 1H, $J = 11.5$ Hz), 4.52 (2d, 2H, $J = 11.5$ Hz), 4.50 (d, 1H, $J = 7.5$ Hz), 4.30 (dd, 1H, $J = 4.5, 10.0$ Hz), 3.95 (dd, 1H, $J = 4.5, 10.0, 10.0$ Hz), 3.82

(dd, 1H, $J = 3.5, 9.5$ Hz), 3.81 (s, 3H), 3.75-3.58 (m, 4H), 3.58-3.45 (m, 3H), 3.43 (m, 1H), 3.45 (s, 3H), 1.79 (s, 3H)

^{13}C NMR (65 MHz, CDCl_3) δ 169.8, 159.9, 138.4, 138.3, 137.82, 137.79, 129.4, 128.3-127.2, 113.4, 105.0, 101.2, 100.3, 84.5, 81.4, 79.7, 78.6, 77.5, 75.5, 74.9, 74.6, 74.3, 73.3, 70.1, 69.0, 68.8, 62.1, 55.3, 55.1, 20.6.

Methyl 2-*O*-acetyl-para-methoxy-4,6-*O*-benzylidene-3-*O*-(2',3',4',6'-tetra-*O*-benzyl- α/β -D-glucopyranosyl)- α -D glucopyranoside (4-35a/4-35b)

Following the same procedure as for compounds **4-36a** and **4-36b**, glucopyranoside **4-33** (415 mg, 1.17 mmol) and **4-31** (882 mg, 1.29 mmol) led to a inseparable mixture of regioisomers **4-35a** and **4-35b** (740 mg, 72% **4-35a/4-35b** = 2:1).



$\text{C}_{51}\text{H}_{56}\text{O}_{13}$, Mol. Wt. = 876.98

$R_f = 0.40$ (H/Ea, 7:3)

IR (neat/ NaCl , cm^{-1}): 1754

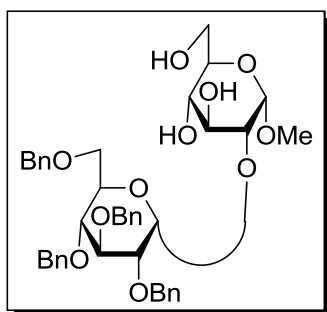
^1H NMR (1:1 mixture, 250 MHz, CDCl_3) δ 7.38-7.23 (m, 38x0.5H), 7.20-7.08 (m, 5x0.5H), 7.00 (m, 0.5H), 6.86 (d, 2x0.5H, $J = 8.9$ Hz), 6.76 (d, 2x0.5H, $J = 8.9$ Hz), 5.58 (d, 0.5H, $J = 3.0$ Hz), 5.48 (s, 0.5H), 5.48 (s, 0.5H), 5.00 (d, 1H, $J = 3.0$ Hz), 4.99 (d, 1H, $J = 3.0$ Hz), 4.95 (m, 4x0.5H), 4.88-4.32 (m, 17x0.5H), 4.27 (dd, 0.5H, $J = 5.0, 10.0$ Hz), 4.26 (dd, 0.5H, $J = 5.0, 10.0$ Hz), 4.05 (m, 0.5H), 3.94-3.82 (m, 4x0.5H), 3.82 (s, 3x0.5H), 3.81-3.70 (m, 5x0.5H), 3.71 (s, 3x0.5H),

3.69-3.55 (m, 5x0.5H), 3.52-3.43 (m, 2x0.5H), 3.42 (s, 3x0.5H), 3.41 (s, 3x0.5H), 3.27 (m, 0.5H), 2.05 (s, 3H), 1.97 (s, 3H)

^{13}C NMR (65 MHz, CDCl_3) δ 170.1, 169.9, 160.1, 159.8, 138.6-137.6, 129.6, 129.3, 128.1-127.2, 113.5, 113.2, 102.9, 101.8, 101.3, 97.3, 97.1, 95.7, 84.5, 82.4, 82.0, 81.1, 79.7, 78.4, 77.5, 77.1, 75.3, 75.2, 74.6, 74.5, 73.6, 73.3, 73.2, 71.9, 70.9, 70.3, 70.1, 68.7, 68.6, 68.5, 68.3, 62.3, 61.7, 55.0, 54.8, 20.7, 20.6.

Methyl 2-*O*-(2',3',4',6'-tetra-*O*-benzyl- α -D-glucopyranosyl)- α -D-glucopyranoside (4-36a)

A solution of **4-34a** (550 mg, 0.63 mmol) in an equimolar mixture of AcOH/THF/ H_2O (60 mL) was stirred at 50°C for 3 h then concentrated *in vacuo*. Flash purification by chromatography (H/A, 4:1 then 1:4) afforded the diol, pure enough for the next step. Thus, the residue was dissolved in MeOH then a catalytic amount of freshly prepared MeONa/MeOH solution was added. After stirring for 3 h, the mixture was concentrated and purified by chromatography ($\text{CH}_2\text{Cl}_2/\text{MeOH}$, 19:1) to afford disaccharide **4-36a** (416 mg, 90%, white crystals).



$\text{C}_{41}\text{H}_{48}\text{O}_{11}$, Mol. Wt. = 716.81

R_f = 0.48 (EA)

t_R = 24.2 min (gradient A)

$[\alpha]_D = +95.1$ (c 0.7, CHCl_3)

mp: 156°C

IR (neat/ NaCl , cm^{-1}): 3441

^1H NMR (400 MHz, CDCl_3) δ 7.32 (m, 18H, Ph), 7.18 (m, 2H, Ph), 5.00 (d, 1H, J = 11.0 Hz, CH_2Ph), 4.92 (d, 1H, $J_{1'-2'} = 4.5$ Hz, $H-1'$), 4.86 (d, 1H, J = 10.5 Hz, CH_2Ph), 4.85 (d, 1H, CH_2Ph), 4.84 (d, 1H, $J_{1-2} = 3.5$ Hz, $H-1$), 4.78 (d, 1H, J = 12.0 Hz, CH_2Ph), 4.65 (d, 1H, CH_2Ph), 4.58 (d, 1H, J = 11.5 Hz, CH_2Ph), 4.51 (d, 1H, CH_2Ph), 4.48 (d, 1H, CH_2Ph), 4.12 (ddd, 1H, $J_{4-5} = 10.0$, $J_{5'-6'} = 2.0$, $J_{5'-6'} = 5.5$ Hz, $H-5$), 4.06 (dd, 1H, $J_{2'-3'} = 9.5$, $J_{3'-4'} = 9.5$ Hz, $H-3'$), 3.88 (dd, 1H, $J_{2-3} = 9.5$, $J_{3-4} = 9.5$ Hz, $H-3$), 3.82 (m, 2H, $H-6'$, $H-6'$), 3.72-3.64 (m, 3H, $H-5$, $H-6$, $H-$

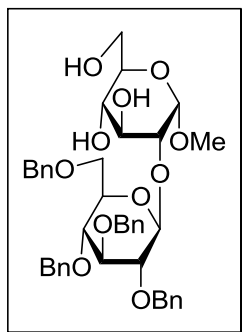
6), 3.60 (dd, 1H, $H-2'$), 3.56 (dd, 1H, $H-4'$), 3.47 (dd, 1H, $J_{4-5} = 9.5$ Hz, $H-4$), 3.45 (dd, 1H, $H-2$), 3.42 (s, 3H, OMe), 2.94 (bs, 1H, OH), 2.28 (bs, 1H, OH), 1.97 (bs, 1H, OH)

^{13}C NMR (65 MHz, CDCl_3) δ 138.6, 137.9, 137.8, 137.5 (Ph), 128.2-127.3 (Ph), 97.0 ($C-1$), 94.8 ($C-1'$), 81.4 ($C-3'$), 79.1 ($C-2'$), 77.4 ($C-4$), 76.8 ($C-4'$), 75.3, 74.9, 73.1, 72.5 (CH_2Ph), 72.0 ($C-3$), 70.7 ($C-5'$), 70.0 ($C-2$), 69.7 ($C-5$), 68.1 ($C-6'$), 61.3 ($C-6$), 54.8 (OMe); LRMS (EI $^+$, m/z , %): 625 (5) (M-Bn^+), 522 (7), 431 (12), 325 (17), 281 (26), 253 (100), 181 (100)

Anal. calcd for $\text{C}_{41}\text{H}_{48}\text{O}_{11}$: C, 68.70; H, 6.75; found: C, 68.90; H, 6.78.

Methyl 2-*O*-(2',3',4',6'-tetra-*O*-benzyl- β -D-glucopyranosyl)- α -D-glucopyranoside (4-36b)

Following the same procedure as for disaccharide **4-36a**, disaccharide **4-34b** (250 mg, 0.285 mmol) led to disaccharide **4-36b** (195 mg, 93%, white powder).



$\text{C}_{41}\text{H}_{48}\text{O}_{11}$, Mol. Wt. = 716.81

$R_f = 0.52$ (EA)

$t_R = 24.6$ min (gradient A)

IR (neat/ NaCl): 3422 cm^{-1}

$[\alpha]_D = +54.7$ (c 0.8, CHCl_3)

^1H NMR (250 MHz, CDCl_3) δ 7.32 (m, 18H, Ph), 7.17 (m, 2H, Ph), 4.93 (d, 1H, $J = 11.0$ Hz, CH_2Ph), 4.92 (d, 1H, $J_{1-2} = 4.0$ Hz, $H-1$), 4.92 (d, 1H, $J = 10.5$ Hz, CH_2Ph), 4.86 (2d, 2H, CH_2Ph), 4.83 (d, 1H, $J = 10.5$ Hz, CH_2Ph), 4.70 (d, 1H, $J_{1-2'} = 8.0$ Hz, $H-1'$), 4.59 (d, 1H, $J = 12.0$ Hz, CH_2Ph), 4.57 (d, 1H, CH_2Ph), 4.52 (d, 1H, CH_2Ph), 3.91 (dd, 1H, $J_{2-3} = 8.5$, $J_{3-4} = 8.5$ Hz, $H-3$), 3.87 (dd, 1H, $J_{5-6} = 3.5$, $J_{6-6} = 11.5$ Hz, $H-6$), 3.80 (dd, 1H, $J_{5-6} = 4.5$ Hz, $H-6$), 3.73-3.61 (m, 4H, $H-3'$, $H-5'$, $H-6'$, $H-6'$), 3.61-3.49 (m, 5H, $H-2$, $H-2'$, $H-4$, $H-4'$, $H-5$), 3.39 (s, 3H, OMe), 3.21 (bs, 1H, OH), 2.71 (bs, 1H, OH), 2.09 (bs, 1H, OH)

^{13}C NMR (65 MHz, CDCl_3) δ 138.3, 138.0, 137.9, 137.8 (Ph), 128.4-127.6 (Ph), 103.8 (C-1'), 99.5 (C-1), 84.8 (C-3'), 82.0 (C-2'), 80.9 (C-4), 77.9 (C-4'), 75.6, 75.1, 74.9, 73.4 (CH_2Ph), 74.6 (C-2), 72.4 (C-3), 70.5, 70.4 (C-5, C-5'), 69.0, (C-6'), 62.1 (C-6), 55.2 (OMe)

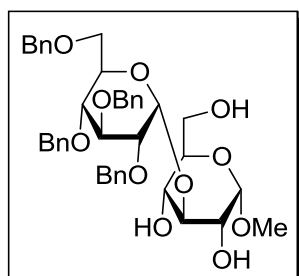
LRMS (EI+, m/z , %): 625 (7) (M-Bn^+), 593 (5), 522 (7), 431 (49), 325 (55), 313 (61), 253 (75), 181 (78), 91 (100)

Anal. calcd for $\text{C}_{41}\text{H}_{48}\text{O}_{11}$: C, 68.70; H, 6.75; found: C, 68.75; H, 6.77.



Methyl 3-*O*-(2',3',4',6'-tetra-*O*-benzyl- α -D-glucopyranosyl)- α -D-glucopyranoside (4-37a) and Methyl 3-*O*-(2',3',4',6'-tetra-*O*-benzyl- β -D-glucopyranosyl)- β -D-glucopyranoside (4-37a)

Following the same procedure as for **4-36a**, the mixture **4-35a/4-35b** (309 mg, 0.352 mmol) was deprotected into the separable (HPLC, H/EA, 3:1) **4-37a** (160 mg, 62%, colorless oil) and **4-37b** (79 mg, 31%, colorless oil).



$\text{C}_{41}\text{H}_{48}\text{O}_{11}$, Mol. Wt. = 716.81

R_f = 0.59 (EA)

t_R = 27.2 min (gradient A)

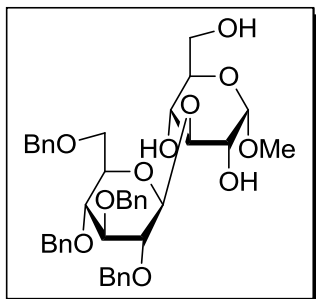
$[\alpha]_D = +80.6$ (c 0.5, CHCl_3)

IR (neat/ NaCl): 3447 cm^{-1}

Data for **4-37a**: ^1H NMR (400 MHz, CDCl_3) δ 7.32 (m, 18H, Ph), 7.15 (m, 2H, Ph), 4.94 (d, 1H, $J = 11.0$ Hz, CH_2Ph), 4.91 (d, 1H, CH_2Ph), 4.91 (d, 1H, $J_{1'-2'} = 4.5$ Hz, $H-1'$), 4.84 (d, 1H, $J = 11.0$ Hz, CH_2Ph), 4.83 (d, 1H, $J = 10.5$ Hz, CH_2Ph), 4.83 (d, 1H, $J_{1-2} = 3.5$ Hz, $H-1$), 4.71 (d, 1H, CH_2Ph), 4.58 (d, 1H, $J = 12.0$ Hz, CH_2Ph), 4.51 (d, 1H, CH_2Ph), 4.50 (d, 1H, CH_2Ph), 4.10 (m, 1H, $H-3$), 4.03 (dd, 1H, $J_{2-3} = 9.5$, $J_{3-4} = 9.5$ Hz, $H-3'$), 3.89 (dd, 1H, $J_{5-6} = 3.5$, $J_{6-6} = 11.5$ Hz, $H-6$), 3.81 (dd, 1H, $J_{5-6} = 4.5$ Hz, $H-6$), 3.73 (m, 1H, $H-5$), 3.70-3.62 (m, 3H, $H-5'$, $H-6'$, $H-6'$), 3.62-3.49 (m, 4H, $H-2$, $H-2'$, $H-4$, $H-4'$), 3.46 (s, 3H, OMe), 3.22 (bs, 1H, OH), 2.11 (bs, 1H, OH), 1.70 (bs, 1H, OH)

^{13}C NMR (65 MHz, CDCl_3) δ 138.3, 137.7, 137.4, 137.1 (Ph), 128.6-127.6 (Ph), 99.7, 99.5 (*C*-1, *C*-1'), 86.9 (*C*-3), 82.3 (*C*-3'), 79.3 (*C*-2'), 77.8 (*C*-4'), 75.6, 74.9, 74.0, 73.4 (CH_2Ph), 71.0, 70.7, 70.5, 70.1 (*C*-2, *C*-4, *C*-5, *C*-5'), 68.3 (*C*-6'), 62.4 (*C*-6), 55.2 (OMe)

LRMS (EI+, *m/z*, %): 625 (3) (M-Bn^+), 522 (3), 431 (55), 325 (65), 313 (49), 91 (100); Anal. calcd for $\text{C}_{41}\text{H}_{48}\text{O}_{11}$: C, 68.70; H, 6.75; found: C, 68.65; H, 6.77.



$\text{C}_{41}\text{H}_{48}\text{O}_{11}$, Mol. Wt. = 716.81

R_f = 0.70 (EA)

t_R = 31.9 min (gradient A)

IR (neat/ NaCl): 3429 cm^{-1}

$[\alpha]_D = +68.3$ (*c* 1.0, CHCl_3)

Data for **4-37b**: ^1H NMR (400 MHz, CDCl_3) δ 7.34 (m, 18H, Ph), 7.18 (m, 2H, Ph), 5.06 (d, 1H, $J = 11.0$ Hz, CH_2Ph), 4.94 (d, 1H, $J = 11.0$ Hz, CH_2Ph), 4.83 (2d, 2H, $J = 11.0$ Hz, CH_2Ph), 4.80 (d, 1H, $J_{1'-2'} = 4.0$ Hz, H -1'), 4.78 (d, 1H, CH_2Ph), 4.58-4.48 (m, 4H, H -1, CH_2Ph), 3.99 (dd, 1H, $J_{5-6} = 4.0$, $J_{6-6} = 11.5$ Hz, H -6), 3.80 (dd, 1H, $J_{5-6} = 5.0$ Hz, H -6), 3.70 (2dd, 2H, $J_{2-3} = 9.0$, $J_{3-4} = 9.0$, $J_{2'-3'} = 9.0$, $J_{3'-4'} = 9.0$ Hz, H -3, H -3'), 3.68-3.60 (m, 3H, H -2, H -5, H -5'), 3.60-3.51 (m, 5H, H -2', H -4, H -4', H -6', H -6'), 3.44 (s, 3H, OMe), 2.33 (bs, 1H, OH), 2.15 (bs, 1H, OH), 1.77 (bs, 1H, OH)

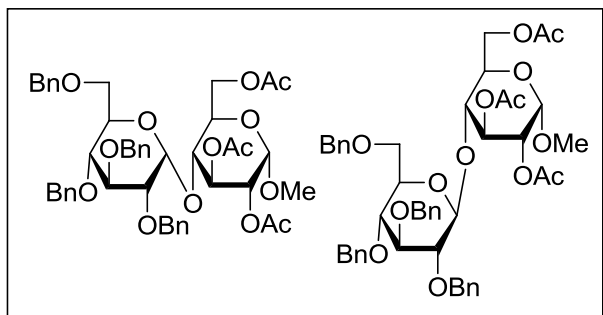
^{13}C NMR (65 MHz, CDCl_3) δ 138.3, 138.0, 137.7, 137.5 (Ph), 128.4-127.7 (Ph), 104.2 (*C*-1'), 99.0 (*C*-1), 86.9 (*C*-3), 84.6 (*C*-3'), 81.9 (*C*-2'), 77.7, 74.3 (*C*-4, *C*-4'), 75.7, 75.1, 73.5 (CH_2Ph), 71.1, 69.6 (*C*-2, *C*-5, *C*-5'), 68.8 (*C*-6'), 62.9 (*C*-6), 55.1 (OMe)

LRMS (EI+, *m/z*, %): 625 (3) (M-Bn^+), 593 (2), 522 (3), 431 (30), 325 (35), 281 (65), 253 (100), 181 (96)

Anal. calcd for $\text{C}_{41}\text{H}_{48}\text{O}_{11}$: C, 68.70; H, 6.75; found: C, 68.70; H, 6.72.

Methyl 2,3,6-tri-*O*-acetyl-4-*O*-(2',3',4',6'-tetra-*O*-benzyl- α/β -D-glucopyranosyl)- α -D-glucopyranoside (4-40a/4-40b)

Following the same procedure as for disaccharides **16a** and **16b**, coupling of compounds **4-38** (351 mg, 1.10 mmol) and **4-31** (1.5 g, 2.19 mmol) led to an inseparable mixture of disaccharides **4-40a** and **4-40b** (730 mg, 79% **4-40a/4-40b** = 2.4:1).



$C_{47}H_{54}O_{14}$, Mol. Wt. = 842.92

R_f = 0.61 (H/EA, 7:3)

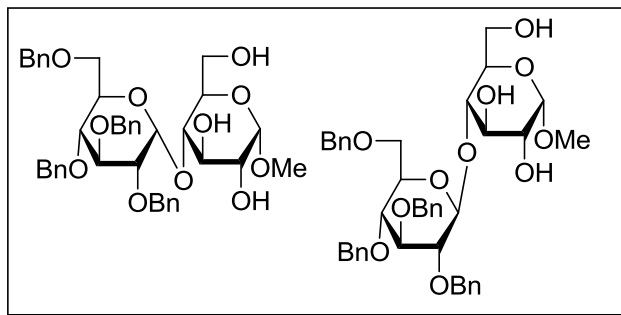
IR (neat/NaCl): 1745 cm^{-1}

^1H NMR (400 MHz, CDCl_3) δ 7.32 (m, 18H), 7.14 (m, 2H), 5.61 (dd, 0.7H, J = 9.5, 9.5 Hz), 5.45 (m, 0.3H), 4.95-4.24 (m, 13H), 3.98-3.41 (m, 8H), 3.40 (s, 3H), 2.11 (s, 3H), 2.04 (s, 3H), 2.03 (s, 0.9H), 1.95 (s, 2.1H)

^{13}C NMR (65 MHz, CDCl_3) δ 170.2, 170.1, 169.7, 138.5-137.5, 128.3-127.3, 102.8, 98.9, 96.3, 84.5, 82.3, 81.1, 80.0, 77.2, 76.4, 75.5, 75.4, 75.3, 75.0, 74.7, 74.5, 73.5, 73.3, 73.0, 71.4, 70.9, 70.6, 70.5, 69.4, 68.7, 68.3, 68.0, 62.6, 61.7, 55.1, 55.0, 20.7, 20.7, 20.5.

Methyl 4-*O*-(2',3',4',6'-tetra-*O*-benzyl- α/β -D-glucopyranosyl)- α -D-glucopyranoside (4-41a/4-41b**)**

A solution of disaccharides **4-40a** and **4-40b** (710 mg, 0.84 mmol) in MeOH (10 mL) was treated with a catalytic amount of freshly prepared solution of MeONa/MeOH. After stirring for 3 h and concentration, the residue was purified by chromatography ($\text{CH}_2\text{Cl}_2/\text{MeOH}$, 19:1) to afford disaccharides **4-41a/4-41b** (545 mg, 91%, **4-41a/4-41b** = 2.4:1).



$C_{41}H_{48}O_{11}$, Mol. Wt. 716.81

$R_f = 0.48$ (EA)

$t_R = 28.1$ min (gradient A)

IR (neat/NaCl): 3412 cm^{-1}

^1H NMR (400 MHz, CDCl_3) δ 7.33 (m, 18H), 7.14 (m, 2H), 5.02-4.71 (m, 6H), 4.61-4.40 (m, 4H), 4.07-3.43 (m, 12H), 3.42 (s, 3H), 2.37 (m, 1H), 2.20 (d, 1H, $J = 8.0$ Hz)

^{13}C NMR (65 MHz, CDCl_3) δ 138.1-136.8, 128.4-127.6, 102.9, 100.2, 99.0, 84.4, 81.9, 81.7, 80.2, 80.0, 78.8, 77.7, 77.5, 75.5, 75.4, 75.1, 74.8, 74.2, 73.9, 73.8, 73.3, 73.2, 72.0, 71.7, 71.2, 70.2, 70.0, 68.4, 61.0, 60.6, 55.2, 55.0

LRMS (EI^+ , m/z , %): 625 (2) (M-Bn^+), 522 (2), 431 (33), 325 (20), 281 (30), 253 (93), 181 (100)

Anal. calcd for $C_{41}H_{48}O_{11}$: C, 68.70; H, 6.75; found: C, 68.77; H, 6.77.

Glycosylations

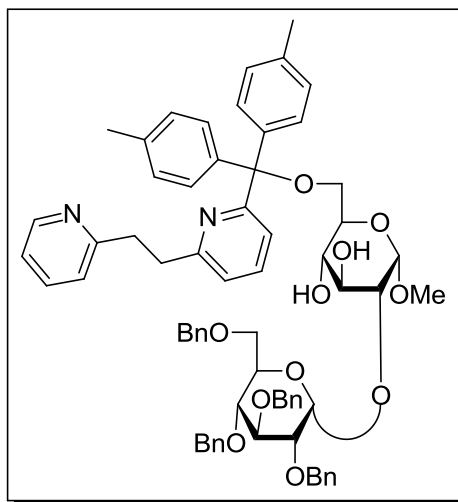
General procedure (Table 1). To a solution of **4-4**, **4-7-4-16**, **4-18** (0.25 mmol) and glucopyranosyl trichloroacetimidate **4-30** (0.25 mmol) in dry CH_2Cl_2 (25 mL) was added a freshly prepared 0.1 M solution of TMSOTf. The resulting mixture was stirred for 1 h then quenched with a drop of Et_3N , diluted with CH_2Cl_2 , washed with 1M NaHCO_3 and brine, dried over MgSO_4 and concentrated *in vacuo*. For the systematic glycosylation reactions, the residue was deprotected without further purification (Table 1).

Deprotection. **4-7**, **4-16**, **4-4** and **4-18** were stirred in a mixture of TFA/ CH_2Cl_2 (1:1, 10 mL) for 5 h. **1c**, **1d** were reacted with TBAF (0.75 mL of a 1M solution in THF, 0.75 mmol) and AcOH (0.05 mL, 1.0 mmol) in THF (10 mL). **4-12-4-14** were heated at 40°C in a mixture of AcOH/ H_2O /THF (1:1:1, 20

mL) for 3 h. **4-10**, **4-11**, and **4-15** were stirred in a MeONa/MeOH solution for 5 h. Standard workup and filtration on a silica gel pad (eluent hexanes/EtOAc 1:1 then 0:1) led to the isolated disaccharides.

Glycosylation-optimized procedure (Table 2). To a solution of **4-4** prepared as reported previously (0.50 mmol) in dry CH₂Cl₂ (50 mL) was added a freshly prepared solution of TMSOTf (2 mL, 0.1 M) and a freshly prepared solution of glucopyranosyl trichloroacetimidate **4-31** (2 mL, 0.50 mmol, 0.25 M) at -50°C. The resulting mixture was stirred for 1 h. This protocol was repeated two to three times (TMSOTf, 2 x 2 mL, trichloroacetimidate 8, 2 x 2 mL). After stirring for a further 3 hours at -50°C, the reaction was quenched with a drop of Et₃N. The resulting mixture was diluted with CH₂Cl₂, washed with 1M NaHCO₃ and brine, dried over MgSO₄ and concentrated *in vacuo*. The crude mixture was next treated with TBAF in THF to cleave any silyl ethers formed. The solution was concentrated and the residue was filtered on a silica gel pad and analyzed by HPLC and further purified by chromatography (H/EA, gradient from 2:3 to 0:5) to afford **4-46a** (120 mg, 22%), **4-46b** (214 mg, 39%), together with another two regioisomers (21 mg, 4% and 39 mg, 7%).

(6-*O*-{[6-(2-pyridin-2-yl-ethyl)-pyridin-2-yl]-di-*p*-tolyl-methyl}-methyl 2-*O*-(2',3',4',6'-tetra-*O*-benzyl- α -D-glucopyranosyl)- α -D-glucopyranoside (4-46a)



$C_{68}H_{72}N_2O_{11}$, Mol. Wt. 1093.31

$R_f = 0.57$ ($CH_2Cl_2/MeOH$, 9:1)

$t_R = 33.2$ min (gradient B)

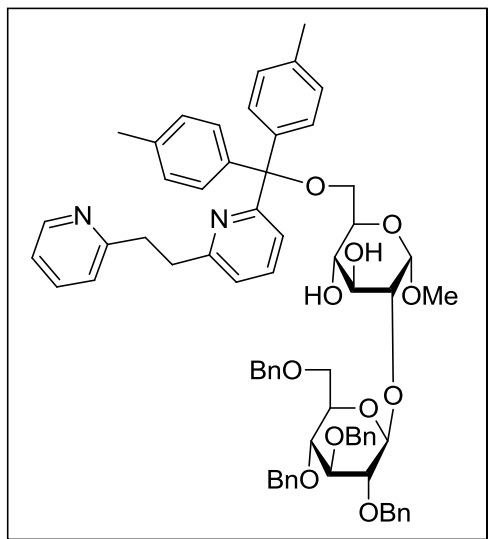
IR (neat/ $NaCl$): 3409 cm^{-1}

$[\alpha]_D = +56.2$ ($c\ 0.8$, $CHCl_3$)

1H NMR (250 MHz, $CDCl_3$) δ 8.45 (d, 1H, $J = 4.5$ Hz), 7.54-6.92 (m, 34H), 6.40-5.80 (bs, 1H (OH)), 5.02 (d, 1H, $J = 11.0$ Hz), 4.95 (d, 1H, $J = 3.5$ Hz), 4.85 (2d, 2H, $J = 11.0$ Hz), 4.79 (d, 1H, $J = 3.5$ Hz), 4.77 (d, 1H, $J = 11.0$ Hz), 4.72 (d, 1H, $J = 11.0$ Hz), 4.62 (d, 1H, $J = 11.0$ Hz), 4.52 (d, 1H, $J = 11.0$ Hz), 4.43 (d, 1H, $J = 11.0$ Hz), 4.27 (d, 1H, $J = 10.0$ Hz), 4.13 (dd, 1H, $J = 9.5, 9.5$ Hz), 4.08 (m, 1H), 3.90-3.53 (m, 9H), 3.42 (s, 3H), 3.44-3.06 (m, 4H), 2.36 (s, 3H), 2.34 (s, 3H)

^{13}C NMR (65 MHz, $CDCl_3$) δ 161.9, 160.9, 160.3, 149.0, 140.8, 140.0, 138.9, 138.4, 137.9, 137.1, 136.9, 136.6, 136.4, 129.3, 128.8, 128.5, 128.3, 127.9, 127.7, 127.6, 123.2, 121.8, 121.2, 121.1, 97.5, 95.6, 86.9, 81.8, 79.6, 77.7, 77.2, 75.5, 74.9, 73.5, 73.4, 72.8, 71.4, 70.1, 69.6, 68.4, 66.1, 55.0, 38.7, 38.0, 21.0.

(6-*O*-{[6-(2-pyridin-2-yl-ethyl)-pyridin-2-yl]-di-*p*-tolyl-methyl}-methyl 2-*O*-(2',3',4',6'-tetra-*O*-benzyl- β -D-glucopyranosyl)- α -D-glucopyranoside (4-46b)



$C_{68}H_{72}N_2O_{11}$, Mol. Wt. 1093.31

$R_f = 0.66$ ($CH_2Cl_2/MeOH$, 9:1)

$t_R = 35.4$ min (gradient B)

IR (neat/ $NaCl$): 3400 cm^{-1}

$[\alpha]_D = +52.3$ ($c\ 0.5$, $CHCl_3$)

mp: $74^\circ C$

1H NMR (250 MHz, $CDCl_3$) δ 8.41 (d, 1H, $J = 3.5$ Hz), 7.54-6.98 (m, 34H), 5.28 (d, 1H, $J = 11.0$ Hz), 4.96 (d, 1H, $J = 11.0$ Hz), 4.93 (d, 1H, $J = 3.5$ Hz), 4.83 (2d, 2H, $J = 11.0$ Hz), 4.80 (d, 1H, $J = 11.0$ Hz), 4.70 (d, 1H, $J = 7.5$ Hz), 4.58 (d, 1H, $J = 11.0$ Hz), 4.55 (d, 1H, $J = 11.0$ Hz), 4.50 (d, 1H, $J = 11.0$ Hz), 4.32-4.10 (bs, 1H, OH), 4.19 (dd, 1H, $J = 9.0, 9.0$ Hz), 3.89 (m, 2H), 3.75-3.53 (m, 8H), 3.58 (m, 1H), 3.45 (s, 3H), 3.47-3.05 (m, 4H), 2.37 (s, 3H), 2.34 (s, 3H)

^{13}C NMR (65 MHz, $CDCl_3$) δ 161.8, 160.7, 160.4, 149.3, 141.1, 139.6, 138.9, 138.7, 138.1, 137.4, 136.9, 136.8, 136.5, 129.5, 128.5, 128.4, 128.3, 128.0, 127.9, 127.6, 127.5, 123.1, 122.3, 121.3, 121.2, 105.3, 99.8, 87.0, 84.7, 81.9, 81.8, 77.7, 75.6, 75.0, 74.6, 74.5, 74.3, 73.4, 71.6, 69.3, 69.2, 66.7, 55.3, 39.1, 38.2, 21.0.

(6-*O*-{[6-(2-pyridin-2-yl-ethyl)-pyridin-2-yl]-di-*p*-tolyl-methyl}-methyl 3-*O*-(2',3',4',6'-tetra-*O*-benzyl- α -D-glucopyranosyl)- α -D-glucopyranoside

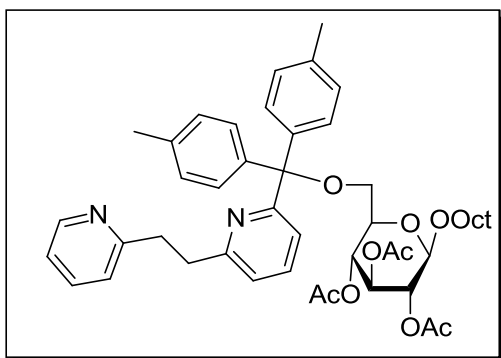
$t_R = 36.8$ min (gradient B).

(6-*O*-{[6-(2-pyridin-2-yl-ethyl)-pyridin-2-yl]-di-*p*-tolyl-methyl}-methyl 3-*O*-(2',3',4',6'-tetra-*O*-benzyl- β -D-glucopyranosyl)- α -D-glucopyranoside

$t_R = 40.5$ min (gradient B).

2,3,4-tri-*O*-acetyl-6-*O*-{[6-(2-pyridin-2-yl-ethyl)-pyridin-2-yl]-di-*p*-tolyl-methyl}-octyl- β -D-glucopyranoside (4-42a)

Following the same procedure as for the preparation of **4-4**, octyl- β -D-glucopyranoside (3.50 g, 12.0 mmol) and **4-27** (1.10 g, 2.79 mmol) led to **4-42**. Acetylation was carried out to facilitate its purification. Thus a solution of acetic anhydride (6.5 mL, excess) in pyridine (30 mL) in CH₂Cl₂ was added to the crude mixture. After stirring for 16 h, the solution was concentrated to provide, after flash chromatography (H/EA, 4:1 then 3:2), **4-42a** (1.03g, 46%)



C₃₉H₄₁N₂O₈, Mol. Wt. = 665.75

R_f = 0.5 (H/EA, 1:1)

IR (neat): 2927, 2856, 1755 cm⁻¹

[α]_D = +25.5 (c 0.10, CHCl₃)

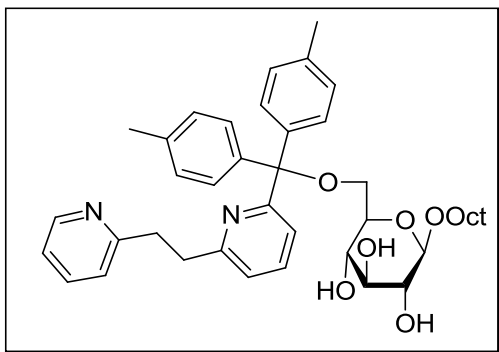
¹H NMR (400 MHz, CDCl₃) δ 8.49 (bd, 1H, *J* = 4 Hz), 7.63 (d, 1H, *J* = 8 Hz), 7.49 (t, 1H, *J* = 8 Hz), 7.43-7.37 (m, 3H), 7.28 (s, 1H), 7.06 (3d, 5H *J* = 7 Hz), 6.85 (d, 1H, *J* = 7.5 Hz), 6.77 (d, 1H, *J* = 7.5 Hz), 5.24 (t, 1H, *J* = 9.5 Hz), 5.15 (t, 1H, *J* = 9.5 Hz), 5.06 (t, 1H, *J* = 8 Hz), 4.50 (d, 1H, *J* = 8 Hz), 3.95-3.89 (ddd, 1H, *J* = 6.5 Hz, 9.5 Hz), 3.57-3.51 (m, 2H), 3.33 (dd, 1H, *J* = 2 Hz, 11 Hz), 3.12-3.07 (m, 5H), 2.31 (s, 6H), 2.05 (s, 3H), 2.00 (s, 3H), 1.76 (s, 3H), 1.67-1.57 (m, 2H), 1.34-1.26 (m, 10H), 0.89-0.85 (t, 3H, *J* = 7 Hz)

¹³C NMR (75 MHz, CDCl₃) δ 170.62, 169.56, 169.08, 162.92, 161.59, 159.44, 149.07, 140.63, 140.16, 136.54, 136.51, 136.27, 129.49, 129.39, 128.19, 128.14, 123.27, 121.01, 120.73, 118.82, 100.91, 86.63, 73.40, 73.37, 71.68, 69.96, 68.79, 62.21, 37.64, 37.31, 31.94, 29.63, 29.43, 26.08, 22.78, 21.17, 20.85, 20.57, 14.23.

HRMS (EI⁺) calc'd for [C₄₇H₅₉N₂O₉ + H]⁺: 795.42151. Found: 795.42232.

6-*O*-{[6-(2-pyridin-2-yl-ethyl)-pyridin-2-yl]-di-*p*-tolyl-methyl}-octyl- β -D-glucopyranoside (4-42)

A solution of **4-42a** (1.03 g, 1.30 mmol) in MeOH (80 mL) was stirred in presence of MeONa (280 mg, 5.2 mmol) for 2 h. The solution was neutralized with IR120H resin, filtered and concentrated to provide pure **4-42** (light yellow foam, 760 mg, 88%).



$C_{33}H_{35}N_2O_5$, Mol. Wt. = 539.64

$R_f = 0.30$ (DCM/MeOH, 9:1)

IR (DCM solution): 3380, 2925, 2856, 1451 cm^{-1}

$[\alpha]_D = +11.9$ (c 0.16, $CHCl_3$)

1H NMR (400 MHz, $CDCl_3$) δ 8.65 (bs, 1H), 7.63, (bs, 1H), 7.59-7.52 (m, 2H), 7.39 (d, 2H, $J = 7.5$ Hz), 7.28 (s, 1H), 7.21 (d, 3H, $J = 8$ Hz), 7.14 (d, 3H, $J = 8$ Hz), 7.08 (d, 3H, $J = 8$ Hz), 4.31 (d, 1H, $J = 8$ Hz), 3.82-3.74 (m, 3H), 3.62-3.59 (m, 1H), 3.49-3.39 (m, 2H), 3.37-3.33 (t, 1H, $J = 8$ Hz), 3.28-3.26 (m, 1H), 3.20-3.18 (m, 2H), 2.37 (s, 3H), 2.30 (s, 3H), 1.60-1.53 (m, 2H), 1.28-1.23 (m, 10H), 0.87-0.84 (t, 3H, $J = 7$ Hz)

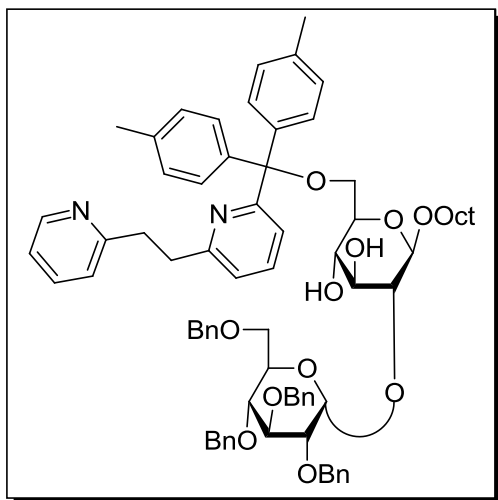
^{13}C NMR (75 MHz, $CDCl_3$) δ 161.82, 160.63, 160.59, 149.43, 142.05, 138.23, 138.14, 137.25, 137.07, 136.90, 130.41, 128.76, 127.87, 123.41, 122.80, 121.70, 121.67, 103.00, 87.24, 75.55, 75.21, 74.33, 73.93, 70.34, 67.86, 39.47, 38.58, 31.92, 29.67, 29.50, 29.31, 26.04, 22.77, 21.26, 21.18, 14.24.

HRMS (EI+) calc'd for $[C_{41}H_{52}N_2O_6 + H]^+$: 669.38981. Found: 669.39095.

(6-O-{{6-(2-pyridin-2-yl-ethyl)-pyridin-2-yl}-di-p-tolyl-methyl}-octyl 2-O-(2',3',4',6'-tetra-O-benzyl- α -D-glucopyranosyl)- β -D-glucopyranoside (4-47a) and (6-O-{{6-(2-pyridin-2-yl-ethyl)-pyridin-2-yl}-di-p-tolyl-methyl}-octyl 2-O-(2',3',4',6'-tetra-O-benzyl- β -D-glucopyranosyl)- β -D-glucopyranoside (4-47b)

Following the optimized procedure for glycosylation, **4-42** (105 mg, 0.157 mmol), **4-31** (3 x 0.63 mL of a 0.25M solution in CH_2Cl_2), TMSOTf (3 x 640 mL, 0.1M solution in CH_2Cl_2) and TBAF (480 μ L, 1M solution in THF) led to a mixture of

isomers from which **4-47a** (21 mg, 11 %), and **4-47b** (32 mg, 17 %) were isolated by flash chromatography (gradient H/EA 1:9 to 3:2).



$C_{67}H_{69}N_2O_{10}$, Mol. Wt. = 1062.27

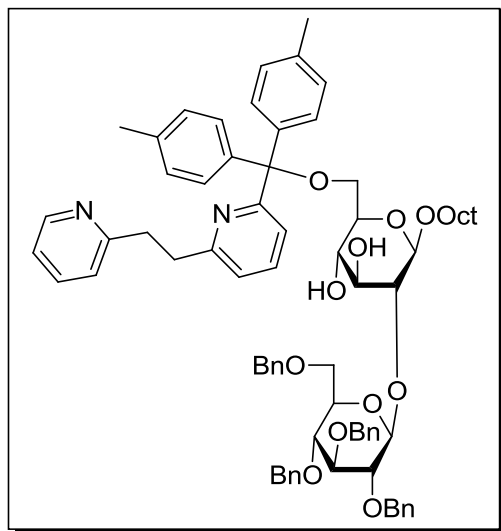
$R_f = 0.2$ (H/EA, 1:1)

$[\alpha]_D = +11.1$ (c 0.11, $CHCl_3$)

1H NMR (400 MHz, $CDCl_3$) δ 8.47 (bd, 1H, $J = 5$ Hz), 7.54-7.47 (m, 2H), 7.39-7.27 (m, 20H), 7.25-7.7.23-7.19 (m, 3H), 7.19-7.16 (m, 3H), 7.13-7.08 (m, 4H), 7.04-7.01 (m, 2H), 5.54 (d, 1H, $J = 3.5$ Hz), 4.99 (d, 1H, $J = 11$ Hz), 4.89-4.77 (m, 4H), 4.65 (dd, 2H, $J = 6.5$ Hz, 12 Hz), 4.61-4.48 (m, 4H), 4.40 (d, 1H, $J = 12$ Hz), 4.08 (t, 1H, $J = 9$ Hz), 3.85-3.68 (m, 7H), 3.68-3.60 (m, 4H), 3.55- 3.47 (m, 1H), 3.42-3.30 (m, 2H), 3.30-3.15 (m, 5H), 3.06 (dt, 1H, $J = 5.5$ Hz, 10 Hz), 3.00-2.92 (m, 1H), 2.37 (s, 3H), 2.32 (s, 3H), 1.54-1.47 (m, 2H), 1.18 (bs, 10H), 0.84 (t, 3H, $J = 9$ Hz)

^{13}C NMR (75 MHz, $CDCl_3$) δ 161.8, 160.8, 160.5, 150.0, 141.6, 139.2, 138.8, 138.7, 138.3, 138.2, 137.7, 137.0, 136.9, 130.1, 128.7, 128.4, 128.4, 128.2, 128.1, 128.1, 128.0, 127.8, 127.7, 127.7, 127.6, 123.4, 122.4, 121.6, 121.4, 103.2, 96.1, 87.1, 82.0, 79.8, 77.9, 77.8, 75.7, 75.1, 75.0, 73.5, 72.2, 70.0, 69.8, 68.6, 67.2, 52.2, 39.0, 38.3, 31.9, 30.0, 29.6, 29.3, 26.1, 25.2, 22.7, 21.2, 21.2, 20.3, 14.2, 13.7.

HRMS (ESI+) calc'd for $[C_{75}H_{86}N_2O_{11} + H]^+$: 1191.63044. Found: 1191.63148.



$C_{67}H_{69}N_2O_{10}$, Mol. Wt. = 1062.27

$R_f = 0.14$ (H/EA, 1/1)

$[\alpha]_D = +9.2$ (c 0.16, $CHCl_3$)

1H NMR (400 MHz, $CDCl_3$) δ 8.45 (d, 1H, $J = 4.5$ Hz), 7.52 (t, 1H, $J = 8$ Hz), 7.44-7.27 (m, 21H), 7.24-7.23 (m, 2H), 7.19-7.15 (m, 4H), 7.10-7.07 (m, 4H), 7.04-7.00 (m, 2H), 5.16 (d, 1H, $J = 11$ Hz), 4.92 (dd, 2H, $J = 7$ Hz, 9 Hz), 4.85-4.78 (m, 3H), 4.63 (dd, 2H, $J = 9$ Hz, 14 Hz), 4.67-4.51 (m, 4H), 4.43 (d, 1H, $J = 7.5$ Hz), 3.86 (dd, 1H, $J = 7.5$ Hz, 16 Hz), 3.81-3.69 (m, 8H), 3.58-3.42 (m, 4H), 3.39-3.34 (m, 2H), 3.26-3.05 (m, 5H), 2.36 (s, 3H), 2.31 (s, 3H), 1.49-1.47 (m, 2H), 1.18 (bs, 10H), 0.85 (t, 2H, $J = 3.5$ Hz)

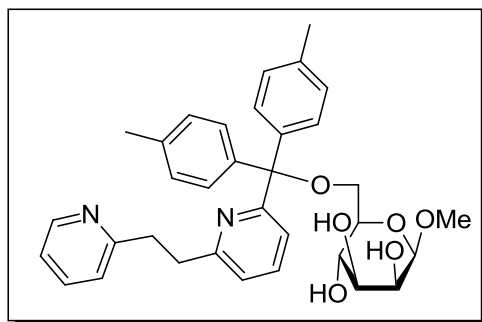
^{13}C NMR (75 MHz, $CDCl_3$) δ 161.9, 160.9, 160.5, 149.4, 141.7, 138.9, 138.8, 138.7, 138.5, 138.3, 137.7, 137.0, 136.8, 136.7, 130.1, 128.7, 128.5, 128.5, 128.4, 128.4, 128.3, 128.1, 127.9, 127.8, 127.7, 127.6, 123.3, 122.2, 121.5, 121.4, 103.1, 102.0, 87.1, 85.1, 82.6, 81.2, 78.1, 76.3, 75.7, 75.1, 75.0, 74.9, 74.3, 73.7, 73.7, 69.8, 69.0, 67.1, 62.5, 52.2, 39.2, 38.4, 36.8, 32.0, 29.8, 29.5, 29.4, 29.0, 28.8, 25.9, 24.8, 22.8, 21.2, 21.2, 20.3, 14.3, 13.7.

HRMS (ESI+) calc'd for $[C_{75}H_{86}N_2O_{11} + H]^+$: 1191.63044. Found: 1191.63061.

6-O-([6-(2-pyridin-2-yl-ethyl)-pyridin-2-yl]-di-p-tolyl-methyl)-methyl- α -D-mannopyranoside (4-43)

Following the same procedure as for the preparation of **4-4** methyl- α -D-mannopyranoside (3.10 g, 16.0 mmol) and **4-27** (1.60 g, 4.06 mmol) led, after

purification by flash chromatography (CH₂Cl₂/MeOH, gradient 98:2 to 9:1), to **4-43** (brown foam, 1.80 g, 85 %).



C₃₄H₃₈N₂O₆ ; Mol. Wt. = 570.68

R_f = 0.35 (DCM/MeOH, 9/1)

IR (CDCl₃ solution): 3372 (broad),
2924, 1451 cm⁻¹

[α]_D = +104.4 (c 0.10, CHCl₃)

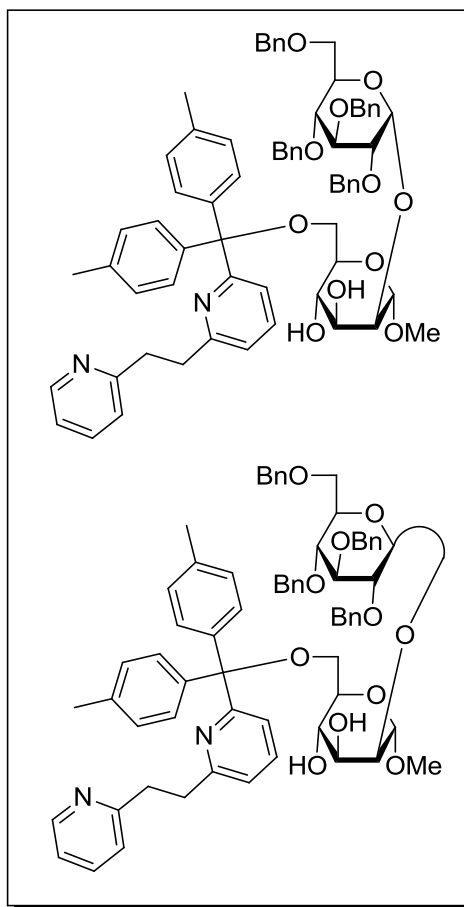
¹H NMR (400 MHz, CDCl₃) δ 8.59-8.58 (d, 1H, *J* = 3.5 Hz), 8.06 (bs, 1H), 7.61-7.55 (m, 2H), 7.43-7.41 (d, 2H, *J* = 8 Hz), 7.30-7.28 (d, 1H, *J* = 8 Hz), 7.23-7.21 (d, 2H, *J* = 8 Hz), 7.18-7.12 (m, 4H), 7.08-7.06 (d, 3H, *J* = 7.5 Hz), 4.68 (d, 1H, *J* = 1 Hz), 4.09-4.07 (m, 2H,), 4.02 (s, 1H), 3.87-3.82 (m, 1H), 3.43-3.39 (t, 1H, *J* = 9 Hz), 3.30 (s, 3H), 3.29-3.20 (m, 2H), 3.15-3.09 (m, 2H), 3.07-3.00 (m, 2H), 2.37 (s, 3H), 2.29 (s, 3H)

¹³C NMR (75 MHz, CDCl₃) δ 161.99, 160.65, 160.52, 149.29, 142.46, 138.13, 137.88, 137.26, 137.21, 136.76, 130.66, 128.77, 127.62, 123.46, 122.91, 121.74, 121.65, 100.83, 87.43, 72.50, 70.62, 70.05, 69.64, 68.59, 55.25, 39.54, 38.65, 21.25, 21.16.

HRMS (EI⁺) calc'd for [C₃₄H₃₈N₂O₆ + H]⁺: 571.28026. Found: 571.28081.

(6-*O*-{[6-(2-pyridin-2-yl-ethyl)-pyridin-2-yl]-di-*p*-tolyl-methyl}-octyl 2-*O*-(2',3',4',6'-tetra-*O*-benzyl-α-D-glucopyranosyl)-α-D-mannopyranoside (4-48a) and (6-*O*-{[6-(2-pyridin-2-yl-ethyl)-pyridin-2-yl]-di-*p*-tolyl-methyl}-octyl 2-*O*-(2',3',4',6'-tetra-*O*-benzyl-β-D-glucopyranosyl)-β-D-mannopyranoside (4-48b)

Following the optimized procedure for glycosylation, **4-43** (90 mg, 0.157 mmol), **4-31** (4 x 0.63 mL of a 0.25M solution in CH₂Cl₂), TMSOTf (4 x 640 mL, 0.1M solution in CH₂Cl₂) and TBAF (480 μL, 1M solution in THF) led to a mixture of isomers from which **4-48a** and **4-48b** (70 mg, 41 %, 1.2:1 mixture) were isolated by flash chromatography (gradient H/EA 1:4 to 3:2).



$C_{68}H_{72}N_2O_{11}$, Mol. Wt. 1093.31

$R_f = 0.14-0.10$ (H/EA, 1:1)

1H NMR (400 MHz, $CDCl_3$) δ 8.51 (d, $J = 4.0$ Hz, 1H), 8.45 (d, $J = 4.0$ Hz, 1H), 7.48–7.46 (m, 1H), 7.46–7.41 (m, 2H), 7.39 (s, 1H), 7.38 – 7.21 (m, 43H), 7.20–7.12 (m, 5H), 7.12–7.00 (m, 12H), 7.00–6.90 (m, 3H), 6.87 (d, $J = 7.6$ Hz, 1H), 5.00 (d, $J = 10.3$ Hz, 1H), 4.92 (dd, $J = 3.6$ Hz, 7.4, 2H), 4.86 (s, 1H), 4.83–4.69 (m, 8H), 4.69–4.64 (m, 2H), 4.59 (s, 1H), 4.57 – 4.48 (m, 5H), 4.47 – 4.38 (m, 3H), 4.21 (t, $J=9.2$, 1H), 4.04 (s, 1H), 4.00 – 3.86 (m, 6H), 3.81 (s, 1H), 3.80 – 3.66 (m, 7H), 3.66 – 3.55 (m, 5H), 3.55 – 3.51 (m, 2H), 3.42 (tdd, $J=4.3$, 12.2, 14.3, 7H), 3.32 – 3.26 (m, 4H), 3.23 (s, 2H), 3.15 (m, 10H), 2.31 (s, 6H), 2.27 (d, $J=5.0$, 6H)

^{13}C NMR (75 MHz, $CDCl_3$) δ 162.25, 162.21, 161.31, 161.16, 160.31, 160.29, 149.31, 149.15, 141.57, 141.06, 140.50, 139.71, 138.71, 138.66, 138.29, 138.15, 138.08, 137.94, 137.75, 137.18, 137.00, 136.84, 136.75, 136.72, 136.70, 136.64, 136.50, 136.45, 136.15, 129.87, 129.62, 129.17, 129.06, 128.7–127.6 (m), 123.51,

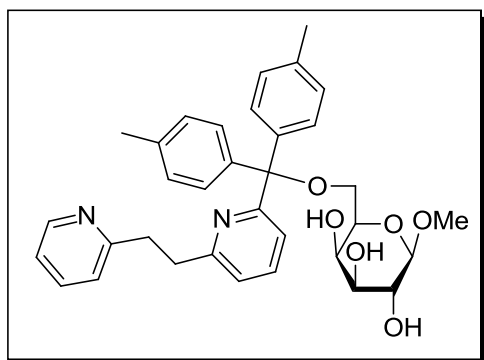
123.45, 121.35, 121.19, 121.14, 103.43, 100.95, 100.20, 99.57, 87.06, 87.05, 86.80, 84.58, 82.23, 81.97, 81.31, 79.76, 79.67, 77.86, 77.61, 75.86, 75.67, 75.24, 75.18, 71.71, 71.50, 71.37, 70.81, 70.60, 70.07, 68.70, 68.67, 66.29, 65.86, 54.89, 54.80, 38.78, 38.68, 38.22, 38.19, 21.18, 21.09.

4-48b HRMS (ESI+) calc'd for $[C_{68}H_{72}N_2O_{11} + H]^+$: 1093.52089. Found: 1093.52043.

4-48a HRMS (ESI+) calc'd for $[C_{68}H_{72}N_2O_{11} + H]^+$: 1093.52089. Found: 1093.51987.

6-O-[[6-(2-pyridin-2-yl-ethyl)-pyridin-2-yl]-di-p-tolyl-methyl]-methyl- α -D-galactopyranoside (4-44)

Following the same procedure as for the preparation of **4-4** methyl- α -D-galactopyranoside (3.10 g, 16.0 mmol) and **4-27** (1.60 g, 4.06 mmol) led, after purification by flash chromatography (gradient 98:2 to 9:1), to **4-44** (brown foam, 330 mg, 14 %).



$C_{34}H_{38}N_2O_6$; Mol. Wt. = 570.68

R_f = 0.35 (DCM/MeOH, 9/1)

IR (CDCl₃ solution): 3361

(broad), 2924, 1451 cm⁻¹

$[\alpha]_D = +99.9$ (c 0.15, CHCl₃)

¹H NMR (400 MHz, CDCl₃) δ 8.65 (bs, 1H), 7.58 (bs, 1H), 7.50 (t, 1H, J = 7.5 Hz), 7.18 (dd, 2H, J = 8 Hz, 21 Hz), 7.08 (d, 8 Hz), 7.03 (d, 1H, J = 7.5 Hz), 4.79 (d, 1H, J = 2.5 Hz), 4.60 (bs, 1H), 3.98 (dd, 1H, J = 6.5 Hz, 8 Hz), 3.92 (bs, 2H), 3.47 (t, 1H, 8.5 Hz), 3.33 (s, 3H), 3.31-3.14 (m, 4H), 3.10 (dd, 1H, J = 5.5 Hz, 8 Hz), 2.37 (s, 3H), 2.31 (s, 3H)

¹³C NMR (75 MHz, CDCl₃) 161.72, 160.92, 160.19, 149.18, 142.05, 138.89, 137.53, 136.73, 136.69, 136.44, 130.08, 128.53, 128.44, 128.02, 123.10, 121.89,

121.40, 121.17, 99.99, 86.96, 70.39, 70.17, 69.26, 69.16, 63.26, 55.35, 38.62, 37.93, 21.09, 21.02.

HRMS (EI+) calc'd for $[C_{34}H_{38}N_2O_6 + H]^+$: 571.28026. Found: 571.28003.

4.7 References

1. David, S.; Hanessian, S. Regioselective manipulation of hydroxyl-groups via organotin derivatives. *Tetrahedron* 1985, 41, 643-663.
2. Tennant-Eyles, R. J.; Davis, B. G.; Fairbanks, A. J. Peptide templated glycosylation reactions. *Tetrahedron: Asymmetry* 2000, 11, 231-243.
3. Cmoch, P.; Pakulski, Z. Comparative investigations on the regioselective mannosylation of 2,3,4-triols of mannose. *Tetrahedron: Asymmetry* 2008, 19, 1494-1503.
4. Richardson, A. C.; Williams, J. M. Selective O-acylation of pyranosides. *Chem. Commun. (London)* 1965, 104-105.
5. Moitessier, N.; Englebienne, P.; Chapleur, Y. Directing-protecting groups for carbohydrates. Design, conformational study, synthesis and application to regioselective functionalization. *Tetrahedron* 2005, 61, 6839-6853.
6. Schmelzer, U.; Zhang, Z.; Schmidt, R. R. Dichloro-cyanoacetimidates as glycosyl donors. *J. Carbohydr. Chem.* 2007, 26, 223-238.
7. Graziani, A.; Passacantilli, P.; Piancatelli, G.; Tani, S. A mild and efficient approach for the regioselective silyl-mediated protection-deprotection of C-4 hydroxyl group on carbohydrates. *Tetrahedron Lett.* 2001, 42, 3857-3860.

[This page was intentionally left blank]

Chapter 5 Regio- and stereoselective glycosylation of position 3 of sugars using directing-protecting groups

The glycosylation method presented in Chapter 4 is regioselective, but not stereoselective. Furthermore, identification of the products is very difficult. In this chapter, we will show that our glycosylation method, applied with a benzoylated glucosyl donor, yields a highly regio- and stereoselective reaction where only a single isomer is obtained which can be identified using 2-dimensional NMR techniques.

5.1 Abstract

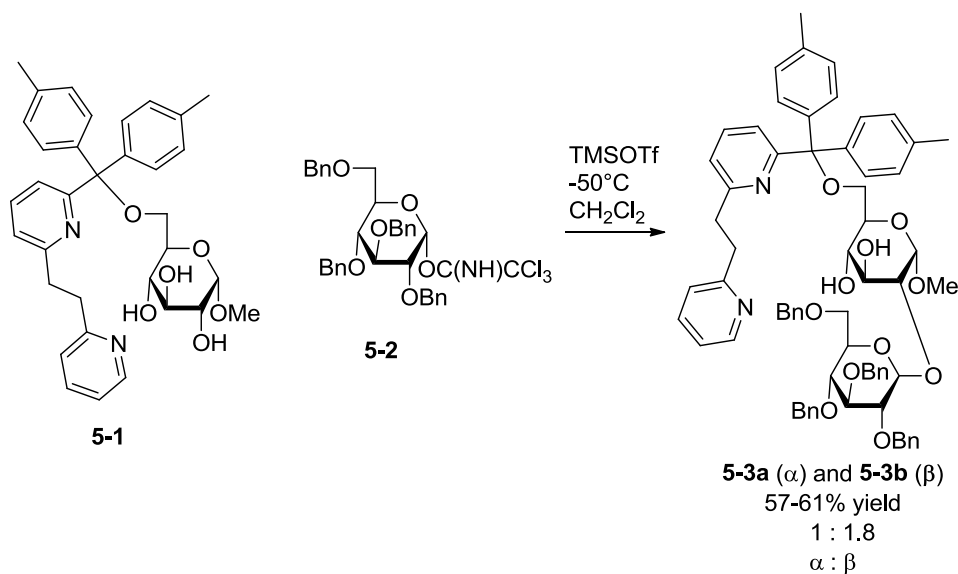
Several years ago, Hanessian (with his Chiron approach) proposed to use carbohydrates as an inexpensive source of chirality. Indeed, D-glucose would be a very useful starting material in many chiral syntheses if it were not for its polyol nature which renders it very complicated to exploit. We showed in Chapter 4 that a di-pyridyl-based protecting group installed at position 6 of a sugar can influence the regioselectivity of reactions by increasing the steric bulk around position 3. This steric bulk renders this position less accessible than position 2 to bulky electrophiles, like glycosyl donors. In practice, when glycosylated with a tetra-benzylated glucopyranose donor, the 6-*O*-di-pyridyl-protected sugar reacts primarily at position 2, although with poor stereoselectivity (57-61% yield of a 1:1.5-1.8 mixture of α/β). We hypothesize that switching to a 2,3,4,6-tetra-benzoylated glucopyranose donor will allow us to control the stereoselectivity of the glycosylation of the 6-*O*-dipyridyl-protected sugars. To prove this hypothesis, we glycosylated a series of 6-*O*-protected glucopyranosides with this 2,3,4,6-tetra-benzoylated glucopyranose donor. Gratifyingly, the stereoselectivity of the glycosylation reaction was optimal, producing only β -linked disaccharides. Interestingly, we also found that the 6-*O*-di-pyridyl-protected sugars were glycosylated at position 3 in an 80-90% yield (and not at position 2 as expected from previous results). Thus, through the use of different glycosyl donors, we can either glycosylate the 6-*O*-di-pyridyl-protected sugar acceptors at position 2 or position 3. The results of Chapters 4 and 5 offer a simple, yet versatile approach to selective carbohydrate functionalization.

5.2 Introduction

5.2.1 Background

Carbohydrate chemists seek to utilize Nature's building block D-glucose as efficiently as Nature does. While Nature possesses a variety of enzymes to perform a reaction selectively on these small, but complex building blocks,

chemists use protecting groups which they install on the building block prior to performing the reaction of interest. However, the multi-step routes using these protecting groups are still far from being as efficient as Nature and its enzymes. We have shown, in Chapter 4, that we could avoid a multi-step strategy to glycosylate position 2 of methyl α -D-glucopyranoside: we enhanced the reactivity of position 2, simply by using a specifically designed, di-pyridyl-based protecting group, regioselectively installed at position 6. The regioselectivity of the glycosylation reaction was altered, in that 6-*O*-protected glucopyranosides, protected with traditional, bulky protecting groups (like a trityl or TBDPS group) were glycosylated mainly at position 3. In this previous chapter, we proved that a properly designed protecting group can orient the glycosylation and therefore addressed the issue of regioselectivity.



Scheme 5.1 Optimized reaction conditions from Chapter 4, for glycosylating a 6-*O*-monoprotected glucopyranoside with a tetra-benzylated glucopyranose donor.

Despite the progress we reported in the previous chapter, the stereoselectivity of the reaction was still in need of improvement. From the glycosylation method we presented in the previous chapter, we consistently obtain a mixture of products, with α - and β -glycosidic linkages (Scheme 5.1), which are difficult to separate (in some cases inseparable) and rarely exceeding a 2:1 ratio of α : β . Our previous strategy relied on the preparation of the 6 possible stereo- and

regioisomers, these reference compounds being used to identify the components of the glycosylation product mixtures. Thus, we needed to synthesize each of these reference compounds separately, through typical protection and deprotection steps and compare these reference compounds to the products obtained from our glycosylation experiments, using HPLC.

5.2.2 Revisiting the challenges of regioselective glycosylation

Recalling the challenges of glycosylation, the method presented in Chapter 4 addressed some of the issues, but not others:

- Regioselectivity: we can glycosylate 6-*O*-protected glucopyranoside, favouring reaction at position 2 over positions 3 and 4, but the selectivity could still be improved upon.
- Stereoselectivity: our method forms the glycosidic linkages that are both α and β , and these isomers are often difficult to separate. Since we always obtain both, this method does not allow us to form one stereoisomer or the other. This issue remains to be addressed.
- Synthetic efficiency: we can glycosylate a minimally protected sugar into a 2-*O*-disaccharide, without the need to perform several tedious steps of protections and deprotections. However, we also needed to prepare several extra reference compounds (using traditional protection and deprotection strategies) in order to identify the products formed. Herein, we will revise this strategy.
- Polyglycosylation: we have minimized the over-glycosylation of the starting material, leading to unwanted trisaccharides.

The main challenges that still could be improved upon are stereoselectivity and efficiency.

5.2.3 Objectives and methods

“Neighbouring group participation” is one of the easiest methods to achieve stereoselectivity in a glycosylation reaction. Switching from the 2,3,4,6-

tetrabenzylated glucopyranose to a 2,3,4,6-tetrabenzoylated glucopyranose donor, the stereochemistry of the acyl group at position 2 will dictate the stereochemistry of the product formed, as illustrated in Figure 5.1.

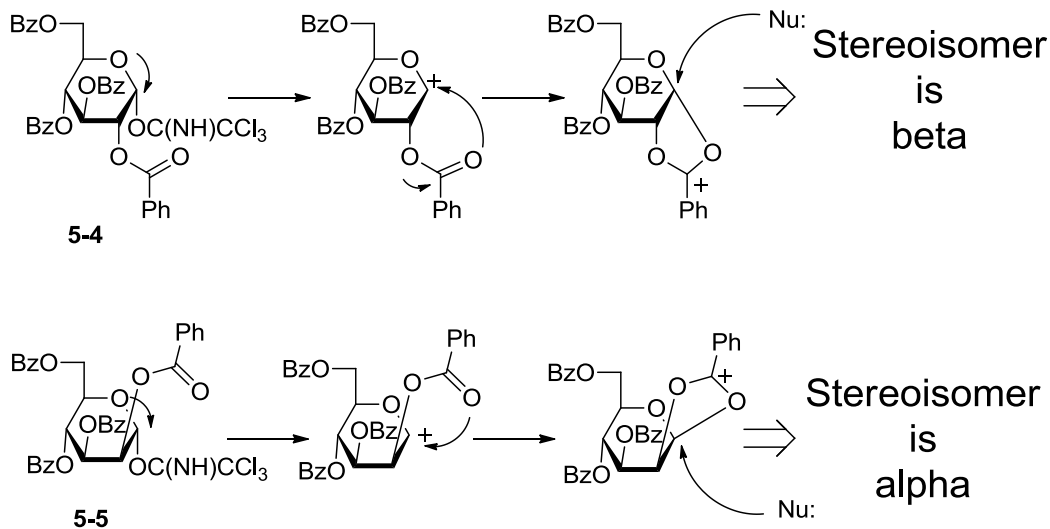


Figure 5.1 Illustration of the neighbouring group participation of an acyl group at position 2 and its effects on the stereoselectivity of a subsequent reaction with a nucleophile.

Using a benzoylated donor instead of a benzylated donor would conveniently eliminate the numerous benzylic protons which clutter the ^1H -NMR spectra of the products from our previous experiments. A disaccharide prepared from a benzoylated donor would thus lead to clearer ^1H -NMR spectra in the region of 6-3ppm. As a result, 2D-NMR analysis of the products would also be easier and appropriate NMR methods should allow us to identify the stereo- and regioisomers, without the need for another set of numerous reference compounds. Herein, we opted for NMR analysis of mixtures and separated isomers in place of HPLC analysis based on reference compounds.

In this chapter, we aimed to develop glycosylation conditions that are both regioselective, controlled by the di-pyridyl protecting group and stereoselective, controlled by the stereochemistry at position 2 of the trichloroacetimidate donor, through neighbouring group participation. To this end, we first glycosylated a small series of 6-*O*-protected glucopyranoside acceptors (including an acceptor having an indol-based protecting group at position 6 acting as a hydrogen-bond

donor) with a 2,3,4,6-tetra-benzoylated glucopyranose trichloroacetimidate donor. We then tested the effect of pre-incubating the di-pyridyl-protected acceptors with TMSOTf prior to glycosylating them. Contrary to the results from Chapter 4, when we switched to the less reactive tetra-benzoylated donor, the glucopyranosides protected with the di-pyridyl-based protecting group were selectively glycosylated at position 3 (80-90% yield) and only the 1,3- β -linked disaccharides were formed. In comparison, the 6-*O*-TBDPS-protected acceptor was glycosylated at both positions 2 and 3 in a nearly 1:1 mixture and in poor yields (38% yield). Our experiments pre-incubating the acceptor with TMSOTf prior to the actual glycosylation revealed that we could switch back to glycosylating the acceptor at position 2. The results of these experiments confirm that our di-pyridyl-based protecting group can be used as an efficient alternative to regioselectively and stereoselectively glycosylate a sugar, instead of a multi-step route of protections and deprotections.

5.3 Results and discussion

To optimize the stereoselectivity of the glycosylation reaction, we prepared a small set of 6-*O*-protected glycosyl acceptors (Figure 5.2). We also had to prepare a new donor, bearing an acyl group at position 2 which would allow us to control the stereochemistry of the new glycosidic linkage.

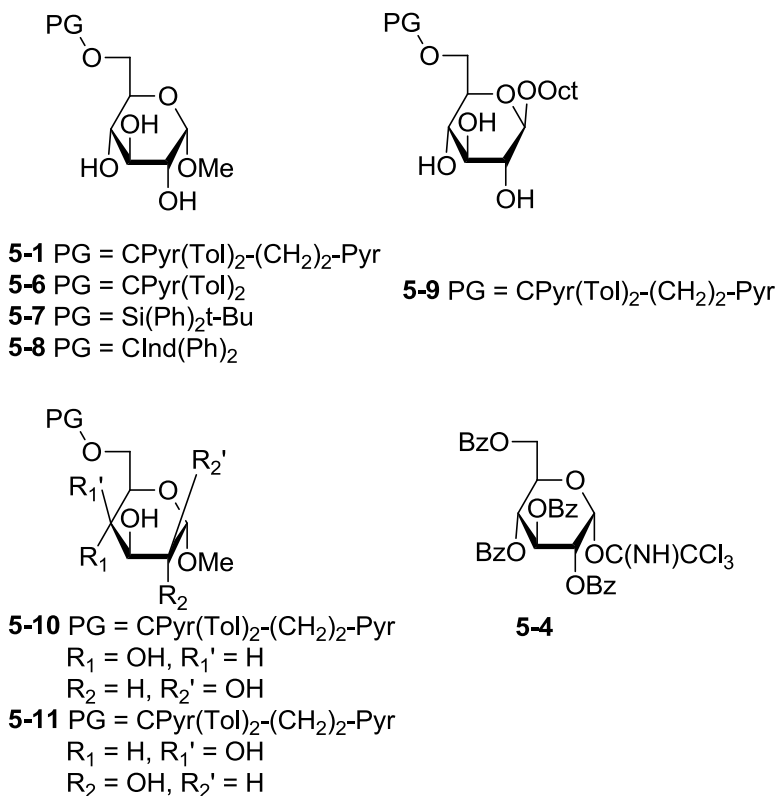


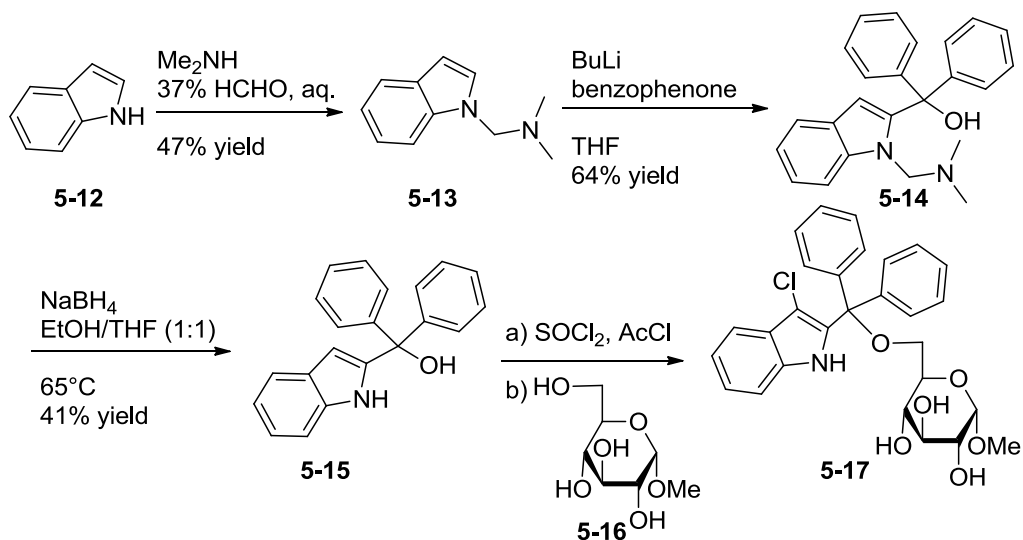
Figure 5.2 Series of 6-*O*-protected glucopyranoside acceptors and 2,3,4,6-tetra-benzoylated glucopyranose donor 5-4 which were used to optimize the regio- and stereoselectivity of the glycosylation reaction.

Given that several groups have reported that 2,3,4,6-tetra-benzoylated donors are significantly less reactive than the tetra-benzylated donor used in Chapter 4,^{1, 2} we added an extra 6-*O*-protected acceptor (**5-8**), featuring an indole ring which we predicted to hydrogen bond with the sugar, hopefully rendering the acceptor more reactive than the acceptors bearing hydrogen bond acceptors.

5.3.1 Preparation of the hydrogen bond donating protecting group and optimization of its coupling to a sugar

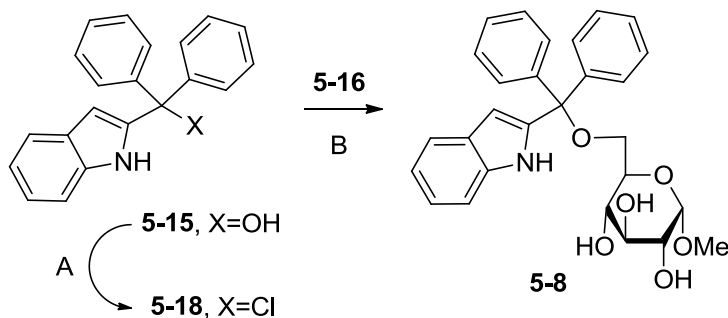
We prepared trityl-like alcohol (**5-15**) from indole (**5-12**) according to Katritzky's method.³ Ironically, in the first step of preparing our hydrogen bond donating directing-protecting group, we performed a Mannich reaction to install a directing-protecting group at position 1 (the amine) of the indole ring, attaching a tertiary amine, as in **5-13**, which could direct lithiation to position 2 instead of

position 3, the most reactive position of the indole ring. Thus, benzophenone could be added selectively to position 2 of the indole ring of **5-13**, yielding **5-14**. Reduction of the protecting group with sodium borohydride next released the indole amine, forming **5-15**. Using chlorination conditions developed for the pyridyl-based protecting groups, we attempted to substitute the chloride for the alcohol. Unfortunately, we chlorinated position 3 of the indole first. Very little indole-protected sugar was recovered, and the little that was had a chloride at position 3 of the indole ring (as in **5-17**).



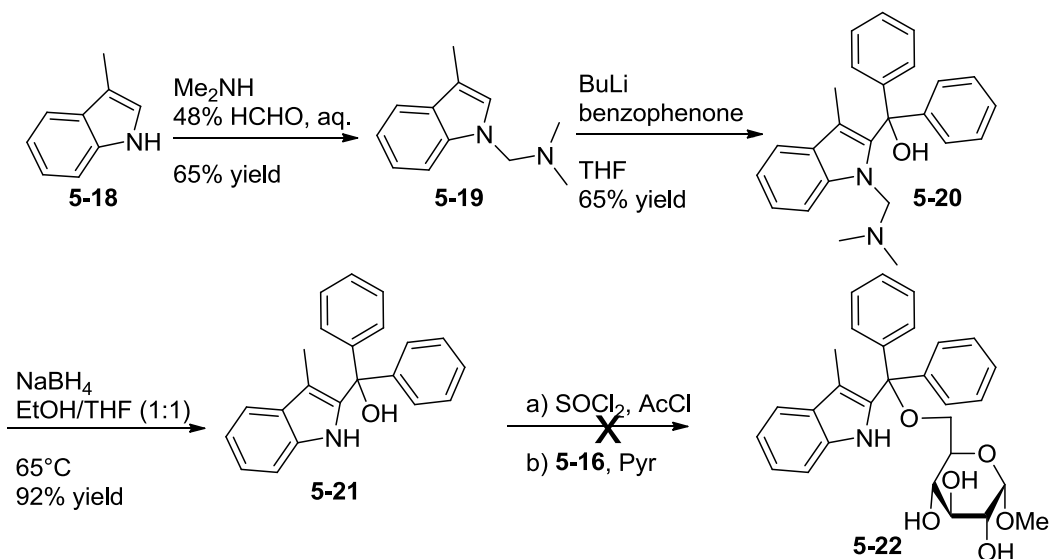
Scheme 5.2 Synthesis of the protecting group **5-15** and its coupling to **5-16**.

Since our initial attempt to install **5-15** onto the sugar failed, we explored other chlorination methods, attempting to optimize the chlorination conditions and successfully couple the indole-protecting group to the sugar with a higher yield (Table 5.1). However, all the methods tested led to little more than traces of the product **5-17** (although chlorinated at position 3 of the indole ring) or decomposition of the indole-protecting group and possibly even some dimerization of the indole-protecting group.

Table 5.1 Methods tested to chlorinate (or mesylate) the indol-2-ylidiphenylmethanol prior to coupling to methyl α -D-glucopyranoside.

A Functionalization of 5-15	B Conditions coupling to 5-16	Yield
SOCl_2 , DMF, DCM, 45°C, O/N	Pyridine, DMAP, rt, O/N	traces
SOCl_2 , DMF, THF, O/N to 48h	Pyridine, DMAP, rt, O/N	0
SOCl_2 , Et_3N , DCM, 45°C, 8h	Pyridine, DMAP, rt, O/N	0
SOCl_2 , Et_3N , DCM, 45°C, 8h	Pyridine, DMAP, 115°C, O/N	0
SOCl_2 , Et_3N , DCM, 45°C, 8h	Pyridine, silica, 115°C, O/N	0
SOCl_2 , DMF, DCM, 45°C, 8h	Pyridine, DMAP, 115°C, O/N	0
SOCl_2 , DMF, DCM, 45°C, 8h	Pyridine, silica, 115°C, O/N	0
MsCl , Et_3N , DCM	Pyridine, DMAP, rt, O/N	0

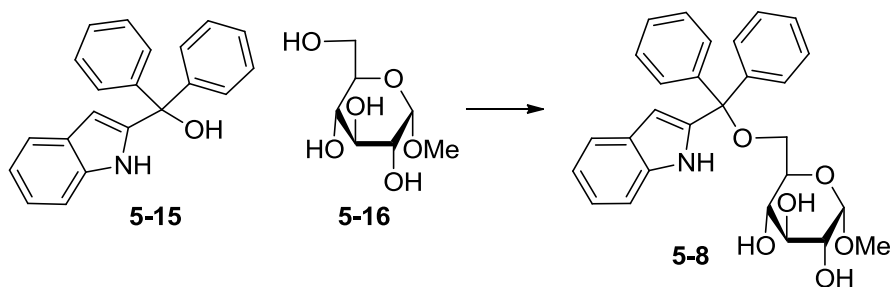
Since chlorination of the indole position 3 seemed to be occurring each time (or decomposition of the indole protecting group), we then synthesized the same protecting group, but starting from 3-methyl indole (**5-18**), so that the reactivity of position 3 would not interfere with our coupling methods (as in Scheme 5.3).



Scheme 5.3 Preparation of 5-21 and its coupling to 5-16.

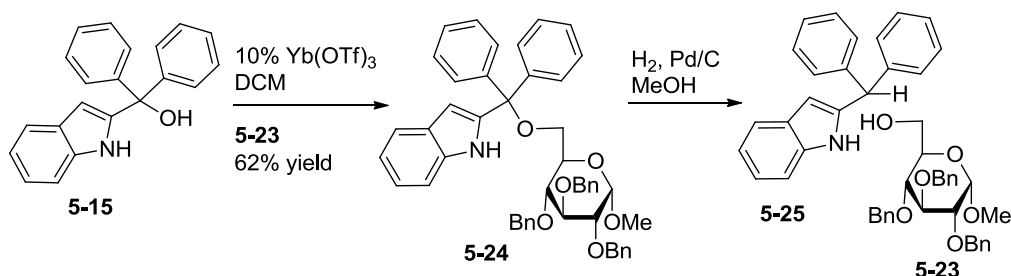
However, we were still unable to successfully chlorinate and couple this new protecting group to **5-16**.

We then investigated alternatives to the chlorination step, testing if we could activate the alcohol using Brønsted or Lewis acids (including $\text{Yb}(\text{OTf})_3$ as a Lewis acid based on Sharma's work⁴), prior to coupling to the sugar, (Table 5.2). However, in each case, we isolated little to none of the desired product. Various solvents were also tested to better solubilize the unprotected sugar, with little success.

Table 5.2 Attempts to directly couple the indyl-diphenyl methanol to a sugar.

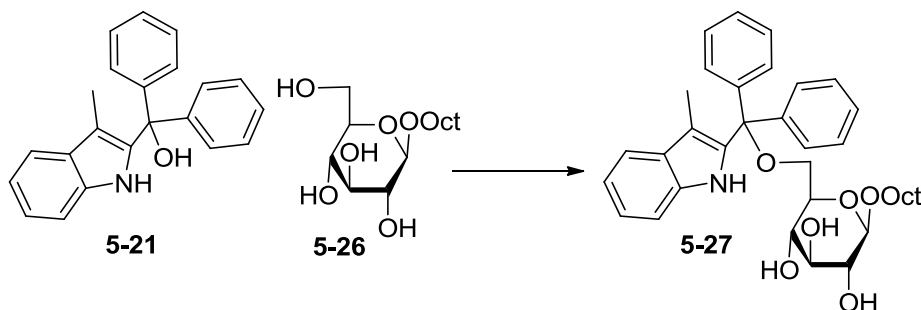
Reagent	Solvent	Temp	% Yield
pTSA	ACN	rt	0
pTSA	DMF	rt	0
pTSA	DMF	150 °C	0
10% Yb(OTf) ₃	DCM	rt	0
10% Yb(OTf) ₃	ACN	rt	traces
10% Yb(OTf) ₃	ACN	65 °C	traces
50% Yb(OTf) ₃	ACN	rt	traces
100% Yb(OTf) ₃	ACN	rt	traces
10% Yb(OTf) ₃	DCM/DMF 1:1	rt	traces
10% Yb(OTf) ₃	DCM/DMF 1:1	rt	traces
10% Yb(OTf) ₃	Bmim.pf6	rt	0
10% Yb(OTf) ₃	H ₂ O/dioxane 1:1	rt	traces
10% Yb(OTf) ₃	DMF	150 °C	5-17 by NMR

We found that the best method to install the protecting group onto the sugar was first using a Lewis acid to activate the protecting group and then coupling it to 2,3,4-tribenzylated methyl α -D-glucopyranoside **5-23** (62% yield). This result proved that one of the major issues with the coupling step could be the solubility of methyl α -D-glucopyranoside, and not activation of the protecting group. Unfortunately, this intermediate was not very useful as the benzyl groups could not be removed by hydrogenation without first hydrogenating at the benzylic position of the trityl-like protecting group, yielding **5-23** and **5-25** (Scheme 5.4).



Scheme 5.4 Coupling the indyl diphenyl methanol to a 2,3,4-tribenzylated methyl α -D-glucopyranoside.

In order to better solubilize the sugar, many researchers have used octyl-glucopyranosides which are soluble in such solvents as chloroform and dichloromethane. Thus, we attempted to couple our protecting group to octyl β -D-glucopyranoside (**5-26**) directly using a Lewis acid (Table 5.3). Optimized coupling conditions involve portion-wise addition of both the sugar and Lewis acid. In fact, too high a concentration of octyl β -D-glucopyranoside (**5-26**) could lead to micelle formation and lower the availability of the 6-OH for coupling, hence lower yields.

Table 5.3 Coupling of 5-21 to octyl β -D-glucopyranoside (5-26).

Reagent	Solvent	Temp	% Yield*
10%Yb(OTf) ₃	DCM	rt	5
10%Yb(OTf) ₃	DCM	45°C	19
10%Yb(OTf) ₃	DCM	rt	50-80 [§]

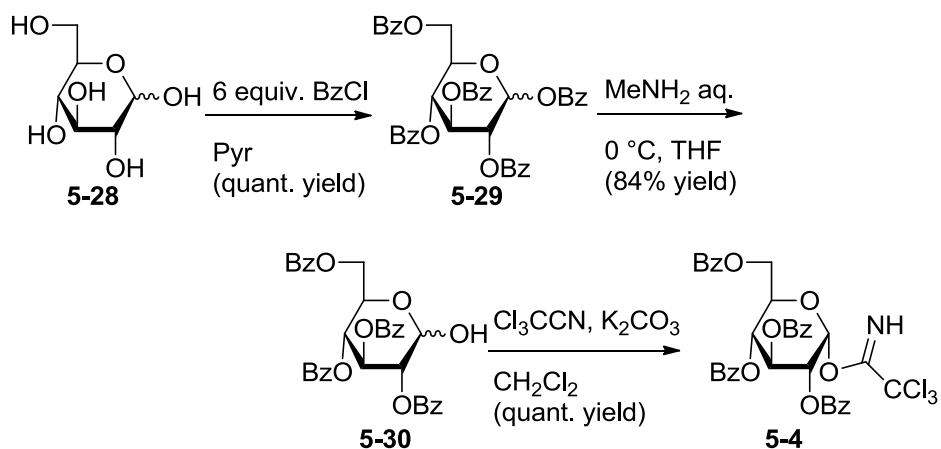
* Yield determined by NMR. [§] 4 equiv. **5-26** used

With this new method for installing **5-21** at position 6 of octyl β -D-glucopyranoside, we obtained a 50-80% NMR yield of **5-27** (35-52% isolated yield).

5.3.2 Regioselectivity of the glycosylation reaction with a benzoylated glycosyl donor

Researchers have widely used the tetra-benzoylated glycosyl donor and several procedures for its preparation have been reported. Starting from D-glucose (**5-28**), we first per-benzoylated **5-29**,⁵ then selectively deprotected the anomeric benzoyl to afford **5-30**. Interestingly, we tested several of the reported methods using a variety of bases to form the trichloroacetimidate **5-4**, but we found that several were irreproducible. In fact, the method which we applied in Chapter 4 to prepare the trichloroacetimidate of 2,3,4,6-tetra-benzyl glucopyranose did not work with the benzoylated sugar. The only base that did work for this step was potassium

carbonate. Furthermore, we found that the formation of the trichloroacetimidate was much slower, requiring 4 to 6 days to go to completion.



Scheme 5.5 Formation of the 2,3,4,6-tetra-benzoylated glucopyranose trichloroacetimidate 5-4.

We then glycosylated our series of acceptors with our per-benzoylated donor 5-4. As mentioned, our previous sets of glycosyl reference compounds (used in Chapter 4) were no longer valid because we changed the donor. Fortunately, products formed with the new donor 5-4 yielded significantly clearer NMR spectra, no longer cluttered with the benzylic protons which prevented any possible 2D-NMR analysis of the products. Thus, rather than preparing another set of reference compounds, we were able to perform extensive 2D-NMR experiments (COSY, HSQC and HMBC) of each product in order to determine the position of the glycosidic linkage formed.

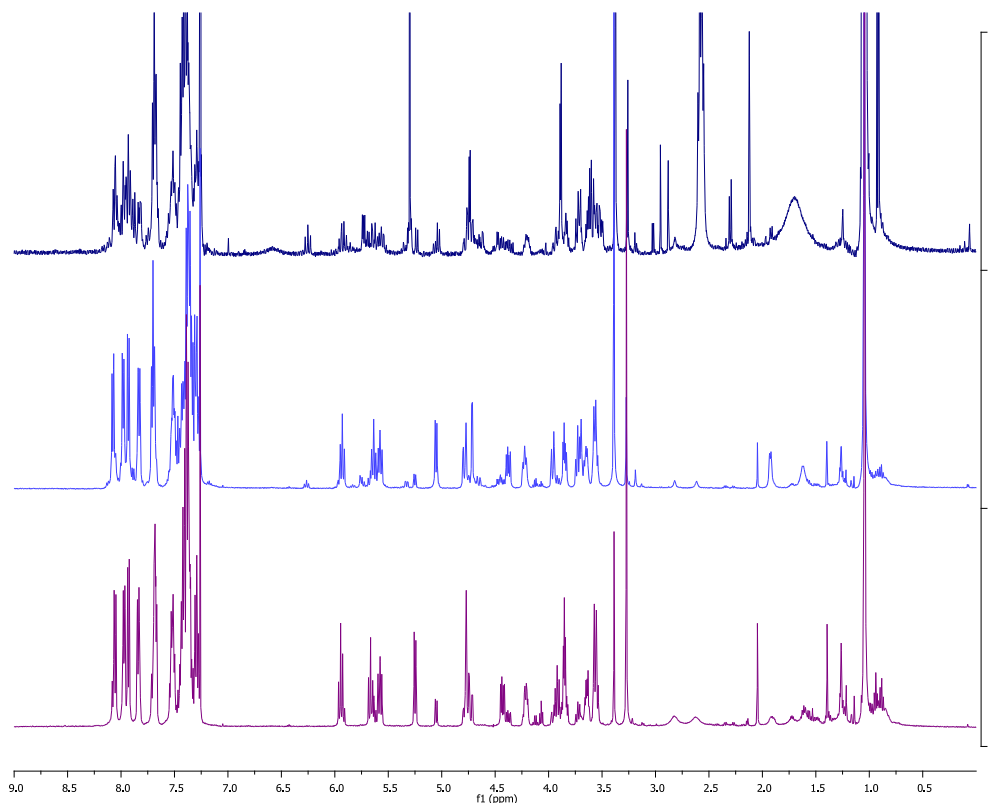


Figure 5.3 Stacked NMR spectra of products of glycosylation of methyl 6-*O*-TBDPS α -D-glucopyranoside (**5-7**), showing the crude mixture (top spectrum, in dark blue) containing only the two disaccharides (middle and bottom spectra, shown in light blue and purple) and the starting material (spectrum not shown).

For example, when we glycosylated methyl 6-*O*-TBDPS α -D-glucopyranoside (**5-7**), we isolated only two disaccharides, as expected from the crude NMR of the reaction (Figure 5.3). We then performed a COSY experiment for each of the disaccharides (Figure 5.4 and Figure 5.5). In a COSY experiment, each axis corresponds to the ^1H -NMR spectrum of the sample. The COSY experiments reveal ^1H - ^1H correlation between protons that are coupled to each other (located on the same or adjacent heavy atoms such as on carbons) as peaks off the diagonal of the spectrum. Combining the information from each peak allows us to assign each signal of the ^1H -NMR spectrum to a proton of the isolated disaccharides.

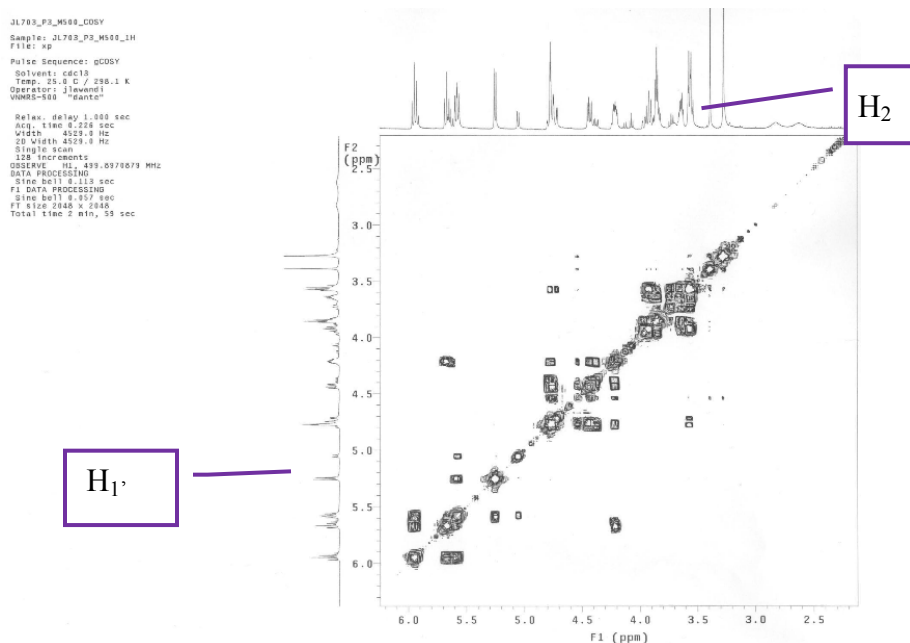


Figure 5.4 COSY of 5-31.

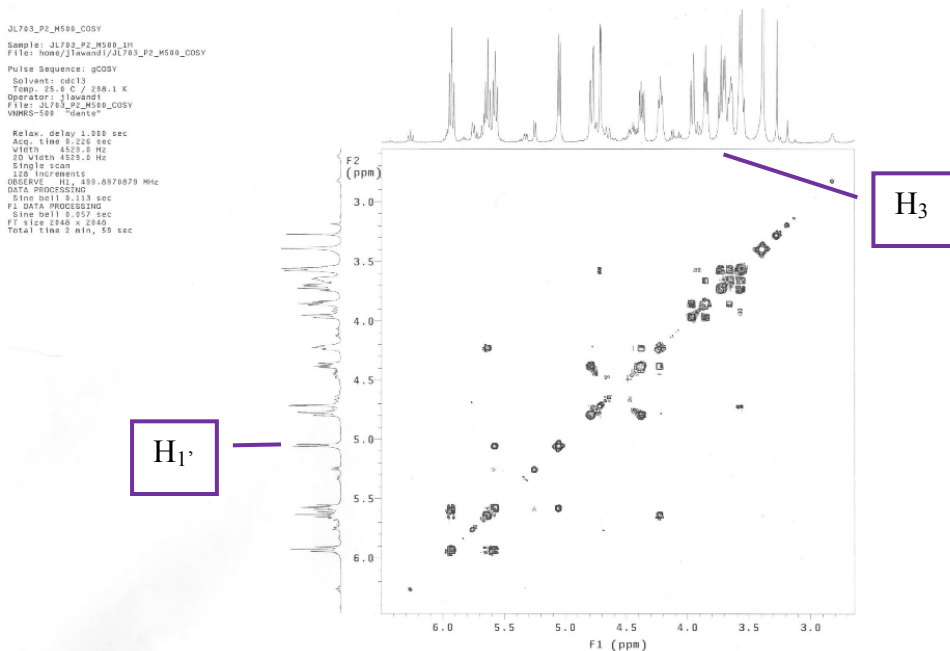


Figure 5.5 COSY of 5-32.

We also performed HSQC experiments (for example, Figure 5.6 and Figure 5.7, as well as others given in the Appendix), correlating ^1H and ^{13}C which are covalently bound. These experiments allowed us to attribute each of the protons

of the disaccharide to a signal in the ^{13}C -NMR spectra and therefore to assign each of the carbon peaks.

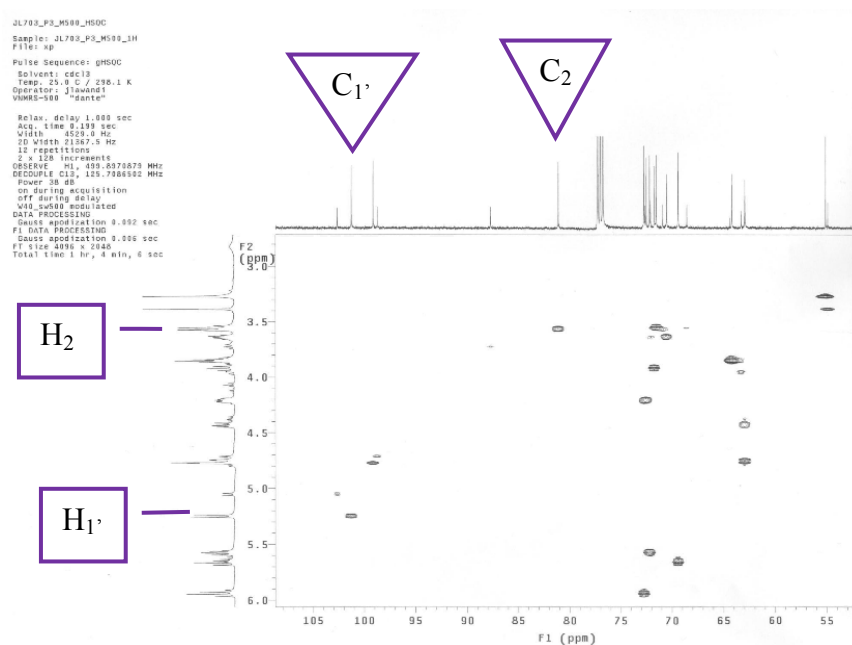


Figure 5.6 HSQC of 5-31.

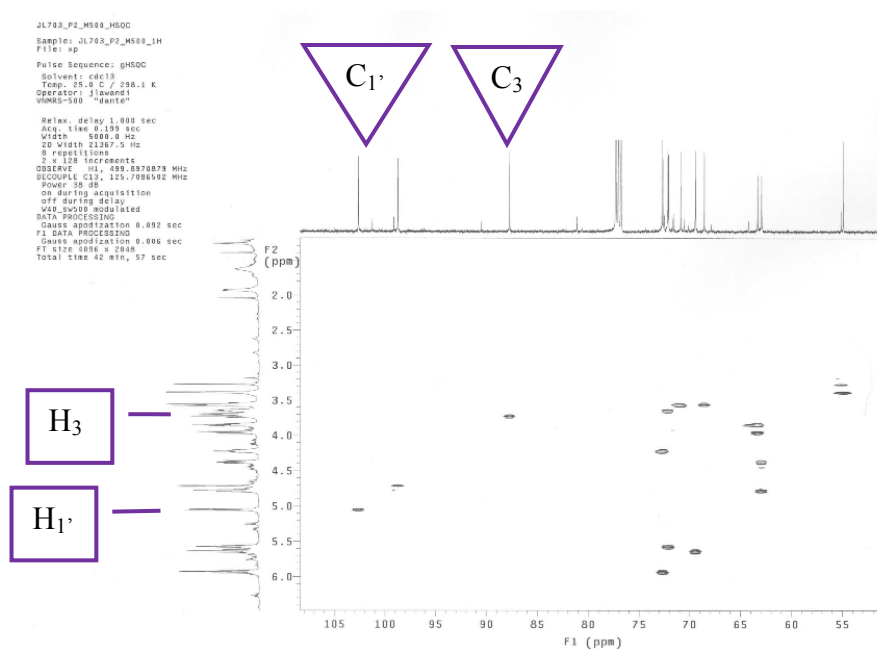


Figure 5.7 HSQC of 5-32.

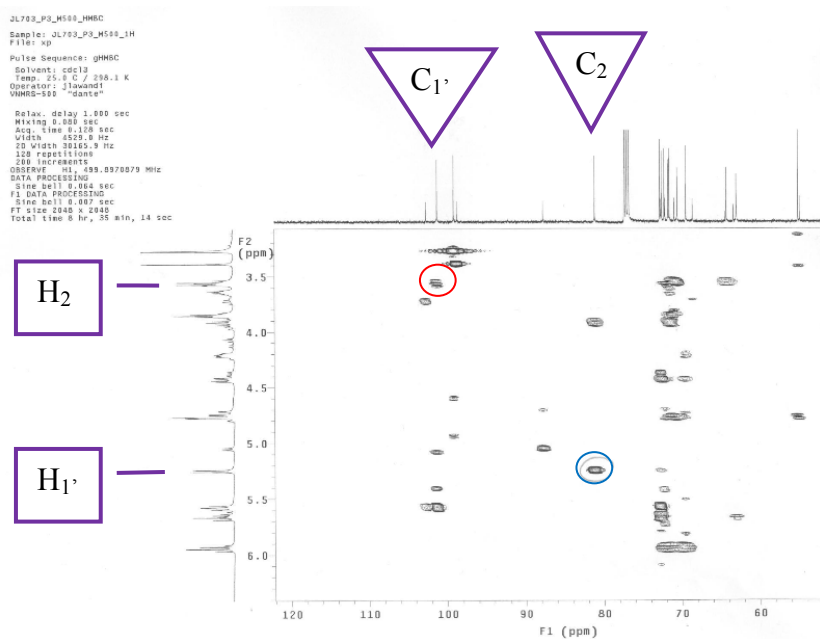


Figure 5.8 HMBC of 5-31. In red, the interaction of C2 with H1' is circled and in blue, the interaction of C1' with H2 is circled.

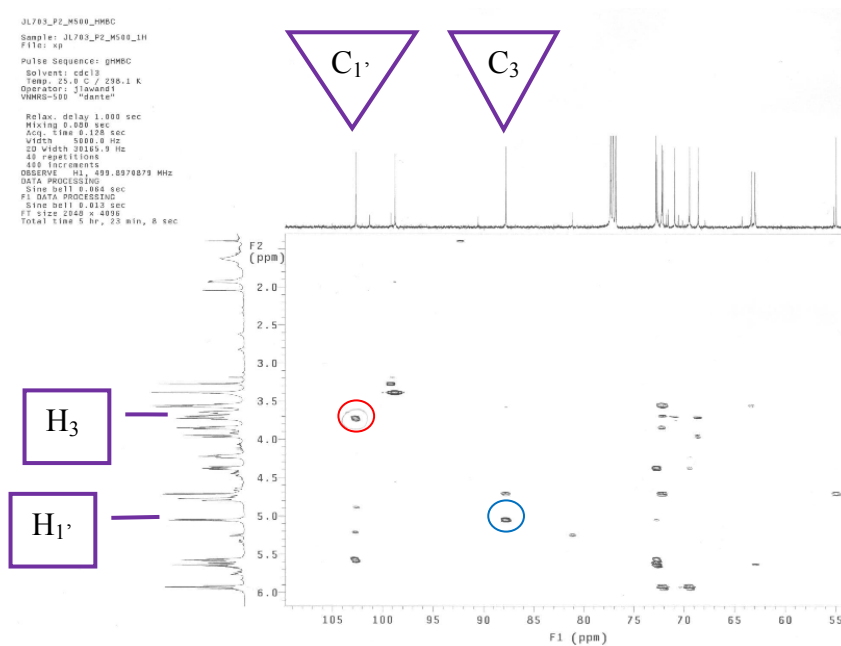
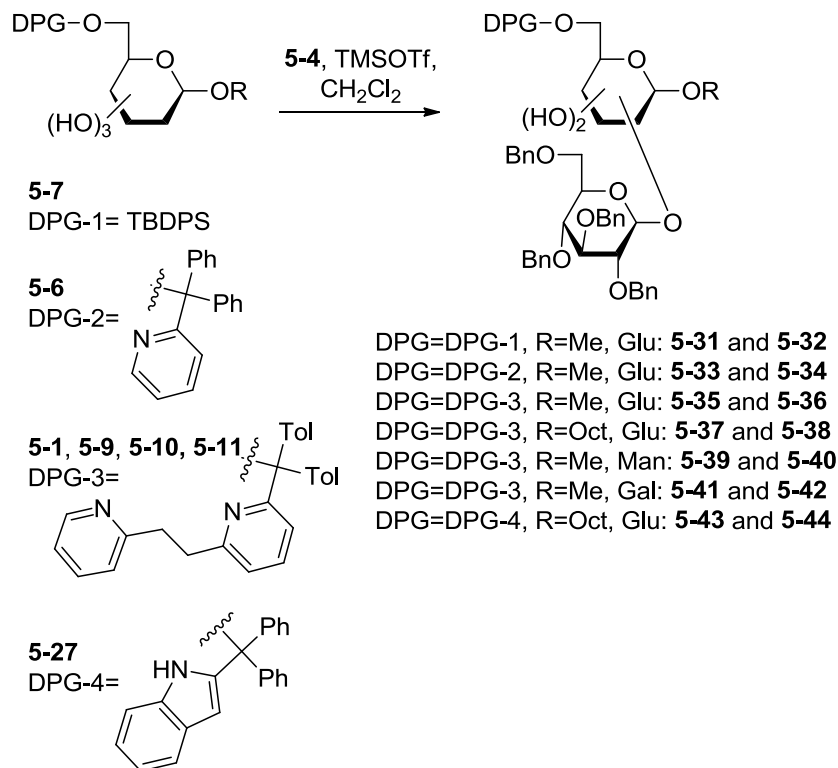


Figure 5.9 HMBC of 5-32. In red, the interaction of C1' with H3 is circled and in blue, the interaction of C3 with H1' is circled

Finally, HMBC (for example, Figure 5.8 and Figure 5.9, as well as others given in the Appendix) reveal correlations between ^1H and ^{13}C which are weakly

coupled (2 or 3 bonds apart). Combined, these experiments helped us identify at which position of the acceptor is attached the donor.

The results of our initial experiments are summarized in Table 5.4. As expected, when we applied our optimized glycosylation method with portion-wise addition of donor **5-4** and TMSOTf, we obtained one single product with both **5-1** and **5-9** in high yields (80-90% isolated yield, entries 3-5). Clearly, the 6-O-di-pyridyl-protected sugars were vastly more selective than the 6-O-protected sugar bearing a TBDPS group (entries 3-5 vs. entry 1). Furthermore, in agreement with the results of Chapter 4, **5-9** was slightly less reactive than **5-1**, while **5-10** and **5-11** were significantly less reactive and in fact hardly reacted at all (entries 6 and 7). Interestingly, from the 2D-NMR studies of all the disaccharides formed, we discovered that both the disaccharides formed in entries 3, 4 and 5 were attached via a 1,3-glycosidic linkage, and not the 1,2-link we were expecting from our previous results with the benzylated donor. Unfortunately, the sugar bearing a hydrogen bond donating indole ring proved to be unstable under our glycosylation conditions, leading to decomposition of the starting material within seconds of adding the Lewis acid to the reaction mixture (entry 8).

Table 5.4 Results of glycosylation experiments performed with 2,3,4,6-tetrabenzoylated glucopyranose trichloroacetimidate (5-4).^{*§}

Entry	Starting material	Reaction temp °C	2- <i>O</i>	3- <i>O</i>	2- <i>O</i> (%) ^a	3- <i>O</i> (%) ^a	SM (%) ^a
1	5-7	-50	5-31	5-32	18	20	62
2	5-6	-50	5-33	5-34	Complex mixture		
3	5-1	+5	5-35	5-36	nd	90	0
4	5-1	-50	5-35	5-36	nd	80	0
5	5-9	-50	5-37	5-38	traces	87	<10
6	5-10	-50	5-41	5-40	nd	nd ^b	>90
7	5-11	-50	5-41	5-42	nd	nd	>90
8	5-27	-50	5-43	5-44	0	0	0 [‡]

^{*} 1,4-glycosylation products were not determined in any of the entries. [§]Yields vary depending on quality of reagents used. [‡] Deprotection of starting material occurred within seconds of adding TMSOTf. ^a Only the β -stereoisomers were isolated.

5.3.3 Effect of pre-incubating the acceptor with TMSOTf prior to reacting with a benzoylated glycosyl donor

For the glycosylations from both Chapter 4 and Chapter 5, performed on the starting materials bearing the directing-protecting groups, we had to treat our crude mixtures with TBAF to remove any TMS groups attached to our products. Given that we only encountered this issue with the sugars bearing the directing-protecting groups, we hypothesized that the terminal pyridyl rings may react with the TMSOTf prior to becoming glycosylated. To test this hypothesis, we titrated **5-1** with increasing amounts of the Lewis acid to see if, in fact, TMS groups were attached to the sugar. The NMR spectra of the resulting mixtures are shown in Figure 5.10.

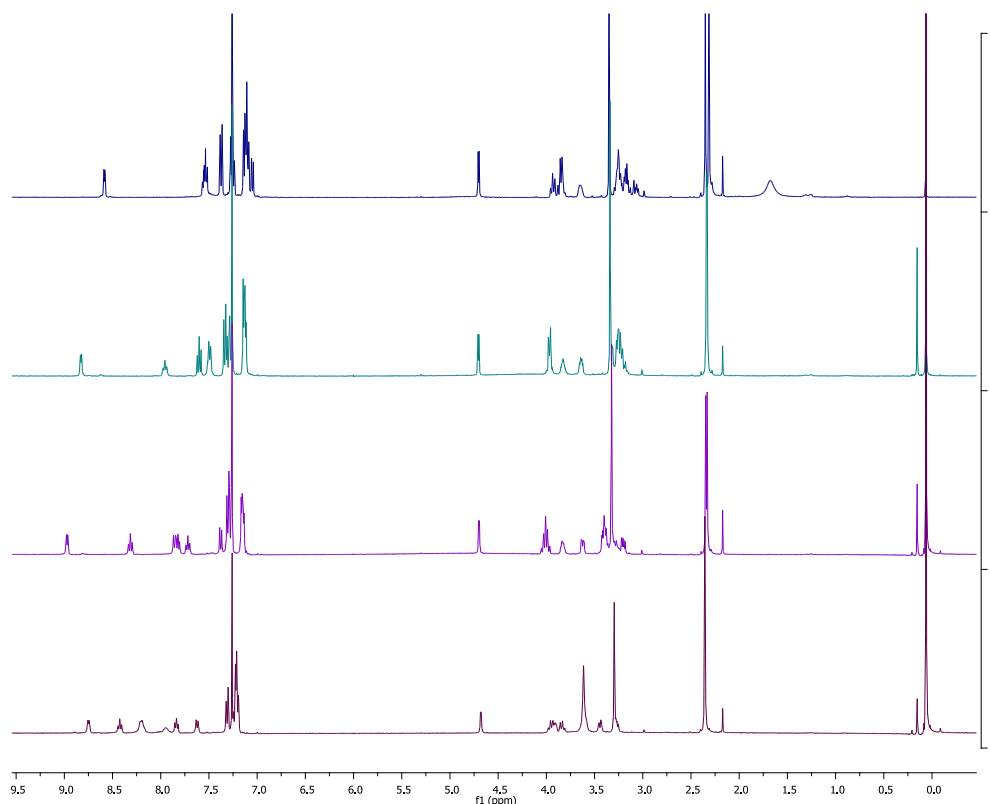
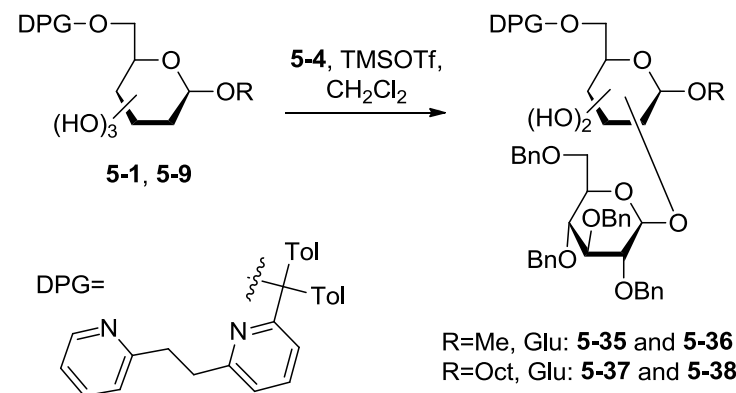


Figure 5.10 NMR titration of the **5-1** with increasing amounts of TMSOTf: 0 equivalents of TMSOTf (indigo), 0.5 equivalents of TMSOTf (teal), 1 equivalent of TMSOTf (purple), 1.5 equivalents of TMSOTf (plum).

From our titration experiment, we clearly see that the presence of TMSOTf affects the entire sugar, including the directing-protecting group. The two tolyl-methyl peaks of the protecting group of **5-1** were clearly distinct from each other by NMR (two singlets at 2.35 and 2.31 ppm, indigo spectrum of Figure 5.10), most likely because the protecting group surrounded and interacted with the asymmetric environment of the sugar. However, with increasing amounts of TMSOTf, these two distinct singlets merge into one (plum spectrum of Figure 5.10), indicating that the protecting group may have moved away from the chiral environment. The aromatic groups of the protecting group were also affected, with noticeable shifts of the ^1H -NMR peaks of the terminal pyridine ring. The TMSOTf also affected the protons of the sugar backbone, which move downfield on the NMR spectra. Although from this information, we can gather that some element (either one of the pyridine ring nitrogen or the sugar hydroxyls) may react with the TMSOTf, we cannot identify the position of the TMS group(s).

Table 5.5 Glycosylation experiment in which the acceptor was pre-incubated with TMSOTf (1 equiv.) prior to adding in the donor (1 equiv.) and more TMSOTf (2-4 equiv.).^{*§}



Entry	Starting material	Reaction temp	2-O	3-O	2-O (%) ^a	3-O (%) ^a	SM (%)
1	5-1	-50°C	5-35	5-36	32	28	40
2	5-9	-50°C	5-37	5-38	16	4	80

^{*} 1,4-glycosylation products were not determined in any of the entries. [§]Yields vary depending on quality of reagents used. ^a Only the β -stereoisomers were isolated.

If the terminal pyridine actually chelates or reacts with the TMSTOf, we expect that position 3 would be less nucleophilic, since the terminal pyridine can no longer activate position 3. This should have an effect on glycosylation, disfavours glycosylation at position 3, but also favours position 2. Therefore, we repeated our glycosylation experiments, this time pre-incubating **5-1** and **5-9** with the Lewis acid, prior to introducing the donor. The results of these experiments are summarized in Table 5.5. As before the 6-*O*-protected methyl α -D-glucopyranoside (**5-1**) was more reactive than the octyl β -D-glucopyranoside (**5-9**) (entry 1 vs. entry 2). However, neither reaction went to completion. Interestingly, by pre-incubating with the Lewis acid, glycosylation at position 2 becomes more prevalent.

5.4 Revised mechanism

Two mechanisms can be envisioned to explain this change in regioselectivity when we switched from the benzylated donor **5-2** to the benzoylated donor **5-4**. In Chapter 4, we proposed two mechanisms that could explain why position 2 of the acceptor was glycosylated with the benzylated donor. The first postulated mechanism begins with the Lewis acid activating the donor, which then reacts with the acceptor. In this case, the regioselectivity would simply be induced by steric effects. Given that the pyridyl rings most likely act as hydrogen bond acceptors interacting with the hydroxyl groups, the bulk of the protecting group around positions 3 and 4 would disavour the reaction at those positions. This is what we observe when we glycosylate our acceptors with the reactive benzylated donor: the sugars react predominantly at position 2, the least hindered position.

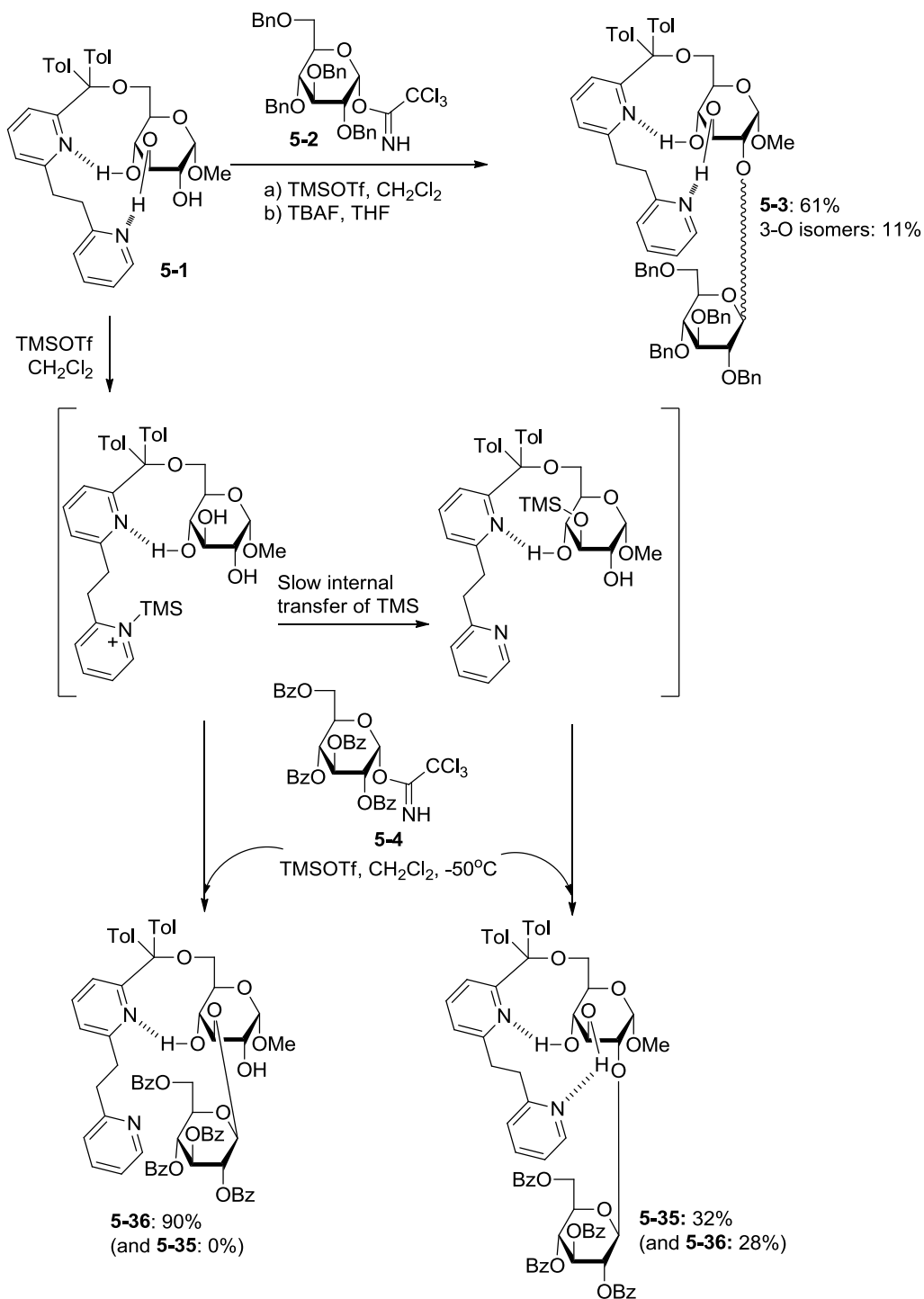


Figure 5.11 Revised postulated mechanism.

The second mechanism would imply the reaction of one of the pyridyl rings with TMSOTf that may be subsequently internally delivered to OH-3, which

would be temporarily protected. Subsequent glycosylation would be regioselective because position 3 was silylated. This would explain the presence of TMS-protected derivatives in the reaction medium (although silylation could also occur after glycosylation). Since the benzylated donors are known to be quite reactive, we expect that the benzylated donor is activated much faster than the Lewis acid / Lewis base reaction. The hydrogen bond between the pyridyl rings and the sugar most likely attenuate the basicity or Lewis basicity of the pyridyl ring. On the other hand, benzoylated glycosyl donors are known to be significantly less reactive.^{1, 2} The most reactive position (position 3 based on previous work⁶) reacts with this unreactive donor. It is also plausible that with this donor, the Lewis acid (TMSOTf) / Lewis base (terminal pyridine ring) reaction may occur more quickly than TMSOTf activation of the donor. In fact, during our experiments, we noted that the acceptor seems unreactive until a full equivalent of TMSOTf is added. It appears that the pyridyl groups may abstract the TMSOTf, prior to its activating the donor, disrupting the hydrogen bond between the pyridyl ring and position 3 and liberating it. Position 3 is now free to react and position 3 is the only position glycosylated. However, if the acceptor is pre-incubated with TMSOTf for a longer period of time and without the presence of any donor, the terminal pyridyl ring may begin to slowly transfer the silyl group from the pyridyl-nitrogen to position 3 of the sugar. Position 3 is therefore no longer available to react and therefore we observed glycosylation of position 2 as well as position 3.

5.5 Conclusion

The pyridyl-based protecting groups used in this chapter are hydrogen bond acceptors which operate by modifying the intramolecular H-bond network observed in non-protected carbohydrates. With our di-pyridyl-based protecting group installed at position 6 of methyl α -D-glucopyranoside, we observed preference for the two 2-O glycosylated isomeric disaccharides when a reactive glycosyl donor was used (Chapter 4). On the other hand, we can selectively

glycosylate at position 3 with a less reactive, benzoylated donor. In fact, with this benzoylated donor, we can selectively form disaccharides at position 3 with isolated yields greater than 80% of only one single stereoisomer. This study clearly demonstrates that these di-pyridyl-based protecting groups, in contrast to traditional protecting groups, can be used in different ways, either to enhance the nucleophilicity of hydroxyl groups, increasing the reactivity at position 3 with small reagents or less reactive glycosyl donors, or to increase the steric hindrance around selected hydroxyls, around positions 3 and 4 for glycosylation with bulky reagents and reactive glycosyl donors.

We have developed a unique strategy to prepare glucose-glucose disaccharides in a highly efficient (yields in the range of 90%), highly regioselective (one single regioisomer) and highly stereoselective (β -anomer only) manner. This methodology improves on all the established methods by providing one single isomer out of the 6 possible in over 80% yield. It also provides a flexible way to produce either 2-O or 3-O isomers starting from the exact same 6-O-protected acceptor.

5.6 Experimental section

5.6.1 General remarks

Solvents were distilled and dried by standard methods; THF and ether, from Na/benzophenone; and CH_2Cl_2 from P_2O_5 . All commercially available reagents were used without further purification. 4 Å molecular sieves were dried at 100°C prior to use. Melting points are uncorrected and recorded with a Büchi capillary tube melting-point apparatus. Optical rotations were measured on a JASCO DIP 140 in a 1dm cell at 20°C. FTIR spectra were recorded using a Perkin Elmer Spectrum One FT-IR. ^1H and ^{13}C NMR spectra were recorded on Varian mercury 400 MHz, 300 MHz or Unity 500 spectrometers. Chemical shifts are reported in ppm using the residual of chloroform as internal standard (7.260 ppm for ^1H and 77.16 ppm for ^{13}C). Mass spectra were recorded on either a Trio 1000 Thermo

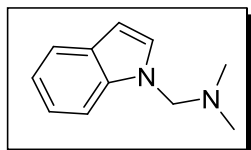
Quest spectrometer in the electron impact mode or a Platform Micromass in the electrospray mode or EI Peak matching (70 eV) on a Kratos MS25 RFA Double focusing mass spectrometer or by ESI on a IonSpec 7.0 tesla FTMS at McGill University. Analytical thin-layer chromatography was performed on Silicycle 60F254 pre-coated silica gel plates. TLC visualization was performed by UV or by development using KMnO₄, H₂SO₄/MeOH or Mo/Ce solutions. Chromatography was performed on silica gel 60 (230-40 mesh).

5.6.2 Synthesis

Synthesis of hydrogen-bond donating protecting group and its coupling to a sugar and other 6-O-protected sugars not mentioned in Chapter 4

1-[(N,N-dimethylamino)methyl]indole (5-13)³

To a suspension of indole **5-12** (5 g, 0.04 mol) in water (15 mL) was added formaldehyde (3.2 mL, 37% aqueous solution) and dimethylamine (4.5 mL, 40% aqueous solution) over 30 min at 0 °C. The mixture was stirred for 3 h, then warmed to rt overnight. The solution was extracted twice with diethyl ether, and the organic phases were combined and extracted with a 2 N HCl solution. The acid extracts were made alkaline with 40 % NaOH solution, then extracted with diethyl ether, dried over Na₂SO₄, filtered, concentrated *in vacuo* to give **5-13** as a clear oil which was directly used in the next step.



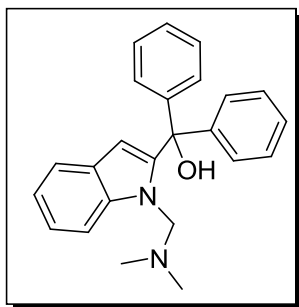
C₁₁H₁₄N₂, Mol. Wt. = 174.24

R_f = 0.5 (Tol)

¹H NMR (400 MHz, CDCl₃) δ 7.64 (d, *J* = 7.9, 1H), 7.47 (d, *J* = 7.7, 1H), 7.25-7.18 (m, 1H), 7.15 (d, *J* = 3.2, 1H), 7.12 (ddd, *J* = 2.5, 4.8, 12.0, 2H), 6.57-6.44 (m, 1H), 4.77 (s, 2H), 2.32 (s, 6H).

[1-[(N,N-dimethylamino)methyl]indol-2-yl]diphenyl-methanol (5-14)³

To a solution of **5-13** (4.01 g, 23 mmol) dissolved in freshly distilled THF (60 mL) under argon was added butyllithium (50 mmol, 31.25 mL, 1.6M in hexane) dropwise over 5 min at -78 °C. The resulting yellow solution was stirred for another 10 min at -78 °C, then warmed to 0 °C over 45 min. The solution was re-cooled to -78 °C and then a solution of benzophenone (9.1 g, 50 mmol in 10 mL THF) was added dropwise. The solution turned dark green. The mixture was stirred for 1 h at -78 °C and then warmed to rt overnight. After quenching with water and extracting with diethyl ether, the organic layer was dried over Na₂SO₄, filtered, concentrated *in vacuo* to give **5-14** as white granules (from CHCl₃-hexane) after a quick filtration through silica (1.4 g, 17 % yield).



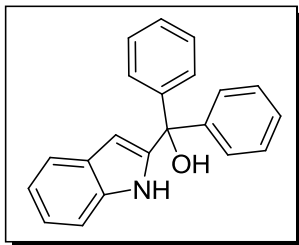
C₂₄H₂₄N₂O, Mol. Wt. = 356.46

R_f = 0.6 (H/EA, 8:2)

¹H NMR (400 MHz, CDCl₃) δ 9.01 (s, 1H), 7.54-7.45 (m, 6H), 7.41-7.28 (m, 6H), 7.20 (t, *J* = 7.3, 1H), 7.08 (t, *J* = 7.4, 1H), 5.86 (s, 1H), 4.11 (s, 2H), 2.16 (d, *J* = 13.0, 6H).

Indol-2-yl-diphenylmethanol (**5-15**)³

To a solution of N-protected indole **5-14** (500 mg, 1.4 mmol) dissolved in ethanol/THF (1:1), was added a large excess of sodium borohydride (65 g, 1.7 mmol). The mixture was refluxed for several hours, then concentrated *in vacuo*. The residue was treated with water, extracted with EtOAc and dried over Na₂SO₄, filtered, concentrated *in vacuo* to yield the product following column chromatograph (CHCl₃) and precipitation to **5-15** as a white powder (171 mg, 41 % yield) with hexanes.



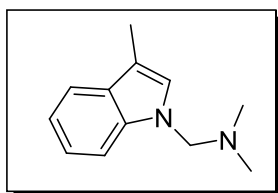
$C_{21}H_{17}NO$, Mol. Wt. = 299.37

$R_f = 0.7$ (H/EA, 8:2)

1H NMR (400 MHz, $CDCl_3$) δ 8.36 (s, 1H), 7.57 (d, $J = 7.7$, 1H), 7.36 (s, 11H), 7.27–7.06 (m, 2H), 6.15 (s, 1H), 3.15 (s, 1H).

3-methyl-1-[(N,N-dimethylamino)methyl]indole (5-19)

To a suspension of 3-methyl-indole **5-18** (1 g, 8 mmol) in water/dioxane (1:1, 4 mL) was added formaldehyde (0.6 mL, 37% aqueous solution) and dimethylamine (1 mL, 40% aqueous solution) over 30 min at 0 °C. The mixture was stirred for 3 h, then warmed to rt overnight. The solution was extracted twice with diethyl ether, and the organic phases were combined and extracted with a 2 N HCl solution. The acid extracts were made alkaline with 40 % NaOH solution, then extracted with diethyl ether, dried over Na_2SO_4 , filtered, concentrated *in vacuo* to give **5-19** as a clear oil (1.1 g, 65 % yield) which was directly used in the next step.



$C_{12}H_{16}N_2$, Mol. Wt. = 188.27

$R_f = 0.3$ (H/EA, 9:1)

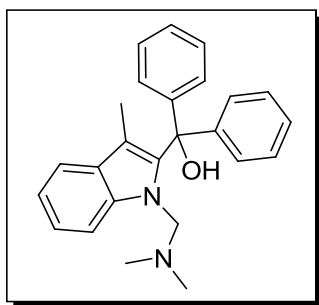
IR (neat/NaCl) 3453 cm^{-1}

1H NMR (200 MHz, $CDCl_3$) δ 7.57 (d, $J = 7.5$, 1H), 7.41 (d, $J = 8.0$, 1H), 7.28 – 7.06 (m, $J = 8.4$, 14.8, 15.3, 2H), 6.93 (s, 1H), 4.70 (s, 2H), 2.33 (s, 3H), 2.30 (s, 6H).

[3-methyl-1-[(N,N-dimethylamino)methyl]indol-2-yl]diphenyl-methanol (5-20)

To a solution of **5-19** (1.0 g, 5.3 mmol) dissolved in freshly distilled THF (15 mL) under argon was added butyllithium (10 mmol, 6.7 mL, 1.6M in hexane) dropwise over 5 min at -78 °C. The resulting yellow solution was stirred for another 10 min

at -78 °C, then warmed to 0 °C over 45 min. The solution was recooled to -78 °C and then a solution of benzophenone (1.92 g, 10 mmol in 2 mL THF) was added dropwise. The solution turned dark green. The mixture was stirred for 1 h at -78 °C and then warmed to rt overnight. After quenching with water and extracting with diethyl ether, the organic layer was dried over Na₂SO₄, filtered, concentrated *in vacuo* to give **5-20** as white granules (from CHCl₃-hexane) after a quick filtration through silica (1.3 g, 65 % yield).



C₂₅H₂₆N₂O, Mol. Wt. = 370.49

R_f = 0.6 (H/EA, 7:3)

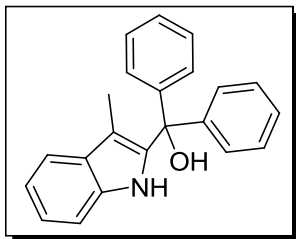
IR (CHCl₃) 3453 cm⁻¹

¹H NMR (300 MHz, CDCl₃) δ 7.57-7.40 (m, 5H), 7.33 (dt, *J* = 3.8, 12.1, 6H), 7.28-7.19 (m, 2H), 7.12 (dd, *J* = 4.3, 11.0, 1H), 4.08 (s, 2H), 2.26-2.09 (m, 7H), 1.35 (s, 3H).

¹³C NMR (75 MHz, CDCl₃) δ 146.68, 139.40, 137.64, 128.99, 128.19, 128.13, 128.08, 127.41, 122.73, 119.44, 119.33, 112.73, 108.65, 78.00, 65.60, 41.39, 9.25.

3-Methylindol-2-ylidiphenylmethanol (**5-21**)

To a solution of N-protected indole **5-20** (426 mg, 1.25 mmol) dissolved in ethanol/THF (1:1, 5 mL), was added sodium borohydride (48 mg, 1.3 mmol). The mixture was refluxed for several hours, then concentrated *in vacuo*. The residue was treated with water, extracted with EtOAc and dried over Na₂SO₄, filtered, concentrated *in vacuo* to yield the product following column chromatograph (CHCl₃) and precipitation to **5-21** as a white powder with hexanes (361 mg, 92 % yield).



$C_{22}H_{19}NO$, Mol. Wt. = 313.39

R_f = 0.25 (H/EA, 8:2)

IR ($CHCl_3$) 3534, 3448 cm^{-1}

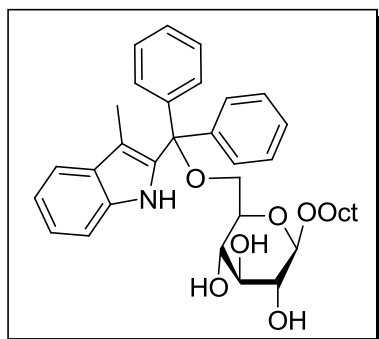
1H NMR (300 MHz, $CDCl_3$) δ 8.08 (s, 1H), 7.56 (d, J = 7.6, 1H), 7.37 (s, 9H), 7.32-6.97 (m, J = 7.4, 17.8, 19.0, 4H), 2.98 (s, 1H), 1.89 (d, J = 0.8, 3H).

^{13}C NMR (75 MHz, $CDCl_3$) δ 144.99, 137.77, 134.27, 129.97, 128.44, 128.00, 127.65, 122.19, 119.34, 118.78, 110.96, 108.81, 79.27, 9.68.



Octyl 6-*O*-3-methylindol-2-ylidiphenylmethyl- β -D-glucopyranoside (**5-27**)

To a stirred solution of **5-21** (350 mg, 1.1 mmol) in DCM (10 mL) was added octyl β -D-glucopyranoside **5-26** (162 mg, 0.56 mmol) every 30 min for a total of 8 additions and $Yb(OTf)_3$ (34 mg, 0.05 mmol) ever 2 hours for a total of 2 additions. The resulting mixture was stirred overnight at rt, then concentrated *in vacuo*. The resulting residue was purified by column chromatography (H/EA gradient, from 8:2 to 1:1) to yield **5-27** as a brown solid (35% yield).



$C_{36}H_{45}NO_6$, Mol. Wt. = 587.75

R_f = 0.22 (H/EA, 1:1)

IR ($CHCl_3$) 3367 cm^{-1}

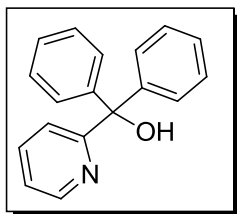
$[\alpha]_D = -28.5$ (c 0.2, $CHCl_3$)



Methyl 6-*O*-(diphenyl-(2-pyridyl)methanol)⁶

To a flask containing butyllithium (28 mL, 0.044 mol) was added a solution 2-bromopyridine (6.66g, 0.042 mol) in diethyl ether (125 mL) at -78 °C. The resulting solution was stirred for 1 h (turned dark orange). A solution of benzophenone (8.2 g, 0.045 mol) in diethyl ether (50 mL) was added dropwise (color change to light yellow) at -78 °C. The resulting mixture was stirred

overnight at rt. Then diluted with CH_2Cl_2 , and then washed with HCl (5 % aqueous). The aqueous extract was washed with diethyl ether, then neutralized with saturated NaHCO_3 aqueous solution, then made basic to pH 9 with aqueous 5M NaOH, and extracted with diethyl ether. The combined organic extracts were washed with water, dried over Na_2SO_4 , filtered, concentrated *in vacuo* to give a white solid after washing with methanol and filtering off the yellow filtrate (8.06g, 73% yield).



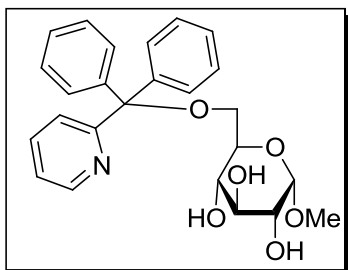
$\text{C}_{18}\text{H}_{15}\text{NO}$, Mol. Wt. = 261.32

$R_f = 0.5$ (H/EA, 1:1)

^1H NMR (400 MHz, CDCl_3) δ 8.60 (ddd, $J = 1.0, 1.7, 4.8$, 1H), 7.64 (td, $J = 1.8, 7.7$, 1H), 7.33-7.27 (m, 10H), 7.16-7.04 (m, 1H), 6.32-6.27 (m, 1H).

Methyl 6-*O*-(diphenyl(2-pyridyl)methyl) α -D glucopyranoside (5-6)⁶

To a slurry of NaH (0.5g, 0.126 mol) in THF was added dropwise at 0 °C a solution of methyl 6-*O*-(diphenyl(2-pyridyl)methanol (2.2 g, 0.0084 mol) in THF. The resulting solution was stirred for 1 h at 0 °C, then SOCl_2 (0.8 mL, 0.011 mol) was added. The solution was warmed to rt over 5 h, diluted with CHCl_3 , washed with aqueous, saturated NaHCO_3 , water and brine, dried over Na_2SO_4 , filtered, concentrated *in vacuo*. To the residue was added a solution of glucopyranoside (4.9 g, 0.025 mol) in pyridine. The resulting solution was stirred for 5 days, then concentrated *in vacuo*, redissolved in CH_2Cl_2 , washed with water, brine dried over Na_2SO_4 , filtered, concentrated *in vacuo*. Following column chromatography (DCM, then DCM/MeOH, 19:1), the oil was precipitated with DCM-hexanes to give a white powder after drying (0.563 g, 15% yield).



$C_{25}H_{27}NO_6$, Mol. Wt. = 437.48

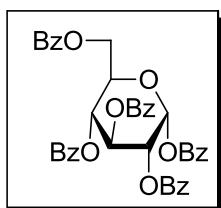
$R_f = 0.3$ (CH_2Cl_2 , CH_3OH)

1H NMR (400 MHz, $CDCl_3$) δ 8.54 (d, $J = 4.1$, 1H), 7.65 (td, $J = 1.8$, 7.9, 2H), 7.45 (d, $J = 7.6$, 4H), 7.41-7.32 (m, 8H), 7.32-7.28 (m, 4H), 7.21 (dd, $J = 5.0$, 7.5, 2H), 4.76 (d, $J = 3.9$, 1H), 4.06 (t, $J = 9.4$, 1H), 3.85 (t, $J = 9.3$, 1H), 3.75-3.58 (m, 4H), 3.30 (s, $J = 16.1$, 4H), 2.89 (s, 1H), 2.16 (d, $J = 9.2$, 1H).

Synthesis of the glycosyl donor

1,2,3,4,6-perbenzoylated α/β -D-glucopyranoside (5-29)

To a solution of **5-28** (5.7 g, 0.032 mol) in pyridine (125 mL) was added dropwise $BzCl$ (24 mL, 0.20 mol) at $0^\circ C$. The solution was slowly warmed to rt and stirred overnight. The crude mixture was diluted with water, then extracted with EA, washed with HCl (5% aq.), brine, dried over Na_2SO_4 , filtered, concentrated *in vacuo* to yield a colorless oil (quant. yield).



$C_{41}H_{32}O_{11}$; Mol. Wt. = 700.69

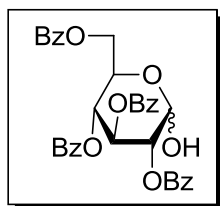
$R_f = 0.8$ (H/EA, 2:1)

1H NMR (300 MHz, $CDCl_3$) δ 8.21 – 8.10 (m, 3H), 8.07 – 7.99 (m, 2H), 7.98 – 7.92 (m, 2H), 7.89 (d, $J = 7.3$, 3H), 7.76 – 7.41 (m, 9H), 7.41 – 7.27 (m, 6H), 6.86 (d, $J = 3.7$, 1H), 6.33 (t, $J = 10.0$, 1H), 5.87 (t, $J = 9.9$, 1H), 5.69 (dd, $J = 3.7$, 10.3, 1H), 4.68 – 4.56 (m, 2H), 4.54 – 4.41 (m, $J = 4.8$, 12.8, 1H).

2,3,4,6-perbenzoylated α/β -D-glucopyranose (5-30)

To a solution of **5-29** (0.032 mol) in THF (200 mL) was added methylamine (13.4 mL, 40% aq. solution) dropwise at $0^\circ C$. The resulting mixture was stirred for 2 h

at 0°C, diluted with Tol and concentrated *in vacuo*. The crude residue was purified by column chromatography (H/EA, 100:25, then 100:35) to yield a brown foam (84% yield).



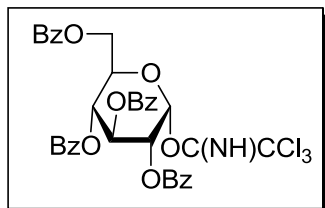
$C_{34}H_{28}O_{10}$; Mol. Wt. = 596.58

$R_f = 0.2$ (H/EA, 2:1)

1H NMR (500 MHz, $CDCl_3$) δ 8.10 (d, $J = 7.1$, 2H), 8.08-8.04 (m, 2H), 7.98 (dd, $J = 6.1$, 7.5, 2H), 7.93 (dd, $J = 7.6$, 9.0, 2H), 7.91-7.84 (m, 2H), 7.61 (t, $J = 7.4$, 1H), 7.58-7.45 (m, 5H), 7.45-7.33 (m, 8H), 7.29 (t, $J = 7.8$, 1H), 6.25 (t, $J = 9.9$, 1H), 5.79-5.71 (m, 2H), 5.32 (dd, $J = 3.6$, 10.2, 1H), 4.73-4.62 (m, 2H), 4.46 (dd, $J = 4.3$, 12.1, 1H).

2,3,4,6-tetra-*O*-benzoyl α -D-glucopyranosyl trichloroacetimidate (5-4)

To a solution of 2,3,4,6-tetra-*O*-benzoyl α/β -D-glucopyranose (1.08 g, 0.0018 mol) in CH_2Cl_2 (10 mL) was added trichloroacetonitrile (0.85 mL, 0.085 mol) and K_2CO_3 (0.89 g, 0.0064 mol). The resulting solution was stirred at room temperature for 4 to 6 days, then filtered through Celite and concentrated *in vacuo*. The residue was used without further purification (1.25 g, 94% yield).



$C_{36}H_{28}Cl_3NO_{10}$; Mol. Wt. = 740.97

$R_f = 0.7$ (H/EA, 2:1)

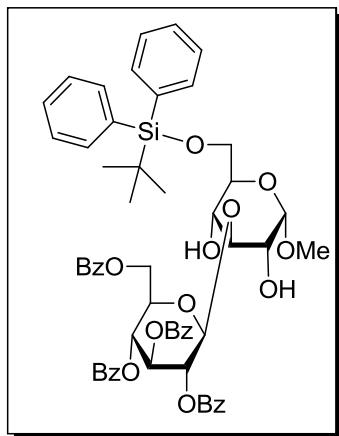
1H NMR (400 MHz, $CDCl_3$) δ 8.63 (s, 1H), 8.08-8.00 (m, 3H), 8.00-7.91 (m, 5H), 7.91-7.83 (m, 3H), 7.54 (dt, $J = 7.4$, 19.8, 4H), 7.43 (dd, $J = 5.1$, 10.2, 5H), 7.37 (t, $J = 7.7$, 5H), 7.30 (t, $J = 7.7$, 3H), 6.83 (d, $J = 3.7$, 1H), 6.27 (t, $J = 10.0$, 1H), 5.82 (t, $J = 9.8$, 1H), 5.62 (dd, $J = 3.7$, 10.2, 1H), 4.69-4.59 (m, 2H), 4.48 (dd, $J = 5.5$, 12.9, 1H).

Glycosylations

General procedure. To a solution of the acceptor (0.50 mmol) in dry CH_2Cl_2 (50 mL) was added a freshly prepared solution of TMSOTf (2 mL, 0.1 M) and a freshly prepared solution of glucopyranosyl trichloroacetimidate **5-4** (2 mL, 0.50 mmol, 0.25 M) at -50°C . The resulting mixture was stirred for 1 h. This protocol was repeated two to three times (TMSOTf, 2 x 2 mL, trichloroacetimidate **8**, 2 x 2 mL). After stirring for a further 3 hours at -50°C , the reaction was quenched with a drop of Et_3N . The resulting mixture was diluted with CH_2Cl_2 , washed with 1M NaHCO_3 and brine, dried over MgSO_4 and concentrated *in vacuo*. The crude mixture was next treated with TBAF in THF to cleave any silyl ethers formed (except in the case of reaction mixtures from **5-7**). The solution was concentrated and the residue was purified by column chromatography (H/EA, gradient from 7:3 to 1:1) to afford the corresponding products.

(6-*O*-[*t*-butyl-di-phenyl-silyl]-methyl 2-*O*-(2',3',4',6'-tetra-*O*-benzoyl- β -D-glucopyranosyl)- α -D-glucopyranoside (5-31**) and (6-*O*-[*t*-butyl-di-phenyl-silyl]-methyl 3-*O*-(2',3',4',6'-tetra-*O*-benzoyl- β -D-glucopyranosyl)- α -D-glucopyranoside (**5-32**))**

Following the general glycosylation procedure, **5-7** (1 equiv.) was reacted with **5-4** (1 equiv.) yielding both **5-31** and **5-32** (18% : 20%, **5-31/5-32**).



$\text{C}_{57}\text{H}_{88}\text{O}_{15}\text{Si}$, Mol. Wt. = 1011.15

R_f = 0.3 (H/EA, 7:3)

IR (CHCl_3) 3494, 1724 cm^{-1}

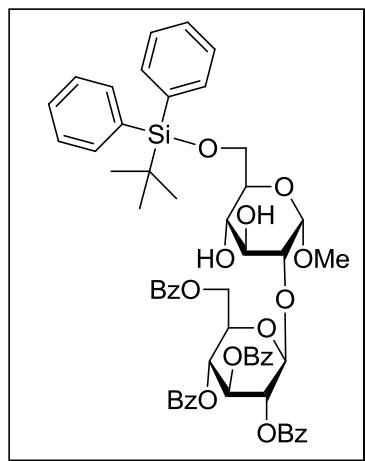
$[\alpha]_D = +54.7$ (c 0.12, CHCl_3)

^1H NMR (500 MHz, CDCl_3) δ 8.08 (d, J = 7.9, 2H), 7.98 (d, J = 7.8, 2H), 7.93 (d, J = 7.7, 2H), 7.83 (d, J = 7.8, 2H), 7.70 (t, J = 7.3, 4H), 7.51 (dt, J = 6.7, 9.4, 3H), 7.47-7.27 (m, 19H), 5.93 (t, J = 9.6, 1.1H), 5.64 (t, J = 9.7, 1H), 5.61-5.54 (m,

1.2H), 5.35-5.30 (m, 0.2H), 5.25 (d, $J = 7.8$, 0.2H), 5.05 (d, $J = 7.9$, 1H), 4.78 (d, $J = 12.2$, 1.2H), 4.72 (d, $J = 3.8$, 1H), 4.67-4.63 (m, 0.2H), 4.50-4.41 (m, 0.4H), 4.38 (dd, $J = 6.7$, 12.1, 1H), 4.26-4.19 (m, 1.2H), 4.14-4.04 (m, 0.2H), 3.96 (d, $J = 10.7$, 1H), 3.93-3.89 (m, 0.2H), 3.85 (dd, $J = 5.5$, 10.8, 1.2H), 3.72 (dd, $J = 8.0$, 17.1, 2H), 3.68-3.63 (m, $J = 5.4$, 1.2H), 3.59-3.53 (m, $J = 9.0$, 2H), 3.39 (s, 3H), 3.27 (s, 0.5H), 2.82 (s, 0.2H), 2.64 (s, 0.2H), 1.92 (d, 0.7H), 1.05 (s, 10H).

^{13}C NMR (126 MHz, CDCl_3) δ 166.37, 166.29, 166.24, 165.96, 165.91, 165.82, 165.55, 165.40, 165.35, 165.33, 136.01, 135.81, 135.80, 135.75, 135.64, 133.83, 133.74, 133.72, 133.68, 133.61, 133.58, 133.55, 133.45, 133.38, 133.26, 130.22, 130.13, 130.03, 130.00, 129.96, 129.89, 129.83, 129.68, 129.67, 129.47, 129.39, 129.30, 129.16, 129.10, 129.05, 128.86, 128.81, 128.68, 128.67, 128.61, 128.60, 128.54, 128.52, 128.46, 128.41, 128.16, 127.86, 127.84, 127.71, 102.78, 101.39, 99.27, 98.86, 90.62, 87.86, 81.24, 77.41, 72.88, 72.77, 72.64, 72.35, 72.32, 72.28, 72.21, 71.82, 71.67, 71.01, 70.63, 70.23, 69.59, 69.52, 68.66, 67.97, 64.33, 63.42, 63.05, 55.21, 55.00, 36.77, 27.06, 26.92, 24.82, 19.47, 19.37.

HRMS (ESI+) calc'd for $[\text{C}_{57}\text{H}_{58}\text{O}_{15}\text{Si} + \text{Na}]^+$: 1033.34372. Found: 1033.34436.



$\text{C}_{57}\text{H}_{58}\text{O}_{15}\text{Si}$, Mol. Wt. = 1011.15

$R_f = 0.2$ (H/EA, 7:3)

IR (CHCl_3) 3494, 1724 cm^{-1}

$[\alpha]_D = +43.4$ (c 0.17, CHCl_3)

^1H NMR (500 MHz, CDCl_3) δ 8.06 (d, $J = 8.2$, 2H), 7.97 (d, $J = 7.1$, 2H), 7.93 (d, $J = 7.3$, 2H), 7.83 (d, $J = 5.8$, 2H), 7.71-7.65 (m, 5H), 7.55-7.49 (m, 4H), 7.45-7.33 (m, 17H), 7.30 (dd, $J = 8.3$, 16.5, 4H), 5.95 (t, $J = 9.6$, 1H), 5.67 (t, $J = 9.7$, 1H), 5.58 (dd, $J = 7.9$, 9.8, 1H), 5.25 (d, $J = 7.9$, 1H), 5.05 (d, $J = 7.9$, 0.3H), 4.77 (d, $J = 3.2$, 2H), 4.73 (dd, $J = 3.3$, 15.1, 1H), 4.43 (dd, $J = 5.8$, 12.2, 1H), 4.40-

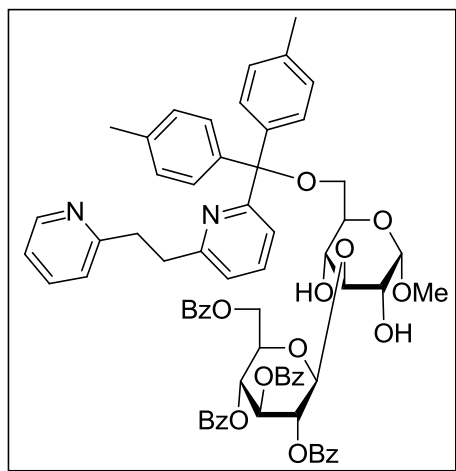
4.34 (m, $J = 12.4$, 0.4H), 4.23-4.18 (m, $J = 6.5$, 0.2H), 4.07 (t, $J = 6.8$, 0H), 3.93 (dd, $J = 7.1$, 16.3, 1H), 3.85 (t, $J = 4.8$, 2H), 3.76-3.69 (m, $J = 9.1$, 0.5H), 3.66-3.61 (m, 1H), 3.58-3.54 (m, 2H), 3.39 (s, 0.8H), 3.27 (s, 3H), 1.04 (s, 11H).

^{13}C NMR (126 MHz, CDCl_3) δ 166.29, 166.24, 165.91, 165.82, 165.55, 165.35, 165.33, 135.81, 135.80, 135.75, 133.83, 133.74, 133.72, 133.68, 133.61, 133.54, 133.44, 133.38, 133.27, 133.26, 130.13, 130.03, 130.00, 129.95, 129.91, 129.90, 129.88, 129.68, 129.67, 129.47, 129.39, 129.15, 128.86, 128.80, 128.66, 128.61, 128.60, 128.46, 128.41, 127.85, 127.84, 127.71, 102.77, 101.39, 99.27, 98.86, 87.86, 81.24, 72.88, 72.76, 72.64, 72.32, 72.28, 72.21, 71.83, 71.66, 71.01, 70.64, 69.53, 68.66, 64.33, 63.42, 63.07, 55.21, 55.00, 36.77, 26.94, 26.92, 24.82, 19.46, 19.37.

HRMS (ESI+) calc'd for $[\text{C}_{57}\text{H}_{58}\text{O}_{15}\text{Si} + \text{Na}]^+$: 1033.34372. Found: 1033.34419.



(6-*O*-[6-(2-pyridin-2-yl-ethyl)-pyridin-2-yl]-di-*p*-tolyl-methyl-methyl 3-*O*-(2',3',4',6'-tetra-*O*-benzoyl- β -D-glucopyranosyl)- α -D-glucopyranoside (5-36)
Following the general glycosylation procedure, **5-1** was reacted with **5-4** yielding only **5-36** (90% yield).



$\text{C}_{68}\text{H}_{64}\text{N}_2\text{O}_{15}$, Mol. Wt. = 1149.24

$R_f = 0.3$ (H/EA, 4:6)

IR (CHCl_3 , cm^{-1}): 3489, 1730

$[\alpha]_D = +59.8$ (c 0.11, CHCl_3)

^1H NMR (400 MHz, CDCl_3) δ 8.50 (d, $J = 4.8$, 1H), 7.99 (dd, $J = 7.3$, 12.3, 5H), 7.92 (d, $J = 7.3$, 3H), 7.83 (d, $J = 7.3$, 2H), 7.59-7.17 (m, 28H), 7.05 (t, $J = 8.5$, 6H), 6.84 (t, $J = 8.3$, 2H), 5.91 (t, $J = 9.7$, 1H), 5.65-5.52 (m, 2H), 5.11 (d, $J = 8.0$, 1H), 4.75 (dd, $J = 3.3$, 8.7, 2H), 4.35 (dd, $J = 6.5$, 12.2, 1H), 4.18 (ddd, $J = 2.7$,

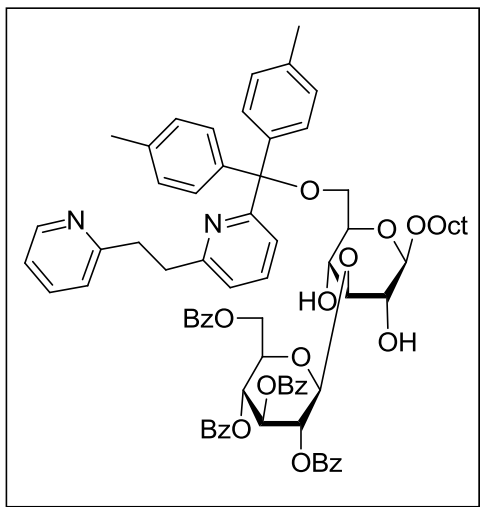
6.4, 9.4, 1H), 4.04 (s, 1H), 3.76 (dd, $J = 7.0, 10.9$, 2H), 3.71-3.57 (m, 2H), 3.43 (s, 3H), 3.33 (dd, $J = 5.8, 10.1$, 1H), 3.13 (s, 4H), 2.32 (s, 6H), 2.00 (d, $J = 7.1$, 1H).

^{13}C NMR (75 MHz, CDCl_3) δ 166.26, 165.83, 165.55, 165.34, 163.10, 161.63, 159.63, 149.20, 141.09, 140.82, 136.55, 136.50, 136.22, 133.71, 133.51, 133.43, 133.27, 130.04, 129.96, 129.89, 129.51, 129.36, 129.27, 129.19, 128.82, 128.70, 128.59, 128.45, 128.40, 128.27, 123.28, 121.04, 120.77, 119.36, 102.52, 87.25, 86.59, 72.80, 72.29, 71.08, 70.94, 69.54, 69.30, 37.62, 21.19.

HRMS (ESI+) calc'd for $[\text{C}_{68}\text{H}_{64}\text{N}_2\text{O}_{15} + \text{H}]^+$: 1149.43795. Found: 1149.43769.



(6-*O*-[6-(2-pyridin-2-yl-ethyl)-pyridin-2-yl]-di-*p*-tolyl-methyl-octyl 3-*O*-(2',3',4',6'-tetra-*O*-benzoyl- β -D-glucopyranosyl)- β -D-glucopyranoside (5-38)
Following the general glycosylation procedure, **5-9** was reacted with **5-4** yielding **5-37** (87% yield).



$\text{C}_{75}\text{H}_{78}\text{N}_2\text{O}_{15}$, Mol. Wt. = 1247.43

$R_f = 0.3$ (H/EA, 1:1)

IR (CHCl_3) 3494, 1730 cm^{-1}

$[\alpha]_D = +21.0$ (c 0.12, CHCl_3)

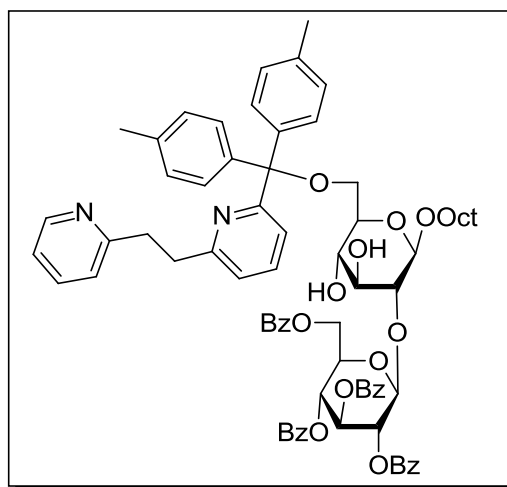
^1H NMR (400 MHz, CDCl_3) δ 8.49 (d, $J = 4.5$, 1H), 8.28-8.23 (m, 1H), 7.98 (t, $J = 8.1$, 6H), 7.93-7.85 (m, 5H), 7.82 (d, $J = 7.4$, 3H), 7.57 (d, $J = 7.9$, 2H), 7.50 (d, $J = 7.2$, 4H), 7.42 (d, $J = 3.0$, 7H), 7.40-7.28 (m, 18H), 7.22 (t, $J = 7.7$, 3H), 7.05 (d, $J = 7.9$, 7H), 6.84 (t, $J = 8.3$, 2H), 5.91 (t, $J = 9.7$, 1H), 5.63-5.52 (m, 2H), 5.10 (d, $J = 8.0$, 1H), 4.73 (d, $J = 10.1$, 1H), 4.37-4.29 (m, 2H), 4.21 (d, $J = 7.9$, 2H), 4.18-4.13 (m, 1H), 4.07 (s, 1H), 3.87 (d, $J = 9.6$, 1H), 3.64 (d, $J = 9.5$, 1H), 3.55-3.50 (m, 2H), 3.48-3.38 (m, 5H), 3.34-3.30 (m, 1H), 3.12 (s, 6H), 2.29 (s, 9H), 1.63-1.57 (m, 5H), 1.28-1.22 (m, 14H), 0.85 (d, $J = 6.8$, 6H).

^{13}C NMR (75 MHz, CDCl_3) δ 171.26, 166.24, 165.82, 165.38, 165.32, 163.07, 161.59, 159.61, 149.16, 141.00, 140.81, 136.50, 136.48, 136.22, 133.67, 133.39, 133.24, 130.00, 129.93, 129.86, 129.47, 129.37, 129.31, 128.82, 128.70, 128.56, 128.51, 128.42, 128.38, 128.23, 123.29, 121.03, 120.75, 119.43, 102.53, 102.49, 88.36, 86.50, 86.35, 75.18, 72.99, 72.72, 72.08, 69.99, 69.61, 64.10, 63.05, 60.51, 37.65, 37.58, 34.78, 31.90, 31.71, 29.82, 29.73, 29.48, 29.35, 26.15, 22.78, 21.18, 14.32, 14.25, 14.21.

HRMS (ESI+) calc'd for $[\text{C}_{75}\text{H}_{78}\text{N}_2\text{O}_{15} + \text{H}]^+$: 1247.54750. Found: 1247.54653.

(6-*O*-[6-(2-pyridin-2-yl-ethyl)-pyridin-2-yl]-di-*p*-tolyl-methyl-octyl 2-*O*-(2',3',4',6'-tetra-*O*-benzoyl- β -D-glucopyranosyl)- β -D-glucopyranoside (5-37)

Pre-incubating **5-9** with TMSOTf (1 equiv.) and then following the general glycosylation procedure, **5-9** was reacted with **5-4** yielding both **5-37** and **5-38** (16% : 4%, **5-37/5-38**).



$\text{C}_{75}\text{H}_{78}\text{N}_2\text{O}_{15}$, Mol. Wt. = 1247.43

R_f = 0.25 (H/EA, 1:1)

IR (CHCl_3) 3463, 1730 cm^{-1}

$[\alpha]_D = +47.2$ (c 0.07, CHCl_3)

^1H NMR (500 MHz, CDCl_3) δ 8.55-8.43 (m, 2H), 8.14-8.07 (m, 1H), 8.03-7.93 (m, 5H), 7.87 (dd, 5H), 7.56-7.29 (m, $J = 71.4$, 23H), 7.22-7.17 (m, 3H), 7.13-6.95 (m, $J = 21.9$, 10H), 5.91 (t, 1H), 5.72 (t, 1H), 5.55 (t, 1H), 5.42 (d, 1H), 4.64-4.56 (m, 1H), 4.51-4.42 (m, 1H), 4.41-4.27 (m, 3H), 4.18-4.08 (m, 2H), 4.02-3.91 (m, 2H), 3.73-3.62 (m, 6H), 3.51-3.38 (m, 4H), 3.31-3.24 (m, 2H), 3.24-3.12 (m, 5H), 3.11-3.04 (m, 3H), 2.32 (d, $J = 31.6$, 10H), 1.69-1.52 (m, 17H), 1.34-1.11 (m, 47H), 0.93-0.78 (m, 20H).

^{13}C NMR (126 MHz, CDCl_3) δ 166.27, 166.03, 165.75, 165.31, 161.92, 160.93, 160.52, 149.45, 141.81, 138.73, 137.81, 137.05, 136.86, 136.66, 133.41, 133.26, 133.11, 133.05, 130.19, 130.04, 130.01, 129.96, 129.93, 129.82, 129.80, 129.16, 129.13, 128.80, 128.75, 128.67, 128.63, 128.48, 128.43, 128.39, 128.33, 128.13, 127.92, 123.31, 122.42, 121.53, 121.44, 101.87, 101.30, 87.16, 81.36, 75.90, 74.63, 73.54, 73.42, 72.86, 72.15, 70.16, 70.00, 67.40, 63.46, 39.36, 38.39, 31.99, 29.87, 29.50, 29.44, 25.98, 22.81, 21.23, 21.16, 14.27.

HRMS (ESI+) calc'd for $[\text{C}_{75}\text{H}_{78}\text{N}_2\text{O}_{15} + \text{H}]^+$: 1247.54750. Found: 1247.54906.

5.7 References

1. Cid, M. B.; Alfonso, F.; Martín-Lomas, M. A comparative study of the influence of protecting groups on the reactivity of chiro-inositol glycosyl acceptors. *Synlett* 2005, 2052-2056.
2. Bohn, M. L.; Colombo, M. I.; Stortz, C. A.; Rúveda, E. A. A comparative study of the influence of some protecting groups on the reactivity of d-glucosamine acceptors with a galactofuranosyl donor. *Carbohydr. Res.* 2006, 341, 1096-1104.
3. Katritzky, A. R.; Lue, P.; Chen, Y. X. An alternative route to 2-substituted indoles via N-aminal-directed lithiation. *J. Org. Chem.* 2002, 55, 3688-3691.
4. Sharma, G. V. M.; Prasad, T. R.; Srinivas, R. B. p-Methoxy diphenylmethanol (MDPM), p-phenyl diphenylmethanol (PDPM), and p-phenylphenyl diphenylmethanol (PPDPM) - protecting groups for alcohols - protection and deprotection. *Synth. Commun.* 2004, 34, 941-950.
5. Egusa, K.; Kusumoto, S.; Fukase, K. Solid-phase synthesis of a phytoalexin elicitor pentasaccharide using a 4-azido-3-chlorobenzyl group as the key for temporary protection and catch-and-release purification. *Eur. J. Org. Chem.* 2003, 3435-3445.
6. Moitessier, N.; Englebienne, P.; Chapleur, Y. Directing-protecting groups for carbohydrates. Design, conformational study, synthesis and application to regioselective functionalization. *Tetrahedron* 2005, 61, 6839-6853.

Chapter 6 Conclusions and contributions to knowledge

In the first part of this thesis, we discussed the potential role of the enzyme prolyl oligopeptidases in diseases. We not only reviewed the reported inhibitors, but we also developed a pharmacophore that researchers could use in the design of novel, selective prolyl oligopeptidase inhibitors. From our review, we found that several researchers are targeting prolyl oligopeptidase, offering mainly pseudopeptidic, but also a few non-peptidic inhibitors. Many of the reports would benefit from a few extra experiments to verify that their inhibitors, which were designed to target POP, are not targeting other prolyl oligopeptidases of the same family. Our review article is in the ASAP the Journal of Medicinal Chemistry have formally accepted our review and it will be published in the coming weeks.

We also designed a series of small bicyclic scaffolds bearing nitriles capable of covalently attaching to the targeted enzyme POP. We not only developed a good inhibitor of POP activity ($IC_{50} = 200$ nM), which is selective for POP over other prolyl oligopeptidase enzymes and membrane permeable, we also learned the importance of the shape of covalent inhibitors. Our results culminated in an article which is now published in the Journal of Medicinal chemistry. Furthermore, we now know which scaffolds must be synthesized next to achieve a more potent and stable POP inhibitor.

In the second part of this thesis, we reviewed the available methods to selectively perform a reaction on a sugar, discovering that although researchers have developed a few methods for selectively functionalizing sugars, few discuss the reasons for the observed selectivity. We also noted that some reports are contradictory to each other, indicating that these methods may be sensitive to subtle differences in conditions which are not described and may influence the products obtained. Amidst this melee of reports, we attempted to organize the methods into logical categories, finding that many researchers utilize and depend on the innate reactivity of the hydroxyls of sugars (most likely arising from an

intramolecular hydrogen bond network) to perform selective reactions on these. We compiled a table summarizing all the methods that can be used to selectively functionalize each of the positions. Outlining such crucial information as starting materials, reagents, conditions and references that would be required to selectively functionalize a position of a sugar, this table will be a valuable reference tool to any researcher aiming to perform a reaction at a specific position of a sugar. This review will be submitted for publication in the coming weeks.

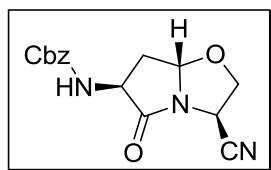
We also successfully applied a protecting group which we designed in 2005 to render glycosylation of the 6-*O*-mono-protected sugar more selective. In fact, with a reactive donor, we could selectively glycosylate at position 2 of the glucopyranosides, usually a less reactive position for this type of reaction. Even though with a less reactive donor, we expected to glycosylate at the same position as with a reactive donor, we surprisingly glycosylated the glucopyranosides at position 3, in yields (> 80% yield) higher than any other reported methods that we know of. We proposed a mechanism to explain our results and revised the role of our protecting group in the reaction since we found that it must participate in the glycosylation reactions we performed. We will expand the scope of this method to other sugars and attempt to develop more user-friendly methods to glycosylate at position 2 or at position 3 of the glucopyranoside.

*“There is nothing like looking, if you want to find something.
You certainly usually find something, if you look,
but it is not always quite the something you were after.”*

J.R.R. Tolkien The Hobbit

Appendix

Supplementary information for Chapter 2

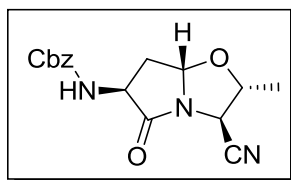


$C_{15}H_{15}N_3O_4$, Mol. Wt. = 301.30

$R_f = 0.35$ (CH_2Cl_2/EA , 9:1)

2-9a: 1H NMR (500 MHz, $CDCl_3$) δ 7.35 (s, 5H), 5.32 (s, 1H), 5.24 (s, 1H), 5.13 (s, 2H), 4.39 (s, 1H), 4.28 (s, 1H), 4.21 (s, 1H), 2.66 (s, 1H), 2.36 (s, 1H), 1.99 (s, 3H), 1.43 (d, 3H).

^{13}C NMR (126 MHz, $CDCl_3$) δ 177.40, 155.84, 135.89, 131.05, 128.94, 128.76, 128.54, 128.39, 116.44, 90.54, 80.61, 67.63, 51.91, 32.07, 29.84, 18.92.



$C_{16}H_{17}N_3O_4$, Mol. Wt. = 315.32

$R_f = 0.55$ (CH_2Cl_2/EA , 9:1)

2-29a: 1H NMR (500 MHz, $CDCl_3$) δ 7.36 (s, 6H), 5.37 (s, 1H), 5.25 – 5.17 (m, 1H), 5.13 (s, 2H), 4.86 – 4.79 (m, 0.5H), 4.80 – 4.72 (m, 1H), 4.65 – 4.57 (m, 0.5H), 4.53 – 4.44 (m, 1H), 4.43 – 4.33 (m, 1H), 4.29 – 4.19 (m, 1H), 4.16 – 4.08 (m, 1H), 4.07 – 3.98 (m, 1H), 3.15 – 3.04 (m, 0.5H), 2.75 – 2.60 (m, 1H), 2.36 (s, 1H), 2.08 – 1.94 (m, 1H).

^{13}C NMR (125 MHz, $CDCl_3$) δ 177.45, 174.39, 155.81, 135.94, 128.76, 128.55, 128.40, 116.77, 116.37, 90.64, 89.12, 70.72, 70.57, 67.63, 67.51, 53.67, 51.79, 45.39, 43.37, 35.01.

Supplementary information for Chapter 5

JL568_majorpure JM409_COSY
Data Collected on:
mdd-mercury480
Archive directory:
/export/home/jlawand/vnmrsys/data
Sample directory:
File: gCOSY
Pulse Sequence: gCOSY
Solvent: CDCl3
Temp: 25.0 C / 298.1 K
Relax: delay 1.000 sec
Acq. time 0.193 sec
Width 3783.7 Hz
2D Width 3783.7 Hz
4 repetitions
60 increments
OBSERVE HI: 400.1218004 MHz
DATA PROCESSING
Sf: time 0.011 0.075 sec
F1 DATA PROCESSING
Sf: time 0.011 0.035 sec
F1 size 1024 x 1024
Total time 5 min

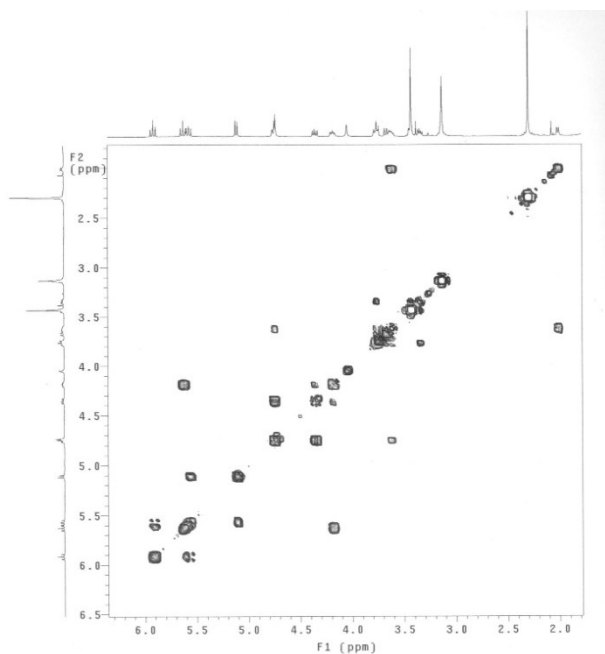


Figure A.1 COSY of 5-36

JL568_P_H500_HSQC
Sample: JL568_P_H500_1H
File: kp
Pulse Sequence: gHSQC
Solvent: cdcl3
Temp: 25.0 C / 298.1 K
Operator: jlawand
VNAME: 150 "dante"
Relax: delay 1.000 sec
Acq. time 0.193 sec
Width 4864.0 Hz
2D Width 21367.5 Hz
8 repetitions
2 x 128 increments
OBSERVE HI: 400.1218004 MHz
DECOUPLE C13: 125.786592 MHz
Power 18 dB
on during acquisition
off during delay
vds_gw500 modulated
DATA PROCESSING
Gauss apodization 0.092 sec
F1 DATA PROCESSING
Gauss apodization 0.006 sec
F1 size 4096 x 1040
Total time 42 min, 57 sec

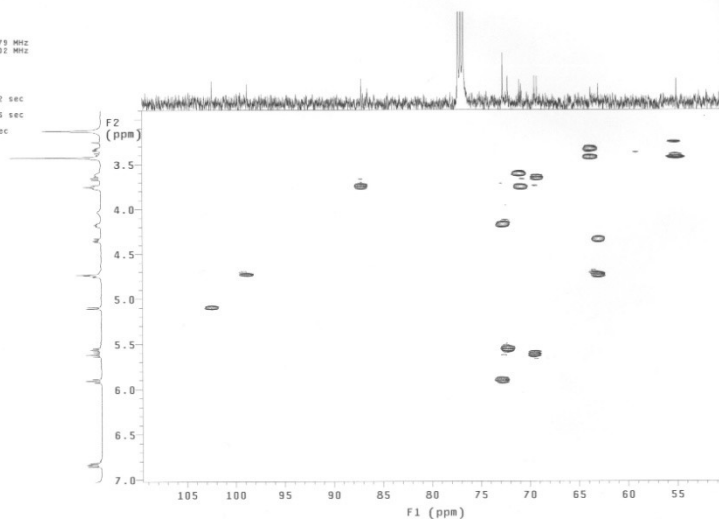


Figure A.2 HSQC of 5-36

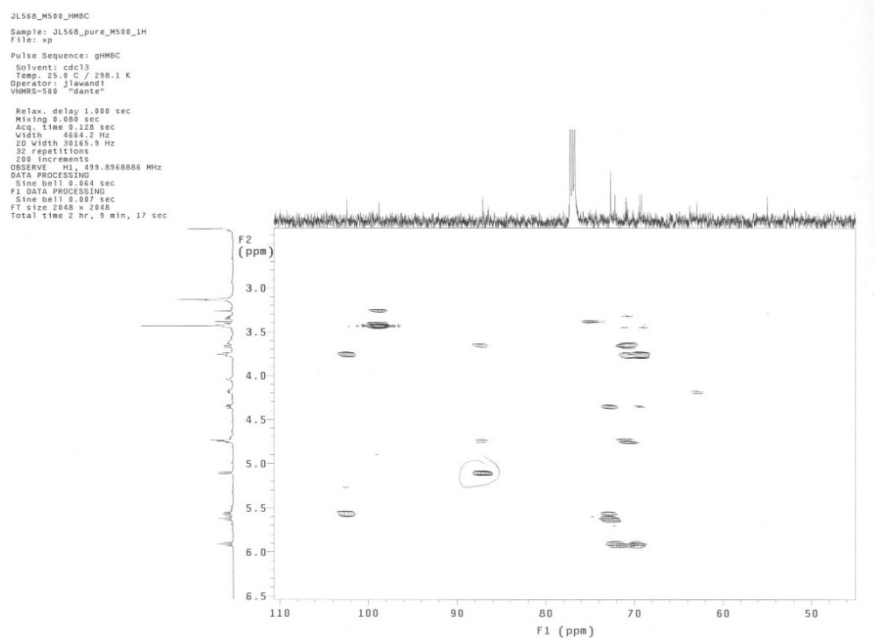


Figure A.3 HMBC of 5-36

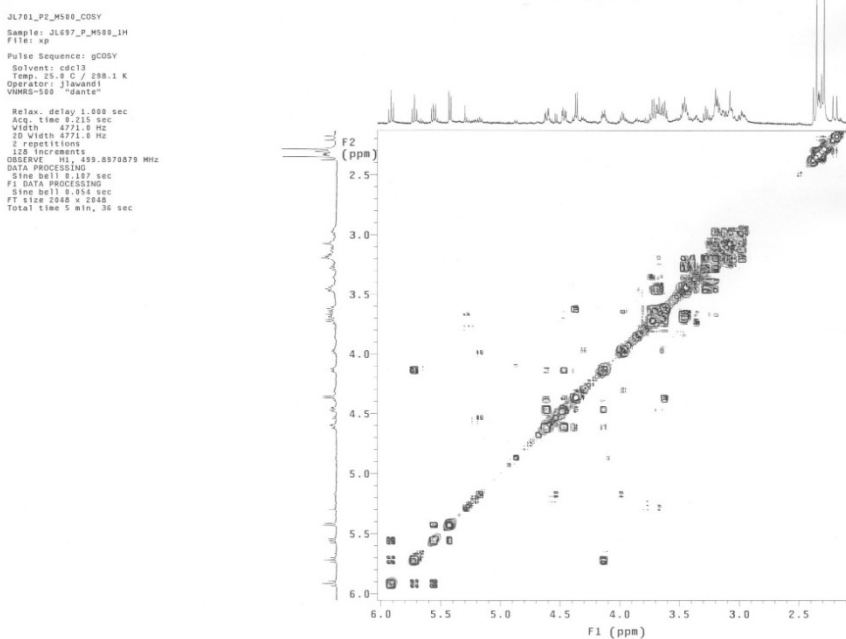


Figure A.4 COSY of 5-37

Appendix

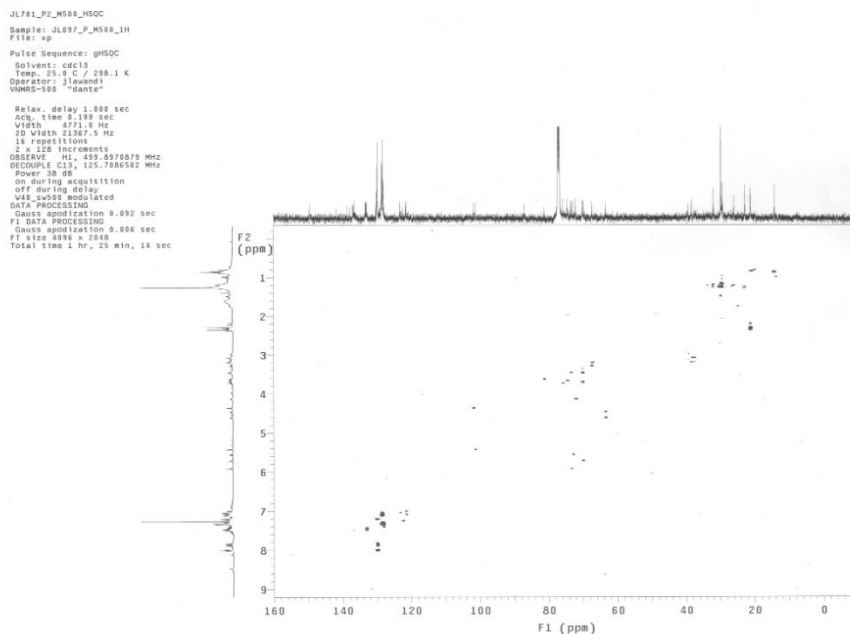


Figure A.5 HSQC of 5-37

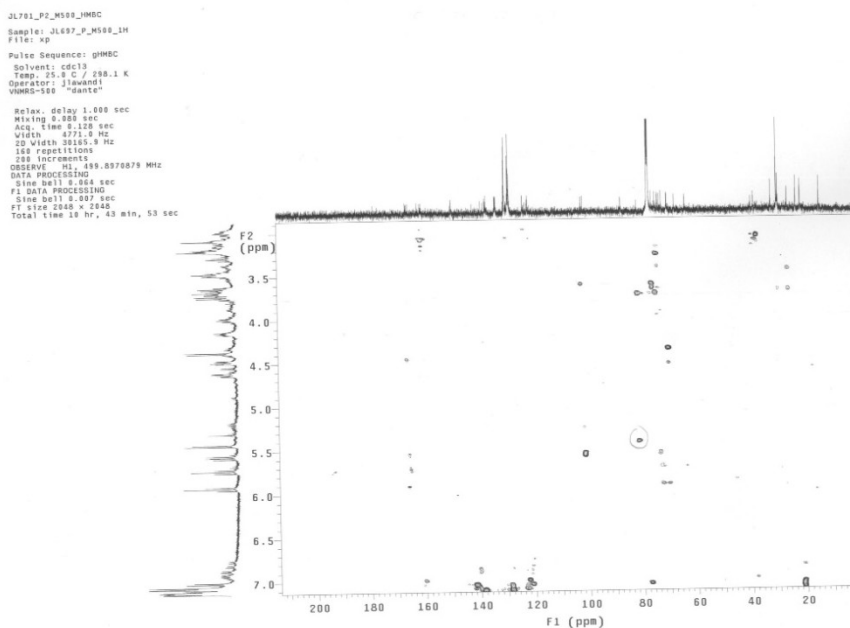


Figure A.6 HMBC of 5-37

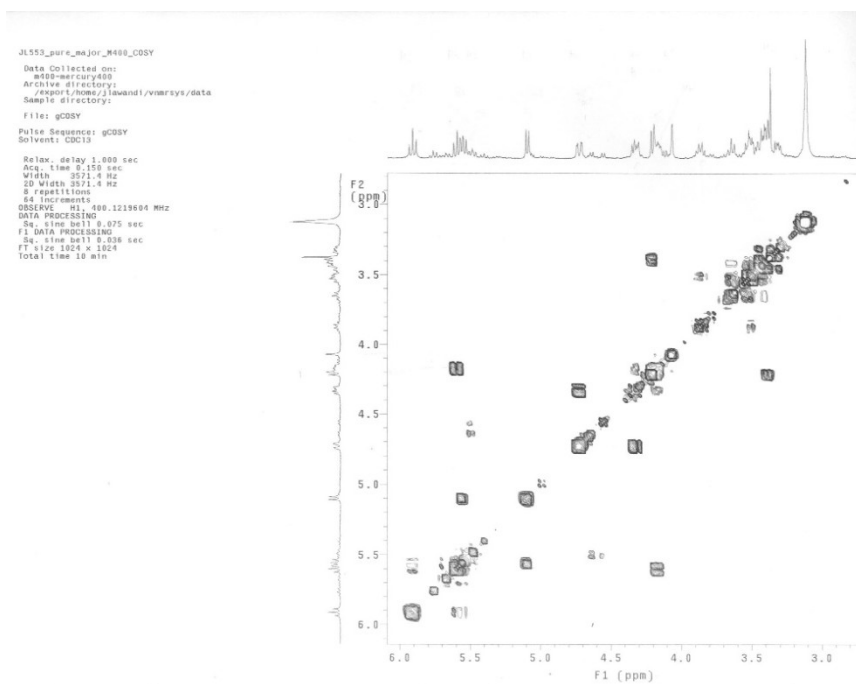


Figure A.7 COSY of 5-38

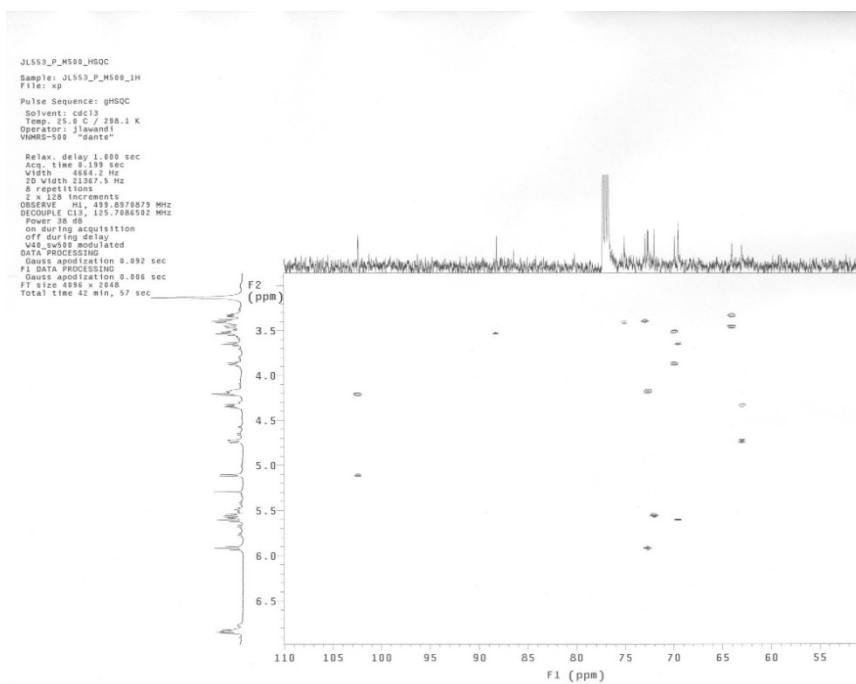


Figure A.8 HSQC of 5-38

Appendix

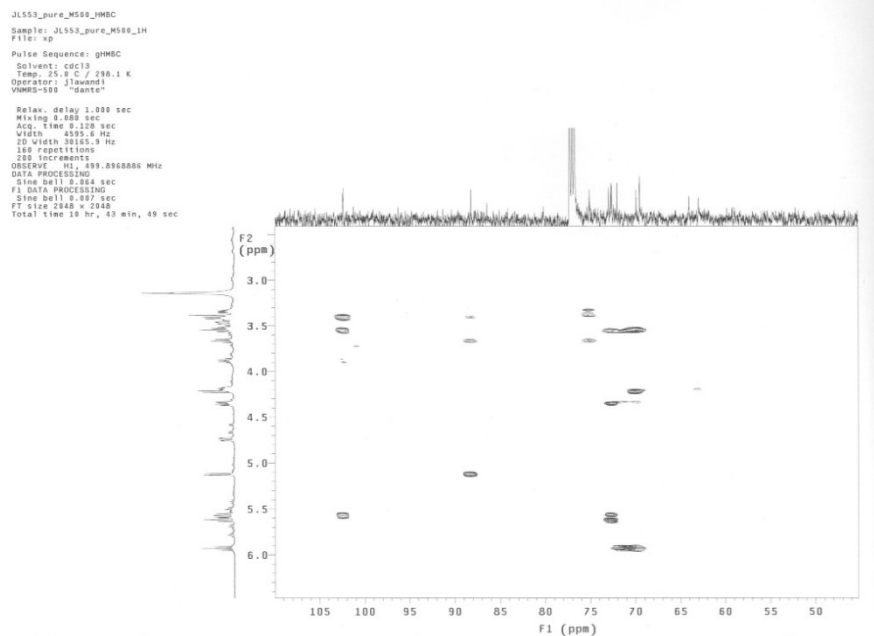


Figure A.9 HMBC of 5-38